School of Architecture, Planning and Landscape

Effect of Roof Shape, Wind Direction, Building Height and Urban Configuration on the Energy Yield and Positioning of Roof Mounted Wind Turbines

Islam Abohela

BSc, MSc

PhD Thesis

(September 2012)

Title page

Thesis Title: Effect of Roof Shape, Wind direction, Building Height and Urban Configuration on the Energy Yield and Positioning of Roof Mounted Wind Turbines

Full name: Islam Mohamed Mahmoud Mohamed Abohela

Qualification: Doctor of Philosophy

School: School of Architecture, Planning and Landscape

Submission Date: September 2012

Abstract

The increasing interest among architects and planners in designing environmentally friendly buildings has led to a desire to explore and integrate renewable sources of energy within the built environment. Roof mounted wind turbines is a technology that presents a high potential for integration within the built environment. However, there is a state of uncertainty regarding the viability of these wind turbines.

This thesis argues that part of this uncertainty is attributed to uninformed decisions about positioning and locating urban wind turbines. This is underpinned by lack of consideration to the wind accelerating effect of different roof shapes, buildings' heights and surrounding urban configurations. This thesis aims to investigate the effect of different roof shapes on wind acceleration and positioning of roof mounted wind turbines covering different buildings' heights within different urban configurations under different wind directions.

To achieve the aim of the thesis, the commercial Computational Fluid Dynamics (CFD) code Fluent 12.1, implementing the Realizable k-ε turbulence model, is used to simulate wind flow around different roof shapes, different buildings' heights and different urban settings. Predictions are comparatively analysed to identify the optimum roof shape for mounting wind turbines. Simulation results indicate that the barrel vaulted roof has the highest wind accelerating effect. The barrel vaulted roof shape case was carried further to investigate the effect of building height and surrounding urban configurations on the energy yield and positioning of roof mounted wind turbines.

The optimum mounting location for each of the investigated roof shapes namely: flat, domed, gabled, pyramidal, barrel vaulted and wedged roofs is identified. Results from the investigation predict a possible increase up to 56.1% in energy yield in the case of a barrel vaulted roof if an informed wind assessment above buildings' roofs is carried out. However, changing the building height and surrounding urban configuration had an effect on choosing the optimum mounting location and the energy yield at that location.

Related Published Work

Journal papers

- Abohela, I., Hamza, N. and Dudek, S. (2013) 'Effect of roof shape, wind direction, building height and urban configuration on the energy yield and positioning of roof mounted wind turbines', *Renewable Energy*, 50(0), pp. 1106-1118.
- Abohela, I., Hamza, N. and Dudek, S. (2011) 'Assessment of wind flow within the built environment', *Built and Natural Environment*, pp. 81-94.
- Abohela, I., Hamza, N. and Dudek, S. (2011) 'Urban Wind Turbines Integration in the Built Form and Environment', *FORUM Ejournal for Postgraduate Studies in Architecture, Planning and Landscape*, 10(1), pp. 23-39.

Conference papers

- Abohela, I., Hamza, N. and Dudek, S. (2012) 'Effect of roof shape, building height and urban configuration on the siting location of roof mounted wind turbines', *PLEA2012 - 28th Conference, Opportunities, Limits & Needs Towards an environmentally responsible architecture* Lima, Perú, 7-9 November 2012. p. Under publication.
- Abohela, I., Hamza, N. and Dudek, S. (2012) 'Validating CFD simulations of wind flow around a surface mounted cube in a turbulent channel flow', *PLEA2012 - 28th Conference, Opportunities, Limits & Needs Towards an environmentally responsible architecture* Lima, Perú, 7-9 November 2012. p. Under publication.
- Abohela, I., Hamza, N. and Dudek, S. (2011) 'Effect of Roof Shape on the Energy Yield and Positioning of Roof Mounted Wind Turbines', *Building Simulation 2011 (BS2011)*. Sydney, Australia. pp. 1203-1210.
- Abohela, I., Hamza, N. and Dudek, S. (2010) 'Assessment of Wind Flow within the Built Environment', *First International Conference on Sustainability and the Future, Future Intermediate Sustainable Cities: a message to future generations*. El Sherouk City, Egypt, 23-25 November 2010. Elain Publishing Company, pp. 298-323.

- Abohela, I., Hamza, N. and Dudek, S. (2010) 'Integration of wind turbines in the built form and environment', *The Second International Conference on Sustainable Architecture and Urban Development*. Amman, Jordan. The centre for the study of Architecture in the Arab Region, pp. 63-78.
- Rashed, A. and Abohela, I. (2009) 'Second Egypt and Sustainable Future: Challenges?!!', *Second International Conference on Whole Life Urban Sustainability and its Assessment*. Loughborough. Loughborough University, pp. 425-440.
- Abohela, I. (2009) 'The Integration of Wind Turbines in Architectural Design', *Third Ain Shams University International Conference on Environmental Engineering*. Cairo, Egypt. pp. 01-14.

Dedication

To my late father Mohamed Abohela who has always been keen on education and would have been proud of his son awarded a PhD degree. And to my mother Saadeya Mohaseb who never gave up on me. This thesis is also dedicated to my sister Eman, my brother Ahmed and their kids who were always a great support and a source of joy during hard times and throughout the journey of the PhD.

Acknowledgments

First and foremost, I thank God, the Almighty, for His providence in my life throughout, especially during my PhD programme. This work could not have been done without the blessings of God.

A studentship from the School of Architecture, Planning and Landscape in Newcastle University made this research possible. As an International student, other scholarships from the Arab British Chamber of Commerce and Newcastle University International Postgraduate Scholarship contributed to covering my living expenses in the UK which helped me in focusing more on my research and finishing on time. I would like to thank these institutions for their help and support.

I would like to express my sincere and deep appreciation and gratitude to my loving family, for long years of prayers, caring and support, for always providing me with the needed support and encouragement. In particular, the patience and understanding shown by my sister and brother who are taking good care of my mother while I am away doing my PhD. Words are inadequate to express my gratitude to my beloved mother whose prayers and blessings kept me going.

Special thanks are due to both my supervisors for their academic input and support. To Dr Neveen Hamza, in whom I found an eminent scholar, sincere and hardworking and an able guide who inspires her students to pursue thorough scholarship. To Dr Steven Dudek, for his detailed and constructive comments, and for his important support throughout this work. I consider myself very lucky to have such a harmonious supervisory team. I acknowledge their care, guidance and patience with due respect and I thank both of them sincerely from the depth of my heart.

At last but not least, thanks to a long list of friends who made the PhD journey an enjoyable and joyful experience. Especially those who have engaged with me in countless thesis related conversations. I would love to thank all my friends one by one, especially Tugce Sanli, for always being there to support me, cheer me up and make me remember that you can still have fun while studying for a PhD.

Table of Contents

List of Figures

Chapter One

Chapter Two

Chapter Three

Chapter Four

Chapter Five

List of Tables

Chapter Two

Chapter Three

Chapter Four

Chapter Five

Chapter Six

List of Symbols, Acronyms and Abbreviations

Symbol	Description
2D	Two dimensions
3D	Three dimensions
A	Swept area of a turbine
ABL	Atmospheric Boundary Layer
AC	Alternating Current
ASCE	American Society of Civil Engineers
AWEA	American Wind Energy Association
BAWT	Building Augmented Wind Turbine
BIWT	Building Integrated Wind Turbine
BMWT	Building Mounted Wind Turbine
BLWT	Boundary Layer Wind Tunnel
BRE	Building Research Establishment
BREEAM	BRE Environmental Assessment Method
C_P	Pressure coefficient
CpL	leeward façade maximum negative pressure coefficient
CpR	Roof maximum negative pressure coefficient
CpW	Windward façade maximum positive pressure coefficient
C_μ	Turbulence model constant
C_s	Roughness constant
CFD	Computational Fluid Dynamics

Symbol	Description
CHP	Combined Heat and Power
C/R	Contra-Rotating
CWE	Computational Wind Engineering
DES	Detached Eddy Simulation
DC	Direct Current
DIY	Do It Yourself
DNS	Direct Numerical Simulation
DWIA	Danish Wind Industry Association
DWT	Ducted Wind Turbine
EM	Electromagnet
EPC	Energy Performance Certificate
f_x, f_y and f_z	Components of the body force per unit mass
FDM	Finite-Difference Method
FEM	Finite-Element Method
FIT	Feed In Tariffs
FVM	Finite-Volume Method
H or h	Building height
HAWT	Horizontal Axis Wind Turbine
k	Turbulent Kinetic Energy
k_s	Roughness height
l	Characteristic linear dimension

Symbol	Description
LCBP	Low Carbon Buildings Programme
LED	Lower Energy Design
LES	Large Eddy Simulation
LIF	Laser-Induced Fluorescence
MCS	Microgeneration Certification Scheme
NIMBY	Not-In-My-Backyard
P	Power extracted from the wind
p	Pressure
PIV	Particle Image Velocimetry
PM	Permanent Magnet
PV	Photovoltaic
RANS	Reynolds Averaged Navier Stokes
Re	Reynolds number
RIBA	Royal Institute of British Architects
RNG	Renormalization Group
RPM	Revolution Per Minute
RO	Renewables Obligation
Rx1	Distance leeward the building where the flow reattaches
Rx2	Reattachment length on top of the roof
Sa	Nodal point
Sp	Saddle point

Symbol	Description
St	Stagnation point
TDR	Turbulent Dissipation Rate
TI	Turbulence Intensity
TKE	Turbulent Kinetic Energy
QR	Quiterevolution
U	Velocity of a turbulent flow at a specific point
$\bar{U}$	Mean velocity taken over a sufficient long period
u'	Fluctuating velocity component
u	X velocity component
u^*	Friction velocity
URANS	Unsteady Reynolds Averaged Navier Stokes
UWT	Urban Wind Turbine
υ	Wind speed
v	Y velocity component
$\mathrm{V}(\mathrm{z})$	Wind speed at reference height z
VAWT	Vertical Axis Wind Turbine
w	Z velocity component
WDR	Wind Driven Rain
X_F	Length of the front recirculation
X_t	Top recirculation
z_o	Roughness length

Symbol	Description
z_p	Distance between the centre of the first cell and the ground
ZEBRA	Zero Emission Building Renewing Alnwick
ZED	Zero Energy Design
δ	Boundary layer height
ε	Turbulent dissipation rate
κ	Von Karman constant
μ	Dynamic viscosity
μ_t	Eddy viscosity
ρ	Air density
τ	Shear stress

Chapter One

Introduction and Methodology

Chapter Structure

1.1 Introduction

1.2 Research Design

1.3 The conceptual framework

1.4 Research Methodology

1.5 Research structure overview

1.6 Conclusion

Chapter 1: Introduction and Methodology

1.1 Introduction

Since the ancient Egyptians exploitation of wind to sail boats on the Nile River, man has tried to tame wind power for his benefit. At the beginning of the first century, Chinese flew kites during battles to signal their troops, Sri Lankans used wind to separate metal from rock ore during the eighths century, Persians invented the first windmill to pump water during the tenth century, Europeans built windmills to grind grain during the thirteenth century and the first windmill to generate electricity is said to have been either built in Scotland in 1887 or was developed in Cleveland, Ohio in 1888 by Charles F. Brush (Andersen, 2007; Walker, 2007; Ages, 2010; Jha, 2010).

Nowadays wind is harnessed and converted into electricity using clustered large wind turbines in wind farms located either offshore or onshore in exposed locations where wind characteristics are ideal for generating power. However, there is a growing opposition to existing wind farms and erecting new ones. The protestors against wind farms argue that wind turbines produce noise pollution, ruin the landscape and jeopardize birds' lives. Thus, there is a growing interest in erecting wind turbines within the built environment to generate electricity where it is needed and avoid spoiling the natural beauty of the countryside (Stankovic *et al.*, 2009).

This thesis investigates wind energy conversion within the built environment focusing on roof mounted wind turbines. The aim of this thesis is to investigate the effect of roof shape, wind direction, building height and surrounding urban configuration on the energy yield and positioning of roof mounted wind turbines. Computational fluid dynamics (CFD) is the wind assessment tool used for assessing wind flow above the investigated roof shapes namely: flat, domed, gabled, pyramidal, barrel vaulted and wedged roofs. The optimum roof shape for roof mounting wind turbines is then used for studying the effect of building height and surrounding different urban configurations on wind flow above it.

This first chapter is divided into four main sections; the first section (1.2) focuses on the research design where the thesis structure is outlined. The second section (1.3) outlines the conceptual framework through discussing the

rationale behind the argument, research aim, hypotheses, objectives, limitations, propositions and the significance of the study. Accordingly, section 1.4 outlines the research methodology, and then the research structure and the thesis chapters overview are outlined in section 1.5.

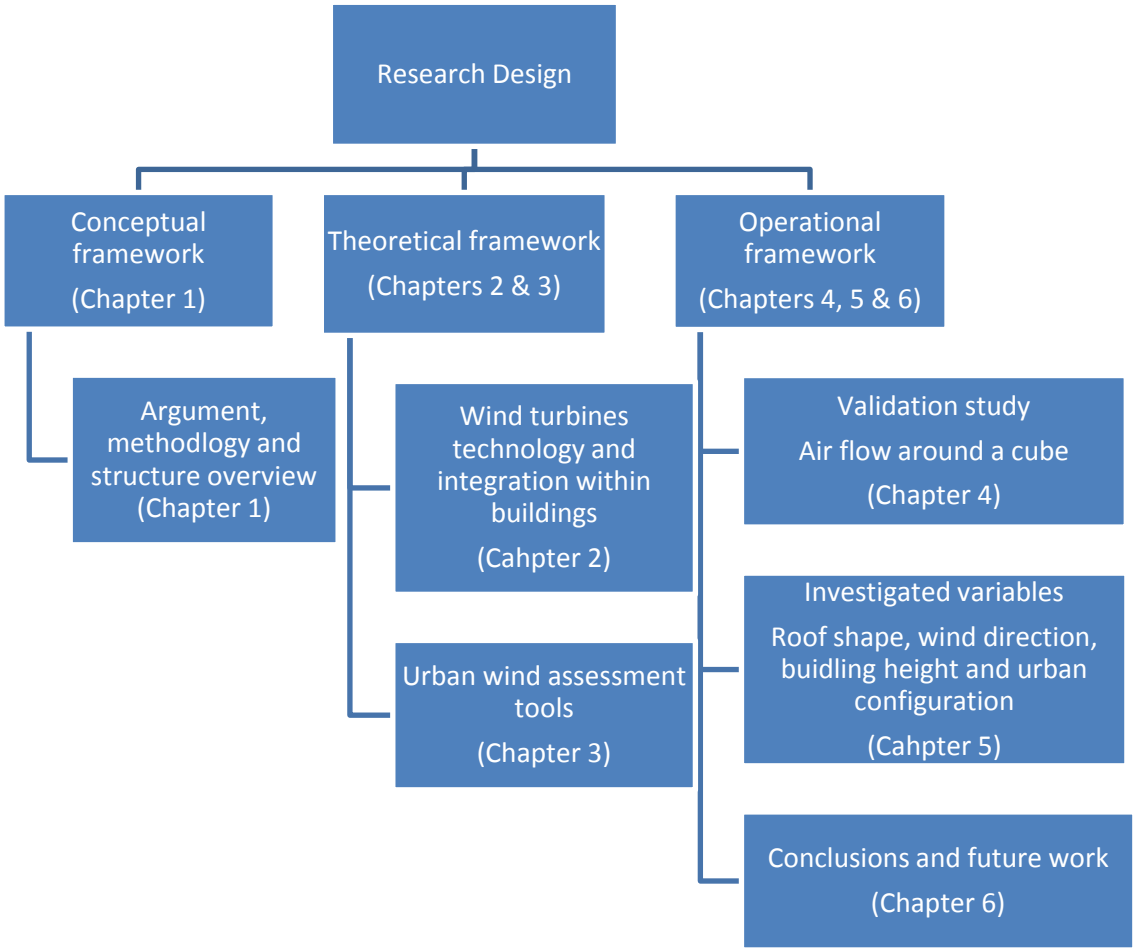

Figure 1.1 Research design.

1.2 Research design

This research is an experimental research where different roof shapes are tested and compared to each other in terms of their effects on wind flow above them for the purpose of identifying the optimum roof shape for mounting wind turbines and the optimum mounting location for each roof shape based on the recorded velocities above the investigated cases.

Accordingly, this research is divided into three main sections forming the conceptual, theoretical and operational frameworks of the thesis (Figure 1.1). The conceptual framework is covered in this chapter, the theoretical framework

constitutes the literature review which is covered in chapters two and three and the operational framework is where the CFD validation and numerical simulations of the investigated wind flow problems are carried out, which is covered in chapters four and five. Chapter six covers the conclusions and recommendations for future work.

1.3 The conceptual framework

1.3.1 *Energy and climate change*

Regardless of the scepticism about climate change and its effect on the planet, the unprecedented Kyoto protocol which was signed by more than 150 countries in Kyoto, Japan on 11 December 1997 was a clear declaration of the importance of combating climate change through reductions in emissions of greenhouse gases. The reductions varied from one country to another, but the overall target was a reduction of 5% below 1990 levels in the period between 2008 and 2012. However, those exceptionally hot summers that happened in 2003, 2005 and 2007 have demonstrated that the rate of warming up happening to the planet is faster than expected (Founda and Giannakopoulos, 2009; Roaf et al., 2009).

According to the Kyoto protocol, the UK is to cut its greenhouse gas emissions by 12.5% below 1990 level by 2008 – 2012. In December 2008, the Committee on Climate Change (2008) advised the UK government on the importance of reducing the emissions by about 50% by 2050 which cannot be achieved unless the power sector is largely decarbonised in addition to implementing new renewable technologies in power, buildings and industry, and transport. Also, the committee acknowledged the importance of the efficiency of using energy through lifestyle changes which would not undermine welfare. These measures would be implemented not only for reducing the greenhouse gases, but also because they have economic, wider environmental and security of supply benefits.

1.3.2 *Buildings and climate change*

Smith (2005) stated that most climate change scientists agree that 90% of the climate change is due to human activity and mainly through the burning of fossil

fuels. However, most of human activities take place inside buildings, this is why the building sector is responsible for about 50% of the greenhouse gas emissions in the world. Thus, cutting down the greenhouse gas emissions from buildings would contribute significantly in combating climate change (Dutton et al., 2005; Roaf et al., 2009). Roaf *et al.* (2009) claimed that modern buildings are becoming more energy profligate and damaging to the environment. However, Mertens (2006) and Stankovic *et al.* (2009) acknowledged that the building sector is trying to reduce its harmful carbon gas emissions due to the growing interest among architects and planners to build Lower Energy Design (LED) or even Zero Energy Design (ZED) buildings where local renewable sources of energy are integrated. Jha (2010) added that LED and ZED buildings are recognized as the most desirable renewable energy schemes because owners of these buildings can be reimbursed at a price set by the utility company, which is roughly three times the price paid to commercial utilities for renewable energy sources in rural areas (more details on these schemes is discussed under section 2.4.5 in chapter two). This emphasises the need to integrate renewables at buildings design stage.

But for this integration to be successful, Smith (2005) noted that there should be a constructive dialogue between architects and service engineers at the inception of a project. However, sometimes it is hard to convince the clients of the importance of integrating systems which would contribute to reducing the greenhouse gases emissions from buildings. In some situations, these measures might need to be enforced by law. For example, in the EU, the Energy Performance Certificate (EPC) is used to enforce reduction of energy consumption by buildings. The same concept applies to the UK where every house or flat in the UK requires an EPC at the point of sale or lease demonstrating the energy efficiency of the building on a scale from A to G. One of the factors that count for the energy efficiency of buildings is the integration of renewable sources of energy in the building (Dutton et al., 2005).

1.3.3 *Green buildings and renewable sources of energy*

Renewable sources of energy have significant advantages such as being infinite and renewable. Some governments have started encouraging the use of renewables; for example China, Scotland, USA, Germany and the Netherlands

have agreed to set a target of producing 30, 50, 50 and 80%, respectively, of their energy from renewables by 2050 (Martinot *et al.*, 2007). For achieving these targets Roaf *et al.* (2009) acknowledged that buildings will have to integrate renewable systems so that each building would generate its own electricity. Since these systems are small in size, they are called micro-renewables or micro-generation technologies.

According to Bahaj *et al.* (2007) and the Department of Energy and Climate Change (2011c), micro-generation technologies have very high potentials for integration within the built environment not only because they satisfy demand and provide decentralised generation but also to help tackle fuel poverty and achieve reductions in emissions. These technologies include:

- Solar thermal panels
- Solar photo-voltaic panels (PV)
- Ground and air source heat pumps
- Wind turbines
- Hydro (including water mills)
- Combined heat and Power (CHP) units
- Fuel cells
- Heat and power generation from biomass, bio-liquids and biogas including from anaerobic digestion.

Among these technologies, Jha (2010) asserted that it is wind and solar power that offer clean electrical energy with lower installation costs, higher reliability and cost effective installations. They have their own disadvantages, but when compared to the other technologies they have higher potentials of implementation.

1.3.3.1 Governmental incentives for implementing micro-generation technologies

In the UK, the government is actively promoting the usage of micro-renewables after a series of reports have shown that micro-renewables could reduce energy demands from conventional sources of energy by up to 5% (Roaf et al., 2009). In 2004 the energy White Paper and subsequently the UK Energy Act have set the initiative through the Clear Skies Initiative to encourage the installation of

micro-generation technologies by providing grants ranging from £500 to £5000 to houses and schools for agreed contracts of micro-renewables installations (Bahaj et al., 2007). According to the Department of Energy and Climate Change (2011c), in the Energy Statement 2010, the UK government has agreed to roll out of a smart grid which would facilitate the management of the two way flows on the local network which come from the micro-generation systems connected to the grid, which will also require the installation of smart meters.

Such initiatives will encourage the advancement in the micro-generation technology making them cheaper and available for a broad sector of the community and in parallel with energy efficient measures, which would have a significant impact on the overall energy demand in buildings (Bahaj et al., 2007). According to the Micro-generation Strategy (2011c) by the Department of Energy and Climate Change, the UK government is providing a range of financial support measures which would benefit the micro-generation sector such as the Feed In Tariffs (FIT) which is a scheme through which the UK government pays people money for generating their own electricity from renewable sources of energy[1]. Also, the Green Deal policy is designed to transform the energy efficiency characteristics of the UK's existing housing stock through providing financing for households to upgrade their energy efficiency performance, creating dwellings that are more suitable for micro-generation and focussing house owners on the potential to take advantage of green technologies.

Watson et al. (2008) acknowledged that the planning policies adopted by the UK government already recognized the need for providing incentives for installing micro-generation systems, however more work needs to be done in terms of having policies that address not only the economics of these systems but also the risk, aesthetics, the need for planning permission and the availability of well-trained installers.

1.3.3.2 Hurdles facing micro-generation technologies

The deployment of micro-generation technologies within the built environment is challenged by a number of hurdles. Roaf *et al.* (2009) pointed out that these

[1] More details on the FIT will be discussed in chapter two.

new technologies are not favoured by large utility companies because they will not make profits in perpetuity from selling the energy, which explains their reluctance to invest in micro-generation technologies which does not help in reducing these systems prices. In addition, they added that there is a need to re-engineer the UK's energy network to cope with the contributions from the small power stations connected to the grid. Other hurdles facing micro-generation technologies include availability of information on the performance and feasibility of these systems.

According to Hyams (2005), these hurdles can be overcome through a set of mass market transformation initiatives which would include delivering a low carbon buildings programme, developing and deploying products, raising awareness and encouraging action, increasing volume and reducing costs and ensuring fair price. However, Dobbyn and Thomas (2005) acknowledged that this field is lacking research both technically and socially which means that there is a lack of information regarding the feasibility of such systems and that discourages people from installing those systems.

1.3.3.3 Advantages of micro-generation technologies

Being independent of the grid and generating on-site electricity is one of the main advantages of integrating micro-generation technologies within buildings, which also comes with economic benefits for the users. In addition to the financial aspects, Mertens (2006) and Collins (2004) added that micro-generation technologies, and especially micro wind turbines, as they are visually more pronounced, have social significances and implications since they help people engage with the idea of combating climate change which would have a direct impact on their consumption of energy and taking more considerate measures to cut down on energy consumption.

Focusing on the social implications of integrating renewables within the built environment, Dobbyn and Thomas (2005) carried out a research to understand people's motivations to be energy efficient, they found that people's engagement with micro-generation technology had a significant effect on their awareness of climate change and impacted positively their attitudes and behaviours in terms of being energy efficient. They stated that:

'Micro-generation usage had an emotional resonance with the users coming from the element of wonder that in this modern era we can make electricity and heat from such eternal and natural sources as the sun and wind. Householders even described generating their own electricity as growing their own vegetables'.

Although some of the micro-generation technologies implemented in the samples examined by Dobbyn and Thomas (2005) produced very modest levels of energy, yet they acknowledged that the behavioural impacts in terms of energy awareness and efficiency were often still considerable. Accordingly, they stressed on the importance of the qualitative impacts of using micro-generation technologies, presenting a real shift in attitude towards energy consumption. Thus, the results cannot only be measured in terms of power generation but the social implications should always be considered. However, it should be noted that installing micro-generation technologies that would not work as expected, might create a feeling of frustration and promotes a bad reputation of these technologies. Thus, more research is needed to ensure the high performance of these technologies which would even have a better impact on the householder's attitudes and behaviours.

The two main pronounced visual micro-generation technologies that promote the idea of combating climate change are the photovoltaic cells and the micro wind turbines. According to Roaf *et al.* (2009) both technologies complement each other during summer and winter, day and night and can provide buildings with significant power supply throughout the whole year. Hyams (2005), acknowledged that micro wind turbines is one of the technologies that could develop into a market-mature technology applicable for widespread adoption.

1.3.4 *Urban wind energy as part of the solution*

According to the Committee on Climate Change report (2008), renewables, in general, can have a significant contribution to the power sector decarbonisation and wind, in particular, can play an important role knowing that the cost of power from wind has fallen fourfold between 1980 and 2008 and it is expected to continue to fall with the advancement in wind turbines technology. Makkawi *et al.* (2009) stated that the cost of wind generated electricity over the years

from 1980 to 2005 has fallen from 20 to 3.7 eurocents/kWh in large-scale systems and is expected to reach 2.0 eurocents/kWh by 2020.

1.3.4.1 Urban wind turbines market growth

In the RenewbaleUK (2011b) annual report on the small wind systems in the UK, it is shown that the annual deployed capacity from small wind systems rose by a record high of 65% (14.23MW) in the twelve months to December 2010, up from the 8.62MW reported for the end of 2009. Although, these numbers diminish when compared to power generated from large scale wind turbines (a single large scale wind turbine can reach 10MW) (Quick, 2010), that was an unprecedented growth in the installed capacity which brought the UK's total installed small wind capacity to 42.97MW at the end of 2009. The report added that the UK could have 1.3 GW of installed small wind system capacity by 2020, if policies are put in place to support it. RenewableUK believes that the current generation capacity of the small wind sector is only a fraction of what might be possible in the future. It is estimated that if barriers to market growth are adequately addressed by 2020, the UK small wind system sector could generate 1,700 GWh (1.7 TWh) of renewable electricity annually. However, there is a state of uncertainty regarding the feasibility and efficiency of these systems and their contribution in decreasing the emitted greenhouse gases from buildings (Dutton et al., 2005; Mertens, 2006; Stankovic et al., 2009).

1.3.4.2 Uncertainties and growing interest in urban wind turbines

This state of uncertainty could be attributed to the complexity of wind flow around buildings and the involvement of many variables affecting wind flow within the built environment. Anderson *et al.* (2008) pointed out that there is a concern that environmentally conscious homeowners, businesses, local government bodies and other organizations will install rooftop wind systems as a signal of their support for sustainability, but may do so without adequate consideration of safety, structural building integrity or turbine performance. The potential consequence of such projects could be the failure of the project due to issues such as underperforming turbines, noise, and vibration. This would lead to the development of a negative reputation for wind energy and the renewable energy industry which has high potentials in replacing conventional sources of energy.

On the other hand, there is a growing interest among architects and planners in integrating wind turbines into the built environment arguing that this integration ensures the generation of electricity in-situ, resulting in reducing the cost of generation and power losses during transmission. In addition, Stankovic *et al.* (2009) argued that building integrated wind turbines would benefit from the concentration effect buildings have on wind, which means an increased energy yield from the wind turbine. But, Lu and Ip (2009) argued that that the symbolism of integrating wind turbines into buildings is their greatest architectural value and it would not be an efficient source of energy based on the fact that cities and buildings introduce too much turbulence into the wind stream in addition to the low mean wind speed within urban areas. Accordingly, Smith (2005) stressed on the importance of accurately assessing wind resources at the installation site to specify to the highest degree of accuracy the optimum mounting locations.

1.3.4.3 Factors affecting the energy yield of urban wind turbines

Makkawi *et al.* (2009), Jha (2010) and Ledo *et al.* (2011) attributed the limited number of urban wind turbines installations to the low wind velocities, high levels of turbulence and unpredictability of wind in terms of speed and direction due to the presence of buildings and other obstacles. Thus, there is a need for special wind turbines which could withstand such conditions and yield enough power which justifies their installation. They added that small wind turbines manufacturers are neither seen to develop wind turbines that operate under low wind speeds and high turbulence intensities, nor work on accelerating wind before reaching the wind turbine. This explains the modest growth rate of building mounted wind turbines, especially when published experimental results in recent years report low performance of urban wind turbines, although it should be noted that none of these reports stated a clear methodology for choosing the mounting location and whether or not it was the best location for mounting the wind turbine.

Blackmore (2008) and Blackmore (2010) asserted that if a turbine is mounted in the wrong location on a house roof, it is possible for the power output to be close to zero for significant periods of time, even when the wind is blowing strongly. Two famous examples of such practice are the Green Building in

Temple Bar, Dublin and the Kirklees Council Building (civic centre 3) in the town centre of Huddersfield, UK (Kirklees Metropolitan Council, 2006; Anderson *et al.*, 2008)[2]. According to Sara Louise (2011), in order to avoid failure of urban wind turbines, it is important to accurately estimate the potential energy yield of the wind turbine before installation, otherwise the technology may be labelled uneconomic while the main problem is that the turbine is installed at the wrong location.

Also, the relatively low wind velocity in urban areas (less than 5m/s) has a direct impact on the energy yield of urban wind turbines. Mertens (2006) and Jha (2010) argued that if wind turbines is to be used within urban areas, the wind has to be accelerated. Wind speed around taller buildings can be appreciably higher than the average free stream wind speed at the same location under the same flow conditions when compared to a vacant site. A similar effect happens when using a concentrator to concentrate wind flow on a wind turbine. Keeping in mind the accelerating effect of buildings, one should use buildings as concentrators or learn about the accelerating effect of different buildings shapes to correctly position the wind turbine.

1.3.5 *Research aim*

The aim of this research is to identify the effect of different roof shapes covering isolated buildings on the energy yield and positioning of roof mounted wind turbines, in addition to investigating the effect of varying wind direction, building height and surrounding urban configuration on wind flow above the investigated optimum roof shape for mounting wind turbines. In order to achieve the aim of this research a set of hypotheses are tested.

1.3.6 *Research hypotheses (Propositions)*

To identify the effect of varying roof shape, wind direction, building height and urban configuration on the energy yield and positing of roof mounted wind turbines, the following eight hypotheses are tested:

[2] The Green Building in Temple Bar installed three small horizontal axis wind turbines which resulted in excessive noise, vibration, and eventual cracking of the turbine blades. The Kirklees Council Building installed two small horizontal axis wind turbines which failed to deliver the expected performance. More details about the two projects are discussed in chapter two.

- Hypothesis One:

Wind regimes around buildings are different from open fields and require specific wind turbines technology. If existing literature on urban wind flow and developing wind turbines technology are reviewed, a set of criteria can be deduced which sets the guidelines for wind turbines technology to be used near to buildings (This hypothesis is tested in chapter 2).

- Hypothesis two:

For assessing wind flow around buildings, CFD simulations can be used to yield consistent results provided that best practice guidelines are followed and validation is carried out (This hypothesis is tested in chapters 3 and 4).

- Hypothesis three:

One of the main reasons behind the low energy yield of urban wind turbines is the low mean wind speed. The presence of a building in wind flow field would increase the wind speed and turbulence intensity in the vicinity of the building. Integrated wind turbines can take advantage of the accelerating effect that occurs (This hypothesis is tested in chapter 5).

- Hypothesis four:

Studying the variation in wind directions may or may not change the optimum mounting location of a roof mounted wind turbine (This hypothesis is tested in chapter 5).

- Hypothesis five:

For each roof shape there is an optimum mounting location for wind turbines. Thus, by assessing wind flow above each roof shape, the optimum mounting location can be identified and the performance of the integrated wind turbine can be improved (This hypothesis is tested in chapter 5).

- Hypothesis six:

Different roof shapes have different effects on wind flow above them. If wind flow above different roof shapes is assessed, there would be a difference in the

accelerating effect from one roof to another (This hypothesis is tested in chapter 5).

- Hypothesis Seven:

Another variable affecting wind flow above buildings' roofs is the building height. Thus, for a single roof shape, if the height of the building is changed, that would have an effect on the air flow above it (This hypothesis is tested in chapter 5).

- Hypothesis eight:

One of the main variables affecting urban wind flow is the urban setting. Thus, it is assumed that different urban configurations would have different effects on wind flow above buildings' roofs (This hypothesis is tested in chapter 5).

1.3.7 *Research scope*

The scope of this research is to investigate the effect of four main independent variables on the energy yield and positioning of roof mounted wind turbines, these are; roof shape, wind direction, building height and surrounding urban configuration. The study provides a scientific methodology to assess optimizing positioning of wind turbines in urban areas to understand the impact of roof shapes as an architectural feature that, maybe, used to enhance wind turbines' energy yield.

What differentiates this research from previous researches is its study of wind flow around different roof shapes for the purpose of integrating wind turbines, thus choosing the optimum roof shape among the studied shapes and the optimum mounting location for each roof shape.

1.3.8 *Limitations*

Computational Fluid Dynamics (CFD) is the tool used for assessing wind flow around the investigated cases in this research. As will be demonstrated in chapter three, different CFD techniques can be used to assess wind flow problems. One of the factors affecting the choice of the CFD technique is the available computational power. According to the available computational power, one of the Reynolds Average Navier Stokes models (RANS), namely the

Realizable *k-ε* turbulence model, has been used which yields reliable results with relatively low computational requirements. However, it should be acknowledged that other techniques such as using Direct Numerical Simulations (DNS), Large Eddy Simulation (LES), Detached Eddy Simulation (DES) or Unsteady RANS, which are known for yielding more consistent results, could have been used if more computational power was available.

Since CFD is an approximation of reality, validation studies are needed to give confidence in the simulation results. As will be discussed in chapter three, there are several techniques for validating the CFD simulation results, one of the most commonly used validation methods is to compare the results with wind tunnel tests results or in-situ measurements. However, since the investigated cases are hypothetical, in-situ measurements cannot be adopted. Thus, running simulation for a certain case and comparing it with a wind tunnel test was adopted. However, a wind tunnel was not available for the researcher. Thus, for overcoming this limitation, the CFD simulations results were compared with published wind tunnel tests for a certain flow case which is common practice in similar researches as will be demonstrated later in this chapter under the validation section (1.4.7), a detailed validation study is carried out in chapter four.

1.3.9 *Significance of the study*

The research hypotheses are derived from theory linking urban wind flow to buildings' shapes and their effect on the performance of urban wind turbines. From the types of integration of wind turbines within the built environment, this research focuses on the roof mounted wind turbines. Thus, the roof shape is the main independent variable to be investigated in this research. Allen *et al.* (2008a), Allen *et al.* (2008b), Peacock *et al.* (2008), Sara Louise (2011) and Balduzzi *et al.* (2012) assessed the performance of urban roof mounted wind turbines based on the energy yield of the installed wind turbine and argued that urban wind turbines are not the best option for in-situ power generations.

However, these researches ignored acknowledging the adopted methodology for assessing and specifying the optimum mounting location for roof mounted wind turbines; changing the mounting location on the same roof can affect the

energy yield of the integrated wind turbine which is one of the hypotheses that will be examined in this research to assess the range of difference in the energy content at different locations above the same roof. Assessing and comparing the energy content at different locations above the investigated roof shapes will help determine the optimum mounting location of a wind turbine.

Thus, this research builds on previous research investigating urban wind flow to cover the gap of specifying the mounting location of roof mounted wind turbines for different roof shapes and determining the optimum roof shape for mounting wind turbines. This is studied under different wind directions, within different urban configurations for different buildings heights. Comparative assessment is undertaken to study the accelerating effect for each roof shape and its effect on the increase in the energy yield of the roof mounted wind turbine compared to a free standing wind turbine at the same location and under the same flow conditions. In doing so, this research tests and sets the guidelines for using CFD as a tool for assessing wind flow within the built environment. The investigation carried out in this research can be extended to understand pedestrian wind comfort, wind loads structural analysis, pollutant dispersion in street canyons and natural ventilation.

1.4 Research methodology

1.4.1 *Research methodologies for assessing wind flow around buildings*

Research in this area generally adopts a scientific approach implementing certain tools for assessing wind flow around buildings through measuring different flow variables such as wind velocity, turbulence intensity, turbulent dissipation rate and pressure coefficients. The main aim behind assessing such variables varies between studying natural ventilation inside buildings, wind loads structural analysis, pollutant dispersion in street canyons or integrating wind turbines within the built environment. In doing so, researchers mostly use one or more of three tools for assessing wind flow, these are in-situ measurements, wind tunnel tests and computational fluid dynamics (CFD).

Van Hooff *et al.* (2011) used a CFD code (Fluent 6.3.26) for studying wind driven rain in stadia. CFD was used for simulating and comparing wind driven rain (WDR) over twelve different generic stadium configurations that are

representative for a wide range of existing stadia. They assessed the WDR through wind flow patterns horizontally and vertically and visualizing rain drops through rain drops trajectories to finally visualise the wetting areas in the stadium. For validation, they depended on previous studies recommending using certain simulation conditions to get reliable results, they argued that using those conditions would lead to accurate CFD simulations. The main reason of using CFD as the tool for generating data in their research was the freedom CFD offers for comparing design alternatives in addition to the visualization capabilities of CFD which is similar to what is investigated and needed in this research as will be demonstrated in chapter three when reviewing the potential tools for assessing wind flow within the built environment.

In a similar study to assess pedestrian wind comfort around a large football stadium in Amsterdam, Blocken and Persoon (2009) used the CFD code Flunet 6.3.26. However, since the stadium was already built, they compared the numerical simulation results with full-scale measurements of mean wind speed at the designated points of investigation. A similar approach is adopted in this research when comparing the obtained results with published in-situ measurements for validation purposes.

Ledo *et al.* (2011) used the CFD code CFX to simulate wind flow above different roof shapes (pitched, pyramidal and flat roofs) to determine the optimum roof mounting location for each roof shape under three different wind directions (0, 45 and 90 degrees). In order to determine the optimum mounting locations, they studied the flow patterns, measured the turbulence intensity and the streamwise velocity at 3 different locations and normalized the values against reference values to determine the change in the flow variables. They validated the CFD simulations by comparing their results with published wind tunnel tests. One of the recommendations of their research is to extend the study to include other roof shapes which is being investigated in this research. In addition, the validation method used in their research could be implemented in this research as will be discussed in chapter four in the validation study.

In another research, Liu *et al.* (2010) implemented the CFD code Fluent 6.1 in studying the effect of airport building's wake on landing aircrafts, they simulated air flow around a hypothetical Y-shaped building under four different wind

directions (0, 22.5, 45 and 60 degrees). They measured the wind velocity along the landing location of the aircraft under different wind speeds, which is similar to what is proposed in this research in terms of comparing the effect of changing wind direction on wind flow above the investigated roof shapes. The CFD simulation results were validated against a set of published wind tunnel tests' results for wind flow around an isolated high-rise building. The adopted validation technique is similar to what Ledo *et al.* (2011) did in their research and would be considered for this research.

In their investigation to study the feasibility of wind power utilization in local urban areas, Lu and Ip (2009) used the CFD code Fluent to simulate wind flow around buildings with different heights, having different spacing between them and covered by different roof shapes (flat and pitched). Both the turbulence intensity and the wind velocity were recorded to determine the best location for mounting wind turbines. However, they did not carry out any other studies to validate the CFD simulation results. But they acknowledged the importance of investigating the turbulence intensity and the wind velocity as the main flow variables affecting the energy yield of the integrated wind turbines.

Huang et al. (2009) investigated the effect of wedge-shaped roofs on wind flow and pollutant dispersion in a street canyon using the CFD code Fluent. They performed a validation study first for a two-dimensional CFD model of a street canyon by comparing the CFD results with published wind tunnel tests, then they used the same conditions for assessing wind flow and pollutant dispersion in urban street canyons of sixteen different wedge-shaped roof combinations by plotting and analysing air velocity vectors and dimensionless pollutant concentration contours inside the urban street canyons. However, it should be noted that studying three dimensional flows is different from two dimensional flows as the flow in reality is in three dimensions and using two dimensional simulations is not considered realistic except for specific flow problems.

Other researchers (Lee and Evans, 1984; Summers *et al.*, 1986; Paterson and Apelt, 1989; Baskaran and Kashef, 1996; He and Song, 1997; Rafailidis, 1997; He and Song, 1999; Theodoridis and Moussiopoulos, 2000; Sun and Huang, 2001; Tutar and Oguz, 2002; Tutar and Oğuz, 2004; Zhang *et al.*, 2005; Blocken and Carmeliet, 2006; Ricciardelli and Polimeno, 2006; Blocken *et al.*,

2007a; Huang *et al.*, 2007; Grant *et al.*, 2008; Jiang *et al.*, 2008) adopted the same approach of using a wind assessment tool for assessing wind flow within the built environment, then using another tool for validating the results. It is noticed that in most of the cases where a comparison between different alternatives is carried out, CFD was used and then one of the cases is compared to wind tunnel tests whether performed by the researcher or cited in literature. In the cases where the buildings existed, in-situ measurements were carried out and compared to the wind tunnel tests or CFD simulations. A more detailed review of the techniques used for assessing wind flow around buildings is discussed in chapter three. And more on the validation is discussed in this chapter in section (1.4.7) and in chapter four.

1.4.2 *Proposed methodology*

Ontologically, this research has foundational assumptions about wind flow within the built environment and generating electricity from wind power, thus the foundational scientific approach is adopted to test and refute the hypotheses and reach the main aim of the research. For reaching the main aim of the research, existing literature on the topic is critically reviewed discussing different types of integration of wind turbines in buildings. Wind turbines have different types based on their technology and the way in which they are integrated within the built environment. Advantages and disadvantages of each type of integration are investigated to determine which type of integration and technology are more relevant to the built environment. Variables affecting wind flow within the built environment are deduced from investigating literature in the field (Chapter two).

Literature on the available tools for assessing wind flow within the built environment is investigated to identify the advantages and disadvantages of each tool, and accordingly, decide upon the relevant tool to be used in this research (Chapter three). The tool used in this research to assess wind flow above different roof shapes is the CFD code Fluent 12.1 which is used as the experimentation tool to generate data for statistical analysis. The rationale behind choosing CFD is discussed in more details in chapter three and the reasons behind choosing Fluent software is discussed in this chapter under section 1.4.6. However, as CFD simulations are approximations of the real

scenarios, they have to be validated by comparing the results with the results of another wind assessment tool. Thus, a detailed validation study is carried out in chapter four. An overview of the validation study is outlined in this chapter under section 1.4.7.

After validating the CFD simulation results, the simulation conditions used for the validation study are used for assessing wind flow above six different roof shapes covering a six meters cube isolated building. Flow characteristics are assessed through plotting the flow patterns around the studied shapes and measuring the turbulence intensities and streamwise velocities and normalizing them at different locations above the roofs. The collected data is parametrically analysed and compared to each other to determine the effect of different roof shapes on wind flow above them under different wind directions. More details on the simulation conditions, results, flow variables and measurements locations are discussed in chapter five.

Simulations are carried out to identify the optimum mounting location above the investigated roof shapes. Comparing the results, the optimum roof shape for roof mounting wind turbines is identified. The optimum roof shape is then investigated further by covering isolated buildings of different heights to identify the effect of height on wind flow above the designated roof shape. Since the hypothetical isolated building scenario is not the most commonly encountered scenario within reality, the investigation is carried further to include assessing wind flow above the optimum roof shape covering different buildings' heights placed within different urban configurations. Accordingly, the effects of height and urban configurations on wind flow above the investigated roof shape are identified (chapter five). These results are interpreted in terms of energy yield of installed wind turbines to determine the feasibility of the accelerating effect of different roof shapes. Thus, the increase in the wind velocity is transferred into an increase in wind energy to identify the potential increase in energy yield for the proposed roof mounted wind turbine.

1.4.3 *Variables affecting wind flow within the built environment*

Existing literature on the integration of wind turbines within the built environment focused on three distinct strands of research, which represent the main three stages for integrating wind turbines within the built environment;

- The first strand focussed on the tools used for assessing wind flow within the built environment such as in-situ measurements, wind tunnel tests, and Computational fluid dynamics (CFD) simulation techniques.
- The second strand is related to the types of integrating wind turbines within the built environment. Four types of integration are identified; building integrated wind turbines, building mounted wind turbines, building augmented wind turbines and ducted wind turbines.
- The third strand focused on the feasibility of integrating wind turbines within the built environment in terms of environmental, economical and social aspects.

Researches across these strands present key variables to be considered by the design team when considering the integration of wind turbines within the built environment. It is also noteworthy mentioning that reviewed literature acknowledged the complex nature of the built environment in terms of the existence of many variables affecting wind flow within the built environment. It is noticed that those variables would fall under three main categories; these are

- Building geometry.
- Surrounding urban context.
- Characteristics of gusting wind.

The rationale behind choosing the variables to be investigated differed from one research to another. However, they would fall under the following categories:

- Either the cases were representing a built case study,
- Or, it was argued that those were the most encountered cases in the built environment,

- Or, the purpose was to keep most of the variables constant for investigating other computational variables in CFD,

- However most of the cases were investigating hypothetical cases.

Examples of these researches include Kindangen *et al.* (1997) who compared the effect of variation in roof shapes on wind flow inside buildings (not around them). Peter *et al.* (2008) discussed changing building geometry in terms of buildings' corners modifications and whole building form on wind flow, but the research was discussing general potentials of form modification without making any tests to investigate the validity of these assumptions. Mertens (2006) investigated and compared basic buildings' forms and their effect on wind flow, but the main aim of the research was to determine the right type of wind turbine to be integrated in the investigated cases.

It is noticed that most of the reviewed researches investigated the variation in only one variable or the interaction between two variables while keeping all other variables constant. According to Kim and Kim (2009) and Stankovic *et al.* (2009) this is attributed to the complex nature of the built environment due to the variety in building morphology which make these studied cases some of other options that could be investigated. Thus, the studied geometrical variables in literature are simplifications of existing geometries within the built environment. In other words, the investigated cases simplify the complex nature of the built environment that may affect wind flow. However, this approach is accepted for understanding wind flow around certain geometrical forms in the absence of other variables.

1.4.4 *Proposed investigated variables*

Since the main concern of this research is the energy yield of roof mounted wind turbines, literature is reviewed for determining the variables affecting the energy yield of roof mounted wind turbines and thus deduce the variables to be investigated in this research. In literature, studying wind flow around buildings was primarily undertaken for purposes other than integrating wind turbines within the built environment (Kindangen et al., 1997; Asfour and Gadi, 2008; Ayata, 2009; Huang et al., 2009). Also, Sara Louise (2011) acknowledged that very little CFD work has been undertaken to consider wind flow at immediately

above roof height, for applications of building mounted wind turbines. Thus, there is a gap in existing literature on investigating urban wind flow above different roof shapes for the purpose of integrating wind turbines.

Of the limited body of research on urban wind flow in relation to roof mounting wind turbines, Ledo *et al.* (2011) studied wind flow around different roof shapes namely; pitched, pyramidal and flat roofs under three wind directions, they concluded that the power density above the flat roof is greater and more consistent than above the other roof types and they asserted the importance of extending the investigation to include other roof shapes. Mertens (2006) analysed flow over a flat roof with a view to developing small wind turbine sitting guidelines focusing on the mounting height and stressed on the importance of the effect of roof shape on specifying where to mount the wind turbine. Phillips (2007) investigated the mounting location for a single wind direction for a gabled roof and recommended extending the investigation to include more roof types and more locations under different wind directions.

In addition, according to a study by the Department of Energy and Climate Change (2011b), for building mounted wind turbines, the main factors affecting wind speed are the geographic location, nearby obstructions such as buildings and trees, the height of the turbine above ground level and the roof shape on which the turbine is mounted. Other publications (Rafailidis, 1997; Dutton et al., 2005; WINEUR, 2007; Blackmore, 2008; Mithraratne, 2009; Sievert, 2009) also asserted that one of the main factors affecting the success of roof mounted wind turbines is the roof shape. Which is similar to what Lu and Ip (2009) acknowledged when they investigated the feasibility of wind power utilization in high-rise buildings in Hong Kong; they asserted that studying the wind concentration effect due to buildings' heights and optimal roof shape can increase the feasibility of urban wind turbines. Accordingly, this research argues that due to the complex nature of the built environment, many variables affect wind flow around buildings. The investigated independent variables in this research are roof shape, wind direction, building height and surrounding urban configuration.

1.4.4.1 The selection of the roof shape variable

Since the roof mounted wind turbine is one of the most popular types of integrating wind turbines within the built environment, it is important to understand the aerodynamics of different roof shapes and their effect on wind flow above them. Thus, the main variable to be investigated in this research affecting the energy yield and positioning of roof mounted wind turbines is the roof shape. Unless the investigated roof is a real built case, one can notice the simplification that takes place for different investigated roof shapes for hypothetical cases. Looking into the built environment, one can notice the various configurations of roof shapes, some of them are pure geometrical forms covering isolated buildings and some are a combination of several geometrical forms. Due to the complexity of the second type and being case specific, it is noticed that existing research focuses on pure geometric forms unless a specific case is being studied.

For the selection of roof shapes to be investigated in this research, the literature review indicates that the mostly investigated roof shapes are:

- Flat roofs (He and Song, 1997; Rafailidis, 1997; Kastner-Klein and Plate, 1999; Kastner-Klein et al., 2001; Richards et al., 2001; Richards and Hoxey, 2004; Richards and Hoxey, 2006; Heath et al., 2007; El-Okda et al., 2008; Richards and Hoxey, 2008; Ayata, 2009; Lu and Ip, 2009; Tominaga and Stathopoulos, 2009; Cheung and Liu, 2011; Hang et al., 2011; Ledo et al., 2011; Mahmood, 2011; Pindado et al., 2011; Zhang et al., 2011; Balduzzi et al., 2012),
- Gabled roofs (Lee and Evans, 1984; Kindangen et al., 1997; Rafailidis, 1997; Kastner-Klein and Plate, 1999; Theodoridis and Moussiopoulos, 2000; Heath et al., 2007; Ayata, 2009; Ledo et al., 2011; Balduzzi et al., 2012),
- Wedged roofs (Kindangen et al., 1997; Kastner-Klein and Plate, 1999; Huang et al., 2009; Lu and Ip, 2009),
- Pyramidal roofs (Kindangen et al., 1997; Ledo et al., 2011),
- Barrel vaulted roofs (Kindangen et al., 1997; Asfour and Gadi, 2008) and
- Domed roofs (Asfour and Gadi, 2008).

However, wind flow above these shapes was not investigated for the purpose of specifying the mounting location of roof mounted wind turbines or comparing them for the purpose of identifying the optimum roof shapes for mounting wind turbines. None of the reviewed researches compared the effect of these roof shapes on the energy yield and positioning of roof mounted wind turbines. Thus, the investigated roof shapes in this research are the flat, domed, gabled, pyramidal, barrel vaulted and wedged roofs. Wind flow above these roof shapes is assessed to determine the best mounting location above each of them and the optimum roof shape among them for mounting wind turbines.

1.4.4.2 The selection of the wind direction variable

Another independent variable which affects wind flow around buildings is the direction of the incident wind. For specific case studies, the prevailing wind is used as the incident wind direction, as for hypothetical cases a variety of incident wind directions can be studied depending on the objective of the investigation. One of the hypotheses in this thesis is that wind direction would have an effect on wind flow above the investigated roof shapes, thus affecting the decision about the optimum mounting location for each roof shape and the optimum roof shape for mounting wind turbines. Accordingly, there is a need for coupling the wind direction with roof shape to identify their effects. And since the investigated roof shapes do not have the same axes of symmetry, different wind directions are investigated for different roof shapes. Generally, five wind directions are investigated, representing all possible main directions of wind:

- 0 degree,
- 45 degrees,
- 90 degrees,
- 135 degrees and
- 180 degrees.

1.4.4.3 The selection of the height variable

According to the Department of Energy and Climate Change (2011b) the height of the building and the mounting location also affects the performance of a roof mounted wind turbine. Thus, the height of the building is one of the independent variables that should be investigated to determine its effect on the energy yield

and positioning of roof mounted wind turbines. In the first set of simulations, the investigated roof shapes covered a cubical building of height 6m, then the wind flow around the investigated roof shapes is assessed and the optimum roof shape for mounting wind turbines is determined under various gusting wind directions. For investigating the effect of the building height, the optimum roof shape is used for investigating the effect of the building height by doubling the height to reach 12m, then doubling it again to reach 24m while assuming the gusting wind to be parallel (0 degree) to the roof profile. Thus the investigated building's heights are:

- 6 meters,
- 12 meters and
- 24 meters.

1.4.4.4 The selection of the surrounding urban configuration variable

Although the isolated building scenario is encountered in rural areas where the need of renewables is more pronounced since these places are most likely not to be connected to the grid (Lee and Evans, 1984; He and Song, 1997; Kindangen et al., 1997; Richards et al., 2001; Richards and Hoxey, 2004; Richards and Hoxey, 2006; Heath et al., 2007; Asfour and Gadi, 2008; El-Okda et al., 2008; Richards and Hoxey, 2008; Tominaga and Stathopoulos, 2009; Cheung and Liu, 2011), this is not always the case within cities were buildings are within certain urban contexts. Thus, it is important to investigate the optimum roof shape covering different buildings' heights placed within different urban configurations. Most of the researches investigating urban wind flows focused on two main configurations, these are:

- Urban canyon configuration (Kindangen et al., 1997; Rafailidis, 1997; Kastner-Klein and Plate, 1999; Theodoridis and Moussiopoulos, 2000; Kastner-Klein et al., 2001; Cheng et al., 2003; Pospisil et al., 2005; Xiaomin et al., 2006; Ayata, 2009; Huang et al., 2009; Lu and Ip, 2009; Cheung and Liu, 2011; Hang et al., 2011; Ledo et al., 2011; Zhang et al., 2011) and
- Staggered urban configuration (Heath et al., 2007; Swaddiwudhipong et al., 2007; Cheung and Liu, 2011; Mahmood, 2011).

Other cases include more specific configurations, where the exact configuration is modelled for specific projects which is either, urban canyon, staggered or a random configuration (Zhang et al., 2005). However, the mostly studied configuration in literature is the urban canyon configuration. Thus, in this research the investigated building is placed within both configurations (urban canyon and staggered) to determine the effect of placing the building within different urban configurations and identify different effects of different urban configurations on the energy yield and positioning of roof mounted wind turbines. The difference in heights is also investigated in this part where the effect of surrounding urban configuration is investigated, this is done through using the same previously mentioned heights (6m, 12m and 24m), in addition to reducing the height of the investigated building in one of the cases to reach 4.5m which is 1.5m lower than the surrounding proposed urban configurations whose buildings heights are 6m.

After investigating the four independent variables (roof shape, wind direction, building height and surrounding urban configuration) and their effect on the energy yield and positioning of roof mounted wind turbines, the collected empirical data from the simulation work is collected and compared to formulate laws about the role of these variables in the energy yield and positioning of roof mounted wind turbines.

1.4.5 *Unit of measurement (flow variables)*

According to Tong (2010) the energy yield of a wind turbine is dependent on the performance coefficient of the wind turbine, the density of the air, the swept area of the turbine and the mean wind velocity. Tong (2010) added that the wind velocity is the main factor affecting the energy yield of a wind turbine since the energy yield is directly proportional to cube the wind velocity. On the other hand, the roof shape affects the wind velocity around the integrated wind turbine, thus for assessing the effect of different roof shapes on the energy yield of the integrated wind turbine, the wind velocity has to be measured at different locations to identify the accelerating effect that happens when wind hits different roof shapes.

However, it is evident that high levels of turbulence are not preferable for the operation of wind turbines, thus another flow variable that needs to be measured is the turbulence intensity in the vicinity of the investigated roofs (Glass and Levermore, 2011). In addition to quantitatively measuring these two flow variables, visualizing the flow patterns through streamwise velocity pathlines around the investigated roof shapes can help in understanding, qualitatively, wind flow around different roof shapes.

Thus, flow patterns are plotted and streamwise velocities and turbulence intensities are measured at different locations above the investigated roof shapes using a Computational Fluid Dynamics (CFD) simulation technique. Results from the CFD simulations are recorded and analysed to determine the optimum roof shape for mounting wind turbines and where on top of each roof shape is the optimum location for mounting a wind turbine. However, in order to assess the accelerating effect that happens when wind hits different roof shapes, the flow variables values are normalized against the values at the same locations under the same flow conditions without the buildings in the flow field. More details about the simulation conditions, measurement location, recorded flow variables and normalizing the recorded values is included in chapter five.

1.4.6 *Proposed wind assessment tool*

According to Paterson and Apelt (1989) and Mertens (2006) the research tools used to understand wind flow within the built environment can be divided into: in-situ measurements, wind tunnel tests and simulation tools based on computational fluid dynamics (CFD) calculations. All of these tools have specific advantages and drawbacks that define the suitability of the tool for a certain analysis. Existing research in this area (Mochida et al., 1997; He and Song, 1999; Murakami et al., 1999; Campos-Arriaga, 2009) favoured wind Tunnel tests and CFD modelling over in-situ measurements for reasons that are discussed in more details in chapter four. However, when comparing wind tunnel tests to CFD simulations, Blocken and Carmeliet (2004) and Chen (2004) argued that CFD simulation can provide an alternative for wind tunnel studies because CFD is less time consuming, less expensive than wind tunnel tests and it is easy to visualize the detailed wind flow within the domain of study. Also CFD has been used for simulating wind flow since the 70s and validated by

researchers as mentioned by Jiang *et al.* (2008) who asserted that CFD simulations agree well with wind tunnel tests in the flow field and wind pressure distribution around buildings and is the most relevant tool for comparing alternatives.

This research involves investigating 27 different wind flow cases, which makes using a wind tunnel impractical due to time and resources limitations. Thus, CFD is used as the wind assessment tool in this research. CFD simulation in this context replaces laboratory testing and full-scale measurements. According to Spalding (1981), the first commercially available CFD code created for general purpose flow problems is PHOENICS. Moving on to the 90s and with the fast advancements in computer technology, many commercial CFD codes entered the market (e.g. Fluent, CFX, STAR-CCM+, FLOW3D, FloVENT, OpenFOAM) and many large consulting firms started using the commercial CFD codes in different applications such as natural ventilation, air flow around buildings, thermal performance of buildings, pollutants dispersion in urban areas, etc. (Hu, 2003; Campos-Arriaga, 2009). Thus, choosing from the available CFD simulation programmes is not straight forward, since almost every software developer argues that their software is the most reliable. This necessitates validating CFD code results before using CFD software for a certain flow problem, the code results should be validated by comparing it with the results of other wind assessment tools which is the main focus of chapter four.

Vardoulakis *et al.* (2011) assessed the performance of four CFD codes; CHENSI, MIMO, VADIS and FLUENT, through simulating wind flow around an isolated single-block building and comparing the results with experimental data, they acknowledged the consistency of the results among the four codes. Herzog *et al.* (2012) compared the results of three CFD codes namely Fluent, MFIX and OpenFOAM with numerical and experimental data existing in the literature for a gas-solid flow problem and they concluded that both Fluent and MFIX yielded better results than OpenFOAM. In their study to validate the CFD code CFX4, Houkema *et al.* (2008) acknowledged that the predictions of CFX4 for a condensation problem were consistent.

In a study by Tominaga *et al.* (2004) to assess the wind environment at pedestrian level around a high-rise building within a building complex using four different CFD codes namely STREAM 2.10, STAR-LT 2.0, Homamde and Fluent 5.0, they acknowledged that all the codes were able to predict the distribution of the scalar velocity at pedestrian level within the actual building complex in reasonable agreement with the measurements except for the wake region and the region far from the target buildings. It is noticed that among the available CFD codes, it is Fluent that is mostly used, Lu and Ip (2009) attributed this to the variety in turbulence models provided by Fluent which makes it one of the first options when considering wind flow problems. In addition to having been validated by many researchers. Accordingly, Fluent software is the chosen CFD code in this research.

1.4.7 *Validation*

Validation studies are essential to give confidence in the CFD simulation results. Reviewing literature, one can notice that validating the CFD simulation results can be done through comparing the results with in-situ measurements or wind tunnel tests. Blocken *et al.* (2010) asserted that in-situ measurements are not often available when studying hypothetical cases. As for real built cases, Blocken and Persoon (2009) asserted that it is preferable to use this validation technique. Thus, for hypothetical cases, it would be convenient to use simple forms and configurations which resemble the main expected flow features around the studied buildings. Such simple cases are widely available in literature, thus decreasing the uncertainties about the CFD simulation. However, for comparing alternatives, it would be impractical to compare each single case with wind tunnel tests as this requires building several scaled models which is uneconomic and time consuming, this is why Huang *et al.* (2009), Liu *et al.* (2010), Ledo *et al.* (2011) and others compared one of their studied cases with published wind tunnel tests.

Other researchers such as Lu and Ip (2009) and Van Hooff *et al.* (2011) suggested that using the CFD code with a certain combination of computational settings and parameters would lead to accurate CFD simulations. It can be added to that, that this might be true provided that those settings and parameters would have been implemented for similar flow problems and

validated with one of the other wind assessment tools. These computational settings and parameters are discussed in more details in chapter three. However, it can be argued that these conditions cannot be generalised on all flow problems as the locations were the flow variables needs to be studied would dictate, for example, which turbulence model to be used to yield consistent results.

Thus, for the validation study in this research a combination of the conventional way of validating CFD simulation results by comparing the CFD results with published wind tunnel tests and the implementation of a set of computational settings and parameters are both implemented. In chapter three a detailed investigation of literature on CFD is discussed and a set of computational settings and parameters are deduced to be implemented in the validation study and then in the operational part of this research. These parameters can be considered as best practice guidelines for using CFD in similar flow problems.

After specifying these parameters, one of the roof shapes is used as the base case and simulation results are compared to published wind tunnel tests, in-situ measurements and validated CFD simulations. The flat roof case (the cube) was chosen for the validation study since a 3D cube immersed in a turbulent channel flow is the most widely studied flow problem in wind engineering. This is due to the simplicity of the shape and the complexity of flow phenomena around the cube (Castro and Robins, 1977; Ogawa *et al.*, 1983; Martinuzzi and Tropea, 1993; Hussein and Martinuzzi, 1996; Lakehal and Rodi, 1997; Richards *et al.*, 2001; Richards and Hoxey, 2002; Schmidt and Thiele, 2002; Cheatham, 2003; Richards and Hoxey, 2004; Gao and Chow, 2005; Richards and Hoxey, 2006; Richards *et al.*, 2007; Richards and Hoxey, 2008; Ariff *et al.*, 2009a; Ariff *et al.*, 2009b; Lim *et al.*, 2009).

Flow patterns along the horizontal and vertical central plans are plotted, in addition to measuring the pressure coefficients along designated points. Then, the simulation results are compared with the published wind tunnel tests results, in-situ measurements and validated CFD simulations results to assess the accuracy and consistency of the simulation results. More details of the validation process and choosing the simulation variables are discussed in chapters three and four.

1.4.8 *The operational framework*

After having confidence in the specified CFD simulation parameters and conditions through the validation study, those conditions and parameters are implemented in the operational part of this research. This operational part is based on analysing data from four sets of simulations:

- The first set of simulations aims to assessing wind flow above six different roof shapes namely; flat; domed; gabled; pyramidal; barrel vaulted and wedged roofs. The wind flow above these roof shapes is assessed through plotting the streamwise velocity pathlines. To investigate the effect of wind direction, simulations were run with different wind directions (0, 45, 90, 135 & 180 degrees) and flow variables namely; turbulence intensities and streamwise velocities where recorded above the investigated roofs.
- The optimum roof shape for mounting wind turbines is determined based on the highest recorded streamwise velocity among all locations above all the roofs. Since it is hypothesised that the building height and the surrounding urban configuration would have an effect on wind flow above buildings, the optimum roof shape is then used to cover buildings of heights 12 and 24 meters respectively and the simulations are run again with wind direction parallel to the roof profile (second set of simulations).
- Then, the identified optimum roof shape for roof mounting wind turbines is used again to cover buildings of height 4.5, 6, 12 and 24 meters and placed within an urban canyon configuration (third set of simulations)
- The previous set of simulations are repeated again but with the buildings placed within a staggered urban configuration (fourth set of simulations) of an array of 6 meter cubes and simulations are run to assess the effect of the surrounding urban context and building height on wind flow above the studied building.

Results are then compared to identify the effect of the independent variables (roof shape, wind direction, height, and urban context) on the dependant variable (streamwise wind velocity). Accordingly, calculations are made to demonstrate the difference in the energy yield between a free standing wind

turbine and a roof mounted wind turbine at the same location under the same flow conditions.

1.5 Research structure overview

This research is divided into three main sections: The first section of the research, which is this chapter, constitutes the conceptual framework of the research focusing on the research design, methodology, structure and thesis chapters' overview. The second section is the theoretical part of the research which includes the investigation of existing literature in light of different factors affecting the performance of urban wind turbines. Section three and the final part of the thesis focuses on the validation study and the CFD simulations of different wind flow cases, comparing them to each other leading to the conclusion of the research and recommendations for future work.

1.5.1 *Chapter one: Introduction and methodology*

The first chapter has explained the conceptual framework for the research focusing on the rationale behind the study, the argument and the relevance of the study derived from the importance of renewable sources of energy, particularly urban wind energy and its advantages. The introduction, aim, hypotheses, objectives, limitations, propositions and significance of the thesis were discussed. Accordingly, the methodology of the research was outlined.

1.5.2 *Chapter two: Wind turbines technology and their integration in buildings*

Chapter two focuses on investigating the basic concepts of wind energy, wind turbines and the hurdles facing the implementation of wind turbines within the built environment. This chapter covers literature on wind turbines technology and aims to providing a critical review of available and developing wind power technologies. Thus, it is divided into three main sections: The first section covers the basics of wind power including the available and extracted power from the wind, different classifications of wind turbines, latest implemented technology in wind turbines and the hurdles facing large scale wind power. The second section focuses on urban wind energy and how it can overcome some of the hurdles facing large scale wind turbines, this section focuses on

understanding wind flow within the built environment for the purpose of exploiting urban wind through small and micro-scale urban wind turbines. Section three focuses on different types of integrating wind turbines within the built environment, highlighting previous attempts to integrate wind turbines within the built environment and the reasons behind their success or failure. This section concludes by reviewing different factors affecting the feasibility of urban wind turbines. Finally the chapter concludes by summarising the key discussed points focusing on the key aspects to be considered when integrating wind turbines within the built environment in terms of the optimum technology and location.

1.5.3 *Chapter three: Urban wind assessment tools*

Urban wind turbines have high potentials provided that a proper assessment of wind resources at the installation site is undertaken. This chapter focuses on investigating the available urban wind assessment tools with the aim of choosing the most relevant wind assessment tool to be used in this research through identifying the advantages and disadvantages of each wind assessment tool and the relevance of each tool for implementation in this research. Thus, this chapter is divided into three main sections; the first section focuses on the effect of macro and micro-scale wind conditions on wind flow at the installation site. The second section focusses on investigating the available wind assessment tools for assessing wind flow within the built environment through identifying their advantages and disadvantages and the fields of application for each, in addition to the relevance of each tool for implementation in this research. The third section discusses in more depth the proposed tool to be used in this research and the different variables to be considered when using that tool to yield reliable results. The chapter concludes by specifying the main criteria to be considered when choosing a tool for assessing urban wind flow, in addition to recommendations regarding choosing the variables for the tool to be used in this research for assessing urban wind flow.

1.5.4 *Chapter four: Validation study: Wind flow around a cube in a turbulent channel flow*

Having concluded the best practice guidelines and the most relevant CFD simulation conditions for this thesis in chapter three, those simulation conditions need to be validated before starting the simulation for the different cases studied in this thesis. For validation purposes the results for CFD simulation of wind flow around a cube in a turbulent channel flow is compared to published in-situ measurements, published wind tunnel tests results and other validated published CFD simulations results. Thus, this chapter is divided into two main sections: the first section critically reviews literature on in-situ measurements of wind flow around a cubic building, wind tunnel tests of wind flow around a cube in a turbulent channel flow and validated CFD simulations of the same flow problem. In doing so, main flow features are discussed qualitatively and quantitatively in terms of streamwise velocities in horizontal and vertical plans, reattachment length, stagnation point location, separation locations and pressure coefficients along the surfaces of the cube. The second section focuses on reporting the CFD simulation results of the same flow problem using the best practice guidelines for running CFD simulations extracted from literature, in addition to explaining the process of specifying the simulation variables such as achieving a horizontally homogeneous atmospheric boundary layer (ABL) profile and choosing the optimum computational mesh through a mesh independence study. In light of the previously reviewed literature, the chapter concludes by assessing the used simulation variables and their relevance for usage in the rest of this research.

1.5.5 *Chapter five: Wind direction, roof shape, building height and urban context effect on the energy yield and positioning of roof mounted wind turbines*

This chapter focuses on studying different wind directions around different roof shapes covering different buildings' heights within different urban configurations. The chapter is divided into three main sections; the first section gives an overview of roof mounting wind turbines, the second section reports the wind flow problems settings in terms of simulations variables, roof shapes, buildings' dimensions, wind directions and urban configurations, the third

section reports the investigated flow variables for the investigated flow problems and is subdivided into three subsections; the first sub-section reports the results of different wind directions for the investigated roof shapes, the second sub-section reports the results of varying the height of the chosen optimum roof shape and the last subsection reports the results of varying the height of the optimum roof shape when placed within different urban configurations. The chapter concludes by reporting the optimum mounting location for each of the investigated roof shapes, the optimum roof shape for mounting wind turbines, the effect of height on wind flow above the roof and the effect of different urban configurations on wind flow above the optimum roof shape.

1.5.6 *Chapter six: Conclusions and future work*

Chapter six concludes the results of the comparative analysis focusing on the effect of different roof shapes on wind flow around roof mounted wind turbines in terms of the energy yield and positioning of roof mounted wind turbines. Also, the effect of different wind directions, changing heights and placing the building within different urban configuration is concluded. Recommendations regarding future related research are outlined. These recommendations focus on CFD simulations, buildings, wind turbines and education.

1.6 Conclusion

This chapter discussed the research design, structure, conceptual framework and proposed methodology. Although there is scepticism regarding the performance of urban wind turbines, it can be argued that with adequate wind resources assessment at the proposed installation site, urban wind turbines can provide buildings with significant amount of power. With the accelerating effect of buildings on wind velocity being evident, using CFD for assessing wind flow around different roof shapes can help determine the optimum roof shape and the optimum mounting location above the investigated roof shapes where maximum wind velocity acceleration takes place. Figure 1.2 explains the sequence of the investigated cases in this research for identifying the effect of roof shapes, wind direction, building height and surrounding urban configuration on the energy yield and positioning of roof mounted wind turbines.

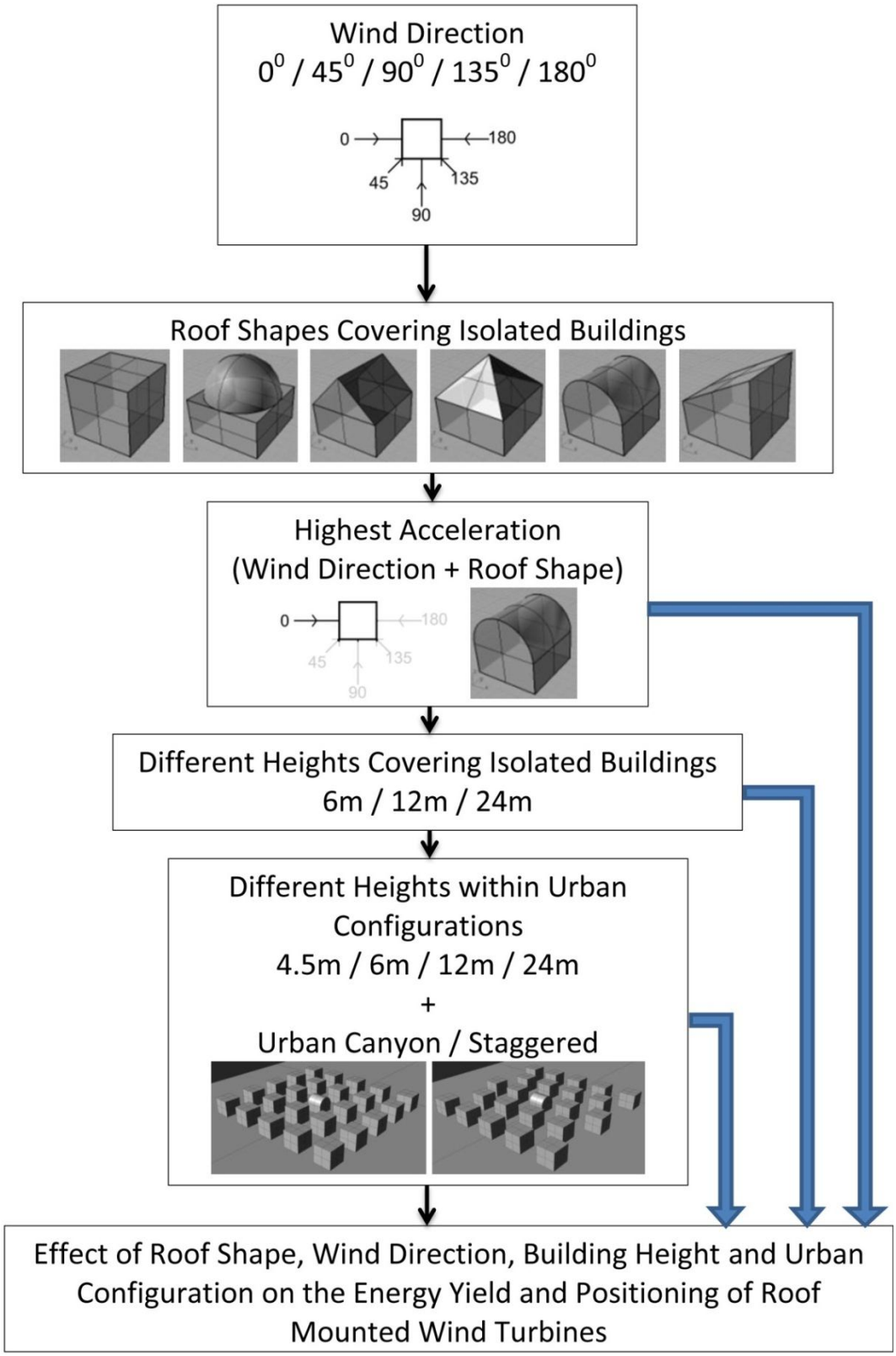

Figure 1.2 Showing the sequence of the investigated wind flow problems to identify the effect of roof shape, wind direction, building height and urban configuration on the energy yield and positioning of roof mounted wind turbines.

Chapter Two

Wind Turbines Technology and their Integration in Buildings

Chapter Structure

2.1 Introduction

2.2 Wind Power and wind turbines

2.3 Urban wind energy

2.4 Urban wind turbines

2.5 Conclusion

Chapter 2: Wind Turbines Technology and their Integration in Buildings

2.1 Introduction

The early utilisation of wind power was limited to providing mechanical power to pump water and grind the grain as well as sailing boats. It is said that the first wind mills on record were built by the Persians in approximately 1700 B.C. (Smith, 2003; Bradshaw, 2006; Manwell *et al.*, 2009). As for the use of wind turbines to generate electricity, Burton (2001) asserted that it can be traced back to the late nineteenth century with the 12 kW Direct Current (DC) wind turbine constructed by Brush in the USA. However, large deployment of wind turbines could not compete well with power generated from conventional sources of energy such as coal and oil until the 1970s. Ackermann and Söder (2002) acknowledged that the first oil price shock at that time drew the attention to the importance of wind power and other energy technologies as a reliable back-up source of electrical power. By the end of the 1990s wind power utilization gained momentum in research and application as one of the most important sustainable energy resources (Ackermann and Söder, 2002).

Smith (2005) acknowledged that the importance of wind power stems from the availability of wind throughout the whole year due to the differential heating of the earth's surface by the sun and the rotation of the earth, which means that the wind power is another form of the conversion of solar power. Joselin Herbert *et al.* (2007) stated that roughly 10 million MW of energy are continuously available in the earth's wind. In addition, about 10% of our electrical power can be supplied by the wind by the year 2020. On the other hand, it is predicted that wind power would capture 5% of the world energy market by the year 2020 especially when keeping in mind that wind energy was the fastest growing energy technology in the 90s, in terms of percentage of yearly growth of installed capacity per technology source. Accordingly, many countries aim to exploiting wind power to replace the power from conventional sources of energy. For example Denmark covers 40% of its electrical needs from wind turbines installations (Ackermann and Söder, 2002; Joselin Herbert *et al.*, 2007).

Thus, the dependency of many nations on wind power is evident. However, there are some concerns about the installation of large scale wind turbines in terms of jeopardizing birds' lives and disturbing the natural beauty of the landscape (Stankovic *et al.*, 2009). Accordingly, the idea of integrating wind turbines on top of buildings' roofs captured the attention of architects and planners in an attempt to play a role in utilizing wind power. But there are some technical issues for installing and operating wind turbines which should be considered before installation. This chapter reviews these technical aspects which architects and planners should be aware of when integrating wind turbines close to buildings. Thus, it is divided into three main sections:

- The first section (2.2) covers the basics of wind power including the available and extracted power from the wind, different classifications of wind turbines, implemented technology in wind turbines and the hurdles facing large scale wind power.
- The second section (2.3) focuses on small and micro wind turbines, which are often referred to in literature as urban wind turbines. This section compares urban wind turbines to large scale wind turbines and how they are advantageous over large scale wind turbines when integrated within the built environment or close to buildings in rural areas. It also focuses on understanding wind flow around buildings for the purpose of exploiting urban wind through small and micro wind turbines.
- Section three (2.4) reviews different types of integrating wind turbines in buildings, evaluating previous attempts to integrate wind turbines within the built environment and the reasons behind their success or failure. This section ends by reviewing different factors affecting the feasibility of urban wind turbines.

2.2 Wind power and wind turbines

The operation of large and small scale wind turbines is similar in many aspects. A wind turbine uses wind energy to generate electricity, which is the reverse of an electrical fan. In other words, wind turbines convert the kinetic energy of the wind into electrical energy through a generator which is one of the main components of a wind turbine. Tong (2010) explained the main components of a wind turbine as the tower, a low-speed rotor consisting of two or three blades

rotating at a speed of 30 to 60 revolution per minute (RPM), an anemometer, a controller, a high speed shaft connected to the rotor through a gearbox operating between 100 and 200 RPM, a pitch motor drive assembly, a yaw motor drive assembly, a nacelle, a wind vane indicator, an alternating current (AC) induction generator operating at high speed, a speed controller unit and other accessories necessary to provide mechanical integrity under heavy wind gusts (Figure 2.1). The generated electricity from a wind turbine depends mainly on wind direction and speed which is captured by the anemometer and the information is sent to the controller that provide data to the yaw motor to turn the rotor to face towards or away from the wind. The gear box in the system converts the slow motion of the slow rotating rotor to higher speed rotation through the high speed shaft which is connected to a generator that produces electricity (Jha, 2010).

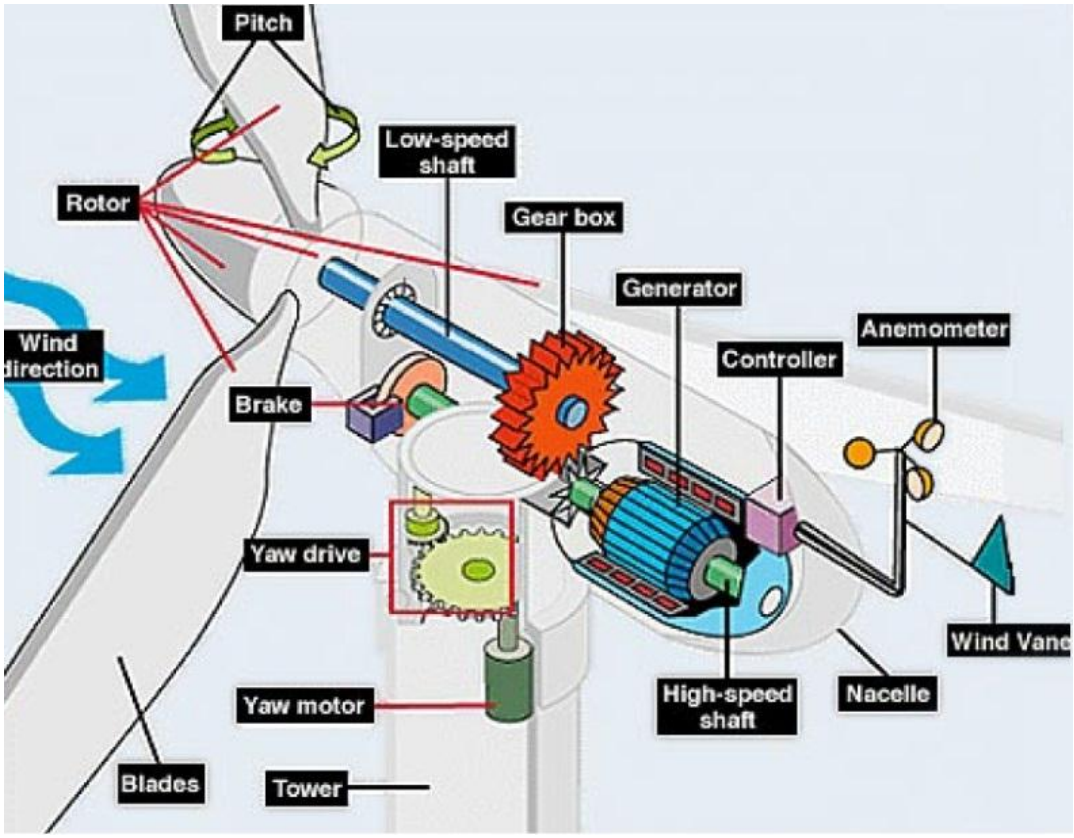

Figure 2.1 Main parts of a wind turbine (Source: http://bertmaes.files.wordpress.com/2009/06/wind-turbine-elements.png, accessed: 20/08/2012).

The concept of generating electricity from wind power is based on converting the kinetic energy in the wind into electric power by converting the power in the wind into mechanical rotational energy through the turbine rotor which rotates in

an electromagnetic field resulting in the generation of electric power. However, according to Eriksson et al. (2008), a wind turbine cannot extract all the energy in the wind as the air mass would be stopped completely in the intercepting rotor area. The Danish Wind Industry Association (DWIA, 2003) and Manwell et al. (2009) added that the maximum extracted power from the wind is known as the Betz limit which was formulated by the German physicist Albert Betz in 1919. Betz's law states that only 59% of the kinetic energy in the wind can be converted into mechanical energy using a wind turbine and the power extracted from the wind (*P*) can be calculated from the following equation:

$$P = \frac{1}{2} C_P \rho A \upsilon^3 \qquad \textbf{Equation 2.1}$$

Where C_P is the power coefficient which differs from one wind turbine to another, ρ is the density of the air, A is the swept area of the turbine and υ is the wind speed and since the power output from a wind turbine is related to the wind speed by a cubic law, Sara Louise (2011) asserted that accurate estimation of the site wind speed is vital for the accuracy of power output estimates. Eriksson et al. (2008) stated that the power coefficient (C_P) represents the aerodynamic efficiency of the wind turbine and is based on theoretical studies and on experimental results from different experiments and is usually around 0.40 for a single wind turbine. Thus, Stankovic et al. (2009) acknowledged that the main objective of wind turbines manufacturers is to get the power coefficient as close as possible to the Betz limit.

In addition to the power coefficient of a wind turbine, other factors such as the wind resources at the installation site largely affect the energy output of a wind turbine. According to the Royal Institute of British Architects (RIBA, 2006), the wind regime at any particular site affects the energy yield of a wind turbine, but in order to assess it accurately, planners should not only rely on the national average, it is important to undergo a site monitoring for one year at least to avoid potentially significant design calculation errors. Another factor is the absence of any obstacles such as tall buildings, trees, or hills that might disturb the wind flow resulting in a reduced mean wind speed and increase in levels of turbulence (Department of Energy and Climate Change, 2011b). However, different types of wind turbines operate under different conditions. Wind turbines can be classified according to different parameters. However, the main three

classifications are based on turbine size, aerodynamic concept (lift or drag) and axis of rotation (vertical or horizontal).

2.2.1 *Size of wind turbines*

Wind turbines vary in size from small scale wind turbines generating few Watts for charging batteries to very large scale wind turbines, reaching each 10MW, providing electricity for hundreds of buildings. The size of a wind turbine or its scale depends on its energy output which is called the rated power. Rated power is the instantaneous output of the turbine at a certain wind speed at a standard temperature and altitude. According to Smith (2003), Smith (2005) and Chiras (2010) wind turbines can be classified according to rated power into small, intermediate and large scale wind turbines.

Smith (2005) described small scale wind turbines as turbines with rated power from few Watts to 20 kW, these machines can either be used to provide direct current (DC) or alternating current (AC), the ones from1 to 5 kW are used mainly for charging batteries and the bigger ones are used to power commercial/industrial buildings and groups of houses. Jha (2010) added that small wind turbines are best suited for applications where electrical power consumption does not exceed 10 kW as in remotely located homes, telecommunication transmitter sites, offshore platforms, water pumping and utility-connected homes and businesses.

Intermediate scale wind turbines have rated power between 20 kW to 100 kW and they are mostly used when small scale and large scale wind turbines do not provide a cost effective operations on the long run. Intermediate turbines are mostly used for distributed generations, telecommunications, village electrification, and water pumping. Above 100 kW, wind turbines are classified as large scale or utility scale wind turbines and these large scale wind turbines are used to power complete neighbourhoods and cities. These wind turbines are found in open fields and the locations where they are sited are called wind farms.

2.2.2 *Lift, drag and hybrid driven type wind turbines*

Another classification of wind turbines is based on the way in which wind forces are distributed on the turbine blades to rotate them. These forces are either lift

force or drag force. The drag force is the force in the direction of the wind while the lift force is the one perpendicular to the wind direction. Kaldellis and Zafirakis (2011) acknowledged that the early windmills used to grind the grain and pump water utilised the drag principle whose turbines' blades are characterised by large surface area and slow moving blades because the rotational speed is limited by the wind speed. Jha (2010) explained that the concept behind the rotation of the blades of a drag type wind turbine is based on the difference in drag of two rotating bodies. A basic drag type wind turbine would consist of two adjacent cups facing opposite directions, the cup with the spherical facing downwind has the highest drag contrary to the one facing the upwind, and this difference in drag forces drives the wind turbine (Figure 2.2).

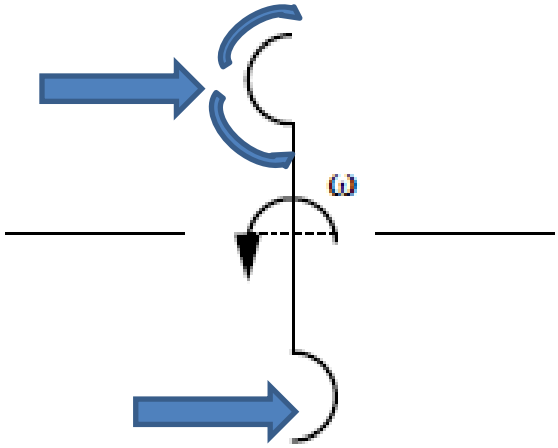

Figure 2.2 Drag driven wind turbine (Jha, 2010).

According to Hau (2006), drag type wind turbines have generally low power coefficient (C_P) which is in the range of 0.16. Their main advantage is that they produce less noise compared to lift type wind turbines due to the low rotational speed which makes them also reliable for areas of low wind speeds as the start up speed is very low. In addition, they require less maintenance than the lift type wind turbines which makes them suitable for integration within buildings.

However, all modern day horizontal axis wind turbines (HAWT) are designed to make use of the lift phenomenon. Lift type wind turbines use aerofoils that interact with the incoming wind. The lift force is a multiple of the drag force and therefore drives the rotor faster to generate more power and, as such, is characterized by fast-moving blades with low surface areas. According to Ackermann and Söder (2002), the vast majority of lift-force wind turbines in the

market significantly outperform the drag type wind turbines in terms of extracting more energy per square metre of swept area and this is their main advantage over drag type wind turbines. Stankovic et al. (2009) acknowledged that modern aerofoil blades are subjected to drag and lift forces as illustrated in Figure 2.3. However, the angle of attack of wind on the blades determines whether the dominant driving forces are lift or drag.

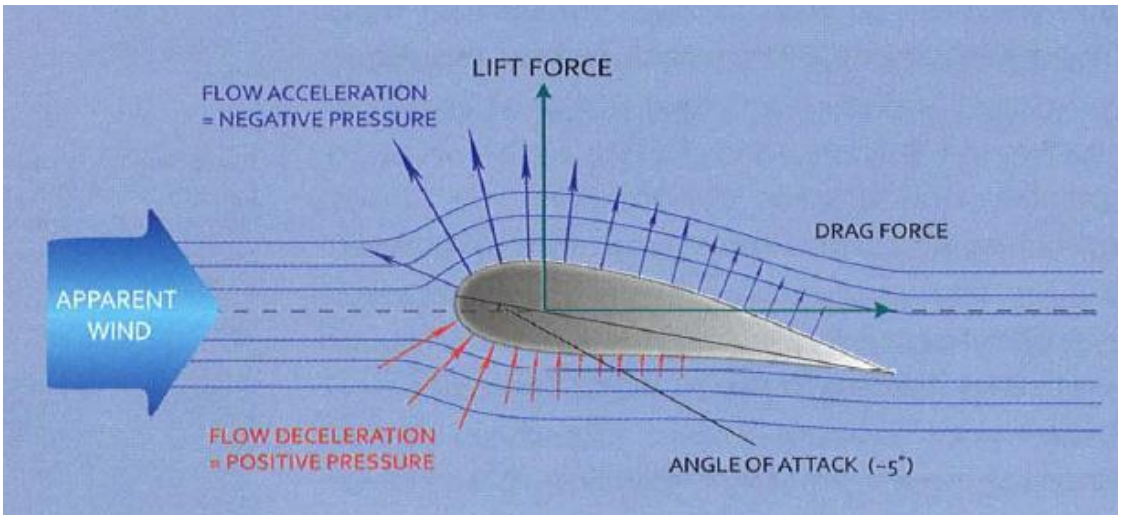

Figure 2.3 Drag and lift forces on an aerofoil shaped wind turbine blade (Stankovic *et al.*, 2009).

2.2.3 *Horizontal and vertical axis wind turbines*

Although wind turbines are classified according to several criteria, any of the wind turbines available in the market would fall under one of two types depending on the axis of rotation. These two types are the horizontal axis wind turbines (HAWTs) and the vertical axis wind turbines (VAWTs) (Figure 2.4). Eriksson et al. (2008) and Bradshaw (2006) mentioned that although many configurations of VAWTs are available in the market, many people associate wind turbines with the horizontal axis type which might be attributed to the fact that for large-scale wind turbines, the market is relying heavily on the three-bladed HAWT as the way forward for multi-megawatt wind turbines.

According to Smith (2005), the HAWTs with two or three blades are the most dominant generator types installed as for the VAWTs they are not as popular as the horizontal axis ones but they are more suitable for installation within the built environment as will be discussed in section 2.4. Accordingly, RenewableUK (2011b) anticipated that the installations of VAWTs will continue to grow with the growth in interest in installing small wind turbines close to buildings. As for

HAWTs they will continue to dominate the open space large scale wind generation market. Since in open spaces, the HAWT is allowed to yaw freely to face the prevailing wind direction, while for VAWT they have the advantage of being able to rotate under different wind directions.

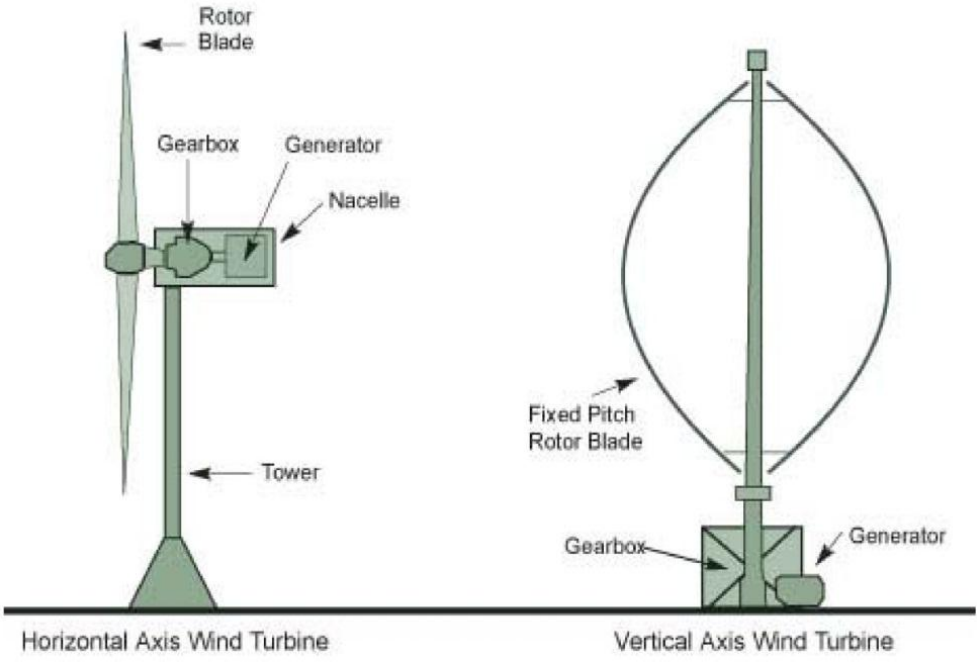

Figure 2.4 Schematic of the horizontal and vertical axis wind turbine (Source: http://www.cbmjournal.com/content/2/1/8/figure/F2, accessed: 21/08/2012).

According to Smith (2005) and Stankovic et al. (2009) HAWTs have received most of the attention in the field of generating electricity from wind energy for the following reasons:

- They are cheaper as they require less material per square metre of swept area, in addition to the reduction of the cost due to mass production and prototyping.
- The technology is robust with a long history of testing.
- They have high efficiency in terms of power output (high C_P).
- Most prototypes are self-starting.

However the disadvantages of HAWTs are:

- They have to be placed at high altitudes away from obstructions; this is why they are not a good option for urban applications.

- They produce more noise especially when using a gearbox and braking system.
- They require substantial foundation support especially when mounted on buildings.
- When used within the built environment where wind frequently changes direction, they yaw frequently to face the wind; this not only undermines power output, but also increases the dynamic loading on the machine with consequent wear and tear.
- Some people consider them visually intrusive.

Thus, most of large scale wind turbines are HAWTs which can be found in open fields and offshore, as for urban areas or where wind tends to regularly change direction, in such conditions VAWTs are preferable for installation.

Different configurations are available for VAWT. However, Ritchie and Thomas (2009) acknowledged that all of them would fall under one of the main three types which are the Savonius turbine, the Darrieus turbine and the H-Darrieus turbine (Figure 2.5), a more detailed review of different VAWTs configurations is included in the review by Bhutta *et al.* (2012). The Savonius is a drag type VAWT which is also called the S rotor turbine due to the S shape plan of the blades. The Darrieus and the H-Darrieus are lift type VAWTs. Among the three types, Jha (2010) acknowledged that the Savonius turbine has the lowest power coefficient and it only operates over a blade tip speed to wind speed ratio equal to or below one, the Darrieus turbine has a power coefficient close to 0.35 at a blade tip speed to wind speed ratio ranging from 0.55 to 0.65.

In their experiments to verify the power coefficient of an H-Darrieus wind turbine, Kjellin et al. (2011) found that the C_P of the turbine is 0.29 at a tip speed ratio[1] of 3.3 and they argued that it can reach 0.39 with improved blades design. Pope et al. (2010) investigated the aerodynamic performance of a new VAWT called Zephyr which has high solidity to cope with the wind conditions within the built environment. The turbine has a unique design that includes stator vanes with reverse winglets (also called stator tabs), in their research they explored the effect of those taps on the C_P of the wind turbine and the

[1] The tip speed ratio of a wind turbine is the ratio of the tangential speed at the blade tip to the actual wind speed (Tong, 2010).

maximum recorded C_P was 0.113 which is relatively low compared to the Darrieus and the H- Darrieus VAWTs.

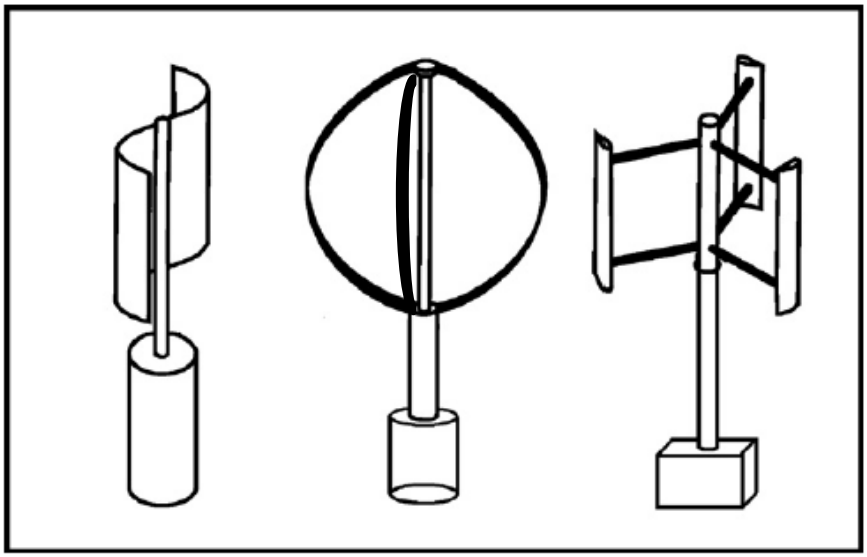

Figure 2.5 Left: Savonius VAWT, Middle: Darrieus VAWT and Right: H-Darrieus VAWT (Ritchie and Thomas, 2009).

Thus, according to Ackermann and Söder (2002), Smith (2003), Smith (2005), (RIBA, 2006), Mertens (2006), Eriksson et al. (2008), Stankovic et al. (2009) and Ritchie and Thomas (2009), the main disadvantages of VAWTs are:

- Most of them have no self-starting capability so they need mechanical start-up.
- Limited options for speed regulations during high wind speeds.
- They have a tendency to stall under gusty wind conditions.
- Low power coefficient, accordingly low energy output.
- Low starting torque.
- They have dynamic stability problems.
- The low installation height limits the operation to lower wind speed environments.

On the other hand VAWTs have advantages which make them a good option especially for usage within urban areas and close to buildings:

- They operate independently of the wind direction (omni-directional), thus turbulence and wind from different directions are handled more effectively.

- The gearbox and the generating machinery can be placed at ground level which facilitates installation, operation and maintenance.
- Requires less maintenance as there are fewer and slower moving parts.
- They emit less noise.
- Some people consider them more aesthetically pleasing.
- They do not require a yawing mechanism.
- The blades have high rotational speeds which offer reduction in gear ratios.

Although VAWTs are not as efficient as HAWTs based on the performance coefficients of each, Riegler (2003) argued that VAWTs are quite competitive with HAWTs when it comes to small and micro-scale wind turbines, thus VAWTs can play their role in areas where HAWTs do not work that well such as in the case of harnessing wind power close to buildings. Müller et al. (2009) have undergone a research on developing the old concept of the first VAWT which was found in the Sistan Basin in the border area between Iran and Afghanistan for the purpose of integration within buildings. Their results showed efficiency which can reach 42% and the integration on top of a high rise building was architecturally acceptable (Figure 2.6).

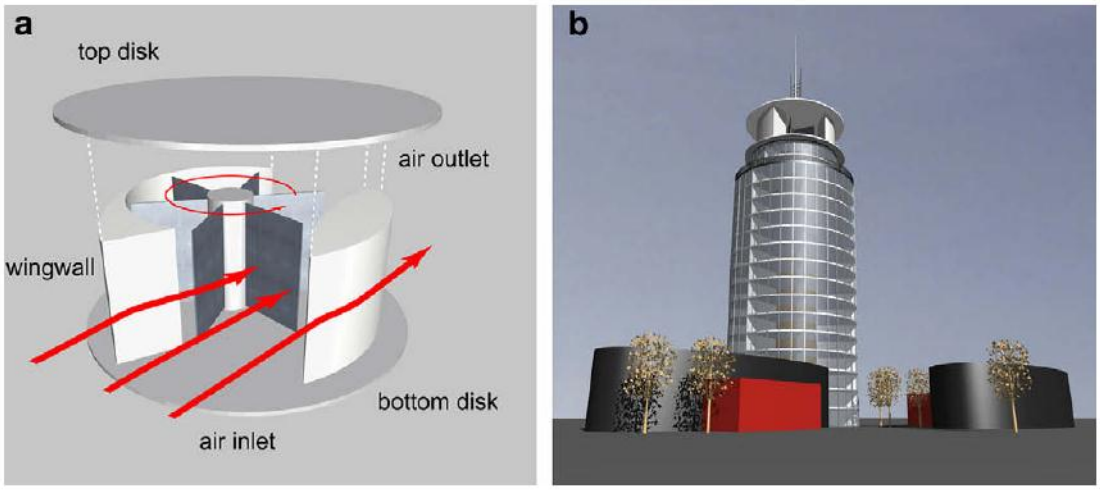

Figure 2.6 Artist's impression of the integration of the developed VAWT on top of a building implementing the concept of the VAWT which was found is the Sistan Basin (Müller et al., 2009).

2.2.4 *Wind turbines blades*

According to Ackermann and Söder (2002), the most common type of wind turbines is the three bladed horizontal axis wind turbine. They are

advantageous over single and double bladed wind turbines in terms of stability, visual aesthetics and lower noise levels. The less number of blades the faster the rotation, the lower the torque and the lower the cost. However, Bradshaw (2006) recommended not to use even number of blades or one blade due to the stability problems for a machine with a stiff structure. According to Jha (2010), most HAWT implement either a two or three bladed rotor and the one bladed rotor is rarely available. The main advantage of single and double bladed rotors is the reduced used material which translates into less cost. However, they rotate faster than three bladed rotors which mean higher noise emissions and higher rates of blades erosion. Also, due to the uneven distribution of the loads of the rotating blades, more dynamic instability is introduced to the structure. Furthermore, the three bladed wind turbines provide better efficiency and improved reliability than the two or single bladed wind turbines.

Recent research has focused on varying the length of the blades (Figure 2.7) for getting more energy output at relatively low wind speeds. According to Sharma and Madawala (2012), this concept is at development stage but it has high potentials since variable length blades can:

- Operate under variable wind speeds which improve their economics.
- Make viable using wind turbines at areas with low mean wind speeds.
- Reduce the need for different size blades for different wind regimes.
- Improve capacity factor without running turbines beyond rated loads.
- Make logistics of shipping easier since they can be shipped in a shortened position.
- Can be retrofitted to existing blades, as well as being designed into new blades.

In their experiments to assess this concept, Sharma and Madawala (2012) explained the concept as a mechanism of extending the blades length when wind speed falls under the rated level, thus increasing the swept area and increasing the power output. Results showed that doubling the blades length will lead to doubling the energy output of a corresponding turbine with fixed length blades. In addition, from an economical point of view, this concept is feasible if the cost of the rotor is kept below 4.3 times the cost of a standard rotor with fixed length blades.

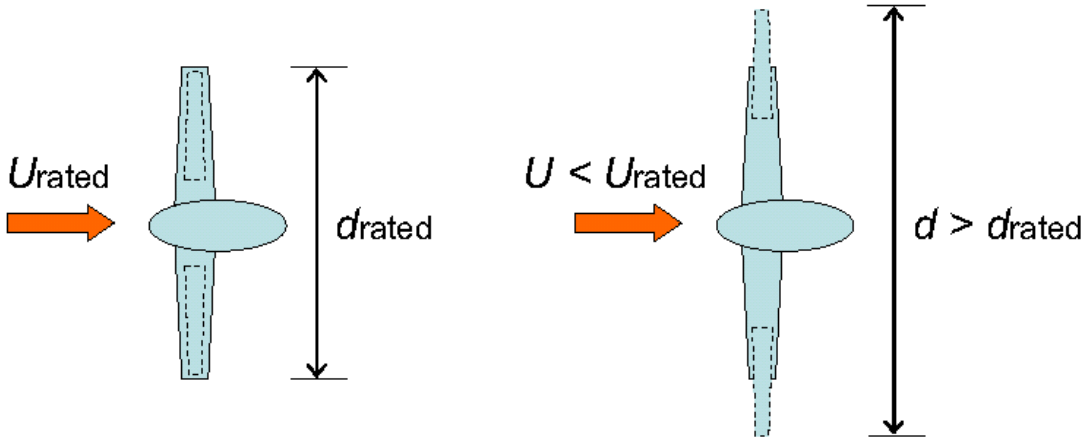

Figure 2.7 Schematic diagram of a turbine with varying blade length (Sharma and Madawala, 2012).

2.2.5 *Power control and protection*

Eriksson et al. (2008) stated that wind turbines are designed to reach their highest efficiency at certain rated wind speed. At that wind speed the power output reaches the rated capacity. If the wind speed exceeds that limit, the wind turbines has to be controlled so that the power output would be in the range of the rated capacity otherwise the wind turbine blades would be subjected to excessive driving forces which will be transferred to the whole structure of the wind turbine putting it to the risk of failure and the wearing out of the turbine components. According to Ackermann and Söder (2002), the available systems for controlling the speed of the wind turbine are the passive stall regulation, active blade pitch control, active stall regulation, yawing and tilting, bending and tip control.

2.2.5.1 Passive stall regulation

This type of control depends mainly on creating an area of turbulence in the leeward direction of the blade when the wind speed exceeds a certain limit. The effect results in a reduction of the aerodynamic forces, and subsequently of the power output of the rotor. In other words, the lift forces are minimized to put the turbine into a stall.Tong (2010) explained that, under passive stall condition when the wind speed is high the wind detach from the blades and consequently the lift forces decrease as explained in Figure 2.8, this results in large aerodynamic forces on the rotor. Stall regulation is simple and does not require a sophisticated control system.

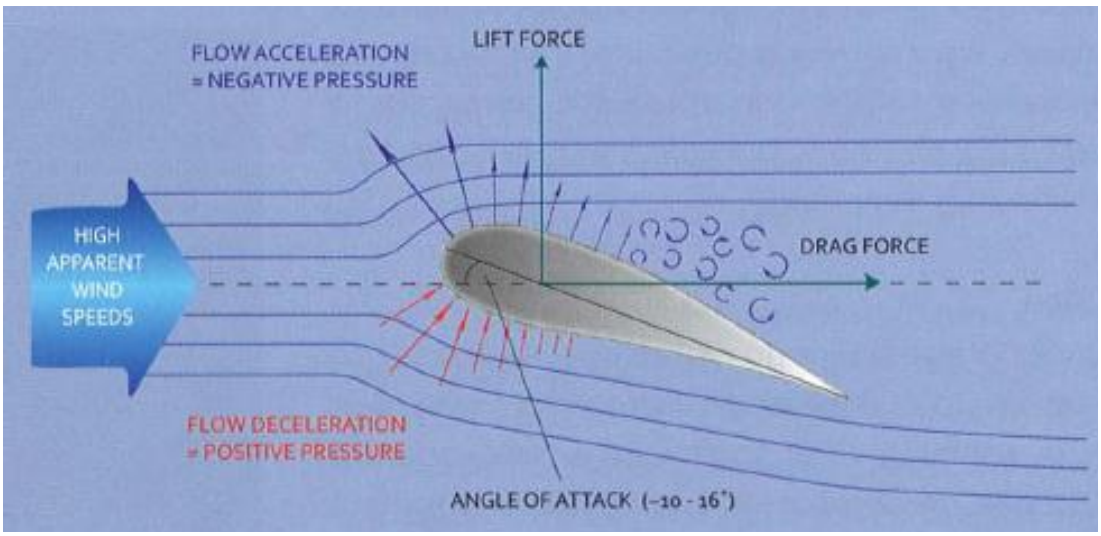

Figure 2.8 At high wind speeds the wind detach from the blades surface and puts the turbine to a stall (Stankovic *et al.*, 2009).

However, such approach requires careful design of the blades due to the complexity of the dynamic process involved and the difficulty of calculating the stall effect for unsteady wind conditions. The main disadvantage of this approach, according to Stankovic et al. (2009), is that during high wind speeds (above the rated speeds) which have high energy content, little energy will be generated. Another problem which faces this technique is the delay in stall phenomenon, Hu *et al.* (2006) attributed this to the centrifugal forces during the rotation of the blades and they asserted that this delay should be accounted for while designing the blades to minimise the power losses due to this phenomenon. These disadvantages can be overcome by another technique which is the active pitch blade where the blades adjust and rotate to keep the energy produced at these high wind speeds constant.

2.2.5.2 Active blade pitch control

This technique is also called pitch regulation, feathering or furling and is based on rotating the whole length of the blade along its longitudinal axis (Figure 2.9) so that the lift forces are eliminated at high wind speeds so that the power output of the rotor remains constant after rated power is reached (Ackermann and Söder, 2002; Stankovic et al., 2009). This rotation takes place by means of a hydraulic system or by using electronically controlled electric motors. In both cases the mechanism is connected to a control system which must be able to adjust the pitch of the blades by a fraction of a degree at a time, corresponding

to a change in the wind speed, in order to maintain a constant power output. This technique allows the turbine to rotate in a no-load mode at high wind speeds with a maximum pitch angle which reduces the thrust of the rotor on the turbine's structure, allowing for a reduction of material and weight.

A pitch controlled wind turbine would generate more power at low wind speeds than stall controlled wind turbines because the blades can be kept at optimum angle. However, the main advantage of stall controlled wind turbine over pitch controlled wind turbines is that at high wind speeds when stall effect becomes effective, the wind oscillations are converted into power oscillations which might be missed by a pitch controlled wind turbine during the pitching of the blades to adapt to different wind speeds (Ackermann and Söder, 2002). Jha (2010) added that with this mechanism, it is theoretically possible to adjust the blades to be in the optimum pitch position at all wind speeds, thus having a relatively low cut in wind speed. As for high wind speeds, this mechanism helps reduce the aerodynamic forces on the structure which will improve the dynamic stability of the wind turbine. However, it should be noted that the power output will still be limited to the rated power of the electrical generator.

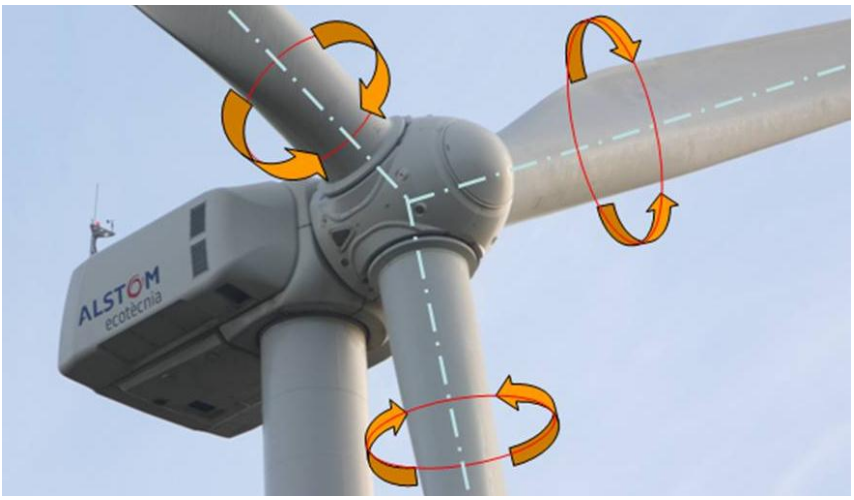

Figure 2.9 A Pitch-controlled HAWT (Source: http://usuaris.tinet.cat/zefir/fotos/000/pitch%20zefir2.jpg, accessed: 21/08/2012).

2.2.5.3 Active stall regulation

Ackermann and Söder (2002) described this type of control as a mix between the pitch and stall approaches. During low wind speeds, the blades are rotated around their longitudinal axis like in a pitch-controlled wind turbine where higher

efficiency is achieved and large torque is guaranteed to achieve adequate turning force. However, when the wind turbine reaches its rated capacity, the blades will pitch in the opposite direction than a pitch-controlled machine does, resulting in increasing the angle of attack of the rotor blades and accordingly putting the blades into a deeper stall. The main advantage of this control system is that it takes advantage of pitch controlled turbines when turning the blade into the low load feathering position, hence reducing the thrust on the turbine in addition to achieving a smoother limiting of power output, similar to that of pitch-controlled turbines without the 'nervous' regulating characteristics of that type. This technique is popular for HAWTs, however for VAWTs, Greenblatt et al. (2012) argued that no attempts have been made to directly control turbine blade dynamic stall using active stall regulation.

2.2.5.4 Yawing and tilting

One of the control methods for avoiding undesirable high wind speeds is to yaw or tilt the blades away from the gusting wind. This can be done passively using a tail fin, as in the case of small scale wind turbines, or actively in the case of large-scale wind turbines using an electric motor. Although Stankovic et al. (2009) noted that it is not preferable to use this technique with large scale wind turbines due to the uneven distribution of loads on the structure of the turbines during yawing which can jeopardise the structural integrity of the turbine, Jha (2010) acknowledged that using the yaw control ensures the dynamic stability and structural protection of a wind turbine in a turbulent environment and recommends using both pitch and yaw regulations to ensure the dynamic stability and safe operation of high capacity wind turbines. Tong (2010) added that, during the process of titling the wind turbine away from high speed winds, possible energy that could have been harvested will be lost. However, Ackermann and Söder (2002) argued that the total value of the lost energy over the lifetime of the wind turbine will usually be smaller than the investments that will be avoided by limiting the strength of the turbine to the cut-out speed.

Research on active yawing systems for large scale wind turbines is available in literature. However, for small and medium wind turbines, which are more likely to be used within the built environment, Wu and Wang (2012) claimed that there is almost no research on active yaw system for small wind turbines. They

developed an active yaw system for small wind turbines arguing that although the advantages of passive yaw system are that the structure is very simple and the system has low manufacturing cost, its disadvantages are the uncontrollable, small yaw moment and unsteady yaw which makes the wind turbine yaw frequently resulting in reducing the efficiency in power generation. The system they developed for small wind turbines suitable for urban wind turbines consists of a yaw motor, a reducer, a worm gear, two yaw bearing and a controller which gives instructions to the yaw system (Figure 2.10).

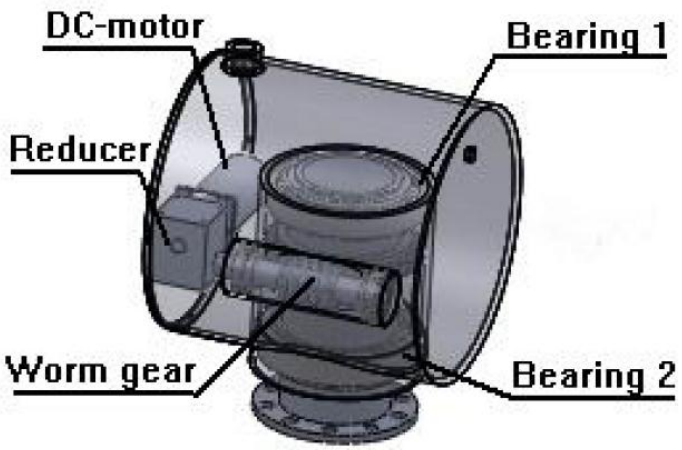

Figure 2.10 Active yaw system for a small HAWT (Wu and Wang, 2012).

The main advantages of that system is that it is compact, simple and low in cost. Their experiments has proven that the active yaw mechanism prototype combined with a controller can be fast and flexible responding to instructions of controller and yaw stably and accurately leading to an increased efficiency in the energy yield of small wind turbines.

Another system was developed by Mejía et al. (2003) who argued that their system can be advantageously utilized, as compared with conventional vanes and other mechanical or electromechanical means, in horizontal axis wind turbines with diameters between 2 and 12 m. The system consists of a rigid short tail with an aerodynamic rotating vane to yaw the rotor smoothly edgewise to the wind direction in strong winds or in gusts, a bumper and a spring (Figure 2.11). The tail will always be aligned with the turbine axis as long as the wind speed does not exceed the rated speed, but if the wind velocity exceeds that limit, the drag force on the vane makes it rotate away from the wind and the

spring would return it to its position after the wind speed returns back to rated speed and in order to avoid an oscillation of the tail, a bumper is recommended.

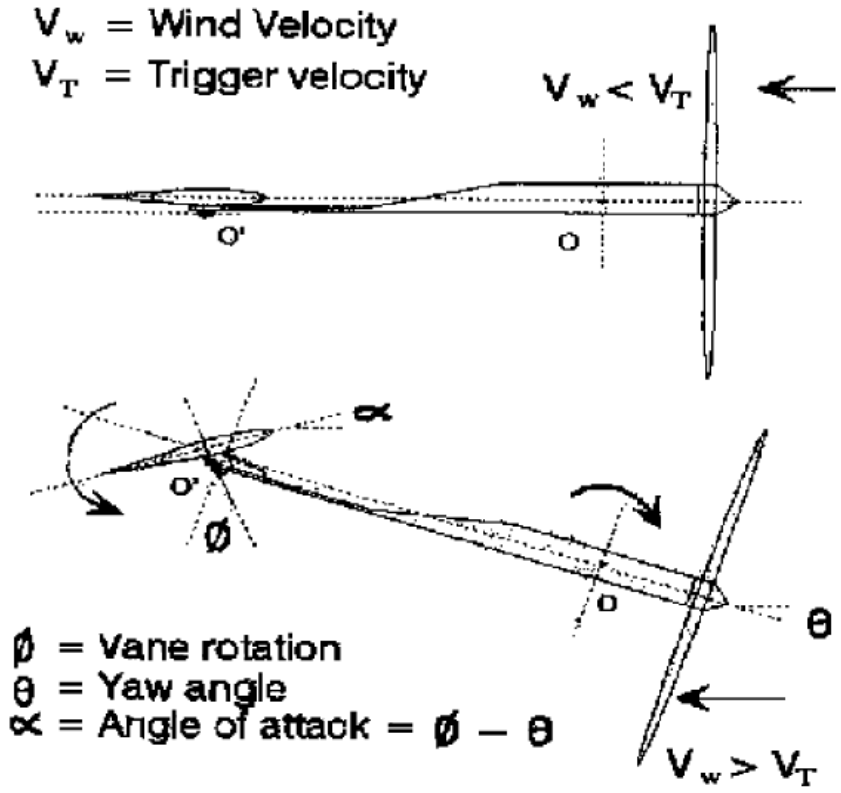

Figure 2.11 The proposed tail vane showing the tilting of the turbine when the wind speed exceeds the rated limit (Mejía et al., 2003).

2.2.5.5 Blade bending and tip control

One of the control techniques implemented in small wind turbines is allowing the blades to bend resulting in decreasing the lift force during high wind speeds. Another technique is to use blades with tip brakes (fins) where those fins are operated at high wind speed or in the event of an electrical power failure (Ackermann and Söder, 2002).

Stankovic et al. (2009) acknowledged that a secondary backup system should be provided which will be one that is less advisable to use on a regular basis to control blade speed such as mechanical brake (which would wear given regular use) or applying a current to the generator (which can cause the generator to burn out). However, a mechanical locking system is required to lock the turbine during maintenance. As for the case of vertical axis wind turbines, Eriksson et al. (2008) acknowledged that passive stall control is the most widely used due to the difficulty of applying any of the other control systems. Also a mechanical

brake is provided as a secondary system which can be placed at the bottom of the tower.

2.2.6 *Generators*

Wind turbines generators convert mechanical energy into electrical energy. This is done by the rotation of the wind turbine blades which drives a shaft connected to a coiled wire placed in a magnetic field. The power generated by the rotor blades is transmitted to the generator by a transmission system. The transmission system consists of the rotor shaft with bearings, brake(s), an optional gearbox, as well as a generator and optional clutches. Zhe et al. (2009) acknowledged that alternating current (AC) generators are available in two types: the synchronous and the induction (asynchronous) generator. The difference between the two types is related to the arrangement of the magnets on the rotor which makes the synchronous generator rotates with a fixed speed while for the induction generator its speed varies according to the wind speed.

The synchronous generator is mostly used with conventional fossil fuel power generating plants and when used for generating electricity from wind power, they are mostly used in standalone systems. This is because the rotational speed is fixed by the grid frequency and the number of pairs of poles of the generator. This means that the structure of the wind turbine will have to withstand extra loads due to sudden wind gusts. A solution to this problem is to decouple the electric connection between the generator and the grid through an intermediate circuit which is connected to a three-phase inverter that feeds the grid with its given voltage and frequency (Ackermann and Söder, 2002; Stankovic et al., 2009).

However, according to the Danish Wind Industry Association (2003), most wind turbines in the world use asynchronous generators to generate alternating current. This type of generator is not widely used outside the wind turbine industry, and in small hydropower units. Burton (2001) stated that induction generators suffer from losing energy in the form of heat energy which reduces their efficiency especially at low wind speeds. However, they are less expensive and are more flexible in terms of operating under variable speed. This is attributed to the unique design of the rotor which makes the asynchronous generator different from the synchronous generator.

The main advantage of an induction generator is the reduced forces on the turbine parts due to the rotation of the rotor with different speeds according to the gusting wind speed. This is reflected in increasing the life time of wind turbine in addition to reducing the structural costs of the foundation of the wind turbine since most of the wind forces is converted into rotational force and then into electrical power (Danish Wind Industry Association, 2003).

2.2.7 *Gear box and direct drive*

For grid connected wind turbines, the current exported to the grid should have the same frequency of the grid current. According to the Danish Wind Industry Association (2003) a 50 Hz AC three phase grid with two, four, or six poles, would have to have an extremely high speed turbine with between 1000 and 3000 RPM, which means that with a 43 metre rotor diameter, that would imply a tip speed of the rotor of far more than twice the speed of sound. Jha (2010) added that the gear box is required to increase the speed typically from 20 to 50 revolutions per minute (rpm) to the 1000 to 1500 rpm required to drive most types of generators. However, this system produces more noise than direct-drives. Thus, when noise elimination is a key concern, direct-drives might be an option. In addition, Eriksson et al. (2008) argued that the gearbox is often associated with breakdown, need for maintenance and power losses.

Stankovic et al. (2009) argued that generators with their magnetic rotors rotating at lower speeds can still produce the same required 'grid compatible' electric output if the length or the diameter of the generator is increased. Eriksson et al. (2008) pointed out that lower-speed designs increase simplicity and reliability, reduce the need for maintenance and extend the life of the machine. In the small-scale wind energy markets most turbines are direct-drive, especially with vertical axis wind turbines as the size of the machine can be overcome by placing the generator on the ground.

One of the methods for reducing the size of the generator is to employ a pair of contra-rotating (C/R) wind turbines that are configured to rotate the permanent magnet (PM) array and the windings in opposite directions. Jung et al. (2005) acknowledged that the C/R wind turbine system combines both the conventional HAWT system and the VAWT system by using a bevel-planetary gear arrangements which makes use of the rotation of both rotors. The main

rotor rotates in an anti-clock wise direction and is located in the downwind location while the auxiliary rotor rotates in a clockwise direction and is located in the upwind location (Figure 2.12). The presence of the two rotors rotating in opposite directions represents a structural challenge in terms of structural stability in addition to the added cost for the two rotors and the structural system. However, from an aerodynamic point of view, the system have many advantages, these are:

- Higher aerodynamic efficiency nearly doubling the direct-drive power capability for a given wind turbine speed, the power coefficient can reach as high as 0.5.
- Free yaw characteristic is possible due to the reduction of the nacelle weight by placing the heavy generator system into the non-rotating region.
- Low starting torque and torque ripple.
- Very high electrical and mechanical efficiencies (including part-load operation).
- Compact size and high specific torque/power.
- Low noise and vibration.
- Simple and inexpensive to manufacture/assemble.
- Modular construction.
- Scalable design.

Figure 2.12 A Contra-rotating (C/R) wind turbine system (Source: http://www.srl.gatech.edu/education/ME6105/Projects/Fa11/folder.2011-09-22.5693359149/img1D.jpg, accessed: 21/08/2012).

Contra-rotating (C/R) wind turbines are relatively new technology which is still under development, and due to the complex phenomenon arising from the aerodynamic interaction between its two rotors, more design parameters could be investigated to increase their efficiency. The research by Lee et al. (2012) investigated the effect of the pitch angles, rotating speed ratios and radius differences of the two rotors on the power coefficient of the wind turbine. It can be argued that with the development of the C/R wind turbines, it might prove to be one of the good options for overcoming the problem of low mean wind speeds at certain areas, especially when considering integrating wind turbines in buildings.

2.2.8 *Permanent magnet and electromagnet*

All electricity generators contain magnets in their parts, this magnet is either a permanent magnet (PM) or an electromagnet (EM). Tong (2010) acknowledged that permanent magnets are mostly used for small scale wind turbines and they are a good option for standalone systems. However, they should be monitored over time to detect any decay in performance due to loss of magnetic strength resulting from overheat or the iron dipoles being misaligned. On the other hand electromagnets are mostly used in large-scale wind turbines where electricity from the grid is used to generate a magnetic field. Booker et al. (2010) added that one of the main advantages of PMs is that they yield high power density at low directly driven speeds which omits heavy and noisy gearbox parts and makes the turbine more acceptable within urban areas since the noise problem is minimised. Thus, research in this area is directed towards developing direct-drive PM generators that are compact, lightweight, quiet, exhibit low vibration and are suitable for mounting on buildings with minimal additional infrastructure.

2.2.9 *Power handling*

The Royal Institute of British Architects (2006) asserted that the most relevant power handling approach is to connect the wind turbine to the electrical grid which requires permission from the local electricity supplier as well as an up-front agreement for power purchase. According to Chiras (2010), the grid is the extensive network of high-voltage electrical transmission lines that crisscross nations, delivering electricity generated at centralized power plants to cities, towns and rural customers. However, the Danish Wind Industry Association

(2003) acknowledged that in order to allow the turbine to rotate with different speeds according to wind speed, thus reducing the forces on the structure, a wind turbine should be indirectly connected to the grid. First the fluctuating alternating current from the turbine is converted to a direct current through a rectifier. Then an inverter is used to convert the direct current to an alternating current with the same frequency of the current in the grid. The wind turbine either feeds all the power it generates to the grid or is directly used on site and feeds the surplus into the grid (Stankovic et al., 2009; Chiras, 2010).

Another way of handling the generated power is to store it and use it at later times. Bradshaw (2006) stated that storage requires batteries which tend to be expensive and take a lot of space, in addition to the need for replacing the batteries after five to eight years for typical lead-acid batteries. Another disadvantage of storing the generated power in batteries is the energy loss which accompanies the conversion of the generated alternating current to a direct storable current, this conversion of energy from electric to chemical and back to electric results in energy loss.

However, other approaches of storing power in other energy forms such as heat energy by heating water or mechanical energy through a flywheel might be a viable approach depending on the required application. For small wind systems found in urban areas, Peacock et al. (2008) acknowledged that connecting small scale wind turbines to the grid is not a problem except in the case of exporting electricity to the grid where the complications remains in metering the exported electricity. They added that the implications of the grid of large levels of distributed generation and the resulting changes needed in the electricity transmission and distribution systems are not yet known which is common for all domestic scale micro generation technologies.

2.2.10 *Hurdles facing wind turbines*

Wind energy has many environmental and economic advantages which encourage developers and governments to invest in them. However, Dannecker (2002) raised questions about the feasibility of wind turbines, the public safety in the vicinity of wind turbines, their visual impact, the noise emissions, their impact on biodiversity and birds, their interference with electromagnetic waves and their irritating effect of flickering sunlight and blade reflected light. Also

Smith (2005) added that most advantageous onshore sites are places of particular natural beauty and these sites are often far away from the grid and centres of population where the power is being used, thus a considerable amount of power is lost due to transmission and there are concerns about their effect on the natural landscape. In the next few subsections, the main hurdles facing wind turbines will be discussed.

2.2.10.1 Public safety, fire and ice throw

These are some of the main problems of wind turbines because they jeopardise the safety of people in the vicinity of wind turbines. Since wind turbines have moving parts in friction with each other, there is a probability of overheating of the parts and eventually catching fire if the cooling system malfunctions. Also during winter time the accumulated ice on the turbine parts is a concern. Ackermann and Söder (2002) asserted that if ice accumulates on the blades of a wind turbine, that would have significant impact on the performance of the wind turbine as it influences the blade aerodynamics as well as the blade load. In a research by Li et al. (2010) they investigated the effect of ice accumulation on a VAWT by attaching clay to the blades and found that the attachment reduced the rotation and power performance and the reduction rates increased as the mass attached and wind speed increased. They attributed this to the unbalance of weight of the rotor and the variation of the aerodynamic characteristics based on the change of aerofoil geometry.

In their research on anti-icing and de-icing techniques for wind turbines, Parent and Ilinca (2011) acknowledged that the accumulation of ice on wind turbines will result in measurement errors during the assessment phase of the operation of the wind turbine, power losses, mechanical failures, electrical failures and safety hazards. Thus, they recommended active heating of the blades in order to minimise the probability of accumulating ice on the blades. However, Chiras (2010) noted that when ice build-up on a wind turbine, the turbine should be shut down until the ice is melted. At that point the ice tends to break up into small pieces and drops to the ground. Eriksson et al. (2008) noted that the problem of ice build-up on VAWT is less severe when compared to HAWTs, due to the lower rotational speed of VAWTs which requires less security distance.

2.2.10.2 Visual effects

Molnarova et al. (2012) considered that there is a dichotomy in the view of wind farms among members of the public since there is enthusiasm about renewable sources of energy including wind turbines but on the other hand there is a concern about the visual impact of wind turbines. In the case of large scale wind turbines, this controversy is true but for urban wind turbine, it is not since the buildings already exist.

Molnarova et al. (2012) argued that wind turbines were almost universally perceived as a negative impact on the landscape. Most of the respondents to their image based questionnaires rejected wind turbines when they were placed in areas of high aesthetic quality, as opposed turbines placed in the least attractive landscapes did not increase negative responses to those landscapes. The number of wind turbines to be installed also played a role in the acceptance of the respondents to wind turbines; although the supporters of wind turbines saw a single turbine as an improvement to the landscape scene, they considered four turbines as deterioration. It is therefore possible that even supporters of wind power can find wind turbines unattractive when their numbers cross certain thresholds.

When some people consider wind turbines as visually intrusive, this also has other implications on their perception of the noise produced by wind turbines. Pedersen and Larsman (2008) investigated the relationship between the visual impact of wind turbines and how people perceive noise emissions from wind turbines. They found that the visual attitude towards the noise source was associated with noise annoyance to different degrees in different situations; a negative visual attitude enhanced the risk for noise annoyance. Thus, it is expected that people who find wind turbines visually intrusive are more likely to complain about the noise emissions from wind turbines especially when they are visible.

2.2.10.3 Noise

The noise emitted by wind turbines is one of the major concerns especially with urban wind turbines where people work and live in the vicinity of those wind turbines. Stankovic et al. (2009) stated that the emitted noise is either

aerodynamic resulting from the friction between the rotating blades and the air or is mechanical which is usually associated with the gearbox. According to Eriksson et al. (2008), the aerodynamic noise is related to the tip speed of the turbine, the higher the tip speed the louder the noise. This is why the VAWT produces less noise than the HAWT since the later has more tip speed. As for the mechanical noise, the VAWT also emits less noise than the HAWT as the drive train components of the VAWT are placed at ground level where the noise can be confined.

Although the noise problem is a major concern when thinking of deploying wind turbines, the problem might be exaggerated as Chiras (2010) pointed out that most of today's wind turbines emit noise in the range of 50 to 60 dB, at the turbine location, which is the same as the noise emitted from trees on a breezy day, what makes the noise from a wind turbine distinguishable from ambient noises is the different continuous frequency of noise from wind turbines. Chiras (2010) also pointed out that the distance from the wind turbine affects the amount of noise heard at a certain location; the farthest from the turbine, the less noise will be heard. However, Ackermann and Söder (2002) and Joselin Herbert et al. (2007) acknowledged that this is a problem which can be solved technically especially when knowing that the emitted noise has successfully been halved over the last few years. In addition to that, Pedersen et al. (2010) asserted that the noise generated by a wind turbine should be assessed in light of the noise levels emitted from other sources at the installation site as in areas near airports or windy locations where the ambient noise level of the wind stream may impact the noise level generated by the wind turbine.

Jha (2010) added that wind turbine manufacturers have made significant efforts in reducing noise levels from wind turbines whether aerodynamic or mechanical noise. Aerodynamically, sharpening the trailing edges of the rotor blades and using new tip shapes has reduced the emitted noise. Mechanically, isolating the gearbox from the nacelles and installing sound deadening insulation have made newer wind turbines significantly quieter. In addition to that, Pedersen et al. (2010) acknowledged that road traffic noise can provide a significant masking of wind farm noise, but only at intermediate levels of wind turbine sound (35–40 dB(A)) when the road noise is louder with about +20 dB than the wind turbine.

Thus, less noise annoyance is expected from a not too near wind farm if residents are already exposed to road traffic sound levels of 55–60 dB(A). However, Pedersen *et al.* (2010) acknowledged that the noise problem is more pronounced at night when the masking effect of surrounding traffic and other noise sources are not present.

2.2.10.4 Biodiversity and birds

Bright *et al.* (2008) acknowledged that the main long term threat to birds is the climate change. On the other hand, one of the main measures to combat climate change, accordingly reduce the threat to birds' lives, is using renewable sources of energy and especially wind power. However, it is argued that wind farms also contribute to the mortality of birds. But according to Stankovic et al. (2009) the issue of biodiversity and birds mortality arose from lack of assessment and consultation with avian experts to avoid birds' migration paths, which is now part of any wind farm development. Accordingly, Bright et al. (2008) proposed a sensitivity mapping system where maps are produced for the paths of migrating birds and compared to proposed developments of wind farms to avoid any potential collision.

However, it should also be noted that Chiras (2010) acknowledged that the total number of birds killed by commercial wind turbines is 50 000 birds per annum, this number diminishes when compared to 270 million birds killed per year by cats only which means that wind turbines are not a main cause for birds mortality. To put the numbers in context, Sovacool (2012) researched the number of birds killed per kilowatt-hour kWh generated for wind electricity, fossil fuel, and nuclear power systems. The numbers showed that wind farms killed approximately 20,000 birds in the United States in 2009 but nuclear power plants killed about 330,000 and fossil fuelled power plants more than 14 million, which means that wind farms are the least cause for birds' fatalities. On the other hand, Carrete et al. (2012) asserted that these numbers might not be indicative of the magnitude of the problem since the current protocols of counting birds at specific points during particular periods of time have low predictive power, they recommend locally inspecting the relationship between mortality at existing turbines and their relative position within the spatial distribution of bird populations as this can guide managers in planning future

wind-farms and in managing currently operating developments to reduce the birds' mortality rates from wind turbines as long as it can be avoided.

2.2.10.5 Shadow flicker, sun ray reflection and property value

Shadow flicker occurs when the blades of wind turbine is in a position between the observer's eye and direct sunlight, as for sun ray reflection it happens when the incident sun ray falls with a certain angle to the blades of a wind turbine and reflects towards the eye of an observer. Both situations should be avoided to minimise nuisance. Jha (2010) asserted that the problem of reflections can be solved with a dull paint, as for the shadow flicker of a turbine blades located in the direct path of the sun's rays can be a nuisance to an observer near an operating wind turbine at visible frequencies below 20 Hz. Stankovic et al. (2009) acknowledged that in some cases the property value might decrease as a result of a wind turbine development or the integration of wind turbine in an urban area due to the noise emissions, and shadow flicker which has created an undesirable environment.

2.2.10.6 Electromagnetic interference

Although Tong (2010) acknowledged that small wind turbines have been widely used to provide electricity for remote telecommunication stations for both commercial and military applications without the report of any signal interference problem, Stankovic et al. (2009) asserted that the problem is true for large scale wind turbines when the blades have metallic components. However, it can be argued that this problem applies to any large obstacle. In the case of small-scale wind turbines for the built environment, Chiras (2010) asserted that these turbines have small blades that do not interfere with such signals. Moreover, the blades of modern wind turbines are made out of glass reinforced plastics, wood, plastic and fibreglass which does not interfere with telecommunications signals. Electronic interference has been a problem only in remote areas where television and radio signals are extremely weak. Even in such areas, adverse effects have been rare and localized.

2.2.10.7 Public's acceptance of wind farms

Wolsink (2000) and Eltham et al. (2008) acknowledged that when wind farms are being constructed, there are often objections from the local population near

the planned project which might result in planning permissions being declined. Although it was believed that these objections are based on the Not-In-My-Backyard (NIMBY) syndrome, Wolsink (2000) and Jones and Richard Eiser (2010) argued that NIMBYism is not the sole reason for objections against wind farms. The results from Jones and Richard Eiser (2010) research showed that the opposition was not determined by the location with respect to the project but is more related to the visibility of the development in addition to a concern about that the development would spoil the landscape, thus if the development is not visible by the locals although it is near to them, it is more likely to be accepted, however, they added that these results cannot be generalized, although they acknowledged that in general terms, local opposition to onshore wind developments is increasing.

Eltham et al. (2008) asserted that in order to reduce the opposition, developers and planning authorities need to engage and consult local populations in the early stages of the project so that concerns and objections can be addressed through effective dialogue between stakeholders which might have an effect in mitigating the proportion of locals responding negatively. Most of the reasons for opposing onshore wind turbines might not be viable for offshore wind turbines. This is why Haggett (2011) stated that offshore sites are more preferred because they are thought to remove the problem of public protests. However, it was argued that the public should also be included in decision-making about offshore wind farms, and that they have a key role which should not be underestimated. Similarly in the case of urban wind turbines and even the publics' opinion is more pronounced since the turbines will be operating within the built environment.

2.3 Urban wind energy

Since some of the hurdles facing large wind turbines can be overcome by small and micro wind turbines, this explains the increase in the deployed capacity of small scale wind turbine in the UK by 65% comparing end of 2010 to end of 2009. The most notably growth was noticed in the 10 – 20kW turbines with 416 units reported to have been installed in the 12 months to December 2010, up from 125 installed in the same size range in 2009 (RenewableUK, 2011b). According to Wu and Wang (2012), in China, the production of the small and

medium wind turbine has increased at a rate of 40% for the last 3 consecutive years and research on small wind turbines has been increasing rapidly due to the demand from the building environment sector. Another reason behind that growth is the financial incentives offered by governments in this sector. In the UK, RenewableUK expects that the contribution of small wind systems will continue to grow in response to continued financial incentives and increasing consumer interest in the small wind market.

As seen in the previous section, large scale wind turbines face some obstacles which encourage the implementation of wind turbines in a nonconventional way. Chiras (2010) argued that these problems are exaggerated and when it comes to urban wind turbines, some of these points are not valid. According to Booker et al. (2010) the main advantage of sitting a wind turbine close to a building is to generate the electricity where it is being used, thus reducing the costs and the energy loses in electricity due to transmission from the point of generation to the point of usage. Ritchie and Thomas (2009) argued that although there are imminent dangers of erecting wind turbines near buildings, their benefits outreaches the disadvantages and summarized those benefits in the following points:

- The probability of facing power shortages or failures is less since it is independent of the electrical utility grid.
- It saves substantial money on utility bills.
- It delivers electrical energy at lower cost especially at remote locations where electrical grids are not available.
- Although it is argued that wind turbines affect home values negatively, the installation can be easily removed, leaving no adverse visible effect at the installation site, thus not jeopardizing the value of a building.
- Unlike steam and gas turbine-based electricity generation systems, they do not require frequent maintenance or employment of operations personnel.
- Wind turbines integrated within cities can offer on-site off-grid electrical energy which is not possible with other conventional sources of energy.
- They do not ruin the natural landscape.

- Minimising the power losses during the transmission process from the point of generation to the point of consumption.
- They reduce the costs of cabling and infrastructure.
- In addition to acting as a visual message of tackling climate change.

Accordingly, the UK government has included local and micro-generation renewable energy schemes in its energy strategy. Thus, micro-generation, including micro wind turbines, is subject to a number of legislative drivers in the UK, including the Microgeneration Strategy, the Low Carbon Buildings Programme, the Renewables Obligation (RO) Order, the Code for Sustainable Homes, the Energy Performance of Buildings Directive, the Feed-in Tariffs and the Renewable Heat Incentive. Small-scale urban wind turbines are eligible for support through the feed-in tariff (FIT) scheme.

According to Walker (2012), the FIT was introduced in the UK in 2010 with the anticipation that it would result, with the RO, in supplying 2% of electricity supply from projects less than 5 MW installed capacity by 2020. The FIT is a price based mechanism, where prices are differentiated by technology. For 50 kW or less installed capacity wind turbines, they should be installed under the Microgeneration Certification Scheme (MCS) to ensure high levels of accuracy in estimating the expected output of the installed wind turbine in order to avoid labelling the technology as uneconomic due to wrong decisions regarding the installation locations and accordingly the expected power output.

However, in order to specify the optimum installation location and in order to efficiently integrate wind turbines within the built environment, Blocken and Carmeliet (2004) acknowledged the importance of understanding the aerodynamics of buildings from a Building Physics point of view. They asserted that, studying wind flow within the built environment has received relatively little attention in the Building Physics community. On the other hand, Hu (2003) acknowledged that studying urban wind flow has many applications in many fields such as the structural responses of buildings, natural ventilation, energy consumption, cladding design, snow accumulation, pollutant dispersion, pedestrian safety and comfort and integrating wind turbines within the built environment.

2.3.1 *Urban wind flow*

Willemsen and Wisse (2007) acknowledged that the correlation between urban geometry and local wind flows is poorly documented in literature and even the existing literature is related to technical issues which is not usable by designers and urban planners. However, according to the WINEUR (2007) report, the main two features characterising urban wind regime are lower annual mean wind speed compared to rural and open areas, and turbulent flow. Stankovic et al. (2009) asserted that one of the rules of thumb when siting a wind turbine within the built environment is to avoid areas of turbulence and low wind speeds. These areas differ according to different arrangements of buildings. But there are some general patterns of wake and disturbance areas as demonstrated in Figure 2.13, to avoid these regions the blades of the wind turbine should be high enough above the roof level; at position A, although the turbine is at low height, it avoids the highly turbulent region as for the positions B, C and D the turbines are located high enough above the highly turbulent region.

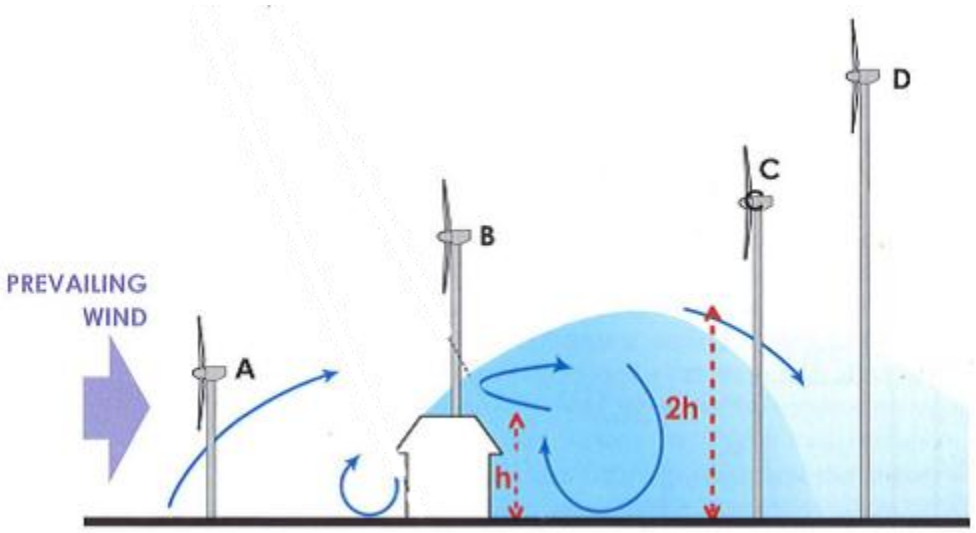

Figure 2.13 Proposed locations for mounting a wind turbine avoiding highly turbulent areas (Stankovic et al., 2009).

Generally, the turbine blades should be located twice the height of the tallest local obstacle to avoid a significant drop in potential performance. It should also be noted that some areas around the buildings are characterised by an increase in wind speed which can be utilised only if the building has been designed with wind energy in mind. In some cases, it is possible to plan and design a whole

development to accelerate and concentrate wind in particular areas using buildings and landscape to create artificial tunnels where urban wind turbines can be installed.

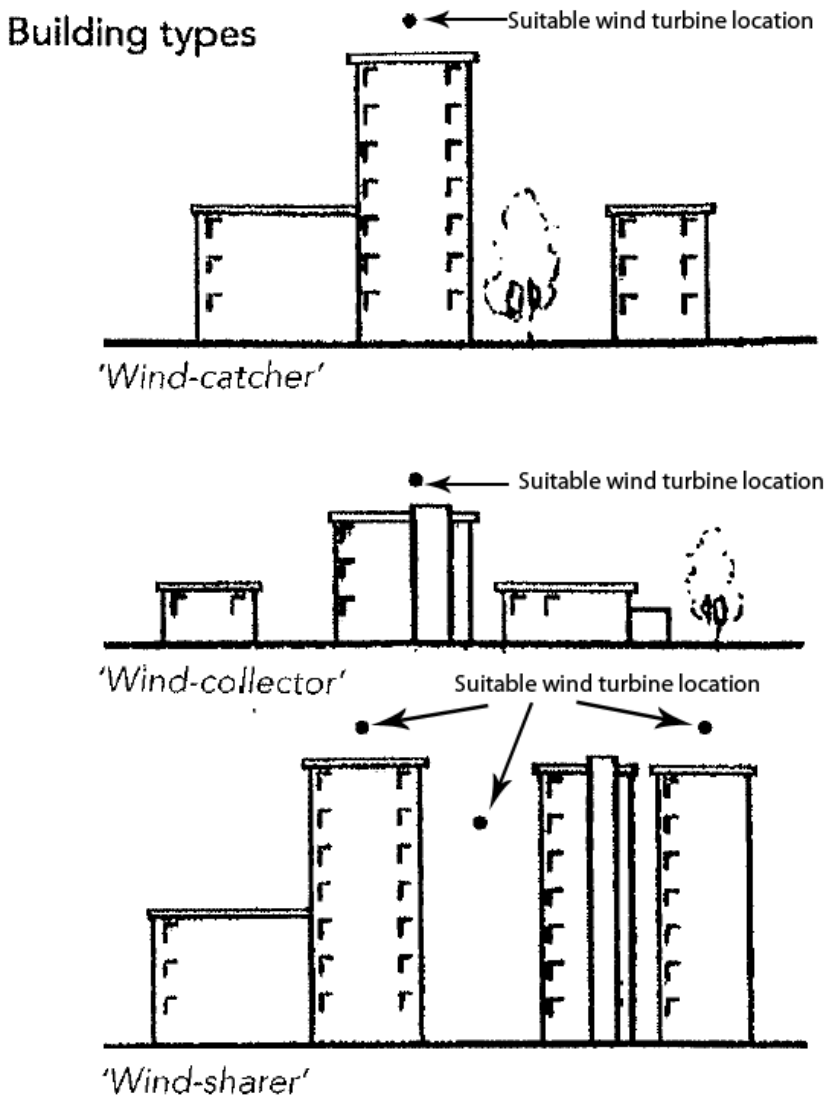

Figure 2.14 Categories of building cluster and their effectiveness for wind generation (Ritchie and Thomas, 2009).

A study by Delft University of Technology and Ecofys examined urban building types and identified three types (Figure 2.14) that are suitable for small-scale wind power utilization, these are:

- The wind-catcher type which is characterized by good height plus relatively free flow which makes small horizontal axis wind turbines suitable for mounting.

- The wind-collector type which has lower height than the wind catcher type and is situated within an area of more roughness height and the wind is more turbulent, which makes the vertical axis wind turbines more preferable.
- The wind-sharer type which can be found in industrial areas and business parks where the roof heights are relatively even and the buildings are spaced out which accelerates wind but with high levels of turbulence (Smith, 2003; Smith, 2005; Ritchie and Thomas, 2009).

2.3.2 *Wind flow around buildings*

According to the WINEUR (2007) report, it is difficult to precisely evaluate and predict wind flow around a building within an urban area due to the unpredictability of wind flow since many variables affect the flow such as vegetation, adjacent buildings, street furniture, moving and stationary vehicles, etc. Sara Louise (2011) and Balduzzi et al. (2012) acknowledged that these features form the surface roughness layer which extends to at least 1 to 3 times of their height where wind flow is highly irregular, unpredictable and strongly affected by the surface features. According to Jha (2010), the variations in the surface features differs from one terrain to another and can be represented by the roughness length (z_o) which varies from 1 x 10^{-4}m over a water surface to 1m over cities (Table 2.1).

Reiter (2010) and Grant and Kelly (2004) described the flow around a simple isolated building as a complex 3D flow which is highly turbulent and transient. The main characteristics of the flow can be quantified as corner effect, passage effect, front vortex, wake effect, separation and reattachment[2]. Dannecker (2002) elaborated that when the wind meets an isolated building or a building which is relatively higher than the surrounding buildings, much of the approaching wind is accelerated and deflected downwards, at the building corners the flow separates and accelerates forming high speed jets which extends in the leeward direction of the building.

[2] A more detailed discussion on wind flow around a typical building will be discussed in chapter four when carrying out the validation study.

Table 2.1 Roughness lengths of terrain surface characteristics (Jha, 2010).

Terrain surface	Roughness length (m)
City	1.0
Forest	0.8
Surface with trees and bushes	0.2
Farmland with closed appearance	0.1
Farmland with open appearance	0.05
Farmland with few buildings	0.03
Bare soil	0.005
Snow	0.001
Smooth sand	0.0003
Water	0.0001

The accelerating effect that takes place is due to the relatively low pressure downwind of the building. This difference in pressure between the leeward and windward direction of the building creates a recirculation area which extends in the leeward direction based on the aspect ratio of the building. However, the effect of the building on the leeward flow will continue for a distance downstream which corresponds to several building heights. Jha (2010) added that this kind of flow is characteristic of a flow around a bluff building[3] where an early separation of the boundary layer from the surface is pronounced contrary to an aerodynamic building where usually a thin boundary layer is attached to the surface of the building. However, it should be noted that the characterization of a building as aerodynamic or bluff depends also on wind flow direction.

[3] Bluff body is the opposite of a streamlined body. Air does not pass smoothly around a bluff body but will separate at some point, leading to areas of reversed flow and high turbulence. Most buildings and structures are bluff bodies, often with sharp edges (source:http://www.ice.org.uk/Information-resources/Document-Library/Glossary-of-wind-terms-used-in-construction, accessed: 14/09/2012).

2.3.2.1 Turbulence

Due to the complexity and the variety in elements forming the built environment, wind patterns around buildings are unpredictable and wind flow is highly turbulent. High levels of turbulence mean an increased energy in wind, but not all this energy is extractable by the integrated wind turbine due to the randomness in the direction of the wind. These conditions are not favourable for horizontal axis lift type wind turbines.

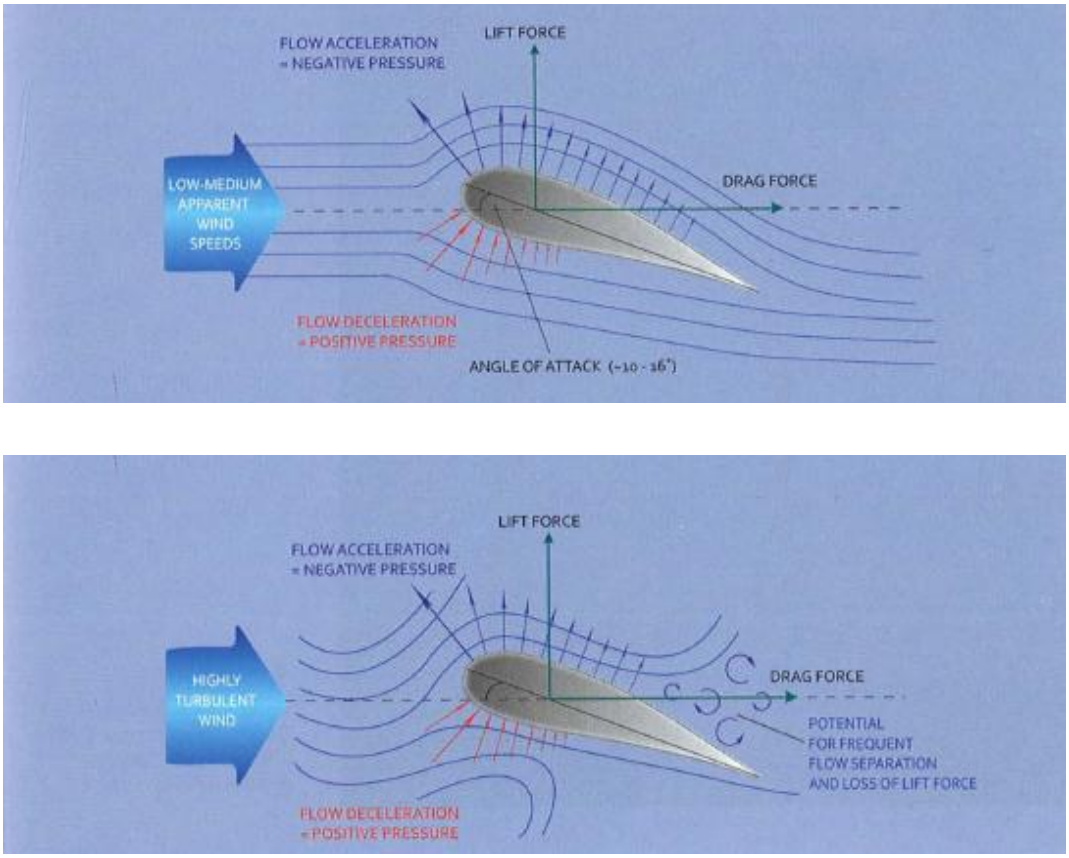

Figure 2.15 Attachment of flow to the blade (top) with the right angle of attack, while flow separates from the blade (bottom) due to skewed flow causing high levels of turbulence leeward the blade (Stankovic *et al.*, 2009).

Accordingly, Devinant et al. (2002) acknowledged that the energy yield of lift-type wind turbines will be decreased as a result of the turbine constantly trying to yaw into the wind and even when aligned with the wind, the wind will hit the blades at a non-optimal direction for the blade design. In Figure 2.15, top image; the wind flows over the blade generating maximum lift and minimum drag, with the flow skewed to the blade, bottom image, less lift is generated and drag increases. This is why Smith (2003) stated that vertical axis wind turbines are more likely to be used within urban areas for energy generation purposes as

they are more able to operate at lower wind speeds and they are less stressed mechanically by turbulence.

However, within urban areas, wind speed increases giving the opportunity for integrating wind turbines on top of high-rise buildings where the building can serve as a mast for the wind turbine. But Jha (2010) noted that turbulence within the built environment is highly dependent on buildings heights, the higher the buildings heights the more turbulence will be generated and the more the wind speed. However, Ritchie and Thomas (2009) noted that at lower altitudes wind speed will be reduced due to the uneven urban terrain, a wind speed not less than 4m/s and turbulence intensity[4] of 10% are good conditions for the operation of wind turbines for energy generation purposes, but these values differs from wind turbines manufacturer to another (Ritchie and Thomas, 2009).

2.3.2.2 Stagnation point, separation and reattachment

According to Freathy and Salt (2010), when wind hits a building or an obstacle the streamlines change direction at a particular location. The streamline which is located at the point of changing direction and the division of the flow takes place, it comes to rest and the wind speed at that point is equal to zero. This point on the building is called the stagnation point which is characterized by maximum pressure since the dynamic pressure in the approaching wind is converted to static pressure (Figure 2.16).

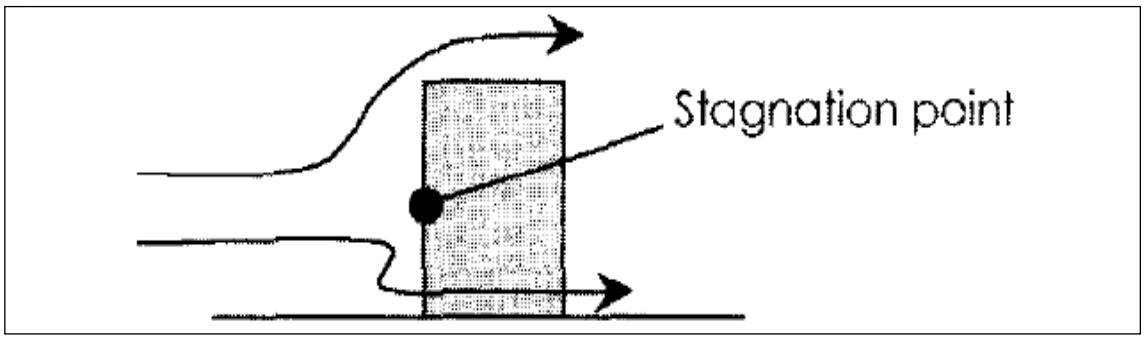

Figure 2.16 Stagnation point (Freathy and Salt, 2010).

[4] Turbulence intensity is the standard deviation of wind speed divided by the mean wind speed based on 1-minute averaged data that is sampled at 1 Hz (source: http://www.smallwindcertification.org/for-consumer/consumer-resources/definitions/, accessed: 04/09/2012).

Separation occurs when the flow separates or goes away from the surface of the building leaving below it a recirculation area where the flow in that area is mostly characterized by flowing in a reverse direction of the main flow. It is called separation to distinguish it from smooth flow which is attached to the surface of the building. Normally separation happens with sharp edged buildings, as for curved buildings separation might happen at the leeward direction of the curved body. The location where the separation occurs is called the separation point. That point has very high energy content due to high levels of turbulence, so if a wind turbine which can withstand high levels of turbulence is installed, it would yield significant amount of electricity (Figure 2.17).

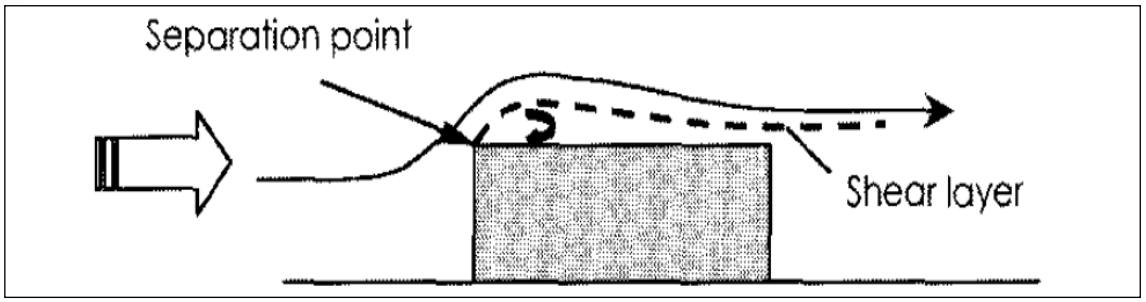

Figure 2.17 Separation (Freathy and Salt, 2010).

If the building is long enough in the downwind direction and the flow around it experience separation, it may reattach again to the building and the streamlines would be flowing parallel to the building surface. The area below the separated region is sometimes called the separation bubble or recirculation area (Figure 2.18) (Freathy and Salt, 2010).

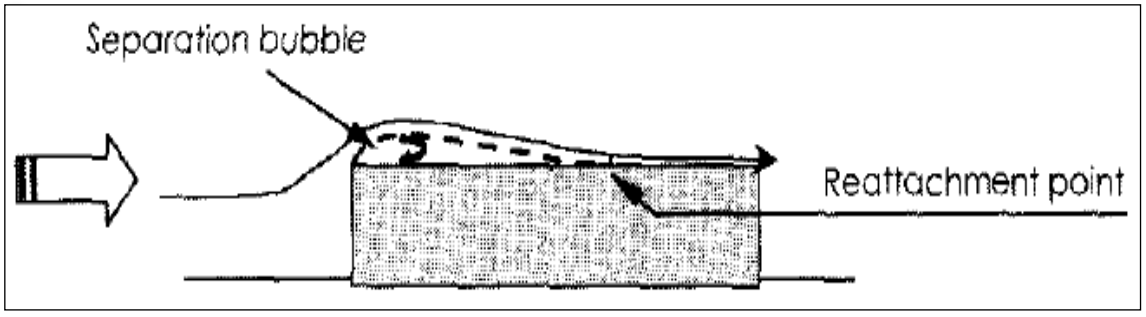

Figure 2.18 Reattachment (Freathy and Salt, 2010).

2.3.2.3 Wake and recirculation zone

Due to the obstruction of the building to wind flow, a recirculation zone is created in the windward direction of the building forming a front vortex (called a standing vortex) at the foot of an isolated building (Figure 2.19). The characteristic length of the vortex and the wind speed in this zone is related to the height of the building (Reiter, 2010).

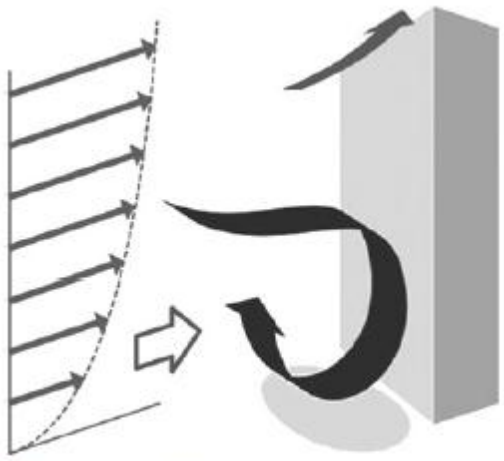

Figure 2.19 The standing vortex windward the building (Reiter, 2010).

2.3.2.4 Accelerating effect of buildings

As in onshore wind farm location specification, sites are chosen where natural acceleration occurs, such as hill tops or slopes up from coastal regions, urban wind turbines can also benefit from the accelerating effect of buildings. Accordingly, when the subject of wind enhancement is approached, visions of aerodynamic shapes accelerating prevailing wind into turbines may be adopted. However, it is more practical to understand and implement the accelerating effect of the most common normal sharp edged buildings, but it should be noted that in order to benefit from the accelerating effect of buildings, they should be designed with wind turbines in mind or else the likely result will be a drop in energy yields (Stankovic et al., 2009).

One of the main urban wind phenomena is the accelerating effect that happens at the edges or corners of buildings. Due to the difference in pressure between the windward and leeward zones (Figure 2.20), the wind speed is increased compared to the wind speed at the same location without the building in place. Reiter (2010) found that this accelerating effect is highly dependent on the

building height and independent of building length. Several simulations were carried out with different buildings heights and constant length and width and it was noticed that the acceleration effect increase with the increase in the building height. Other simulations were carried out varying building's length and fixing building height and the results were not changing. Thus, it was confirmed that building height is a key parameter influencing the accelerating effect around a single building: the higher the building, the more the accelerating effect.

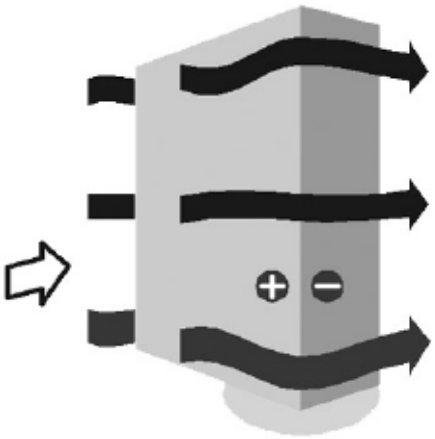

Figure 2.20 The accelerating effect that happens at the corners of buildings due to differential pressure (Reiter, 2010).

Other areas of wind acceleration within the built environment are the passages between buildings (Figure 2.21). This is called the double corner effect, where two adjacent buildings squeeze the wind between them which leads to an increase in the wind speed. Fixing a passage width of 8m and varying the buildings' height, Reiter (2010) noticed the increase in wind speed between the two buildings with the increase in height. Comparing this case with the accelerating effect of a single isolated building, it was noticed that the magnitude of acceleration in the double corner effect is more than that of the single corner effect. It was also noticed that the double corner effect does not exist if the passage width is less than 6m. Similar results were obtained by Blocken et al. (2008).

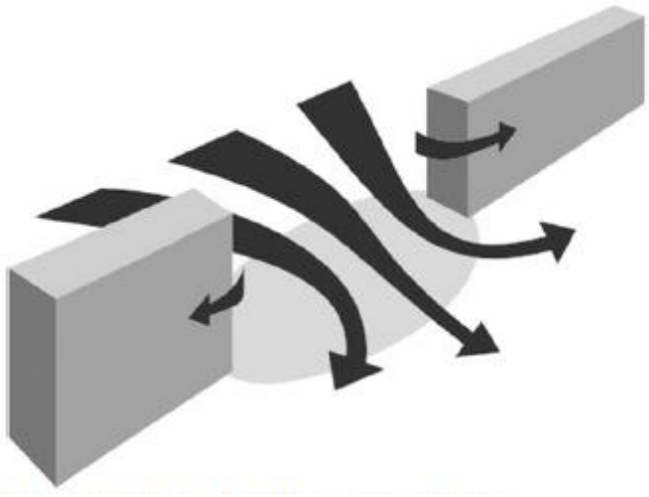

Figure 2.21 The accelerating effect in the passage between two buildings (Reiter, 2010).

Blocken et al. (2008) acknowledged that one might expect more increase in wind speed at the passage between two buildings if the two buildings are arranged in a converging configuration rather than a diverging configuration. Blocken et al. (2008) acknowledged that this assumption was previously based on the Venturi effect which has been defined as the increase in fluid speed or flow rate due to a decrease of the flow section. They argued that this effect is only valid for flow within closed channels which is not the case for the built environment where the flow is not confined and only part of the approaching flow passes through the passage between the two buildings while most of it flows over and around the building (Figure 2.22).

Their simulations and wind tunnel test revealed the validity of their assumptions. They attributed this to the wind-blocking effect which refers to the slowdown of wind speed upstream of the buildings. This effect is more pronounced for the converging arrangements that catch the wind and significantly slow down a large mass of air over quite a large distance upstream of the passage causing the wind to flow over and around the buildings than being forced through the narrow passage opening. However in the case of the diverging configuration, such blocking effect does not exist leading to more wind acceleration between the diverging configuration rather than the converging configuration.

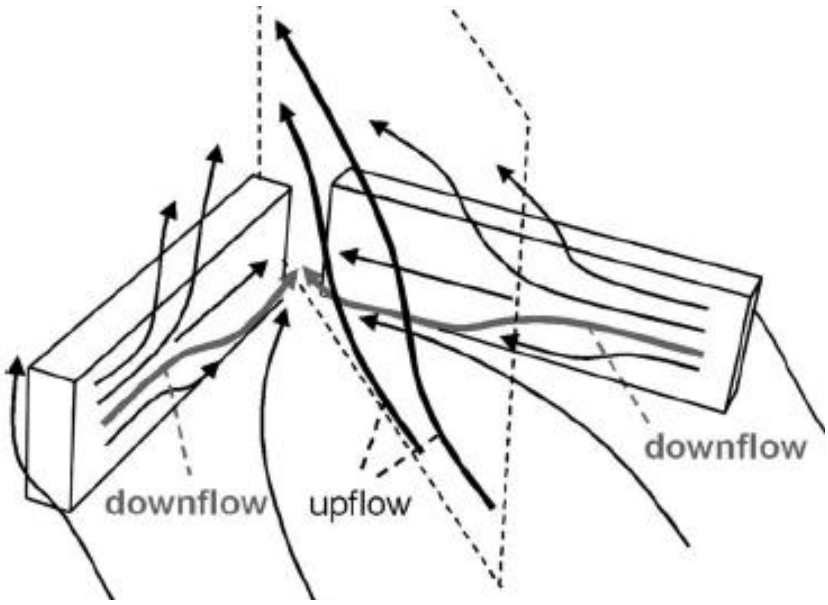

Figure 2.22 3D of the flow through the converging configuration showing the escape of the flow above the converging configuration (Blocken *et al.*, 2008).

2.4 Urban wind turbines

With the advancements in wind turbines technology, small and micro wind turbines can overcome the unfavourable wind condition in urban areas. For example, according to Bahaj et al. (2007), the emergence of urban wind turbines in the UK is driven by the advancements in turbines design and technology in addition to the available financial incentives offered by the government in light of the increasing energy prices and the growing interest among the public in urban wind turbines although there is a paucity of knowledge in the public domain to confirm this. Also, Grant and Kelly (2004) added that the emergence of urban wind turbines is due to the shift in approach from centralised power production to production of heat and power at the point of use. However, Booker et al. (2010) pointed out that the success of wind turbines installations in the urban or built environment has been variable and considering transferring familiar technologies to urban wind turbines is not straight forward or might not even be applicable. Thus, they argued that more research is still needed to develop new typologies of VAWTs and HAWTs designs which implement more efficient generators able to cope with the urban wind characteristics.

Ackermann and Söder (2002) noted that urban wind turbines are different from large scale wind turbines in many aspects. In terms of blades design, small-

scale wind turbines require different aerodynamic profile to large–scale wind turbines due to the difference in tip speed to wind speed ratio. Blades of large scale wind turbines are more advanced in terms of aerodynamic design than small scale wind turbines which affect to a great extent the coefficient of performance of the wind turbine. The high tip speed ratio of the small-scale wind turbines have a direct impact on the transmission-generation system which is most likely to be a direct driven, variable speed system with a permanent magnet which requires a power converter if a constant frequency is needed. Direct driven systems are more reliable and require less maintenance. Also, small-scale wind turbines power and speed regulation systems are different from large-scale wind turbines, mechanically controlled pitch and yaw systems are used which is different from the electronically controlled system of the large-scale wind turbines. In addition, small–scale wind turbines have relatively tall towers in relation to the rotor diameter, as they need to reach undisturbed wind flow above windward obstacles.

Also, Bahaj et al. (2007) acknowledged that urban wind turbines will always suffer from being installed in unfavourable locations compared to large scale wind turbines due to their sitting at low heights within dense urban areas. They also added that it is not evident that urban wind turbines would be the norm in urban areas due to the changing wind directions in urban areas, since the wind flow at such low altitudes will be governed by local effects where turbulence will be prominent in such cases, thus the way forward for urban wind turbines would be at seaside locations where sea breezes occurs and at the countryside and suburban locations where the obstacles are less.

Thus, Booker et al. (2010) acknowledged that there are a number of technical issues which need to be addressed when developing wind turbine systems for urban areas, these are:

- System type: static, integrated with building/structure, yawing system, with/without collector and/or diffuser;
- System attributes: self-starting, safe, low noise, low vibration, robust design to the service conditions, minimal maintenance, low installation weight, high power per active volume of material;

- Location: aesthetics, building/infrastructure strength, electromagnetic interference with existing electrical installations, space for other equipment e.g. inverters, monitoring devices etc.

Another aspect which Stankovic et al. (2009) also pointed out is the difficulty of the sourcing of small-scale wind turbines when compared to large ones. However, they argued that old low capacity wind turbines can be reengineered and used within the built environment. But in order to maximise the energy yield of the integrated wind turbines within the built environment, the WINEUR (2007) report asserted that the following points should be considered:

- Turbines should be preferably placed on large buildings with a flat roof.
- Investigate which turbine type and model is the best for the chosen building and location.
- Deploy multiple turbines at the same location if possible.
- Investigate if the building and the surroundings are suitable for urban wind turbines (UWTs) deployment.
- Ensure acceptance of the turbines in the neighbourhood.
- Investigate the visual impact: the blade movements may bring a certain dynamic appearance to the area, however flicker or general visual disturbances are also possible.
- Concentrate the deployment in certain targeted areas.
- Ensure that the turbines are recognised in the spatial development plan and that the deployment plans respect the vision other stakeholders have about the location.
- Give enough attention to the aesthetic aspects of the integration. The turbine needs to visually integrate well with the building and the area.

In terms of integrating wind turbines within the built environment, there are four main types of integration. According to Dannecker (2002), wind turbines integrated within the built environment are classified based on their positioning in relation to the buildings. The main aim is to capture high speed low turbulence winds. Thus, urban wind turbines are either

- Freely standing on very high posts within the built environment (building integrated wind turbines) or

- Mounted on buildings' surfaces such as roof tops (building mounted wind turbines) or
- Fully integrated within the building (building augmented wind turbines) or
- They can be within ducts in the building (ducted wind turbines).

2.4.1 *Building integrated wind turbines (BIWTs)*

Dutton et al. (2005) described building integrated wind turbines as free standing wind turbines which are capable of working close to buildings and taking advantage of the augmentation in wind flow caused by surrounding buildings, they can be retrofitted into existing urban areas or incorporated in the design of a new urban area where the whole design account for the existence of the wind turbine. Although the building integrated wind turbine may yield more power than the building mounted wind turbines, the cost per kilowatt tends to be relatively high (compared to medium/large scale wind turbines) in part to cover for required foundations, tower and cabling.

Figure 2.23 The building integrated wind turbine in a BP station in London (Stankovic *et al.*, 2009).

Example of this type is the small standalone turbine at the Mile End Ecology Centre in London and the wind turbine at a BP station, Wandsorth, London which is a 6kW turbine with blade diameter 5.5m (Figure 2.23) (Aguiló et al., 2009). Another example of this type is the installation of three 15kW wind

turbines at the ZEBRA (Zero Emission Building Renewing Alnwick) project (Figure 2.24) where the predicted energy supply was 60,000kWh/year.

Figure 2.24 The three 15kw wind turbines at the ZEBRA project (Source: http://alnwick.journallive.co.uk/news/alnwick-divided-by-willowburn.html, accessed: 14/09/2012).

According to the WINEUR (2007) report, this type of integration within the built environment is usually implemented where open areas and fields are available within the built environment such as school playing fields and parks. According to Stankovic et al. (2009), the main consideration for this type is the support system of the wind turbine. Lattice towers or cable supported steel towers can be used. Lattice towers have to be secured and look secured as well in terms of thickness of the tower, which would have cost implications, as for cable supported towers, enough space should be available for the extended supporting cables.

The height of the tower is an issue as well as the wind turbine should be mounted at heights where turbulence is minimum and wind speed is adequate. However, this might be limited by planning constrains or manufacturers specifications for towers. This is why it is important to make a complete assessment for the wind resources at the proposed site and choose the suitable wind turbine. Towers of building integrated wind turbines can also be implemented as support for advertisements, energy generation, branding, street lighting, urban art, or signposting (Figure 2.25). However, the effect of these elements on local wind flow should be carefully assessed in order not to affect the energy yield of the wind turbine (Stankovic et al., 2009).

Figure 2.25 BIWT towers used for advertisements and publicity (Stankovic *et al.*, 2009).

2.4.2 *Building mounted wind turbines (BMWTs)*

According to the Royal Institute of British Architects (RIBA, 2006), building mounted wind turbines are gaining interest among the public. However, one of the main obstacles facing this type is obtaining planning permission, but there are few examples of permitted roof mounted wind turbines in some local councils, most of these are HAWTs as VAWTs are still under development. These installations are more likely to contribute to the electricity supply within the built environment. Dutton et al. (2005) and Webb (2007) described building mounted wind turbines as physically linked to buildings where the building acts as a vertical post for positioning the wind turbine to exploit the desirable wind flow augmentation caused by the building.

Since, the built environment is so complex, Anderson *et al.* (2008) argued that the urban context would have a great effect on the flow on top of the roof and most likely it is going to be highly dynamic, turbulent and includes a vertical component. Even on the same roof, the conditions can differ significantly from one location to another. Accordingly Dannecker (2002) acknowledged the importance of specifying the optimum mounting location on top of the roof.

According to the WINEUR (2007) project, the most influential parameter affecting local wind flow above the roof is the shape of the roof. Dutton et al. (2005) also noted the importance of the effect of roof shape on local wind flow and acknowledged the need for investigating the effect of different roof shapes on wind speed and turbulence intensity and how would that increase the energy yield of roof mounted wind turbines, which is the aim of this research. In addition to choosing the optimum mounting location, the building should be structurally capable of supporting the wind turbine and also the building should provide reduction in vibrations and noise emissions.

Anderson *et al.* (2008) studied the Green Building in Temple Bar, Dublin, as an earlier attempt for mounting three small horizontal-axis wind turbines combined with solar hot water and photovoltaic collectors (Figure 2.26). The application resulted in excessive noise, vibration, and eventual cracking of the turbine blades. The wind turbines were determined to be uneconomical and were eventually replaced by photovoltaic cells.

Figure 2.26 Left: The Green Building in Temple Bar, Dublin / Right: The Kirklees council building (civic centre 3) in the town centre of Huddersfield, UK (Anderson *et al.*, 2008).

Another example is the Kirklees council building (civic centre 3) in the town centre of Huddersfield, UK which was retrofitted to house a large array (143m^2) of solar photovoltaic panels and two 6kW wind turbines to generate electricity and a set of solar energy collectors (48m^2) to heat the building's water (Figure 2.26). The Council wanted to demonstrate leadership in reducing its building's carbon footprint by around 8% and reduce dependency on grid generated electricity. The estimated electricity generated from the photovoltaic array and the wind turbine was estimated at 5% of the total electricity demand. However, similar to the Green building in Temple Bar, the wind turbines failed to generate

a reliable electricity supply and were eventually disconnected from the grid and left to promote a demonstration of good intentions. Roof mounted wind turbines in both cases were seen as an expensive add on. In the case of Kirklees council building £15,000 were spent on preparing the roof to take the structural load, vibration and improve the insulation of the roof (Kirklees Metropolitan Council, 2006).

However, according to Smith (2003), it can be argued that similar projects retrofitting existing buildings with urban wind turbines are not always a feasible approach, but if the building was designed in the first place with wind power in mind, the results might be better. These concerns about noise, vibration and energy yield can be eliminated if wind assessment is carried out and the right wind turbine is used at the optimum mounting location. It was argued that the triple-helix vertical-axis quietrevolution (QR) wind turbine is ideal for urban situations (Figure 2.27). It is rated at 6kW, producing 10,000 kW hours per year at average wind speeds. Free-standing, it is around 14m high with a swept area of 3m. Mounted above buildings; its height is 8m. In addition, it is cost-effective which makes it attractive to business and housing developers.

Figure 2.27 Quietrevolution (QR) VAWT (Source: http://www.quietrevolution.com/, accessed: 21/08/2012).

Ritchie and Thomas (2009) acknowledged that in the future it is likely to see combined systems of wind turbines and PV modules fully integrated with the roof design. In their conceptual design of a building mounted wind turbine,

Sharpe and Proven (2010) argued that building mounted wind turbines should be flexible in design to be fitted either on top of the roof or on the edges of buildings, they developed a new concept for a Darrieus VAWT called Crossflex which has a flexible blade system, utilising a lightweight cowling system which provides augmented airflow and improved visual integration into buildings, it also has a modular form which can be sited on ridges and corners of buildings to provide useful levels of generation (Figure 2.28).

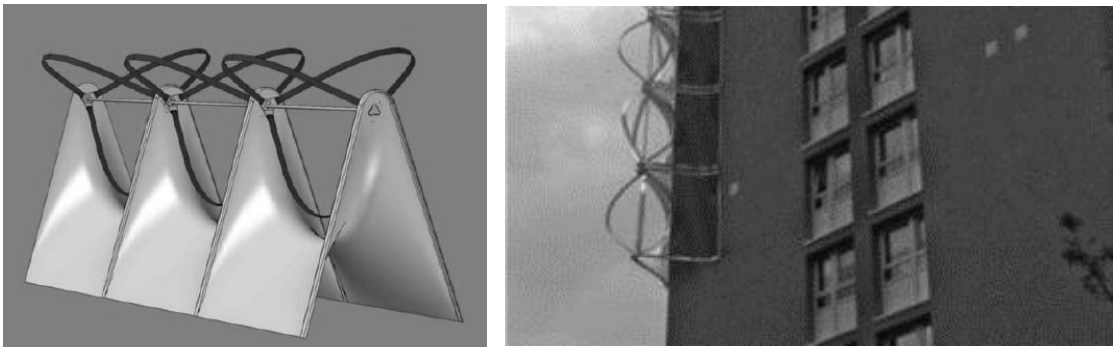

Figure 2.28 Left: Crossflex concept image, Right: graphical representation of installing the Crossflex VAWT to the edge of a building (Bhutta *et al.*, 2012).

Although each installation is case specific, there are some basic guidelines, extracted from literature (Smith, 2003; WINEUR, 2005; Bahaj et al., 2007; WINEUR, 2007; Encraft, 2009; Müller et al., 2009; Stankovic et al., 2009), for mounting wind turbines over roof tops, these are:

- For flat roof mounted HAWT, it should be placed near the middle of the roof at a height between 35 to 50% of the height of the building.
- If it is not possible to mount the turbine high enough due to planning limitations or any other reason, it is preferable to use VAWT which can withstand high levels of turbulence.
- If a wind turbine to be mounted at the edge of the building, there should be a vertical clearance between the building edge and the sweep of the turbine to avoid areas of turbulence.
- The building integrating the wind turbine should be higher than surrounding buildings with about 30 to 50% of the height of the surrounding buildings.
- A complete wind assessment should be carried out keeping in mind the prevailing wind direction and its effect on building orientation.

- The minimum wind speed at the site should be more than 5 m/s and the turbulence intensity less than 10%.
- Suitable supporting structure and access for a crane are important.
- Measures must be taken to provide adequate strength in the building structure which is not easily achieved in retrofit situations.

2.4.3 *Building augmented wind turbines (BAWTs)*

According to Dutton et al. (2005) and Jha (2010), BAWTs are those wind turbines capable of providing concentrated energy from aerodynamically shaped buildings. In this type of integration the form of the building harnesses wind to be driven towards a turbine. The building form acts as a support for the integrated wind turbines and a wind collector. Here, the architect plays a major role in sculpting the building to be based on aspects related to aerodynamics and a successful installation of BAWT requires a comprehensive knowledge of buildings aerodynamics, wind energy, wind energy conversion and cost-effective concentration schemes. The building design may require some modifications based on wind flow assessment using wind tunnel tests or CFD simulations. Smith (2003) acknowledged the increasing interest among architects in incorporating wind turbines in their designs and using the form of the building to funnel wind. Denoon et al. (2008) illustrated a number of new developments that were based on the principle of aerodynamic building form to enhance the performance of the integrated wind turbines. For example Figure 2.29 includes the Bahrain World Trade Centre, Pearl River Tower in China, Strata SE1 project in London, all implemented BAWTs (Peel and Lloyd, 2007; Cochran and Damiani, 2008).

The Bahrain World Trade Centre Tower is formed to collect and squeeze wind flow between the two towers where the horizontal axis wind turbines are placed. Killa and Smith (2008) stated that the funnelling of the Bahrain World Trade Centre towers has the effect of amplifying the wind speed at the turbine location of up to 30% which would result in the turbines providing the building with 11% to 15% of the electrical energy needs. Frechette and Gilchrist (2008) argued that the same funnelling effect is implemented in the Pearl River Tower where the building incorporates four large openings, approximately 3 x 4 meters wide. The facades are shaped to decrease the drag forces and optimize the wind

velocity passing through the four openings. These openings function as pressure relief valves for the building.

Figure 2.29 From left to right: Bahrain World Trade Centre, Pearl River Tower in China, Strata SE1 project in London (Peel and Lloyd, 2007; Cochran and Damiani, 2008).

Mithraratne (2009) acknowledged that building form manipulation based on wind flow assessments would play an important role in reducing the turbulence around buildings by 10–15% which is responsible for reducing energy production from building integrated wind turbines. A concept patented by Altechnica of Milton Keynes demonstrates the form of the roof can be implemented to accommodate wind turbines (Figure 2.30).

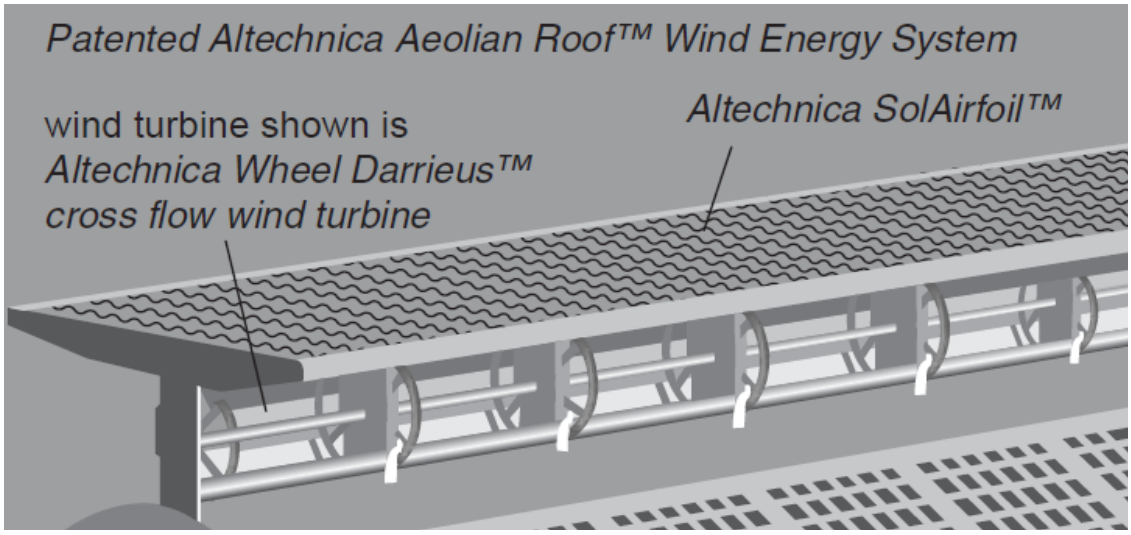

Figure 2.30 Altechnica's Aeolian Roof (Source: http://what-when-how.com/wp-content/uploads/2011/07/tmp1E51_thumb2.jpg, accessed: 21/08/2012).

The system is designed to be mounted on the ridge of a roof or at the apex of a curved roof section. Rotors are incorporated in a cage-like structure which is

capped with an aerofoil wind concentrator. The flat top of the aerofoil can accommodate PVs where the rotors are mounted at the apex of a curved roof, the effect is to concentrate the wind in a manner similar to a cowling. The advantage of this system is that it does not become an over-assertive visual feature and it is perceived as an integral design element. It is also a system which can easily be fitted to existing buildings where the wind regime is appropriate.

Another concept design for BAWT is the 'flower-tower' by Bill Dunster Architects in their SkyZed concept which is a multi-storey residential block consisting of four lobes which, on plan, resemble four petals of a flower. Smith (2003) noted that the curved shapes of the four parts serve to accelerate wind towards the central void of the composition where vertical axis wind turbines are integrated (Figure 2.31). It is said that the form of the building would increase the wind velocity at the turbines location four times more than if the building was not there. This would be sufficient to power several vertical axis turbines stacked over each other.

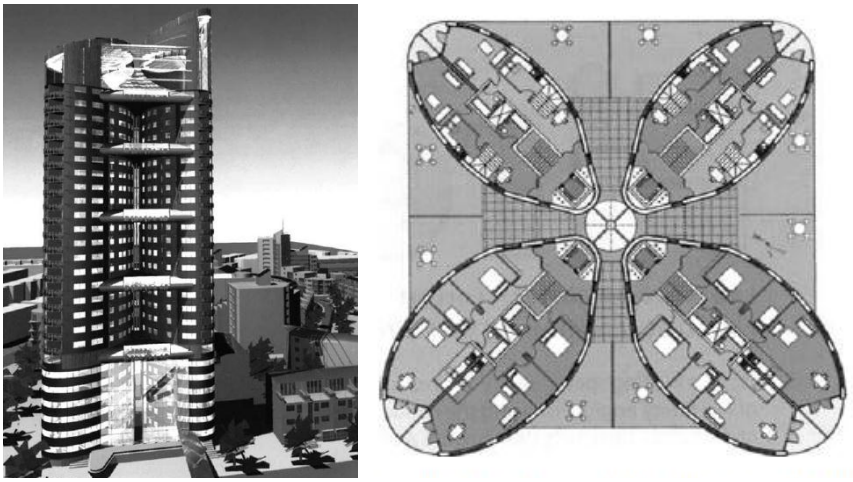

Figure 2.31 SkyZed tower: 3D model (left) and plan (right) (Smith, 2003).

Although Dannecker (2002) acknowledged in 2002 that the idea of integrating large power vertical axis wind turbines within aerodynamically shaped buildings was still developing and only appearing in designer's ideas and sketches for futuristic buildings like the concept zed tower of Future systems in 1989 (Figure 2.32), it can be argued that this is still true as only few buildings such as the Bahrain World trade Centre, Pearl River Tower and Strata SE1 buildings has been built since then and it is so hard to get data on the performance of the

integrated wind turbines to assess their performance. Accordingly, Müller et al. (2009) noted that it cannot be assumed that such projects will become the norm as urban wind turbines may not always be visually appropriate and hence not be put forward by architects and designers. Therefore, a successful wind turbine design needs to be integrated to add to the architectural value of the building.

Stankovic et al. (2009) acknowledged that this approach requires careful design of the spaces around the integrated wind turbines in order to maximise the usage of the spaces which are sculpted based on aerodynamic concepts, otherwise sculpting the building to capture wind would result in spaces which cannot be used architecturally. In addition, Dannecker (2002) asserted that it is not practical to aerodynamically shape the building as a flow augmenter to work as a huge power plant, rather than that the utilisation of simple wind power devices within the usual structure of conventional buildings like roof mounted wind turbines or ducted wind turbines are more practical . Example of this is the implementation of ducted wind turbines which can be integrated as modular units within the building structure. According to the WINEUR (2007) report, this kind of integration will minimise the visual impact and their small size will keep possible noise emissions minimal.

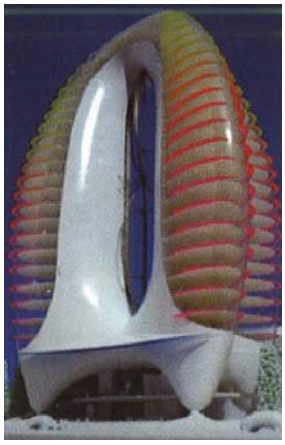

Figure 2.32 Project ZED conceptual building integrating VAWT (Stankovic *et al.*, 2009).

2.4.4 *Ducted wind turbines (DWTs)*

Another form of the turbine confined in a casing for wind concentration purposes is the ducted wind turbine (DWT). According to Grant and Kelly (2004), unlike conventional wind turbines, DWTs were initially developed for

integration into the built environment. The main features of DWTs are that they are mostly a VAWT and the blades are fully enclosed in a casing (Figure 2.33). The casing is used to guide the horizontal flow vertically through the VAWT where the difference in pressure between the inlet and the outlet of the unit is utilised to turn the VAWT. The form of the duct, the inlet, the outlet and the installation of spoilers play a major role in the energy yield of the installed wind turbine (Dannecker, 2002).

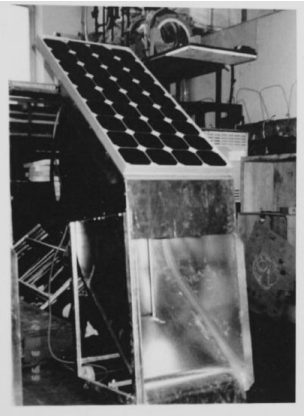

Figure 2.33 Casing of a ducted VAWT (Dannecker, 2002).

Smith (2003) acknowledged that a development from the 1970s has placed the turbine blades inside an aerofoil cowling (Figure 2.34) and a prototype was developed at the University of Rijeka, Croatia, where the energy yield of such configuration is claimed to have increased by 60% compared to free standing, unconfined wind turbine. This is attributed to the accelerating effect of the aerofoil concentrator which enables the turbine to operate at slower wind speed as it collects more wind from different directions and directs it towards the blades of the turbine.

However, at high wind speed, there is the danger of excessive stresses on the blades, but this was solved by introducing hydraulically driven air release vents into the cowling, which are activated when the pressure within the cowling is too great. The main problem which remains is the extra initial cost of the machine due to the usage of extra material for the cowl, but this can be ignored on the long run when compared to the increase in energy yield.

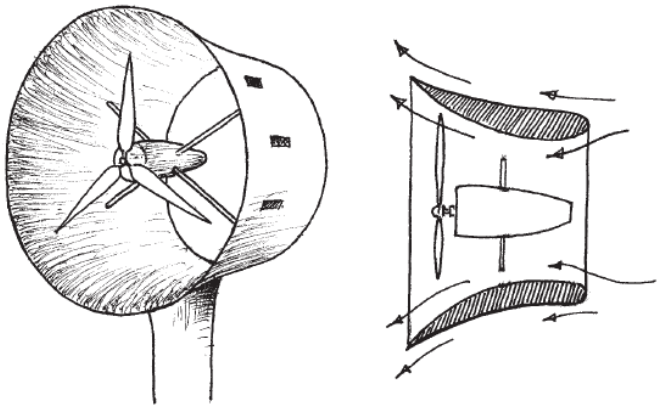

Figure 2.34 Wind turbine with cowling wind concentrator (Smith, 2003).

Grant and Kelly (2004) acknowledged that the enclosure of the blades in a duct has several advantages:

- More secured in the case of blade shedding or failure.
- More energy yield than the conventional wind turbines due to higher pressure differences.
- Easily integrated within the architectural design.
- Visually, less obtrusive.

On the other hand, Sharma and Madawala (2012) added that it should be noted that if wind speed exceeds 16m/sec the improvement in the shaft performance will not be significant. In addition, adding a concentrator requires more material and might not be economic, especially when comparing the increase in energy yield from a ducted wind turbine with a slightly bigger rotor size wind turbine. Thus a careful economic assessment should be undertaken before making the decision of using ducted wind turbines as they are usually more expensive than normal wind turbines.

2.4.5 *Feasibility of small and micro wind turbines*

According to the Royal Institute of British Architects (RIBA, 2006), large scale wind turbines are considered one of the most feasible renewable sources of energy, this is attributed to the reduced unit output cost due to the large scale of installations. This is not the case for small and micro wind turbines where the capital cost is very high per kW installed, in addition, other constrains include siting location, visual intrusions and noise which make its social feasibility also questionable. However, they still have the advantage of generating electricity

where it is being used, thus sparing the extra costs of distribution networks and avoiding loses in electrical power due to transmission. Thus, in order to assess the feasibility of an urban wind turbine installation, not only the economic aspects should be considered, but also other environmental and social aspects should be considered.

Stankovic et al. (2009) acknowledged that the educational value of installing wind turbines within the grounds of educational facilities, the added value to a development in terms of increasing the iconic status and visibility of sustainable design aspects, in addition to the value of sending a visual message for tackling climate change are some social aspects which should be considered when studying the feasibility of urban wind turbines. The Department of Energy and Climate Change (2011b) stated that these aspects would increase the societies acceptance of urban wind turbines and encourage more people to consider installing urban wind turbines. However, more research is needed to identify the effect of these systems in the behaviour of individuals in terms of consuming power as it might lead to make people more relaxed about using as much power as they want as the source is renewable. However, Stankovic et al. (2009) asserted that the economical aspect will always be the main objective for installing wind turbines within the built environment.

The WINEUR (2007) report stated that the feasibility of most of the projects integrating wind turbines within the built environment is measured in terms of the financial revenue of the investment which is directly related to the energy yield of the integrated wind turbine which in turn is very dependent on the annual mean wind speed. The Royal Institute of British Architects (RIBA, 2006), explained that the importance of the wind speed to the energy yield of a wind turbine stems from the correlation between the energy yield and the wind speed which is a cube function, which means that if the wind speed doubles the energy yield will increase eight times. However, it is still hard to predict the wind speed within the built environment. This is why the WINEUR (2007) report stressed on the importance of avoiding any obstacle at the site that might reduce the wind speed at the hub height of the turbine.

Eriksson et al. (2008) added that in addition to the energy yield of a wind turbine, other factors should be included for assessing the feasibility of urban

wind turbines such as the cost of installation and the maintenance cost. The amount of captured energy is dependent on the efficiency of the wind turbine which is measured by the power coefficient or performance coefficient (C_P), as for the maintenance cost it should be minimised to keep the total cost low. For this point the VAWTs are advantageous over HAWTs since VAWTs are simpler in structure and have fewer movable parts requiring less maintenance than HAWT. In addition VAWTs have most of the electrical parts at ground level which is more accessible than those of the HAWTs which is mostly located at the top of the tower.

Ackermann and Söder (2002) and Joselin Herbert et al. (2007) noted that the costs of electricity from wind power have fallen about one-sixth since the early 1980s and it is still going down. However, at today's electric utility rates, Bradshaw (2006) considered the initial machinery cost of urban wind turbines is still so high and wind power can only be economically justified on the basis of anticipating rapidly rising utility electric rates. Ahshan et al. (2008) acknowledged that the site of installation plays an important role in determining the feasibility of urban wind turbines. For example in remote sites where electricity services are not present, wind power is more likely to be more economical than installing and buying fuel for an electrical generator or extending utility power to the site if it is 1 km away from the nearest grid point and the wind speed at the site is 5 m/s or more.

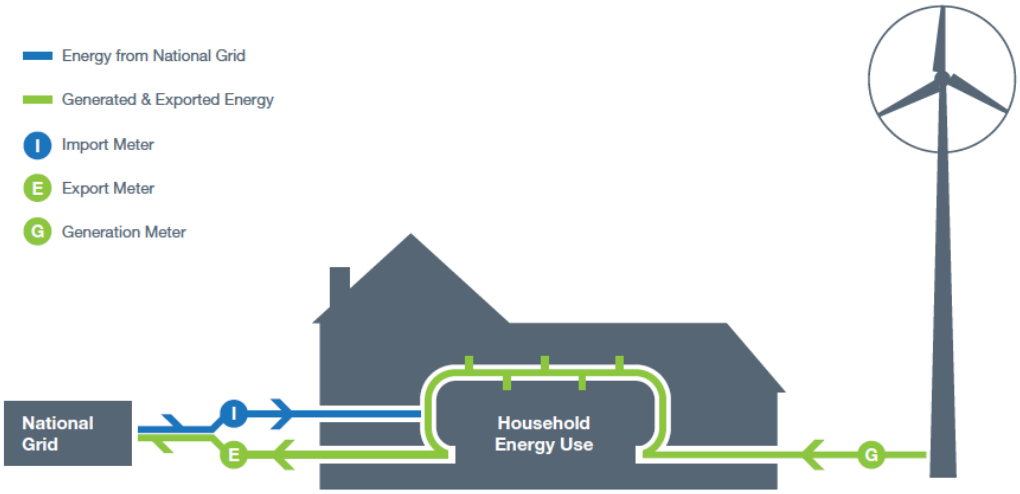

Figure 2.35 Schematic diagram of the metring system of a wind turbine connected to the grid (Stankovic *et al.*, 2009).

RenewableUK (2011a) acknowledged that one of the main factors affecting the feasibility of urban wind turbines is the financial support provided by governments for installing these systems; the Feed-in Tariff (FIT) is one of the financial incentives which guarantees households and businesses payment for producing their own electricity from renewable sources of energy. These financial schemes work through setting a price for the generated electricity in addition to setting another price for any surplus electricity exported to the grid. If accurate wind data is available, the owner of the system can easily asses the costs and revenue from the installation. In order to join the scheme in the UK, the owner has to select a wind turbine that has qualified for the Microgeneration Certification Scheme (MCS) and let an MCS-accredited installer install it. Accordingly the energy company is obliged to pay the user for the generated used and exported energy which is a tax-free income for domestic customers. Special metering system is required for calculating the exported and imported power from the installed wind turbine (Figure 2.35).

Table 2.2 Different prices of generated and exported power for different turbines sizes (Stankovic *et al.*, 2009).

Power (kw)	Generation tariff [5] (p/kwh)	Export tariff[6] (p/kwh)
0 - 1.5	34.5	3
1.5 – 15	26.7	3
15 - 100	24.1	3

The generation tariffs vary according to the size of the installed technology, for example a 1.2 kW wind turbine will be paid just over 34p/kWh, while a 6kW wind turbine will be paid 26.7p/kWh. In addition to that, the tariffs are index-linked which means that payment rise each year with inflation. Table 2.2 demonstrates the different prices for generation and export for different wind turbines sizes. Table 2.3 is a breakdown of the costs and revenue of generating electricity for a year for an 11kW wind turbine (Stankovic et al., 2009).

[5] These tariffs are accurate for new installations until march 2012

[6] Some energy suppliers will offer over and above the guaranteed minimum of 3p/kwh

It should be noted that with the increase in the rated power of the turbine the FIT decreases which reflects the Government's support of small and micro wind systems. However the FIT is regularly under revision and it is noticed that it has decreased since its implementation which reflects the development in the technologies which is reflected in the increase in the energy yield which encourages the users to install the systems and the government to reduce the support as the technology is running towards being more efficient and feasible.

Another example is a 6kW Proven wind turbine (Figure 2.36) which was installed by the Felstead family near Ashford in Devon; the turbine and the foundations coasted them £23,000 and in light of the FIT they are expecting a payback period of around eight years (RenewableUK, 2011a).

Table 2.3 Breakdown of the costs and revenue of generating electricity for a year for an 11kW wind turbine (Stankovic *et al.*, 2009).

Generation	0.267p x 28 000kwh (Generation tariff x Total energy)	£7 476
Export (50%)	0.03p x 14 000kwh (Export tariff x Exported energy)	£420
Reduced bills	0.15p x 14 000kwh (Retail price x Onsite use)	£2 100
Annual		-£250
Total yearly earning		£9 746

Peacock et al. (2008) confirmed the importance of subsidies in raising the feasibility of urban wind turbines, another form of the governmental support is the UK Government's Low Carbon Buildings Programme (LCBP) where grants are available for domestic urban wind turbines applications in the form of a maximum of £1000 per kW of installed capacity subject to an overall maximum of £2,500 or 30% of the relevant eligible costs whichever is lower. Table 2.4 shows a comparison between the FIT since 2010 and the proposed tariffs from October 2012 by the Department of Energy and Climate Change.

Another example is a 6kW Proven wind turbine (Figure 2.36) which was installed by the Felstead family near Ashford in Devon; the turbine and the

foundations coasted them £23,000 and in light of the FIT they are expecting a payback period of around eight years (RenewableUK, 2011a).

Figure 2.36 Left: 11 kW Gaia HAWT, Right: 6kW Proven HAWT (RenewableUK, 2011a).

Peacock et al. (2008) confirmed the importance of subsidies in raising the feasibility of urban wind turbines, another form of the governmental support is the UK Government's Low Carbon Buildings Programme (LCBP) where grants are available for domestic urban wind turbines applications in the form of a maximum of £1000 per kW of installed capacity subject to an overall maximum of £2,500 or 30% of the relevant eligible costs whichever is lower.

Table 2.4 FIT since 2010 to October 2012 (Source: http://www.decc.gov.uk/en/content/cms/consultations/fits_rev_ph2a/fits_rev_ph2a.aspx, accessed: 09/09/2012).

Power (kw)	FIT Year 1 2010/11 (p/kwh)	FIT Year 2 2011/12 (p/kwh)	FIT Year 3 2012/13 (p/kwh)	Proposed FIT October 2012(p/kwh)
0 - 1.5	37.9	37.9	35.8	21
1.5 – 15	29.3	29.3	29.3	21
15 - 100	26.5	26.5	26.5	21

In Skeffling which is a small farming village in East Yorkshire, they installed a 6kW wind turbine which they considered more cost effective than PV, the costs

of the turbine in total was £22,052.86 and they received 50% of that total cost as a grant (LCBP grant) which means that they would be saving £1,040 per year if the annual energy yield is around 8000kWh. In Crediton, Devon, Mr John Lightfoot installed the same wind turbine and he is producing twice as much electricity as he consumes (Department of Energy and Climate Change, 2011a).

Another factor affecting the decision on the feasibility of an urban wind turbine is the payback period of the installed wind turbine. Bahaj et al. (2007) acknowledged that if the payback period is greater than the life time of the wind turbine, it is not suitable from a financial perspective to install the wind turbine. Taller buildings are preferable for mounting wind turbines within the built environment where better wind resources are available in addition to the increase in the size of the building allows for installing wind turbines with larger rotor diameter, leading to better annual energy yields.

In a study by Peacock et al. (2008) to assess the payback period of a roof mounted wind turbine at two different wind regimes; low and high, although there was a great difference between the two cases in terms of energy yield, it was noticed that even for the high wind regime the installation was not economical based on the payback period because for a significant period of the year the turbine is not producing any electricity, they found that the payback period varied between 11.6 to 20.4 years for a wind turbine whose life time is 20 years. Thus they argued that for an urban wind turbine to be feasible, high wind regime should be available, grants and subsidies should be implemented and turbine prices has to fall to as low as 60% of their current level which cannot be achieved unless there is a mass production of urban wind turbines and these measures could reduce the payback period to 5.5 to 11.9 years for high wind sites, which is another reason for taking advantage of the accelerating effect of buildings and specifying to a high degree of accuracy the optimum location for mounting the wind turbine.

2.5 Conclusion

In light of reviewed literature it can be argued that urban wind turbines have high potentials and can overcome many of the hurdles facing large scale wind turbines especially with the advancement in small and micro scale wind turbines

technologies. The main advantage of urban wind turbines is that they provide electricity where it is used, thus cutting down on the extra infrastructure costs of cabling and cutting down on power losses due to transmission. However, small and micro wind turbines would not prove feasible until there are high levels of demand which would result in mass production of turbines' components, accordingly reducing the capital cost of the turbine. Until then, governmental support for such projects is mandatory provided that the wind condition at the installation location is acceptable.

Although planners and architects are showing more interest in exploiting urban wind power, there is a lack of knowledge in regard of choosing appropriate turbine mounting location and turbine type. This chapter has investigated the required knowledge for integrating wind turbines within the built environment in terms of understanding the characteristics of wind power, wind flow within the built environment and different types of integrating wind turbines within buildings. In light of the reviewed literature, it was found that both the mean wind velocity and the turbulence intensity at the installation site are the main factors affecting the energy yield of the wind turbines.

In terms of turbine technology it can be argued that for the integration of a turbine within the built environment to be successful, it is recommended:

- Using vertical axis wind turbine (VAWT) to cope with the high levels of turbulence. However, it should always be noted that VAWT have lower power coefficient than HAWTs which will have an impact on the energy output.
- Blades implementing lift forces are more preferable than drag type blades since the first tend to have more power coefficient.
- Latest technology should be implemented; for example the contra-rotating rotating wind turbines system and the concept of a smart wind turbine by Sharma and Madawala (2012) which have adjustable blades can be implemented to operate the turbine and generate electricity even at relatively low wind speeds.
- An active yaw system like the one proposed by Wu and Wang (2012) would make the wind turbine yield more electricity than self-driven yawing system.

- Using an induction, permanent magnet generator rather than a synchronous generator implementing an electromagnet.

As for understanding wind flow within the built environment, in order to decide about the optimum possible location for urban wind turbines, it is recommended to:

- Mount wind turbines on top of high rise buildings; 30-50% higher than the surrounding urban context.
- Avoid areas with high roughness length where surrounding buildings have the same height as the proposed mounting location.
- Avoid areas with high levels of turbulence or areas around buildings where flow separation occurs. But it should be noted that these areas have high energy content and VAWT can be used.
- Take advantage of the accelerating effect of buildings on wind.
- Place wind turbines between building and preferably buildings with diverging configurations.

As for the type of integration, any of the reviewed types can be used provided that the previous points are taken into consideration and more importantly, a complete wind assessment should take place at the proposed site to understand wind flow at the installation location to avoid areas of high levels of turbulence and choose areas with wind speed relevant to the rated wind speed of the proposed wind turbine. Different tools are available for assessing wind flow at the installation site. These tools include in-situ measurements, wind tunnel tests and computational fluid dynamics (CFD). The next chapter will focus on investigating these tools and comparing them to each other in order to specify the optimum wind assessment tool to be used in this research.

Chapter Three

Urban Wind Assessment Tools

Chapter Structure

3.1 Introduction

3.2 Wind resource estimation

3.3 Urban wind assessment tools

3.4 CFD as a tool for assessing urban wind flow

3.5 Conclusion

Chapter 3: Urban Wind Assessment Tools

3.1 Introduction

As seen in the previous chapter, wind speed is one of the main factors affecting the energy yield of wind turbines and accordingly their feasibility. Thus, assessing wind speed at the installation site is important for estimating the performance of wind turbines especially in urban areas where different variables affect wind flow at the installation location. These variables include urban settings, surface cover and vegetation (Yuen et al., 2004; Lei et al., 2006; Syngellakis and Traylor, 2007). In addition to assessing the local wind flow, Joselin Herbert et al. (2007) acknowledged that the study of geographical distribution of wind speeds, characteristic parameters of the wind, topography and local wind flow and measurement of the wind speed are essential in wind resource assessment for successful application of wind turbines. Urban wind assessment is carried out using a variety of available tools including in-situ measurements, wind tunnel tests and computational fluid dynamics (CFD) simulations. Each tool has its advantages and disadvantages.

This chapter focuses on investigating the available urban wind assessment tools with the aim of choosing the most relevant wind assessment tool to be used in this research through identifying the advantages and disadvantages of each wind assessment tool and the relevance of each tool for implementation in this research. Thus, this chapter is divided into three main sections; the first section (3.2) focuses on the effect of macro and micro-scale wind conditions on wind flow at the installation site. The second section (3.3) focusses on investigating the available wind assessment tools for assessing wind flow around buildings. The investigation is carried out through identifying their advantages and disadvantages and the fields of application for each, in addition to the relevance of each tool for implementation in this research. The third section (3.4) discusses in more depth the proposed tool to be used in this research and the different variables to be considered when using that tool to yield reliable results. The chapter concludes by discussing the main criteria to be considered when choosing a tool for assessing urban wind flow, in addition to recommendations regarding choosing the variables for the tool to be used in this research for assessing urban wind flow.

3.2 Wind resource estimation

Available wind resources depend primarily on macro-scale (continental) and meso-scale (regional) conditions. However, within the built environment, wind resources mainly depend on the micro-scale (local) conditions which differ from one urban area to another depending on its geometrical features. Macro-scale and meso-scale wind conditions can be initially assessed using data from nearby weather stations, as for micro-scale wind conditions they should be inspected using different wind assessment tools. In addition to wind speed, it can be argued that other factors affect the feasibility of integrating wind turbines within the built environment which results from the interaction between air flow and different obstacles forming urban areas. Stankovic et al. (2009) asserted that undesirable turbulence occurs within the built environment which results in reducing the energy yield of urban wind turbines, these areas of turbulence can be determined using available wind assessment tools and accordingly decisions about the optimum way of integrating wind turbines into buildings could be reached.

3.2.1 *Macro-scale wind conditions*

Wind conditions in different geographic areas on earth are governed by some natural phenomena. The most influential phenomenon which drives wind from one place to another is the difference in solar radiation between the equator and the poles. This difference in energy, accordingly temperature, creates areas of different pressures which dictate the air movements known as the prevailing winds. In weather maps, these differential air pressure areas are represented by isobars (Figure 3.1) (Dannecker, 2002; Hu, 2003). In addition to the forces produced by these pressure differences, other forces resulting from the rotation of the earth and the curvature of its surface govern the atmospheric motions at higher altitudes (1000m – 2000m). However, at low altitudes in the atmospheric boundary layer those forces are less important compared to drag and frictional forces at the surface (ASCE, 1996).

Ackermann and Söder (2002) added that the air movement due to different thermal conditions of the masses can be found as a global phenomenon, i.e. jet stream, as well as a regional phenomenon. The regional phenomenon is determined by orographic conditions, e.g. the surface structure of the area as

well as by global phenomena. The wind conditions in this area, known as the boundary layer, are influenced by the energy transferred from the undisturbed high-energy stream of the geostrophic wind to the layers below as well as by regional conditions. Due to the roughness of the ground, the wind stream near the ground is turbulent.

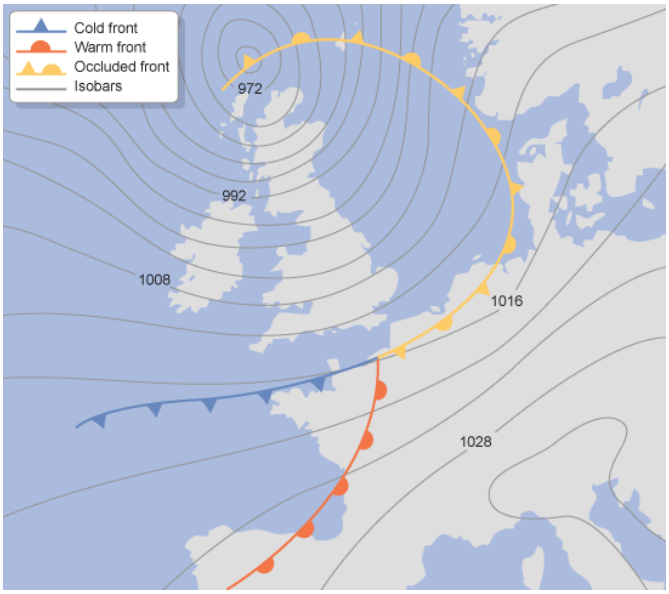

Figure 3.1 A weather map showing isobars as contour lines. (Source: http://www.bbc.co.uk/schools/gcsebitesize/geography/images/clim_038.gif, accessed: 20/08/2012)

These phenomena results in three main components which are key to wind energy resource assessment. According to Stankovic *et al.* (2009), the first factor is the annual mean wind speed. The annual mean wind speed in a certain location depends on the location with respect to the prevailing wind as well as the roughness of the terrain the wind has to pass over in order to reach that specific location. It can be calculated by dividing the sum of the hourly average values of the whole year by the number of hours in a year (8760 hours). The second factor is the wind speed distribution profile which reveals the frequency of different wind speeds along the year, this factor is important for determining the available power in the wind as the energy available in the wind is directly proportional to cube the speed of wind. As for the third factor, it is the wind direction which is a major concern when integrating wind turbines within the built environment, especially if the wind turbine is to be integrated in the form of the building as the whole building should be oriented in a way to harness the prevailing wind. This factor is not very important for large scale

wind turbines in wind farms due to the possibility of the turbine yawing to face the prevailing wind.

3.2.2 *Micro-scale wind conditions*

According to ASCE (1996), the main factors affecting micro-scale wind conditions are the geographic features, different elements forming the built environment, and terrain roughness. Terrain roughness affects to a great extent the characteristics of wind around buildings. Stankovic *et al.* (2009) identified three separate terrains with three different aerodynamic roughness (z_0): city centre terrain (z_0 > 0.7), suburban terrain (z_0 = 0.25 - 0.3) and an open field terrain (z_0 = 0.01- 0.03). The atmospheric boundary layer (ABL) velocity profile has the shape of a power law curve which is displaced a distance d from the ground depending on the roughness of the terrain. Figure 3.2 shows how accessible winds can easily be reached in open fields while in urban areas the corresponding accessible wind is at much higher altitudes or even may never reach the same speeds as in open fields.

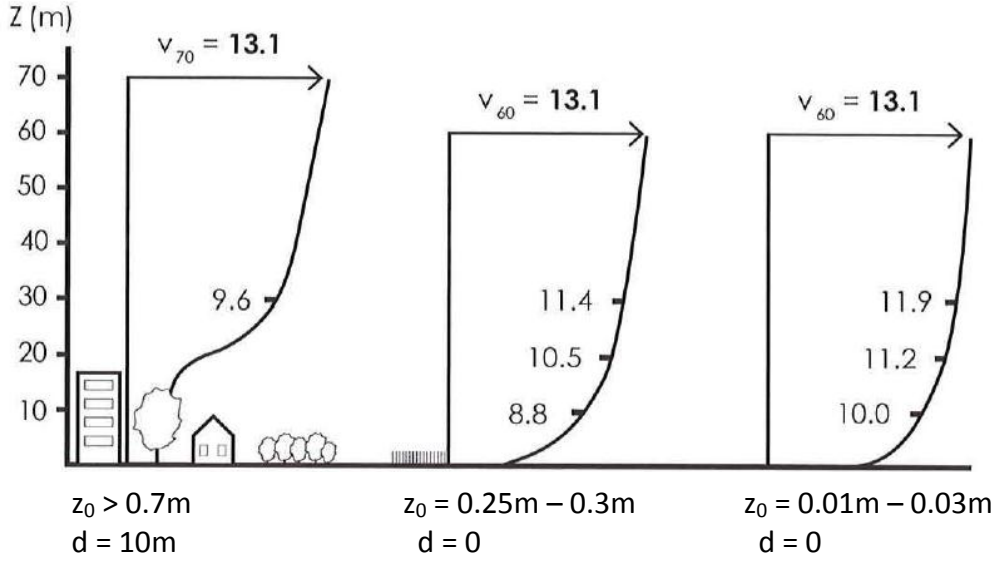

Figure 3.2 Wind speed profiles with different terrains of different aerodynamic roughness where z_0 is the roughness length and d is the displacement of the profile in urban areas (Stankovic et al., 2009).

Thus, it is important when the macro-scale wind conditions are appropriate for urban wind turbines installation, to make a full assessment of wind resources at the specified location to determine whether or not it is feasible to install wind turbines. Chiras (2010) acknowledged that for large scale wind turbines, the

locations of wind farms are chosen carefully in order to make best use of the wind resources. In the case of small scale wind turbines within urban areas a complete assessment of wind resources in the proposed site is important due to the variety of variables affecting wind flow within urban areas. Urban wind energy is considered reliable if it is treated as a complimentary source of energy.

3.3 Urban wind assessment tools

According to Paterson and Apelt (1989), Mertens (2006) and Jha (2010) the most common research tools used to understand wind flow within the built environment are:

- In situ measurements.
- Wind tunnel tests.
- Computational fluid dynamics simulations (CFD).

All of these tools have specific advantages and drawbacks that define the suitability of the tool for a certain analysis. Campos-Arriaga (2009) confirmed that these tools when properly used can lead to informative data which would be implemented in making good design decisions about integrating wind turbines in a building or in an urban area. The energy yield of the integrated wind turbine depends mainly on the annual mean wind speed, in other words, higher wind speeds produce more electricity. Thus, the accurate assessment of wind resources affects to a great extent the decisions about the feasibility of integrating wind turbines within the built environment (WINEUR, 2007).

3.3.1 *In-situ measurements*

Plate (1999) asserted that in-situ measurements or full scale investigation using specific anemometers is the most accurate among the available tools, especially when the assessment is aimed for retrofitting existing buildings with urban wind turbines. For the purpose of integrating wind turbines within the built environment, the required data is related to three main variables which are the wind speed, wind direction and turbulence intensity. The instrument used to collect this data is called anemometer. There are many types of anemometers; mostly used is the cup anemometer. Anderson *et al.* (2008) and Stankovic *et al.* (2009) acknowledged that cup anemometers can be used to determine wind

speed and some of these cup anemometers are fitted with vanes to correlate wind speed with wind direction (Figure 3.3).

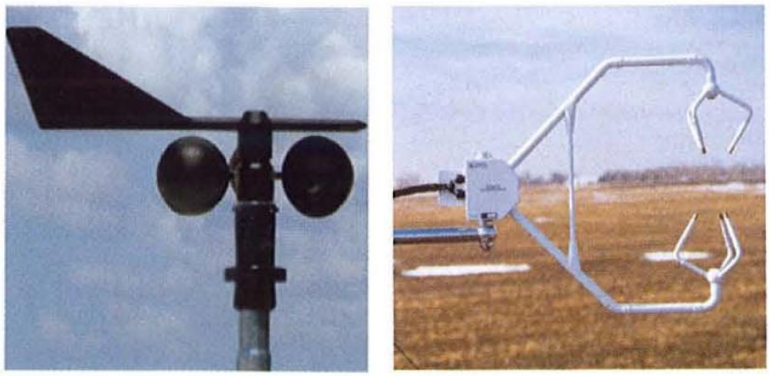

Figure 3.3 Left: Cup anemometer with a weather van. Right: Sonic anemometer (Stankovic *et al.*, 2009).

However, Anderson *et al.* (2008) asserted that other measurements such as temperature, humidity, and barometric pressure are also important for calculating values such as air density, which is important in determining the power available in the wind. Cup anemometers are not capable of measuring turbulence which is a main feature of air flow within the built environment. Sonic anemometers are used to assess turbulence as well as wind speed and direction and they are advantageous over other types of anemometers in detecting the vertical component of wind. In addition, they require less maintenance as they do not have any moving parts (Figure 3.3). But they require a greater data logging capacity and are considered expensive compared to other wind monitoring devices which are usually considered inexpensive.

According to the WINEUR (2007) report, in order to obtain accurate results from the anemometer for the purpose of installing urban wind turbines, it is important to mount the anemometer at the exact location of the proposed wind turbine which should be selected carefully based on the prevailing wind direction, avoiding nearby obstacles and areas of expected turbulence where possible. In addition, Stankovic *et al.* (2009) asserted that the collected data should be over a one year period of time with time interval between each recorded reading ten minutes and to put the data in context it is normalized against the collected weather data over 30 years. This long period of time for monitoring is one of the main drawbacks of in-situ measurements. In addition, this is a costly process

due to the involvement of man-power to carry out the monitoring and the maintenance of the anemometer.

Willemsen and Wisse (2002) noted that in-situ measurements are embedded with errors that could reach 20% especially at pedestrian level in the built environment. Kaganov and Yaglom (1976) and Morris *et al.* (1992) attributed this to the over-speeding effect which is a consequence of the property of the cup anemometer that responds more quickly to an increase in the wind speed than to a decrease of the same magnitude which means that the recorded data will have higher values than the real ones. On the contrary, cup anemometers which are fitted with vanes tend to record wind speeds lower than real ones due to failure to instantaneously align with the prevailing wind direction and since wind direction changes quickly within the built environment, the response time of these anemometers is very slow which results in missing recording some of the dynamic nature of urban wind.

Another factor which would add to the expenses of in-situ measurements is the cost of erecting the mast and obtaining necessary planning permissions for erecting the mast for a long period of time to gather the needed information. These expenses when compared to the size of the installed urban wind turbine and its energy yield, might not encourage users to count on in-situ measurements for assessing wind resources at the proposed installation site (Anderson *et al.*, 2008). Accordingly, Stankovic *et al.* (2009) asserted that it is important to implement other assessment tools such as wind tunnels and CFD simulations which provide a quick and relatively low cost means of assessing wind flow within the built environment.

Easom (2000) argued that for in-situ measurements, the most apparent advantage is that they do not suffer from any scale mismatch due to Reynolds number[1], wind shear and turbulence intensities or from blockage effects. On the other hand, they are costly and time consuming. It is, moreover, impossible to control the approach flow conditions, which will inevitably obscure details in the

[1] Reynolds number (Re) is a dimensionless number that gives a measure of the ratio of inertial forces to viscous forces and consequently quantifies the relative importance of these two types of forces for given flow conditions. $Re = \frac{\rho v l}{\mu}$ Where ρ is the density of the fluid, v is the velocity of the fluid, l is a characteristic linear dimension and μ is the dynamic viscosity.

observed data. Easom (2000) added that the error of measurements could possibly be larger for full-scale observations compared to well controlled wind tunnel tests, which should be borne in mind when using them for calibration. Yang (2004b) acknowledged that the error range experienced in full-scale measurements can reach 10-15%.

3.3.2 *Wind tunnel tests*

According to Sara Louise (2011), a good substitute of in-situ measurements, where extraneous variables are more difficult to control, is the wind tunnel where the test environment is more controlled. Wind tunnel tests are largely used in investigating wind loads on different structures in the built environment, assessing pedestrian wind comfort, dispersion of pollutants within urban areas, integrating wind turbines within the built environment, in addition to validating other tools for assessing wind flow (Yassin *et al.*, 2005; Stathopoulos, 2006; Gomes *et al.*, 2007; Howell *et al.*, 2010; Chen and Liou, 2011; Ross and Altman, 2011; Carpentieri *et al.*, 2012). However, in order to best benefit from these tests, the American Society of Civil Engineers (ASCE, 1996) recommended that wind tunnel tests to be carried out at an early stage of the project to allow for proper design adjustments.

In literature, wind tunnel tests are usually referred to as physical experiments or scale modelling. Cook (1985) asserted that for a long time wind tunnel tests have been a standard approach which was well tested and validated and can be considered one of the best ways for simulating natural wind. According to Baskaran and Kashef (1996) and Plate (1999) this tool was originally developed for aeronautic and industrial engineering but was then widely used in testing physical scaled buildings models. However, Lawson (2001) acknowledged the great difference between the application of wind tunnels in aeronautic and industrial engineering and in buildings aerodynamics. It was argued that the main difference which required the development of new wind tunnel techniques is the complexity of air flow around buildings when compared to the relatively still flows around aircrafts. This is attributed to the fact that wind gusts in urban areas from different directions and the shapes of buildings are bluff shapes which cause the flow to separate unlike the smooth attached flow around the sleek shapes of wings and fuselages.

Blocken and Carmeliet (2004) confirmed that the first wind tunnels did not simulate wind flow correctly because they had wind speed of equal values throughout the cross section of the wind tunnel, which is not the case for the atmospheric boundary layer which is characterized by the variation in mean wind speed with height. Early literature focused on this aspect which resulted in the emergence of wind tunnels which took into consideration the increase in wind speed with height. Campos-Arriaga (2009) acknowledged that the data obtained from these tests are, to a great extent, considered reliable if the wind tunnel used is an atmospheric boundary layer wind tunnel (BLWT) and the model is accurately constructed with all surrounding elements affecting wind flow.

Jones *et al.* (2004) described these wind tunnels as being 2-5 m wide, with a long working section of 15-30 m, and use air at atmospheric pressure. Maximum operating speeds are usually in the range of 10-50 m/s. However, it is not generally required to use the actual wind speeds as long as same Reynolds numbers are maintained. Measurements are generally made as dimensionless ratios, for instance the ratio of speeds at two points in the model (e.g. between a point on the ground and a fixed reference point). The American Society of Civil Engineers (ASCE, 1996) acknowledged that in addition to the wind speed, other features has to be simulated as well, especially when simulating wind flow within urban areas where the flow is more likely to be turbulent. Various devices such as spires, vortex generators, and fences are placed at the entrance of the test section to generate acceptable mean and turbulent flow conditions similar to full-scale conditions. Other similarity requirements should also be considered to run an accurate simulation and minimize the errors due to scaling. Jha (2010) asserted that similarity in scaling includes:

- Geometric similarity where the ratios of linear dimensions are equal.
- Dynamic similarity where the ratios of forces are equal.
- Kinematic similarity where particle paths are geometrically similar.

Other modelling requirements which are considered as the minimum modelling requirements for an accurate wind tunnel simulation are:

- Modelling the vertical distributions of the mean wind speed and the intensity of the longitudinal turbulence component.

- Modelling the important properties of atmospheric turbulence, in particular the relevant length scale of the longitudinal turbulence component, with the same scale approximately as the same scale as that used to model buildings or structures.

- The longitudinal pressure gradient in the wind tunnel test section should be sufficiently small as not to significantly affect the results.

Provided that these similarity and modelling requirements are satisfied, Hu (2003) asserted that wind tunnel tests yield reliable results comparable to full scale measurements which makes it a relevant tool for assessing wind flow around buildings. However, Blocken and Carmeliet (2004) considered adhering to these similarity requirements to be one of the disadvantages of wind tunnel testing. In addition, they pointed out that wind tunnel measurements are usually point measurements which require the implementation of very costly techniques such as Particle Image Velocimetry (PIV) and Laser-Induced Fluorescence (LIF).

In addition to the cost, Hu (2003) considered using wind tunnels as time-consuming, especially when modifications are required for comparing alternatives because the models need to be reshaped or even rebuilt, accordingly the instrumentation are required to be tuned again which also requires a thorough knowledge of the operation of the instruments from the users. On the other hand, Denoon *et al.* (2008) found it difficult to accurately model the effect of turbulence in a wind tunnel because the wind tunnel is limited by its size, this is why a complete accurate simulation of wind flow is not yet possible, which means that the results obtained from wind tunnel testing will have errors that should be considered.

Furthermore, Tominaga and Mochida (1999) asserted that wind tunnel equipment is not readily available to many planners, designers, and architects. Accordingly, they miss the advantages of implementing wind tunnel tests during the design stage which consequently limits the efficiency of their designs. This problem was overcome by CFD simulation codes which are relatively new and

inexpensive wind assessment tool compared to wind tunnel tests. However, Reiter (2010) argued that wind tunnels still yield consistent results and continue to be a reference in wind engineering for validation of other wind assessment tools.

However, it should be noted that when using wind tunnels for modelling wind flow around buildings, especially low rise buildings, the main challenge is to reproduce the details of the studied building in the scaled model. In order to reproduce the details of the flow field around such buildings, a moderately large scale is required. Tieleman (2003) recommended utilising models of low-rise buildings that have a scale not smaller than 1:50. Richards *et al.* (2007) argued that the use of such a large scale inevitably means that the largest turbulence length scales in the wind tunnel are much smaller than the scaled full-scale equivalents. In such situations, the modeller must decide whether to match the turbulence intensity, the integral length scale or neither which would affect the accuracy of the results. Therefore Easom (2000) argued that the novel use of 1:1 scale CFD and experimental models should, in theory, eliminate this detrimental effect.

3.3.3 *Computational fluid dynamics (CFD) simulations*

According to Asfour and Gadi (2007) and Versteeg and Malalasekera (2007), CFD is based on solving the fundamental governing equations of fluid dynamics that describe the exact behaviour of a Newtonian fluid[2], including the effects of turbulence. As in the case of wind tunnel tests, CFD was developed mainly for aeronautic and aerospace applications. However, Wainwright and Mulligan (2004) argued that CFD can be used in many other fields. Moreover, Blocken and Carmeliet (2004) asserted that CFD can provide an alternative for wind tunnel tests if proper validation studies are carried out. CFD simulations are considered by Reiter (2010) a good research tool for studying wind flow around buildings for architectural and urban design purposes as they can directly yield

[2] A Newtonian fluid is a fluid whose stress at each point is linearly proportional to its strain rate at that point. For a Newtonian fluid, the viscosity, by definition, depends only on temperature and pressure, not on the forces acting upon it. If the viscosity does depend on the forces acting upon it then the fluid is said to be non-Newtonian (source: http://www.mathscareers.org.uk/viewItem.cfm?cit_id=383223, accessed: 14/09/2012).

detailed wind flow characteristics at every point around the studied configuration of buildings (Blocken and Carmeliet, 2004).

According to Jones *et al.* (2004), CFD was primarily used in buildings for assessment of internal air flows and ventilation, but recently these techniques have been widely used for full three-dimensional external wind flows. In addition, Asfour and Gadi (2007) acknowledged that some of the applications of CFD in the built environment are in the field of predicting airflow rate, air velocity, air temperature, airflow patterns inside and around buildings and assessing pedestrian wind environment and micro-scale atmospheric environment around human body.

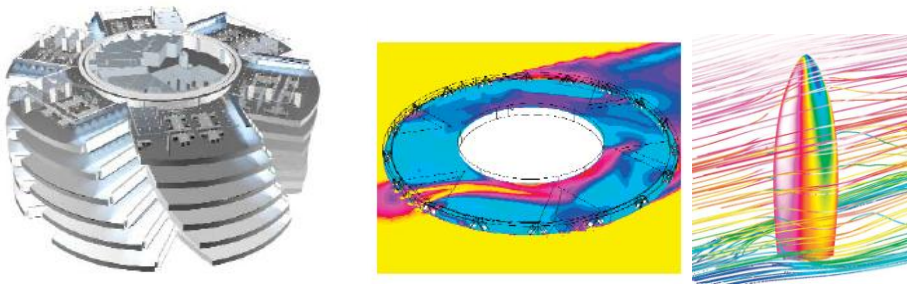

Figure 3.4 Model of several floors in the Swiss Re building (left), CFD simulation showing airflow through one of the floors (middle) and CFD simulation of air flow around the whole building (right) (Source: http://www.fluent.com/about/news/newsletters/06v15i2/a5.pdf, accessed: 14/09/2012).

Even small practices have started using CFD simulation due to their relatively low cost compared to other tools. Currently, CFD is used in modelling the potential of introducing natural ventilation in high rise buildings. This could be taken a step further to look into the possibility of enhancing the building form to improve wind power generation. Swiss Re building by Fosters and Partners was extensively modelled to enhance natural ventilation in its atriums throughout the building height as well as assessing reducing the wind turbulences on pedestrians. The tapering shape of the bottom part of the building is a direct respond to the CFD simulation results to provide a comfortable pedestrian wind environment (Figure 3.4) (Kitson and Moran, 2006).

Since the emergence of CFD in the 70s and its application in assessing wind flow around buildings, researchers have agreed about the advantages of CFD simulations which can be summarised in the following points:

- Due to the rapid increase and advancement in computational power, CFD is getting more and more cost effective especially when compared to wind tunnel tests and full scale measurements (Stathopoulos, 2006).

- Unlike wind tunnels, CFD simulations are not bounded by the similarity constrains previously mentioned. In addition, they give quantitative and qualitative data regarding the characteristics of air flow throughout the whole domain of study not just at few specific points limited by the accessibility of the measuring instruments (Hu, 2003; Jones *et al.*, 2004; Blocken *et al.*, 2010; Reiter, 2010).

- Augenbroe (2004) and Jones *et al.* (2004) acknowledged that the main advantage of CFD simulation which encourages architects and engineers to broadly use it, is the speeding up of studying the effects of design iterations at preliminary design stages. Moreover, simulation tools can provide a better understanding of the consequences of design decisions, which increases the effectiveness of the design process as a whole (Wainwright and Mulligan, 2004; Versteeg and Malalasekera, 2007).

- Unlike wind tunnel tests, in CFD, full scale simulations are carried out which is a significant advantage when large buildings or big urban areas are studied. Wind tunnel tests are limited by the cross section of the wind tunnel (Wainwright and Mulligan, 2004).

- Researchers conceded that the main advantage of CFD being its powerful visualisation tools as results are easily amenable to graphical representations (Mochida *et al.*, 1997; He and Song, 1999; Murakami *et al.*, 1999; Wainwright and Mulligan, 2004; Stathopoulos, 2006).

As for the drawbacks of CFD simulations and issues that must be taken into consideration in any CFD simulation, they are also well documented and can be summarised in the following points:

- Denoon *et al.* (2008) stated that CFD simulation is weak in the field of assessing wind flow in very dense urban environments which can be attributed to the insufficient computational power available to accurately model the effects of turbulence in the built environment.

- CFD requires mathematical background and knowledge of fluid dynamics, the quality of the CFD is highly dependent on the experience of the user and his/her insights into the problems concerned. Wainwright and Mulligan (2004) acknowledged that this combination of skills is not widely available and is not quickly learnt. The danger lies in inexperienced users using the code and interpreting the results in a wrong way (Hu, 2003; Syngellakis and Traylor, 2007; Campos-Arriaga, 2009).

- All commercial CFD codes contain variables which the user has to specify. Some of these variables are the turbulence model, type of grid, boundary conditions, discretisation scheme, etc. Care is required in specifying these variables because the output might completely change if the specified variables are wrongly specified (Sørensen and Nielsen, 2003; Blocken *et al.*, 2010).

- The results output by a CFD code are not necessarily a valid solution for a particular fluid flow problem. Thus, existing recommendations and best practice guidelines should be followed, then validation studies should be carried out. In cases where data are not available to validate or calibrate the CFD model, Wainwright and Mulligan (2004) suggested that care must be taken not to interpret too much into the results.

Comparing the advantages and drawbacks of CFD simulation it can be argued that CFD could be the most appropriate tool for assessing urban wind if the user has adequate training and knowledge of fluid dynamics and relevant computational power is available. Jones and Whittle (1992), Clifford *et al.* (1997) and Jones *et al.* (2004) argued that with the increasing advancements in computational power, CFD techniques will be the obvious pathway for assessing wind flow within the built environment.

3.3.4 *Relevance of different tools for assessing urban wind flow*

It can be argued that engineers, planners and architects favour both CFD simulations and wind tunnel tests over in situ measurements (Mochida *et al.*, 1997; He and Song, 1999; Murakami *et al.*, 1999; Campos-Arriaga, 2009). Blocken and Carmeliet (2004) and Chen (2004) argued that CFD simulation can

provide an alternative for wind tunnel studies because CFD is less time consuming, less expensive than wind tunnel tests and it is easy to visualise the detailed wind flow within the domain of study.

In addition, when comparing the results obtained from wind tunnel tests and CFD simulations, Jiang *et al.* (2008) asserted that CFD simulations agree well with wind tunnel tests in the flow field and wind pressure distribution around buildings but the differences between the results obtained from the two tools are more apparent at ground levels. Campos-Arriaga (2009) attributed this to the treatment used at the near wall region (roughness and mesh specifications at pedestrian level) in the CFD simulation tool. The near wall treatment significantly influences the accuracy of numerical solutions, because it is in that region where the solution variables have large gradients, and the momentum and other scalar transports occur most vigorously. Therefore, representing the flow in these regions will lead to accurate turbulence simulation and accordingly consistent results.

Jones *et al.* (2004) acknowledged that there is agreement in general flow trends, which means that the problem is in the wind environment simulated in both tools. In a practical application, these differences could lead to different design decisions which mean that further work is required for identifying these problems in both, detailed wind-tunnel measurements and CFD turbulence simulation. In a study by Kim *et al.* (2009) comparing wind tunnel tests and CFD simulations, the measurements showed discrepancies from 2% to 30% depending on the wind direction. However, they asserted that the results could still be used because the flow pattern distribution was similar between the wind tunnel test and the CFD simulation.

In terms of cost, all the tools available for assessing wind flow within the built environment are relatively expensive and since most accurate results could be obtained by in-situ measurements which is the most expensive and time consuming tool, therefore CFD simulation and wind tunnel testing need to be developed to improve the estimation of urban wind speeds without having to rely on in-situ measurements. Table 3.1 concludes the observations about wind assessment tools in the built environment in terms of accuracy, usage as a

visualisation tool, preference of usage for existing and future planned developments, cost, required time for assessment and availability to architects.

Table 3.1 Comparison between in-situ measurements, wind tunnel tests and CFD simulations.

	Tools arranged in descending order
High Accuracy	In Situ Measurements – Wind Tunnel – CFD
High Visualization	CFD - Wind Tunnel - In Situ Measurements
Assessing wind flow in existing urban areas	In Situ Measurements – CFD – Wind Tunnel
Assessing wind flow for future planned urban areas	CFD – Wind Tunnel – In Situ Measurements
Lowest cost	CFD – Wind Tunnel – In Situ Measurements
Less time consumed	CFD – Wind Tunnel - In Situ Measurements
Availability to architects	CFD – Wind Tunnel – In Situ Measurements

It can be seen from the table that of all the tools used for assessing wind flow in the built environment, architects favour CFD simulation over other available tools because of its potentials in comparing design alternatives, its high visualisation representation and its ease of use when compared with other wind assessment tools. On the other hand, it should be noted that care should be taken when using CFD codes and the users should have appropriate training and background to use the code in confidence. In addition, any CFD study should first follow published recommendations and best practice guidelines and then validated by other available tools such as wind tunnel test.

3.4 CFD as a tool for assessing urban wind flow

Many of the commercial CFD codes developers declare that their codes are user-friendly and easy to use. This is, indeed, one of the advantages of commercial CFD codes compared to other wind assessment tools, but the danger lies in the codes being used by persons who are not adequately trained or lack the basic background for understanding fluid flow physics. With the wide

use of commercial CFD codes in assessing thermal performance of buildings, wind flow within and around buildings, architects are getting more interested in using the code themselves, but some architects lack the training and background for using the codes.

This was one of the topics discussed in the IBPSA seminar titled "*Building Performance Simulation in Architectural Discourse"* held at the school of Architecture, Planning and Landscape in Newcastle University on 8 October 2010 where the participants were a mix of architects, academics, researchers, engineers and architecture students. There was an agreement between the attendees on the importance of integrating CFD modelling and basics of physics within the architectural curriculum to avoid the misuse of the codes.

However, it can be argued that personal experience in using the code is also very important for obtaining sensible results. One of the examples that demonstrated the importance of personal experience in using the code is the study made by Chen and Zhai (2004) who asked a group of mechanical engineering graduates to use a CFD code to solve a flow problem. The study reported that none of the students reached the correct result in the first attempt. Accordingly, Hu (2003) asserted that the quality of a CFD model and the reliability of its predictions are greatly dependent on users' experience and their insights into the problems concerned. Thus, it is important to introduce in this section the background theories of CFD and the techniques for solving fluid flow problems. This section reviews how the CFD modelling is commonly used along with an overview of the requirements for a successful CFD simulation. The requirements will then be implemented as guidelines for choosing the parameters for the CFD simulations in this research.

3.4.1 *CFD numerical simulation of fluid flow*

CFD is a computerised numerical technique based on solving the fluid flow equations. Blocken *et al.* (2007b) acknowledged that in the case of wind flow around buildings, the lower part of the atmospheric boundary layer (0 - 200 m) is the flow of interest. This boundary layer is characterised by negligible variations in fluid's properties in addition to high level of turbulence. Turbulent flows can be described by solving the continuity and momentum equations known as the Navier-Stokes equations. These equations are named after the

two eighteenth century scientists Claude Navier and George Stokes who independently obtained the equations in the first half of the nineteenth century. These equations are based on the fundamental governing equations of fluid dynamics; the continuity, the momentum and the energy equations which represent the conservation laws of physics. Since this research focuses on air flow problems and no heat transfer is involved, the equations of concern here are the continuity equation and the momentum equation.

The continuity equation is based on the law of conservation of mass which ensures that the change of mass in a control volume is equal to the mass that enters through its faces minus the total mass leaving its faces. The momentum equation is based on Newton's Second Law of Motion (conservation of momentum) which states that the rate of change of momentum of the fluid particles is equal to the total force due to surface stresses and body forces acting in an aligned direction of a chosen coordinate axis. Navier and Stokes combined these principles and expressed them in a set of partial differential equations. Assuming that the flow is incompressible and the flow nature is three dimensional, the 3D form of the equations would be:

Continuity equation

$$\frac{\partial u}{\partial x} + \frac{\partial v}{\partial y} + \frac{\partial w}{\partial z} = 0$$

X-component of the momentum equation

$$\rho \frac{Du}{Dt} = -\frac{\partial p}{\partial x} + \frac{\partial \tau_{xx}}{\partial x} + \frac{\partial \tau_{yx}}{\partial y} + \frac{\partial \tau_{zx}}{\partial z} + \rho f_x$$

Y-component of the momentum equation

$$\rho \frac{Dv}{Dt} = -\frac{\partial p}{\partial y} + \frac{\partial \tau_{xy}}{\partial x} + \frac{\partial \tau_{yy}}{\partial y} + \frac{\partial \tau_{zy}}{\partial z} + \rho f_y$$

Z-component of the momentum equation

$$\rho \frac{Dw}{Dt} = -\frac{\partial p}{\partial z} + \frac{\partial \tau_{xz}}{\partial x} + \frac{\partial \tau_{yz}}{\partial y} + \frac{\partial \tau_{zz}}{\partial z} + \rho f_z$$

Where *u, v* and *w* are the x, y and z velocity components respectively, *p* is the pressure, ρ is the fluid density, τ is the shear stress, f_x, f_y and f_z are the components of the body force per unit mass acting on the fluid (Anderson, 1995; Cebeci, 2005; Versteeg and Malalasekera, 2007).

Computationally, all the boundaries and spaces included in the computational domain have to be arranged in the form of nodes with regular or irregular order which is known as the mesh or grid. This mesh divides the domain, spatially, into a finite number of nodes where calculations can be carried out at regular intervals simulating the passage of time. According to Liaw (2005), this process of presenting the flow problem in the form of discrete numerical data is known as discretisation. Generally, there are three major parts of discretisation in solving fluid flow: equation discretisation, spatial discretisation and temporal discretisation

Equation discretisation is the process through which the governing partial differential equations are translated into numerical analogue solvable by the computer. These equations can be solved by a number of techniques such as the finite-difference method (FDM), the finite-element method (FEM) or the finite-volume method (FVM). FDM is known for its simplicity and ease in obtaining higher order accuracy discretisation. However, FDM only applies to simple geometries because it employs a structured Cartesian mesh. FEM is known for its application around complex geometries because of the application of unstructured mesh. But numerically, it requires higher computational power compared to FDM. As for FVM, it can be used for both structured and unstructured meshes, it is more efficient and easier to program in terms of CFD code development (Liaw, 2005). Hu (2003) asserted that the FVM is the most commonly used due to its simplicity in depicting the conservation laws of mass, momentum and energy in a finite volume of a fluid.

CFD codes have several methods for solving these equations. However, Franke *et al.* (2004) asserted that the numerical method used must be at least second-order accurate. First order scheme should not be used for the final solution but can be used for initial iterations. Higher order schemes are costly in terms of computational power but the computational efficiency of these higher order schemes is much greater. Freitas (1993) added that, it has been demonstrated

many times that, for first order schemes, the simulations yield inaccurate results, even some journals like the Journal of Fluid Engineering has a policy of not publishing results from first order schemes. The process of solving the equations is iterative and the computer keeps repeating solving the equations until the solution converges or a predefined value of residuals is reached (Hu, 2003). The lower the residuals value the more numerically accurate the solution. In most CFD codes and industrial applications a residuals value of 0.001 is used which Franke *et al.* (2007) considered too high to have a converged solution and recommended the reduction of the residuals of at least four or five orders of the magnitude. According to Liaw (2005), a residuals value in the range of 10^{-4} to 10^{-6} is targeted to achieve convergence of the solution.

The second category of discretisation is the spatial discretisation which is the process of dividing the computational domain into small sub-domains making up the mesh where fluid flow can be described mathematically by specifying its properties at all mesh points in space and time. All meshes in CFD comprise nodes at which flow parameters are resolved. Generally, there are two main types of meshes: the structured mesh and the unstructured mesh. The structured mesh is more suitable for simple shapes such as square or rectangular sections. But for more complex shapes the unstructured grid is implemented because it is formed of tetrahedral which can fit any shape but with higher computational cost. In addition to these two types, Liaw (2005) included a third type called the multi-block structured mesh, which could be considered a subcategory of the structured mesh because the computational domain is subdivided into different areas with different structured mesh resolution. The main advantage of this technique is the reduction in computational cost compared to the unstructured mesh, in addition to a higher degree of control when meshing complex geometries.

The third category of discretisation is the temporal or time discretisation which is related to unsteady simulations. Generally, temporal discretisation splits the time in the continuous flow into discrete time steps. In time-dependent formulations, there is an additional time variable (t) in the governing equations compared to the steady state analysis. This leads to a system of partial

differential equations in time, which comprise unknowns at a given time as a function of the variables of the previous time step. Thus, unsteady simulation normally requires longer computational time compared to a steady case due to the additional step between the equation and spatial discretisation (Blazek, 2001). However, any code possesses a number of parameters which the user specifies to set the problem conditions. Without considerable experience in solving CFD problems, the user might specify inadequate conditions for the flow problem resulting in unreliable results. Accordingly, the next part of this section investigates the CFD modelling parameters which should be taken into consideration to minimise errors and uncertainties in the results. Afterwards, these recommendations would be used as guidelines for the CFD simulations in this research.

3.4.2 *CFD modelling parameters*

Uncertainties are embedded within CFD codes, even for an experienced user there are many physical and computational parameters required for a consistent simulation (Castro and Graham, 1999; Hu, 2003; Campos-Arriaga, 2009). This is why many publications address the issues of quality control and best practice guidelines for CFD modelling (Sørensen and Nielsen, 2003; Chen and Zhai, 2004; Franke *et al.*, 2004; Wit, 2004; Franke *et al.*, 2007; Blocken *et al.*, 2010). These guidelines address all the steps of a CFD modelling focusing on five main categories; defining the physical model, the geometry of studied problem, the computational domain dimensions, the computational domain boundary conditions and the computational mesh.

3.4.2.1 Defining the physical model

Defining the physical model means specifying the basic equations describing the physics of the flow and different turbulence models for solving these equations. Theoretically, flow problems can be solved without any turbulence models by directly solving the Navier-Stokes equations without applying any approximation. This method is known as the direct numerical simulation (DNS) and it requires a very fine mesh to capture all the relevant scales of the flow from the smallest eddies to the largest ones and their variations at each time step are also resolved. Hu (2003) asserted that the number of cells and time steps required is too large to be computed using available computing resources

and it is not practical to implement DNS in solving turbulent flow problems unless there is a considerable advancement in computer technology so that the number of grids beyond 10^9 can be calculated in an acceptable amount of time. Spalart (2000) estimated that 80 years is needed for computer power to develop to an extent that DNS is able to simulate flow at Reynolds numbers of engineering interest, assuming that computer power increases by 100% every year.

Thus, according to Hu (2003), Liaw (2005) and Franke (2007) the system of equations has to be simplified to be numerically solvable. This is done by averaging the basic equations to filter out the many scales of turbulent flow. This averaging results in the production of additional unknowns (turbulence stresses or sub-grid stresses) solvable by turbulence models which possess a set of equations that account for turbulence of flow based on some simplified assumptions. Many turbulence models have been proposed to solve turbulent flows and most of these models can be classified either as space-filtered models or time-averaged models. The most commonly used method for solving turbulent flows is the time-averaged method which is usually referred to as the Reynolds Averaged Navier Stokes (RANS) model. In the RANS model all aspects of turbulence are modelled. On the other hand, the space-filtered models directly simulate the large eddies and models the small eddies with some assumptions. However, it still needs to resolve the flow fields at each time step which requires high computational power but less than that of the DNS because it does not resolve the small eddies which does not affect the mean flow. The Large Eddy Simulation (LES) model is a space-filtered model.

Liaw (2005) acknowledged that LES is considered one of the most accurate models for predicting air flow around buildings. It is classified as a space filtering method in CFD where a filter function is implemented to differentiate between large scale and small scale eddies. The filter function uses a length scale which is the characteristic filter width of the simulation. Eddies larger than that length scale are resolved directly (simulated), while those smaller than the length scale are approximated (modelled). This method has shown high accuracy in simulating main turbulence properties like the transient behaviour of separation, recirculation downstream of windward edges, and von Karman

vortex shedding in the wake of an obstacle which the steady RANS models do not accurately simulate (Franke *et al.*, 2004; Blocken *et al.*, 2010). However, Hu (2003) argued that this accuracy comes with a high computational cost.

Vardoulakis et al. (2011) pointed out that the main advantage of LES is its accuracy in reproducing the mean and fluctuating data, but it is still impractical to use due to the large computational power needed to run the simulations. However they added that if adequate computational power is available, LES can be used in producing datasets as a benchmark for assessing other turbulence models such as the RANS based turbulence models or any other less complex turbulence models. Lei *et al.* (2006) pointed out that another disadvantage of LES, which applies to all other models except the steady RANS, is the lack of detailed validation and sensitivity studies for LES for atmospheric boundary layer flows. This is not the case for RANS simulations where many guidelines and best practice documents can be found in literature. Thus, in most cases the RANS models are still the first choice.

RANS method itself possesses many models, each has its advantages and disadvantages and the model to be used should be chosen with great care because choosing the relevant turbulence model has the largest impact on the results. Thus, it is important to decide in the first place whether the flow problem requires a steady or an unsteady treatment. Since the atmospheric boundary layer flow is mostly turbulent, an unsteady treatment is required in principle. Which requires that the averaging to be over small time intervals or ensemble. This approach is called unsteady RANS (URANS). According to Blocken *et al.* (2010), URANS can be a good option in flows characterised by low-turbulence approach flow and when the unsteadiness is predetermined such as von Karman vortex shedding in the wake of an obstacle.

However, Franke *et al.* (2007) stated that few studies have implemented URANS and since it requires high mesh resolution, it is recommended to use LES or detached eddy simulation (DES). The latter is a hybrid modelling strategy which employs both the RANS and the LES models. RANS model is implemented near the wall region and away from the wake region, while LES is implemented in the wake region of the flow where unsteadiness is found. This strategy saves considerable computational time compared to only implementing

LES in the whole computational domain. However when comparing DES to RANS, Franke *et al.* (2007) asserted that DES requires much greater computational time than RANS. In addition, it requires highly accurate inflow boundary conditions based on experimental data which is rarely available in practice resulting in few applications of DES to wind engineering problems.

Steady Reynolds Average Navier Stokes (RANS)

As mentioned earlier, RANS method is a time-filtered method which is one of the reasons of its popularity because in most engineering purposes it is unnecessary to resolve the details of the turbulent fluctuations as the information obtained from time-averaging flow properties is sufficient. This is why Versteeg and Malalasekera (2007) acknowledged that the vast majority of turbulent flow computations has been and for the foreseeable future will continue to implement RANS turbulence models. In the RANS approach to turbulence, for each time dependent variable, it can be decomposed into a mean value and a fluctuating component (Figure 3.5). For example the velocity of a turbulent flow at a specific point in time equals to the mean velocity of the flow plus the fluctuating velocity component:

$$U = \bar{U} + u'$$

Where $\bar{U}$ is the mean velocity taken over a sufficient long period of time and u' is its fluctuating component.

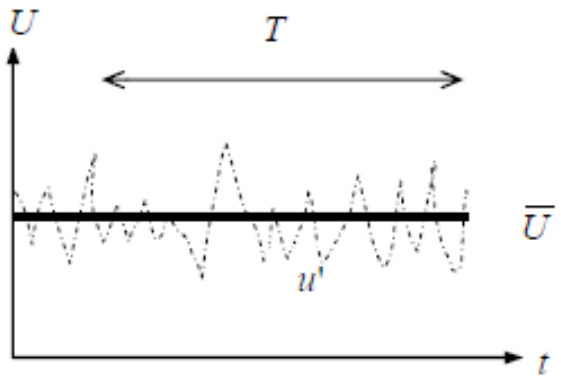

Figure 3.5 Time averaging of turbulence using RANS models (Versteeg and Malalasekera, 2007).

Substituting Eq. ($U = \bar{U} + u'$) into then Navier-Stokes equations, the RANS equations can be obtained:

$$\frac{\partial U_i}{\partial t} + U_i \frac{\partial U_i}{\partial x_j} = -\frac{1}{\rho}\frac{\partial P}{\partial x_i} + \frac{\mu}{\rho}\frac{\partial}{\partial x_j}\left(\frac{\partial U_i}{\partial x_j} - \rho\overline{u'_\iota u'_\jmath}\right)$$

Where U_i are the mean velocities, P is the mean static pressure and $\rho\overline{u'_\iota u'_\jmath}$ are turbulent, or Reynolds stresses which are the stresses contributed by turbulent fluctuations. The existence of the stress terms means there is no longer a closed set of equations, and turbulence model assumptions are needed to estimate the unknowns to solve this closure problem. However, the time averaging implemented by RANS turbulence models leads to a steady description of the turbulent flow which raises questions about their efficiency in modelling turbulent flow. Franke *et al.* (2007) argued that RANS turbulence models are still an adequate representation of the wind tunnel's reality as the time averaged approach flow conditions of the tunnel do not change.

RANS models have been developed based on the concept that a velocity scale and a length scale are sufficient to describe the effect of turbulence in a flow. RANS turbulence models are classified depending on the number of extra transport equations that needs to be solved along with the RANS flow equations (Versteeg and Malalasekera, 2007). The simplest turbulence models are the zero equation turbulence models in which there are no transport equations involved and the velocity and length scales are calculated directly from local mean flow quantities. The drawback of this turbulence model is that it considers the flow isotropic which means that it neglects the process of convective and diffusive transport which are important features of some flows like rapid developing flow and this makes this turbulence model not suitable for modelling complex wind flow around buildings (Hu, 2003).

For such complex flow, there are the seven extra transport equations model called the Reynolds stress model (RSM) which takes into account the anisotropic nature of turbulent flow which leads to more accurate results. However, this turbulence model is computationally more demanding among the RANS models, therefore this turbulence model is not the most commonly applied to engineering flows (Liaw, 2005). The most commonly used RANS turbulence models are the two equations models, of these turbulence models it is the *k*-ε turbulence models that are widely used and most popular of all RANS turbulence models.

Standard k-ε turbulence model

The standard *k-*ε turbulence model is a two equations turbulence model developed by Launder and Spalding where the two equations predict the turbulent kinetic energy (*k*) and its dissipation rate (ε). Lei *et al.* (2006) acknowledged that these two physical quantities help in determining the Reynolds stresses terms, thus closing the RANS equations. The standard *k-*ε turbulence model is the most popular RANS turbulence model used to predict various industrial and engineering flows. Versteeg and Malalasekera (2007) attributed this to the following:

- It is one of the earliest two equations models, thus it is well established and the most widely validated turbulence model.
- Simplest turbulence two equations turbulence model for which only initial boundary conditions need to be supplied.
- Robust formulation and computationally inexpensive.
- Proven excellent performance for many industrial relevant flows.

However, its limitations are also well documented. It is agreed that the main limitations of the standard *k-*ε turbulence model are:

- Excessive production of turbulence kinetic energy in regions of flow impingement resulting in over prediction of the eddy viscosity (μ_t) around a stagnation point.
- Poor performance in flow separation under the action of adverse pressure.
- Flow recovery after reattachment is poorly predicted.
- Fails to resolve flows with large strains such as swirling flows and curved boundary layers flow.
- It has a limited applicability restricted to fully turbulent wall bounded and free shear flows.

- It is not sensitive to free stream turbulence
- It cannot be trusted in flows that involve strong streamline curvature

Vardoulakis *et al.* (2011) added that the standard *k-ε* turbulence model has proven to be very robust and efficient with respect to computational requirements and that is the main reason behind its wide implementation in studying environmental modelling applications. However, its deficiencies are well known and documented. To improve the performance of the standard *k-ε* turbulence model in the above mentioned areas, other two equation models have been developed; these are the renormalized *k-ε* turbulence model and the realizable *k-ε* turbulence model (Hu, 2003; Liaw, 2005; Mertens, 2006; Versteeg and Malalasekera, 2007).

Renormalized k-ε turbulence model

According to Lei *et al.* (2006), a mathematical technique called Renormalization Group (RNG) methods was implemented to derive a closure scheme for the RANS equations. The resulting turbulence model is the RNG *k-ε* turbulence model which is a two equations model for predicting the turbulent kinetic energy (*k*) and its dissipation rate (*ε*). Hu (2003) added that the RNG *k-ε* turbulence model is a modified version of the standard *k-ε* turbulence model where the constants of the standard *k-ε* turbulence model have been replaced with different values and a correction term was added to the dissipation rate (ε) in order to eliminate the excessive production of turbulent kinetic energy (*k*) in the impinging areas and it has proven an improved performance in calculating separated flows. However, it showed poor prediction of flow reattachment in the wake which renders it unsuitable for flow simulation around buildings, especially when the surrounding flow fields are the main concern.

Realizable k-ε turbulence model (used model is this research)

The realizable *k-ε* turbulence model is relatively a new model compared to the former two models. The model was developed based on modifying the dissipation rate (*ε*) equation to satisfy certain mathematical constraints on the normal stresses consistent with the physics of turbulent flows. As for the

turbulent kinetic energy (k) equation, it is the same as that in the standard k-ε turbulence model. The most noteworthy feature is that the production term in the dissipation rate (ε) equation does not involve the production of k, and this modification is believed to better represent the spectral energy transfer of turbulent flows (Lei *et al.*, 2006). Campos-Arriaga (2009) acknowledged that in the realizable k-ε turbulence model, the eddy viscosity (μ_t) is no longer constant but related to gradients in the main flow. Moreover, this model reduces the excessive production of turbulent kinetic energy around the stagnation point and is best used for simulating urban wind flow. According to Mertens (2006) the realizable k-ε turbulence model should give better results for:

- The spreading rate of planar and round jets
- Boundary layers under strong pressure gradients
- Separation
- Recirculation

Lei *et al.* (2006) asserted that all three k-ε turbulence models cannot completely and accurately reproduce all measured data when employed to simulate air flow over geometrical complex intersection model but the measured data showed that the realizable k-ε turbulence was still the best one among the three turbulence models. However, Gosman (1999) pointed out that there is no clear superior turbulence model that can work well with all application and the performance of each turbulence model is highly application dependant. The only reliable guide to select the turbulence closure model is the obtained experience on a similar problem. In an investigation by Blocken *et al.* (2011) to study the application of CFD in building performance simulation for the outdoor environment, they studied different turbulence models and concluded that the Realizable k-$\boldsymbol{\varepsilon}$ is the optimum model in terms of yielding consistent results with relatively required low computational power.

3.4.2.2 Geometry of studied problem

Dutton *et al.* (2005) asserted that air flow within urban areas is highly complicated and including all the details of the built environment in the

simulation model will be computationally very expansive. On the other hand Menter *et al.* (2002) pointed out the importance of reproducing the area of interest with as much details as possible. Franke *et al.* (2007) added that the building at which wind effects are of main interest requires the greatest level of detail, and features greater than 1m should be represented, as for buildings further away could be represented as simple blocks. However, including these details in the model would directly affect the dimension of the domain as there are relationships between buildings' dimensions and the dimensions of the computational domain as will be discussed in the following section.

3.4.2.3 Computational domain dimensions

The computational domain represents the geometry of the region of interest and it cuts off the surroundings, thus the boundary condition of the domain approximates the conditions of the surroundings. The positioning of these boundaries plays an important role in the accuracy of the simulation and the size of the computational domain in the vertical, lateral and flow directions depends on the area that shall be represented.

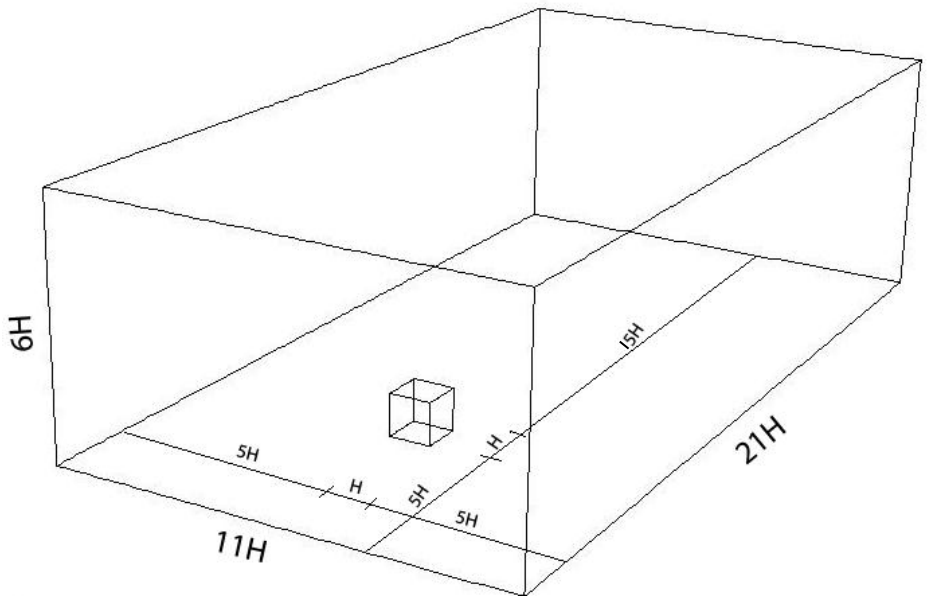

Figure 3.6 Computational domain dimensions for a flow around a surface mounted cube of height H.

In the vertical direction, Cowan *et al.* (1997) and Tominaga *et al.* (2008) agreed that the vertical extension of the domain should be 5H away from the tallest building of height H which makes the domain height equals to 6H. Franke *et al.*

(2007) added that maintaining this vertical distance is necessary for preventing an artificial acceleration of the flow over the building. The lateral extension of the domain is calculated based on fulfilling a blockage of 3%, where the blockage is defined as the ratio of the projected area of the building in flow direction to the free cross section of the computational domain. This would lead to a distance of approximately 2.3H between the building's sidewalls and the lateral boundaries of the computational domain. However Cowan *et al.* (1997) and Tominaga *et al.* (2008) recommended using 5H leading to a blockage of 1.5%.

As for the extension of the domain in the flow (longitudinal) direction, this area is divided into two regions; one is the extension of the domain in the windward direction and the other is the extension of the domain in the leeward direction. For the extension of the domain in the windward direction Cowan *et al.* (1997), Hu (2003), Franke *et al.* (2004) and Tominaga *et al.* (2008) recommended a distance of 5H between the inflow boundary and the windward facade of the building. For the extension of the domain in the leeward direction, they agreed a distance of 15H between the leeward facade of the building and the outflow boundary. Figure 3.6 demonstrates the vertical, lateral and longitudinal dimension of a computational domain enclosing a building of height H.

3.4.2.4 Computational domain boundary conditions

According to Blazek (2001), the domain represents a truncation of part of the surrounding of the flow problem, thus this truncation leads to artificial boundaries, where these boundaries have to prescribe values of certain physical quantities. Assigning these physical quantities to the boundaries should be treated with care as an improper implementation can result in inaccurate simulation of the real flow problem, as well as its effect on the stability and convergence speed of the solution. Thus, boundary conditions are assigned to the boundaries of the computational domain to simulate the physical quantities in the real flow problem. There are five main boundaries which need to be assigned in external flow problems; these are the inflow boundary condition, outflow boundary condition, bottom boundary condition, top boundary condition and the sides boundary conditions. The sides and the top boundary conditions are mostly treated in the same way.

For the inflow boundary condition, an atmospheric boundary layer profile (ABL) should be prescribed as an inlet profile. Jha (2010) stated that wind speed varies with height and the wind profile can either be represented by a power exponent or a logarithmic function which describe the changes in mean wind speed as a function of height (Figure 3.2). According to Franke *et al.* (2007), for the inflow boundary condition, a logarithmic velocity inlet profile is usually prescribed. This velocity profile can be obtained from the logarithmic profile corresponding to the upwind terrain through the roughness length (z_0) or from the profiles of the wind tunnel tests, the turbulence quantities at the inlet can be obtained from the assumption of an equilibrium boundary layer which means that the production and dissipation rates of the turbulent kinetic energy are equal to each other.

According to Jha (2010), using the logarithmic function to compute the velocity profile can be described using the following equation:

$$\frac{V(z)}{V(10)} = \frac{\ln\left({}^{z}/_{z_0}\right)}{\ln\left({}^{10}/_{z_0}\right)}$$

where $V(z)$ is the wind speed at operating height z (m/sec), z_0 is the roughness length, and $V(10)$ is the wind speed (m/sec) at a reference height 10 m from the ground. It should be noted that either the power exponent or a logarithmic function can be used to calculate the mean wind velocity or speed at a given height if the mean wind velocity is known at the reference height (z). Parameter z_0 represents the roughness length for the type of terrain involved (Figure 3.2) (Jha, 2010). Another way of obtaining an atmospheric boundary layer (ABL) velocity profile is the empirical formulation known as the power law:

$$V(z) = V_G \left(\frac{z}{z_G}\right)^{\alpha}$$

Where $V(z)$ is the wind velocity (m/s) at a height z (m), α is the exponent dependent on terrain conditions, V_G is the wind velocity at the gradient height and z_G is the gradient height. According to Hu (2003), the values in the equations depend on the conditions of the terrain being rural, suburban or urban (Table 3.2). According to the American Society of Civil Engineers (ASCE, 1996), the advantage of the power law model is its simplicity and its accuracy is

sufficient for most wind engineering applications. On the other hand, Hu (2003) asserted that the power law models are purely empirical lacking the support of proven theory and they are not good in representing velocity profile close to the ground.

Another important characteristic about the inlet velocity profile which Blocken *et al.* (2007b) and Hargreaves and Wright (2007) outlined is the horizontal homogeneity of the velocity profile along the computational domain, which means that the flow variables should not change until the built area is reached. Horizontal homogeneity means that the inlet profile, the approach flow profile and the incident profile are the same (Figure 3.7). Fulfilling this requirement is dependent on the roughness of the bottom wall boundary and on the boundary condition at the top boundary of the computational domain. This is why sensitivity tests in an empty computational domain are important prior to the actual simulation with the obstacle models present.

Table 3.2 Values of z_G and corresponding α (Jha, 2010).

Type of terrain	z_G, gradient height (m)	α
Open terrain with very few obstacles e. g. open grass or farmland with few trees, hedgerows and other barriers etc; prairie, tundra shores and low islands of inland, lakes; deserts.	300	0.16
Terrain uniformly covered with obstacles 10 to 15 m in height; e. g. Residential suburbs; small towns; woodland and shrub, small fields with bushes, trees and hedges.	430	0.28
Terrain with large and irregular objects; e. g. centres of large cities, very broken country with many windbreaks of tall trees, etc.	560	0.40

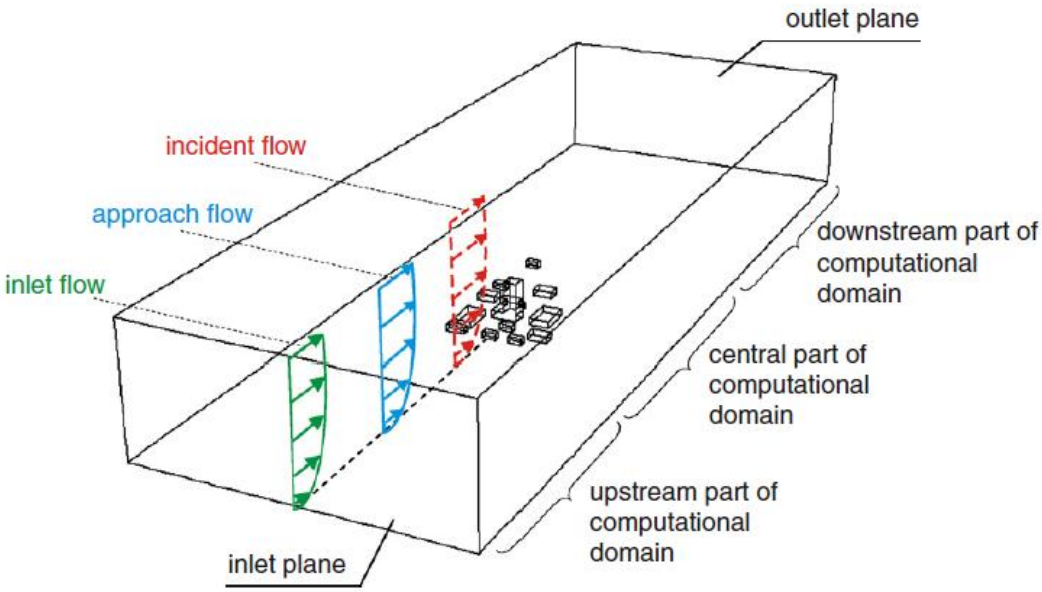

Figure 3.7 Inlet, approach and incident flows is a computational domain with the indication of different parts of the domain (Blocken *et al.*, 2007b).

The bottom boundary condition of the domain is usually prescribed as no-slip wall boundary which significantly affects the flow in the area near the wall because the velocity at the wall surface becomes zero and the shear stress reaches the maximum value. One of the aspects related to the wall boundary condition which affects the accuracy of the solution is the roughness of the implemented wall. Franke *et al.* (2007) asserted that most CFD codes implement sand-roughened surfaces with a corresponding roughness height (k_s) for the roughness of the wall. In such case, Blocken *et al.* (2007b) acknowledged that four requirements should be simultaneously satisfied:

- High mesh resolution in the vertical direction close to the bottom of the computational domain
- Maintaining the horizontal homogeneity of the atmospheric boundary layer (ABL) profile upstream and downstream the computational domain
- The distance between the centre of the first cell away from the bottom boundary (z_p) and the bottom wall boundary to be greater than the roughness height ($z_p > k_s$)
- Roughness height equal to thirty times the roughness length (z_0) ($k_s = 30\, z_0$).

The roughness length differs according to the nature of the terrain, Cook (1985) suggested the values of z_0 for six recognizable terrain types in the UK for design of wind load on buildings and structures (Table 3.3). However, Blocken *et al.* (2007b) added that although it is logical to have $z_p > k_s$ as it is not physically meaningful to have mesh cells with centre points within the physical roughness height, this would lead to a coarse mesh. Thus, it is suggested to alleviate the requirement $z_p > k_s$[3].

Table 3.3 Categories of terrain and roughness parameters (Cook, 1985).

Category	z_0 (m)	Remark
0	0.003	Corresponding to large expanses of water, mudflats, snow covered farmland and large flat areas of tarmac
1	0.01	Corresponding to flat grassland, parkland or bare soil, without hedges and with very few isolated obstructions
2	0.03	Meteorological standard, basic terrain roughness corresponding to typical UK farmland, nearly flat or gently undulating countryside, fields with corps, fences or low boundary hedges and few trees
3	0.1	Corresponding to farmland with frequent boundary hedges, occasional small farm structures, houses or trees
4	0.3	Corresponding to dense woodland, domestic housing typically between10% and 20% plan-area density
5	0.8	Corresponding to city centres, comprising mostly four-storey buildings, or higher, typically between 30% and 50% plan-area density

[3] More on specifying the roughness height will be discussed in the validation chapter when discussing the horizontal homogeneity of the ABL profile as the roughness height is one of the main factors affecting the horizontal homogeneity of the ABL profile.

The top and side boundary conditions play an important role in maintaining the homogeneity of the inflow profile. This is done by prescribing constant shear stress at the top and the sides which corresponds to the inflow profile. Franke *et al.* (2007) acknowledged that a free slip condition at a rigid lid is sometimes used. Blocken *et al.* (2007b) suggested another way of doing this by prescribing the values for the velocities and the turbulence quantities of the inflow profile at the height of the top boundary over the entire top boundary.

Franke *et al.* (2007) asserted that the best results can be obtained by assigning symmetry boundary conditions for both top and side boundaries which enforces a parallel flow at the top and the sides of the domain which means that the velocity component normal to the boundary, as well as other flow variables, will vanish which might be different from the inflow boundary profile. Thus a symmetry boundary condition is suggested to be used.

The outflow boundary is the boundary behind the studied area where all or most of the fluid leaves the computational domain. Either an outflow or a constant static pressure is used as a boundary condition. The outflow boundary conditions means that all the derivatives of all the flow variables are forced to vanish, corresponding to a fully developed flow. This might lead to the flow re-entering the domain which might cause the solution not to converge. Thus, the boundary should be placed far away from the studied area as stated earlier in the domain dimensions section (3.4.2.3) (FLUENT, 2006).

3.4.2.5 The computational mesh

Asfour and Gadi (2007) asserted that the creation of the mesh is one of the important variables to consider for a successful CFD simulation as it is one of the main factors affecting the quality of a CFD simulation. Tu *et al.* (2008) acknowledged that most of the time spent in a CFD project in industry is spent in constructing a mesh that allows for a compromise between desired accuracy and computational cost. However, there is general agreement about the importance of carrying out test runs on different mesh sizes and configurations until the solution does not change significantly with the change in mesh sizes and configurations in what is called mesh independence test (Liaw, 2005; Ariff *et al.*, 2009a; Salim and Cheah, 2009).

The mesh resolution should gradually be refined until a constant solution is achieved. However, Franke *et al.* (2007) limited this test to three systematically refined/coarsened meshes. The ratio of cells for two consecutive grids should be at least 3.4, when this is not applicable due to computational limitations, it is advised to locally refine the mesh in the area of interest or areas where important physical phenomena are likely to occur. Hu (2003) suggested refining the mesh in the areas upwind and in the wake of an obstacle due to the complicated nature of flow in these areas which results from differences in pressure and mixing effects of momentum transfer.

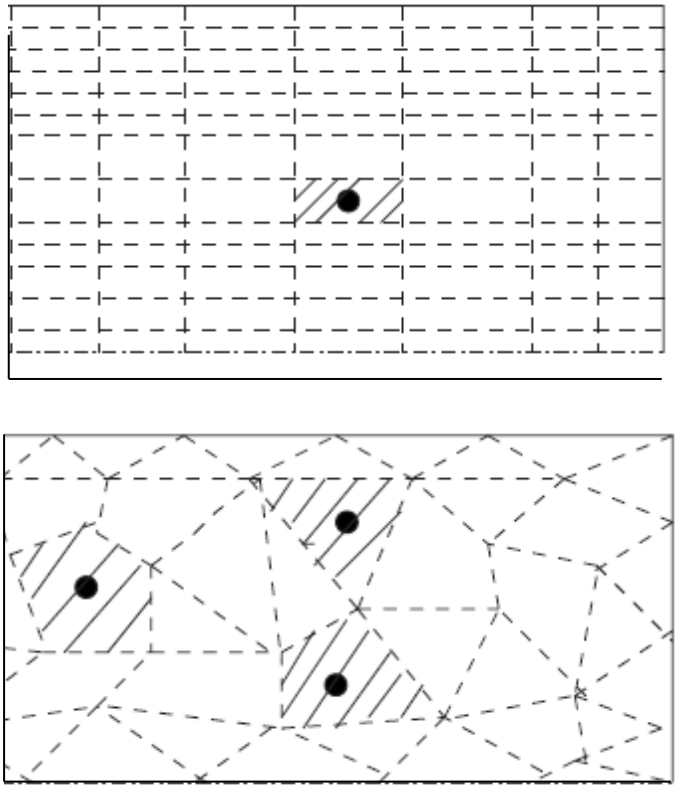

Figure 3.8 Top: structured mesh, Bottom: unstructured mesh (Date, 2005).

Zhang *et al.* (2010) argued that it is hard to give recommendations in advance about mesh resolution because this is very problem dependant. However, they added that there are general recommendations regarding the geometry of the mesh. Generally, the generated mesh should preserve the correct geometry forms of all the objects within the computational domain. The ideal arrangement of the mesh cells is to be equidistant, especially in areas of high gradients. However due to computational requirements stretching and compression can be

implemented, thus Franke *et al.* (2004) recommended a ratio not exceeding 1.3 between two consecutive cells.

Another measure of the mesh quality is the angle between the normal vector of a cell surface and the line connecting the midpoints of the neighbouring cells. Ideally these should be parallel (Ferziger and Peric, 2002). As for the shape of the computational cells, hexahedra are preferable to tetrahedral. Hexahedral cells are the building unit of structured mesh while tetrahedral constitutes most of the cells in unstructured meshes (Figure 3.8).

Hu (2003) argued that structured meshes are advantageous over unstructured meshes in terms of computational cost as the neighbour connectivity simplifies the programming task and the matrix of the algebraic equation system has a regular structure. However, the main disadvantage of structured meshes is that they are ideal only for geometrically simple domains. But it can be argued that this could be overcome by increasing mesh resolution near complicated geometries. On the other hand, unstructured mesh can fit any geometrical shape as they are made of tetrahedral. In addition, they are easily controlled and refined where higher mesh resolution is required. But this comes with high computational cost because node locations and neighbour connections need to be specified with a more complicated algebraic equation system no longer in a form of regular, diagonal structure as in the structured grid. Therefore more time and storage are needed for calculations to take place.

3.4.3 *Errors, uncertainties and validation of CFD simulations*

The study by Chen and Zhai (2004) demonstrated that the quality of a CFD flow simulation is highly user dependant. Hu (2003) attributed this to the many physical and numerical parameters which might puzzle even experienced users. Castro and Graham (1999) acknowledged that even though the user might think the right decisions were made and even the results look reasonable, the solution is far from the reality because the problem solved is actually another flow problem based on inaccurate or wrong assumptions. The large number of parameters affecting the quality of CFD flow simulation introduces errors and uncertainties which are either errors and uncertainties in modelling the physics of the flow or numerical errors and uncertainties.

According to Franke *et al.* (2007), the errors and uncertainties in modelling the physics could be due to:

- Simplification of physical complexity which takes place when implementing turbulence closure models to average the Navier-Stokes equations (LES & RANS) instead of directly solving the equations (DNS) due to limitations in computational power. These approximate models introduce errors and uncertainties to the results of the numerical solution.

- Usage of previous experimental data for the adjustable parameters within the turbulence model such as the turbulence intensity, roughness values, viscosity related variables, etc. This experimental data are embedded with errors themselves thus introducing uncertainty to the CFD simulation.

- Simplification of the geometrical details of the objects surrounding the area or object of interest which is due to either the lack of the required information or the limitations in computational power to model all surrounding objects. These missing details add to the uncertainty of the CFD simulation.

- Approximation of surrounding environment through physical boundary conditions because the computational domain only represents part of the real surrounding environment. Prescribed boundary conditions influence to a great extent the behaviour of the flow within the domain which adds to the uncertainty of the simulation and can also lead to errors or even the solution not converging if the boundary conditions are inadequate.

As for the numerical errors and uncertainties, they could be due to:

- Code programming errors, these errors cannot be controlled by the code users but should be detected and fixed by the code developers.

- The accuracy of the computer known as “computer round-off errors” and depends on the precision of different computers in terms of the finite representation of numbers. It is recommended to use double precision in CFD simulation which requires 64 bits of storage.

- Spatial and temporal discretisation which represents the difference between the exact solution of the partial differential equation and the numerical approximation obtained by finite discretisation in space and time. These errors could be kept to a minimum by careful distribution and refinement of the mesh.

- Iterative convergence which occurs when the numbers of iterations are insufficient to obtain a converged solution or the iterations are stopped too early. The iterative convergence error is the difference between this intermediate solution and the complete solution. These errors can be controlled by monitoring the residuals values to make sure that the residuals have reached a steady state predefined values in the range of 10^{-4} to 10^{-6}.

All previously mentioned errors can be controlled and kept to a minimum by the code user except the computer programming errors which are the responsibility of the code developers. Although the code users are urged to take every measure to keep the errors as minimum as possible, a mistake or unwise choice might be made during the course of simulation due to lack of experience or computational resources. Thus, Castro and Graham (1999) argued that the best CFD simulation is not necessary to be identical with wind tunnel tests for validation purposes. However, a margin of error or discrepancy is acceptable. Summers *et al.* (1986) suggested a 20% discrepancy, which is the same commonly used percentage when comparing wind tunnel tests with full-scale measurements. Stathopoulos and Baskaran (1996) considered a discrepancy of 30% to be acceptable in CFD modelling of wind flow around buildings, which is the same percentage Hu (2003) considered satisfactory when comparing computations and experiments.

Thus, due to the errors and uncertainties in CFD simulations, validation studies are essential for assessing the quality of the results and reducing the uncertainties in CFD simulations. Another way of reducing the uncertainties in CFD simulations is to consult earlier validation studies. However Blocken *et al.* (2010) still argued that the results from validation studies can easily be obscured by numerical errors and the statement of Ferziger and Peric (2002) on

turbulence model, although made more than a decade ago, it is still believed to be true today:

"Which model is best for which kind of flows (none is expected to be good for all flows) is not yet quite clear, partly due to the fact that in many attempts to answer this question numerical errors played a too important role so clear conclusions were not possible … In most workshops held so far on the subject of evaluation of turbulence models, the differences between solutions produced by different authors using supposedly the same model were as large if not larger than the differences between the results of the same author using different models ."

3.5 Conclusion

Three main urban wind assessment tools were discussed in this chapter; in-situ measurements, wind tunnel tests and CFD simulations. The advantages and disadvantages of each tool were investigated and it can be argued that CFD simulation is the most relevant tool for implementation in this research since CFD is the most relevant tool for comparing design alternatives and this research mainly focuses on comparing alternative roof shapes and their effect on the energy yield and positioning of roof mounted wind turbines. Thus, CFD as a tool for investigating urban wind flow was investigated further to reach a conclusion about the requirements for a consistent CFD simulation through investigating the main potentials and constrains of using different CFD simulation parameters for assessing wind flow around buildings.

It can be concluded that the set of requirements for a consistent CFD simulation is strongly dependant on the availability of adequate computational power and availability of experimental data for validation purposes. Although DNS, LES, DES and URNAS methods yield more reliable results, their implementation in studying wind flow around buildings is few when compared to Steady RANS models. Accordingly, there is a lack in literature for detailed validation for these methods. This is not the case for RANS models where many guidelines and best practice documents can be found in literature. Table 3.4 summarises the main concluded requirements for carrying out a consistent CFD simulation.

Table 3.4 Requirements for a consistent CFD simulation.

Solution method	Second order Schemes or above should be used for solving the algebraic equations.
Residuals	In the range of 10^{-4} to 10^{-6}.
Mesh	Multi-block structured mesh. Carrying out sensitivity analysis with three levels of refinements where the ratio of cells for two consecutive grids should be at least 3.4. Mesh cells to be equidistant while refining the mesh in areas of complex flow phenomena. If cells are stretched, a ratio not exceeding 1.3 between two consecutive cells should be maintained.
Turbulence model	Realizable k-ε turbulence model.
Accuracy of studied buildings	Details of dimension equal to or more than 1 m to be included.
Domain dimensions	If H is the building height; Lateral dimension = 2H+Building width. Flow direction dimension = 20H+Building dimension in flow direction. Vertical Direction = 6H. While maintaining a blockage ratio below 3 %.
Boundary conditions	Inflow: Horizontally homogenous log law ABL velocity profile. Bottom: No-slip wall with standard wall functions. Top and side: Symmetry. Outflow: Pressure outlet.

Although it has been demonstrated that these requirements would lead to a high quality CFD simulation, it is mandatory to validate the CFD simulation

using another wind assessment tool to minimise the errors and uncertainties in the CFD code. It can be argued that implementing these parameters in studying wind flow around a 3D cube immersed in a turbulent channel flow would be adequate for validating the CFD simulation results later in this research. This would be done by comparing the results with the data sets from published researches investigating wind flow around a cube in a turbulent channel flow which is the focus of the next chapter.

Chapter Four

Validation Study: Wind Flow around a Cube in a Turbulent Channel Flow

Chapter Structure

4.1 Introduction

4.2 Wind flow around a cube

4.3 CFD simulation of wind flow around a cube in a turbulent channel flow

4.4 Conclusion

Chapter 4: Validation Study: Wind Flow around a Cube in a Turbulent Channel Flow

4.1 Introduction

As seen in the previous chapter; CFD simulation, as a wind assessment tool, is embedded with errors and uncertainties. Thus, Blocken *et al.* (2011) asserted the importance of validating CFD simulations against other wind assessment tools to gain confidence in the simulation results. Accordingly, for validating the results of a CFD simulation, the flow problem has to be solved using another wind assessment tool. Blocken *et al.* (2011) acknowledged that for assessing wind flow within the built environment, in-situ measurements are not often available. Thus, it would be convenient to use simple forms and configurations which resemble the main expected flow features around the studied objects. Results from wind tunnel tests for such simple cases are widely available in literature, thus decreasing the uncertainties of the CFD simulation.

In this chapter wind flow around a cube in a turbulent channel flow is investigated using the commercial CFD code Fluent 12.1. For validation purposes the results are compared to published in-situ measurements, published wind tunnel tests and other validated published CFD simulations for a 6m cube. In-situ measurements, wind tunnel tests results and validated CFD simulation results for wind flow around a full scale 6m cube at the Silsoe Research Institute is available in literature and is used for comparison in this research. Thus, this chapter is divided into two main sections:

- The first section (4.2) reviews literature on in-situ measurements of wind flow around a cubic building, wind tunnel tests of wind flow around a cube in a turbulent channel flow and validated CFD simulations of the same flow problem. In doing so, main flow features are discussed qualitatively and quantitatively in terms of main flow features, streamwise velocities in horizontal and vertical plans, reattachment length, stagnation point location, separation locations and pressure coefficients along the surfaces of the cube.
- The second section (4.3) focuses on reporting the CFD simulation results in this thesis of the same flow problem using the best practice guidelines for running CFD simulations extracted from literature in the previous

chapter, in addition to explaining the process of specifying the simulation variables such as achieving a horizontally homogeneous atmospheric boundary layer (ABL) profile and choosing the optimum computational mesh through a mesh independence study.

In light of the previously reviewed literature, the CFD simulation results will be assessed by comparing the obtained results with the published in-situ measurements, wind tunnel tests and validated CFD simulations. Accordingly, the simulation variables used in the validation study will be reviewed and updated for further use in the simulations in the rest of the research.

4.2 Wind flow around a cube

The most widely studied flow problem in wind engineering is a 3D cube immersed in a turbulent channel flow. This is due to the simplicity of the shape and the complexity of flow phenomena around the cube. In a preliminary study by the author to compare different flow phenomena around some basic shapes (cube, prism, dome, vault, pyramid and a cone), it was noticed that of all the investigated basic shapes, it is the cube which demonstrated highest variety in flow phenomena; the largest number of deviated flows, separation, reattachment, recirculation, side vortices, leeward vortices, backflow, shear layers, stagnation point and upward drafts.

The same results and rational behind using a simple cube for validation studies was reported by Vardoulakis *et al.* (2011) and Seeta Ratnam and Vengadesan (2008). It is evident that the cube immersed in a turbulent channel flow is extensively investigated in existing literature and used in many CFD studies to validate CFD simulation work (Castro and Robins, 1977; Ogawa *et al.*, 1983; Martinuzzi and Tropea, 1993; Hussein and Martinuzzi, 1996; Lakehal and Rodi, 1997; Richards *et al.*, 2001; Richards and Hoxey, 2002; Schmidt and Thiele, 2002; Cheatham, 2003; Richards and Hoxey, 2004; Gao and Chow, 2005; Richards and Hoxey, 2006; Richards *et al.*, 2007; Richards and Hoxey, 2008; Ariff *et al.*, 2009a; Ariff *et al.*, 2009b; Lim *et al.*, 2009).

Two of the mostly cited references in literature on wind flow around a cube are the researches by Murakami and Mochida (1988) and Martinuzzi and Tropea (1993). They have noticed that as the flow approaches the building it divides into four main streams; the first stream is deviated over the building, the second

stream is deviated down the windward facade and the other two streams deviate to the two sides of the building (Figure 4.1). At the point of deviation a stagnation point is formed with maximum pressure situated at that point. From that point the flow changes direction to lower pressure zones of the facade; upwards, sidewards and downwards. The air flowing downwards forms a standing vortex in front of the windward facade.

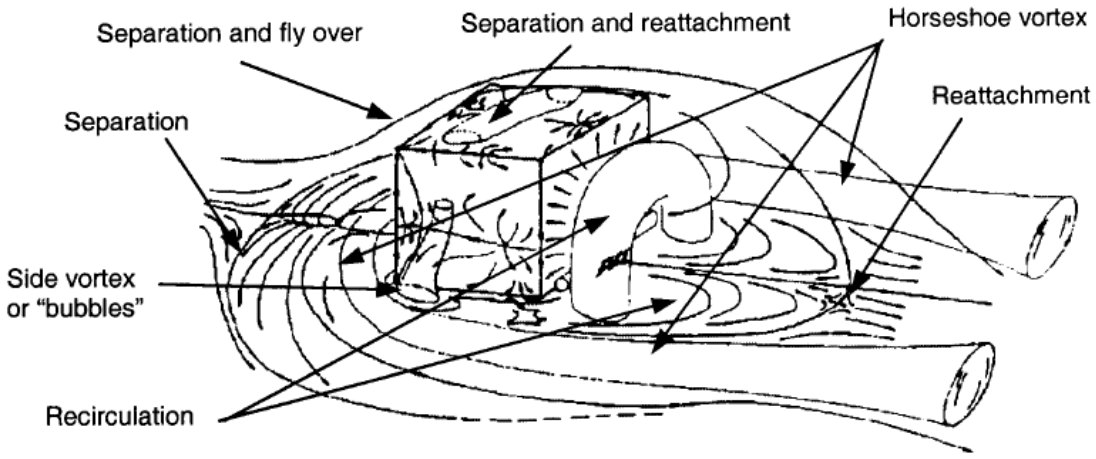

Figure 4.1 Schematic representation of the flow field around a cube (Martinuzzi and Tropea, 1993).

Corner streams and flow separation areas are formed at the sides and on top of the building due to the formation of 3 vortices, the corner streams subsequently merge into the general flow around the corners. A low pressure zone is formed downwind the building which results in the formation of a backflow or a recirculation area were the flow direction is opposite to the main flow direction. This backflow is responsible for the formation of slow rotating vortices behind the building. Between these vortices and the corner streams an area with a high velocity gradient exists which is called the shear layer and these are situated at the buildings corners where flow separation occurs. Seeta Ratnam and Vengadesan (2008) added that the most visible feature of the flow is the formation of a horseshoe vortex around the cube which is formed due to the separation in the flow near the connection between the obstacle and the lower channel wall on both sides of the obstacle, the separated flows then merge together downwind the obstacle (Figure 4.1). A more detailed visualization of the flow around the cube is included in Figure 4.14 under section 4.2.3.

The accuracy of the wind assessment tool is measured by its ability to capture qualitatively the previously mentioned flow features. In addition to that, quantitatively, specifying to the highest degree of accuracy the locations and values of each of the specific flow features. In the following sections, the results from published in-situ measurements, wind tunnel tests and validated CFD simulations for wind flow around a cube will be reviewed, compared to each other and to the obtained CFD simulation results from this study.

4.2.1 *In-situ measurements*

Hölscher and Niemann (1998) asserted that long term in-situ measurements (at least for a year) have contributed considerably to understanding turbulent flows and developing wind tunnel tests and CFD simulations. However, Eliasson *et al.* (2006) and Roth and Oke (1993) noted that in-situ measurements are scarce in literature and if found they are case specific and mostly focusing on assessing pollutants dispersions within street canyons and pedestrian wind comfort. For this reason, a 6m cube has been constructed at Silsoe in an open country exposed position, at the Silsoe Research Institute to provide a facility for fundamental studies of the interactions between the wind and a structure (Figure 4.2). Detailed measurements have been made of surface pressure on the cube and of the wind velocities in the region around the cube. Mean pressure coefficient data from the Silsoe 6m cube are compared with published wind tunnel data and with the detailed results from the Windtechnologische Gesellschaft comparative wind-tunnel testing program (Richards *et al.*, 2001).

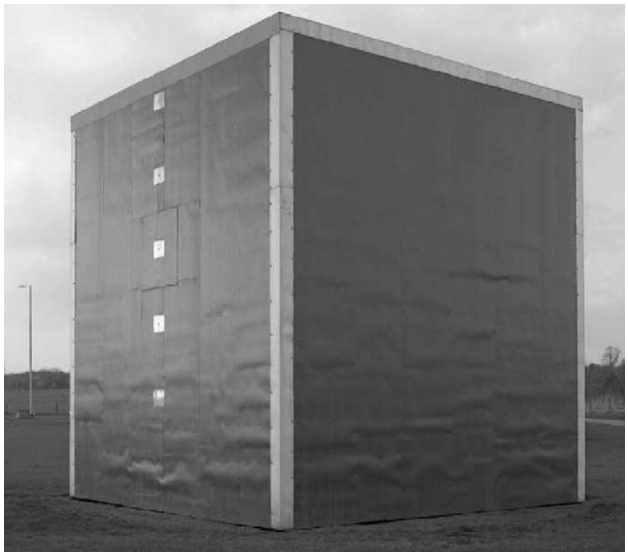

Figure 4.2 The 6m cube at the Silsoe Research Institute (Richards *et al.*, 2001).

The measurements by Richards *et al.* (2001) for wind speed at the Silsoe cube location are matched by a logarithmic profile with a roughness length z_o = 0.006 to 0.01m. They compared their results for pressure distribution along the cube's surfaces with those from the wind tunnel tests of Castro and Robins (1977) and others. They argued that the results of Castro and Robins (1977) are the most comprehensive and most widely referenced set of data for pressures on a cube. Figure 4.3 shows that with the wind perpendicular to one face, there is general agreement on the windward facade pressures between wind-tunnels and the full-scale measurements. However, for the roof and leeward façade there are some discrepancies in the values but the pressure distribution is the same. Richards *et al.* (2001) and Vardoulakis *et al.* (2011) argued that this is due to pressures being sensitive to approach flow conditions and scale, i.e. velocity profile, turbulence, variation in the cube to roughness height ratio and Reynolds number.

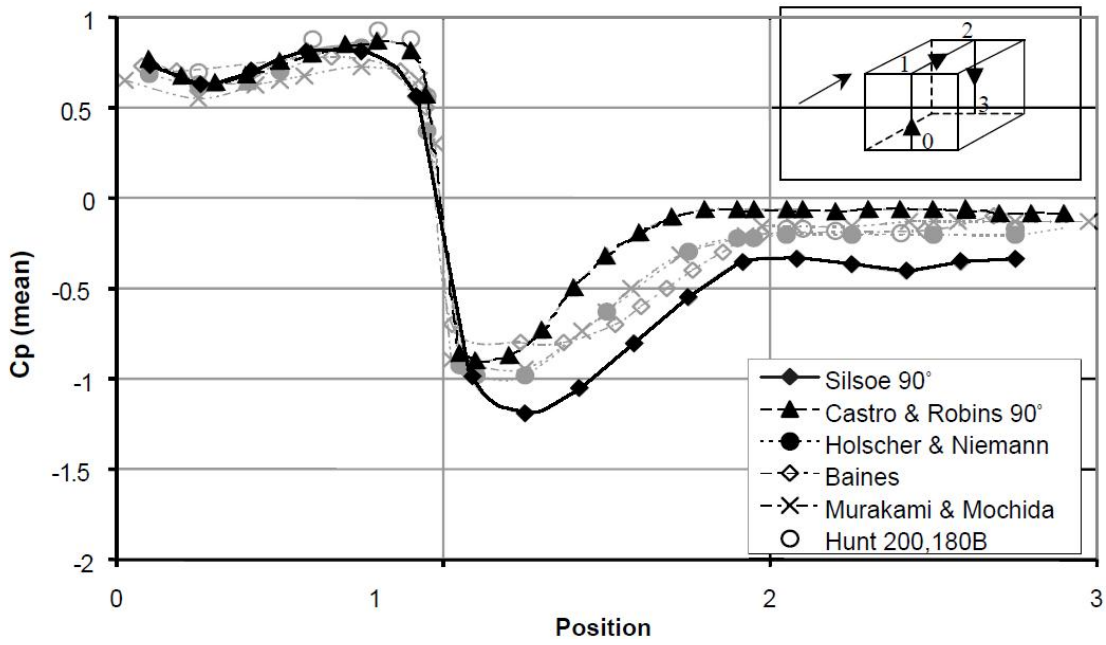

Figure 4.3 Wind tunnel tests results of the vertical central section mean pressure coefficients with the wind normal to one face (0^0) including the Silsoe full-scale test (Richards et al., 2001).

Similar observations were recorded when comparing the results to those from Hölscher and Niemann (1998) (Figure 4.4) as the full scale measurements were in agreement with the average of the 15 wind tunnel tests at the windward façade, but discrepancies were found on the roof and the leeward façade. However, results from Richards *et al.* (2001) agreed best for the three surfaces with wind tunnel tests results number eight. Detailed results from Hölscher and

Niemann (1998) showed that the maximum range of pressure coefficients for all the wind tunnel tests is between 0.67 and 0.92 which occurred about three-quarters of the way up the windward facade. More discrepancies are noticed between the wind tunnel tests across the roof and at the leeward façade although the basic shape of the pressure distribution is the same. It should be noted that at both locations the in-situ measurements over-predicted the pressure coefficients in comparison to the wind tunnel tests.

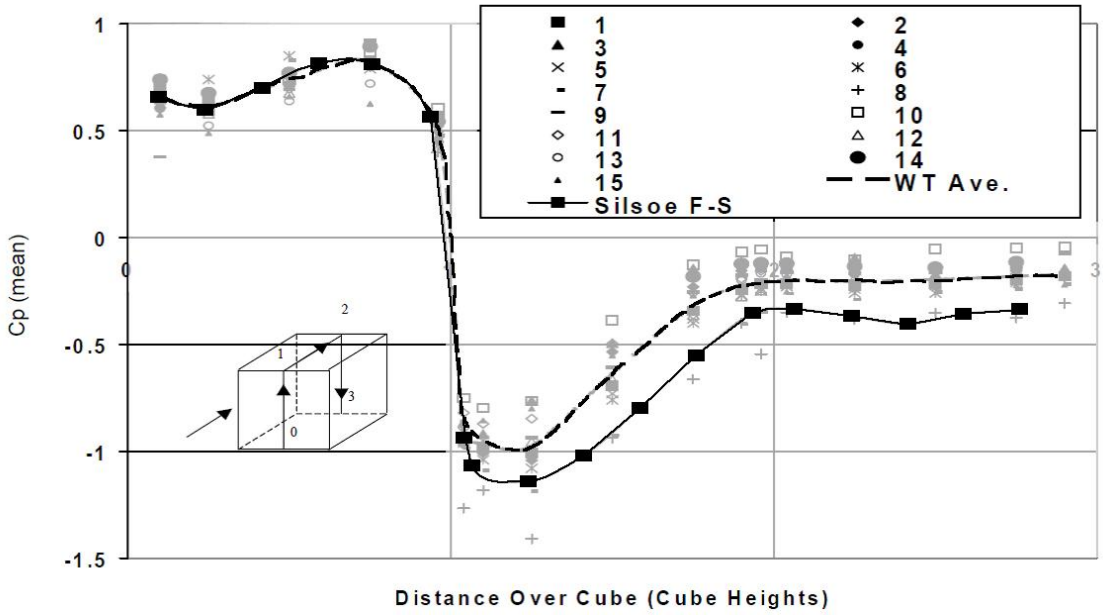

Figure 4.4 Vertical central section mean pressure coefficients with wind normal to one face (0^0) from the Windtechnologische Gesellschaft comparative wind-tunnel testing program, including the Silsoe full-scale test (Hölscher and Niemann, 1998).

In addition to measuring the pressure distribution on the surfaces of the cube and comparing it to the results from wind tunnel tests for validation purposes, Richards and Hoxey (2006) acknowledged that comparing the flows in terms of locations of separations and reattachments are also important for determining the consistency of the results especially when the flow is perpendicular to one of the faces of the cube. In order to specify the reattachment point on top of the roof, Richards and Hoxey (2006) used five ultrasonic anemometers to measure flow velocity above the roof of the Slisoe 6m cube.

The results showed that the reattachment point on top of the roof along the cube centreline was near the location x/h = 0.6 (Where h is the characteristic length of the cube and x is the length on top of the cube in the streamwise direction when the origin is at the windward edge). It should be noted that the

reattachment length is dependent on the wind direction as well which means that if wind changes direction, the reattachment will happen at a different location. Richards and Hoxey (2006) measured the reattachment length under different wind directions and acknowledged that the reattachment length decreases with the increase in the incident angel of the wind. These results were consistent with other full-scale and wind tunnel tests as can be seen in Table 4.1 which shows that the reattachment length ranges from no reattachment with very low turbulence levels in the onset flow to no separation with high onset flow turbulence which suggests a relationship between the reattachment length and the levels of turbulence.

Table 4.1 Characteristics of the full-scale and wind tunnel tests and the associated reattachment lengths ranked in order of longest to shortest reattachment length which corresponds to lowest to highest turbulence intensities as explained by Richards and Hoxey (2006).

Reference	Tool used	Cube height	Reattachment length
Castro and Robins (1977)	Wind tunnel (Laminar flow)	60mm	No reattachment
Ogawa *et al.* (1983)	Wind tunnel with no roughness	80mm	No reattachment
Murakami and Mochida (1988)	Wind tunnel	NA	≈ 0.7h
Richards *et al.* (2001)	Field measurements	6m	≈ 0.6h
Ogawa *et al.* (1983)	Field measurements	1.8m	≈ 0.55h
Castro and Robins (1977) BL[1]	Wind tunnel	200mm	≈ 0.3h
Ogawa *et al.* (1983)	Wind tunnel (6cm roughness)	80mm	No separation

[1] BL = Boundary Layer wind tunnel

4.2.2 *Wind tunnel tests*

Since in-situ measurements are costly, time consuming and it is difficult to control the approaching flow conditions due to the unpredictability of wind which would inevitably obscure the results. Thus, it can be argued that a well-controlled environment such as wind tunnels or CFD simulations can yield more consistent results than in-situ measurements. For CFD simulation implementing RANS, Franke *et al.* (2004) suggested that the best wind assessment tool to be used to validate the CFD simulation results is the wind tunnel as wind tunnels use steady-state boundary conditions which comply with the underlying definition of the statistically steady RANS results. Hölscher and Niemann (1998) also acknowledged that wind tunnel experiments are the primary tool for predicting either wind effects on structures or dispersion of air pollutants and although full scale measurements are embedded with errors, they are still considered as the true result by comparison to which the performance of the wind tunnel model is measured.

As mentioned earlier, the wind tunnel results from Castro and Robins (1977) are the most comprehensive and most widely referenced set of data for wind flow around a cube in literature. They used two different flow types; the first is a uniform upstream flow and the second is an atmospheric boundary layer (ABL) profile (Figure 4.5). This section focuses on the second type as it is closer to reality and will be used in further simulations in this research. They produced the ABL profile in a 2.7 x 9.1m wind tunnel using a series of vorticity generators mounted across the wind tunnel with a relatively small barrier wall mounted upstream and distributed roughness elements downstream which resulted in an ABL whose thickness is 2m. The roughness length (z_0) was about 0.02% of the ABL height, so that z_0/h = 0.02. The cube height was 1/10 of the boundary layer height (δ) and was positioned at a distance 3.5δ downstream of the vorticity generators. Castro and Robins (1977) reported gradients in the velocity, shear stress and turbulent intensity throughout the longitudinal section of the tunnel which reached 3% per boundary layer thickness which they considered very small.

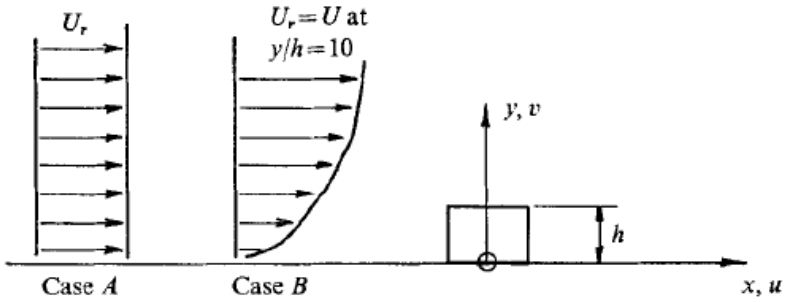

Figure 4.5 Case A and Case B for the velocity profile used (Castro and Robins, 1977).

Figure 4.6 shows the results of the surface pressure coefficients along the centreline of the cube on the windward façade, the roof and the leeward façade in the case of the wind perpendicular to the windward facade.

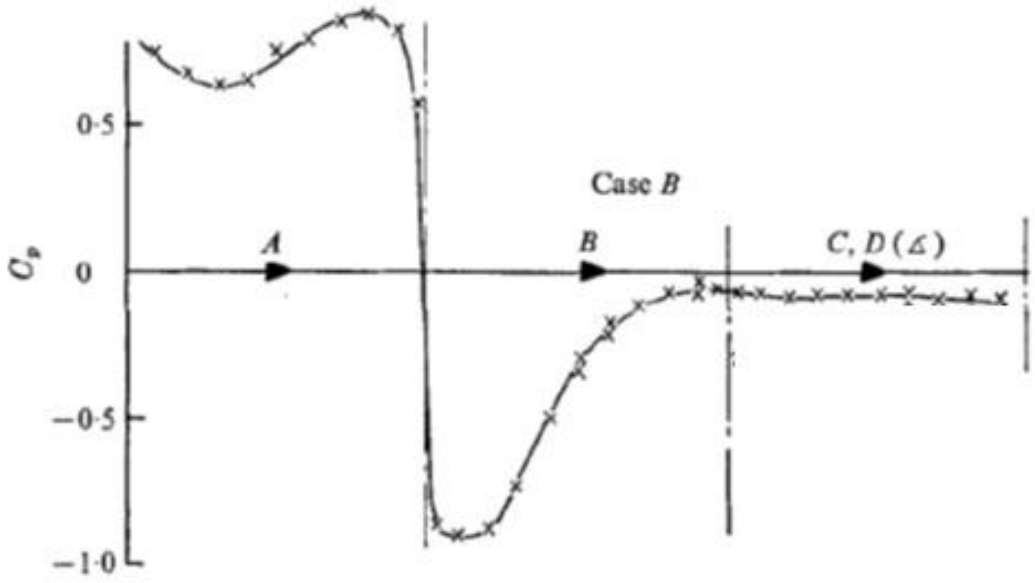

Figure 4.6 Surface pressure coefficients along the centreline of the cube when normal to the incident flow (Castro and Robins, 1977).

In terms of flow velocity, measurements showed that the flow returned to initial upstream conditions around x/h = 8.5 as for the separation and reattachment on top of the roof; the thickness of the negative velocity region was found to be only 5% of the cube height and the reattachment occurred around x/h = 0.3.

Richards and Hoxey (2006) stated that they had access to the results data sets from Castro and Robins (1977) and acknowledged that there was a considerable difference between the roof pressures from the uniform boundary

layer and the ABL where there are high suctions near the windward edge and a much lower suction towards the leeward edge, this resulted in the flow reattaching on top of the roof at a location approximately 0.3h across the roof (x/h = -0.2).

In another attempt to assess the accuracy and capabilities of wind tunnel tests in simulating full-scale flow field, Hölscher and Niemann (1998) reported the results of a research programme where twelve laboratories from Germany, Austria, Denmark, the Netherlands and Switzerland studied wind flow around a cube in a turbulent channel flow.

ABL profile was generated corresponding to a suburban terrain with a profile exponent α = 0.22 ± 0.02, the Reynolds number (Re) was to be beyond 5 x 10^5 and the blockage ratio less than 5% to ensure the development of the general flow pattern for wind flow around a surface mounted cube in a turbulent channel flow which is dominated by the cube sharp edges.

Although, the Re number for the smallest model was 2x 10^4 and the Re number for the largest model was 3 x 10^5, Hölscher and Niemann (1998) considered the results acceptable since the global flow pattern was simulated reasonably and the blockage ratio did not exceed 2.54. Figure 4.7 shows the distribution of the pressure coefficients along the centreline of the cube's windward facade, roof and leeward facade.

The figure shows the average of the 15 wind tunnel tests where some of them exhibit significant deviations, especially on the roof and the leeward side, Hölscher and Niemann (1998) attributed this to the difference in turbulence intensities in each case which strongly affects the reattachment on the roof and accordingly the pressure at the windward façade. They suggested removing the deviated measurements so that better averages mean pressure distribution is achieved for usage in validation and quality assurance studies.

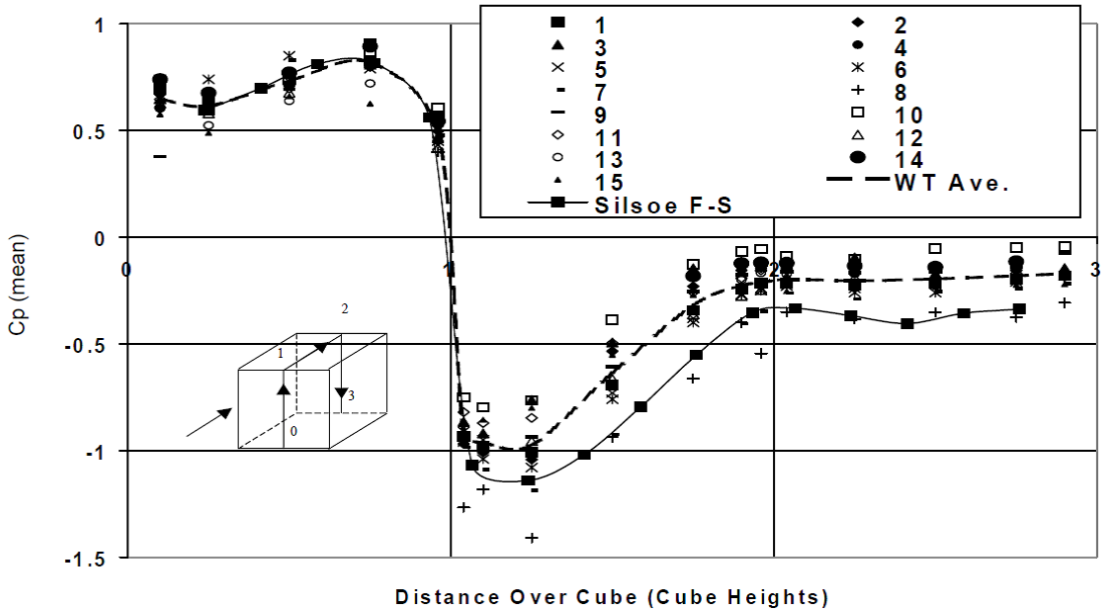

Figure 4.7 Vertical central section mean pressure coefficients with wind normal to the windward façade from the 15 wind tunnel test, their average and the Silsoe full-scale test (Hölscher and Niemann, 1998).

The Silsoe 6m cube was also modelled in a wind tunnel to compare the results of the full-scale measurements with the wind tunnel test. Richards *et al.* (2007) ran wind tunnel test for the Silsoe cube in the University of Auckland boundary layer wind-tunnel. The scale of the wind tunnel model was 1:400 yielding a cube whose edge length is 150mm (Figure 4.8). All of the tappings on the Silsoe Cube were modelled together with some additional taps, such that both vertical centreline planes, all four faces at mid-height and six rows of six taps on one-quarter of the roof were included. However in order to assess the effect of the orientation of the tappings, two tests were carried out with the corner pressure taps oriented in two different directions.

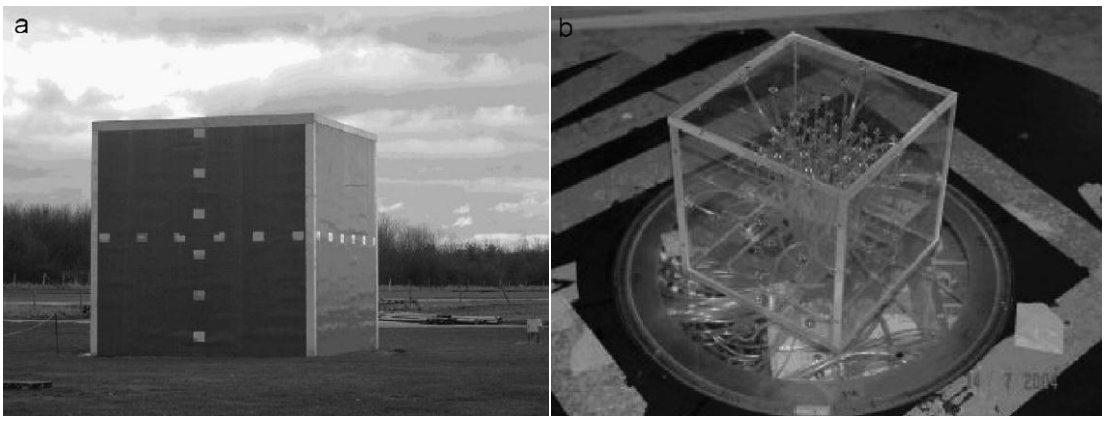

Figure 4.8 Right: the Silsoe 6m cube, Left: the scaled model for the wind tunnel test (Richards *et al.*, 2007).

Richards *et al.* (2007) pointed out that previous comparisons between wind tunnel test and in situ measurements suffered from discrepancies in pressure distributions on top of the roof and on the leeward façade due to difference in levels of turbulence, however they argued that the University of Auckland boundary layer wind-tunnel use turbulence values which are similar to theirs of the full scale measurements of the Silsoe cube, thus they were expecting that the results from the wind tunnel test to be similar to the full-scale measurements. Figure 4.9 shows that there is a good agreement between full scale and the wind tunnel test, however changing the orientation of the tapings had a slight effect on the pressure distributions as in case A the tapings were facing the windward direction while in case B the tappings were facing the leeward direction. This suggests that the positioning of the corner roof taps may be slightly modifying the flow reattachment behaviour and hence the mean pressure distribution.

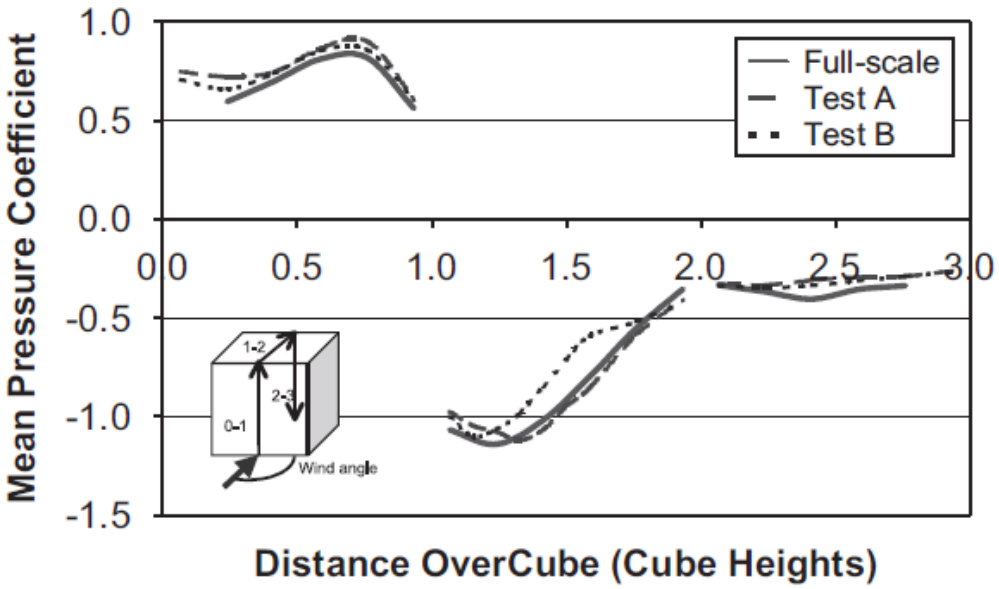

Figure 4.9 Vertical centreline mean pressure distribution for the full scale and the two cases with different tappings orientations (Richards *et al.*, 2007).

4.2.3 *CFD simulations*

CFD simulation is another valid tool for assessing wind flow around buildings. However due to the embedded errors and uncertainties in CFD simulations, it has to be validated by wind tunnel tests. In addition, wind tunnel tests can be used to assess the performance of different CFD codes in simulating wind engineering problems. Vardoulakis *et al.* (2011) used two quality-assured and

fully documented experimental datasets produced in the wind tunnels of the Meteorological Institute of Hamburg University, Germany, for evaluating four numerical models namely; CHENSI, VADIS, MIMO and FLUENT. The first dataset is for the CEDVAL cube of specific length 0.125m which was studied in a conventional-type boundary layer wind tunnel with a 15m long and 1m high test section and a 4m wide turn table. The other data set is for the ATREUS cube whose specific length was 0.19m which was built for the purpose of that study. The tunnel used is a multi-layered stratified closed circuit wind tunnel. The return section is made up of nine horizontal ducts of rectangular shape; the height and width of their cross sections are 0.12 and 2.3 m, respectively. The usable length of the test section of the wind tunnel is about 4.5 m^2.

Table 4.2[3] shows the comparison between locations of the stagnation point, separation and reattachment of the flow for the four numerical codes and the two wind tunnel tests (CEDVAL and ATREUS). It can be noticed that both wind tunnels tests did not yield the same results for all three characteristic lengths. The discrepancy in the stagnation point location was 6%, the separation 13% and the reattachment 16%. It was again noticed that more agreement is found at the windward facade while more discrepancies were found on top of the roof and at the leeward direction of the cube. As for the four numerical codes; for the stagnation point, FLUENT agreed best with the CEDVAL cube while MIMO agreed best with the ATREUS cube, for the separation VADIS agreed best with the CEDVAL cube while CHENSI agreed best with the ATREUS cube and for the reattachment VADIS agreed best with the CEDVAL cube and the ATREUS cube. However, all the results for the four numerical codes were within the acceptable range.

According to Vardoulakis *et al.* (2011), the need to validate CFD simulations against wind tunnel tests and full-scale measurements stems from previous results showing that similar numerical models, based on the same physical principles and mathematical formulation and using the same input and

[2] More information about the two wind tunnels is available at http://www.mi.unihamburg.de/Facilities.311.0.html

[3] Z is the height at which the stagnation point occurs, H is the height of the building, X_F is the length of the front recirculation and X_R is distance leeward the leeward façade where the flow reattaches.

boundary conditions gave significantly different results. Simulation approaches other than RANS modelling approach, such as LES, can give more accurate and consistent results and are becoming increasingly popular. However, they are still computationally expensive. Thus, RANS approach is still considered the most widely used approach.

Table 4.2 Comparison between the characteristic lengths of the flow for the four numerical codes and the two wind tunnel tests (CEDVAL and ATREUS) (Vardoulakis et al., 2011).

Model	Stagnation (Z/H)		Separation (X_F/H)		Reattachment (X_R/H)	
	CEDVAL	**ATREUS**	**CEDVAL**	**ATREUS**	**CEDVAL**	**ATREUS**
Wind Tunnel	0.64	0.70	-0.88	-0.75	1.5	1.34
CHENSI	0.62	0.80	-0.74	-0.77	2.18	1.89
VADIS	0.72	0.80	-0.83	-0.53	1.33	1.23
MIMO	0.68	0.79	-0.73	-0.50	2.27	2.19
FLUENT	0.65	0.88	-0.72	-0.55	2.24	1.60

In a study by Richards and Hoxey (2006) to assess the effect of using different turbulence models on the flow around a cube in a turbulent channel flow (the Silsoe 6m cube), they compared the results from three different turbulence models, namely the k-ε model, the RNG model and the MMK model and compared the results with the wind tunnel test results from Castro and Robins (1977) for both cases of a uniform inlet flow and an ABL turbulent flow.

Figure 4.10 shows that with the MMK turbulence model the flow did not reattach on the cube roof and so the pressures were relatively uniform, similar to the results of the uniform flow in Castro and Robins (1977). Using the k-ε

turbulence model, the flow did not separate at the windward edge of the roof which resulted in high suction occurring at this edge and then decreased rapidly with distance across the roof. Only when using the RNG turbulence model, the flow separated and reattached and created a roof pressure distribution similar to the turbulent ABL flow in Castro and Robins (1977).

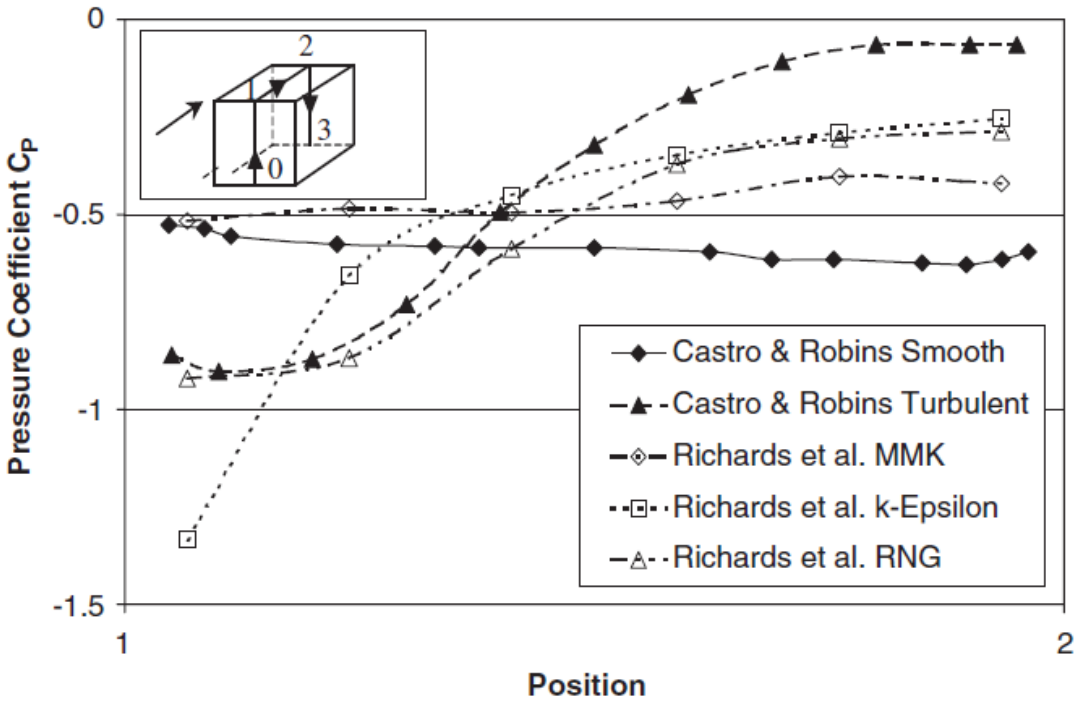

Figure 4.10 Centreline mean pressure coefficients across the roof for the two wind tunnels tests and the results of using three different turbulence models (Richards and Hoxey, 2006).

In a study by Beyers *et al.* (2004) to investigate the drifting snow surrounding a 2m cube structure, they used measured data for applying an ABL profile and the *k-ε* turbulence model was used to solve the flow turbulence quantities. Figure 4.11 shows the computational domain dimensions used for the numerical simulation and the specified boundary conditions. It should be noted here that the provided diagram by Beyers *et al.* (2004) is not proportional and the provided domain dimensions do not agree with the best practice guidelines which was mentioned in the previous chapter. A 91 x 80 x 41 grid was employed for the final simulation after making a grid independence study which ensured that the solution is grid independent. The grid was refined near the edges of the cube to ensure capturing velocity gradients in these areas. The second order discretization schemes were used to solve the convection and the viscous terms of the governing equations.

The simulation was run and the results were then compared with those from Castro and Robins (1977) and Paterson and Apelt (1989). Beyers *et al.* (2004) argued that Castro and Robins (1977) provided the first experimental data for a cube fully immersed in a turbulent boundary layer where 50 000 <Re_l<100000[4]. As for Paterson and Apelt (1989), they compared these measured data with their numerical simulation employing the *k-ε* turbulence model. Figure 4.12 shows the results of the pressure coefficients along the centreline of the cube on the windward facade, roof and leeward façade from Beyers *et al.* (2004) compared to the results from the above-mentioned researchers.

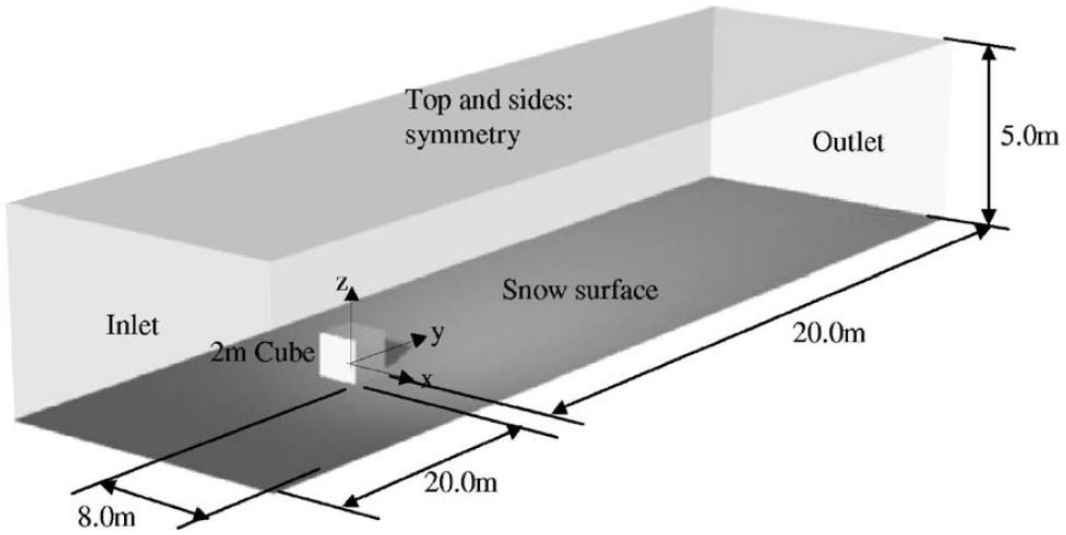

Figure 4.11 Computational domain for the simulation of the snow accumulation surrounding a 2 m cube (Beyers *et al.*, 2004). It should be noted that it has been demonstrated in this work that the dimensions are not proportional and do not agree with the best practice guidelines for domain dimensions.

In previous comparisons between full scale measurements and wind tunnel tests where there were good agreements on the windward façade, discrepancies were found on the roof and the leeward façade. The simulation results here have discrepancies with the wind tunnel test on the windward façade and the roof while the agreement was found to be on the leeward façade. Even when comparing the results with the numerical simulation by Paterson and Apelt (1989), the same discrepancies occurred. Beyers *et al.* (2004) attributed the discrepancy in the prediction of the negative pressure on

[4] The '*l*' refers that the specific length used for calculating the Reynolds number which is the height of the cube in this case.

the windward corner of the top face to the need for more mesh refinement, as for the discrepancy on the roof is attributed to the inaccuracy of the *k-ε* turbulence model in capturing the separation layer accurately. It was noticed that the CFD simulations under-predicted the pressure coefficient on the roof compared to the wind tunnel test results.

However, Beyers *et al.* (2004) argued that their simulations qualitatively compares favourably with the results from Castro and Robins (1977) and Paterson and Apelt (1989). Based on the plots of the horizontal and vertical streamwise velocity vectors of the flow around the cube (Figure 4.13), Beyers *et al.* (2004) compared different characteristic lengths of the flow with the results from Paterson and Apelt (1989). Accordingly, they considered the results compare favourably only qualitatively as there were significant discrepancies in the registered values. However, based on the literature review in this work, it can be argued that if the domain dimensions shown in Figure 4.11 were the used dimensions, this would affect the simulation results and might be one of the sources of discrepancies in the results.

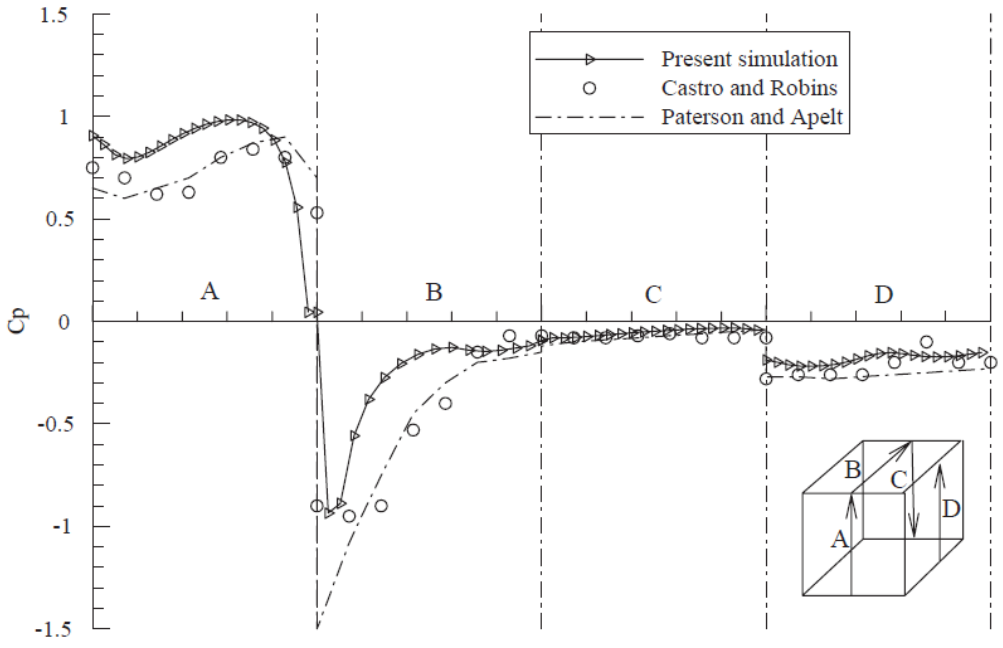

Figure 4.12 Pressure coefficients calculations on the cube surface from Beyers *et al.* (2004), Castro and Robins (1977) and Paterson and Apelt (1989) (Beyers *et al.*, 2004).

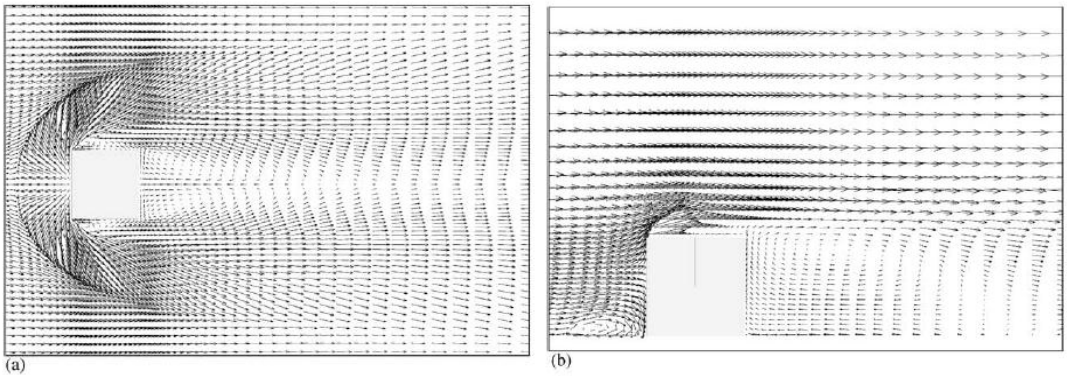

Figure 4.13 (a) Vector field plot for horizontal plan at z/h = 0.06 (b) Vector field plot for vertical plan at y/h = 0.0 (Beyers *et al.*, 2004).

In a study by Seeta Ratnam and Vengadesan (2008), they investigated the optimum two equation turbulence model for the complex flow structure which involves recirculation, separation and reattachment. Thus, they used the standard k–ε, low-Reynolds number k–ε, non-linear k–ε model, standard k–ω and improved k–ω models to solve the closure problem of a three dimensional incompressible flow over a cube placed in a fully developed turbulent flow. Then they compared the results with the results of the DNS from Yakhot *et al.* (2006). They concluded that the improved k–ω model gives overall better predictions of the flow field. The non-linear k–ε model gives better prediction when compared to standard k–ε and low Reynolds number k–ε models.

They constructed a computational domain of dimensions16h x 3h x 7h (where h is the cube height). However, these dimensions are considered too small when compared to the recommendations for domain dimensions for similar flow problems. Accordingly, a false accelerating effect is expected to occur around the obstacle, especially above the roof where the distance between the roof and the top boundary is only 2h while it should be at least 5h to avoid such effect as mentioned earlier in this work when discussing the domain dimensions under section 3.4.2.3.

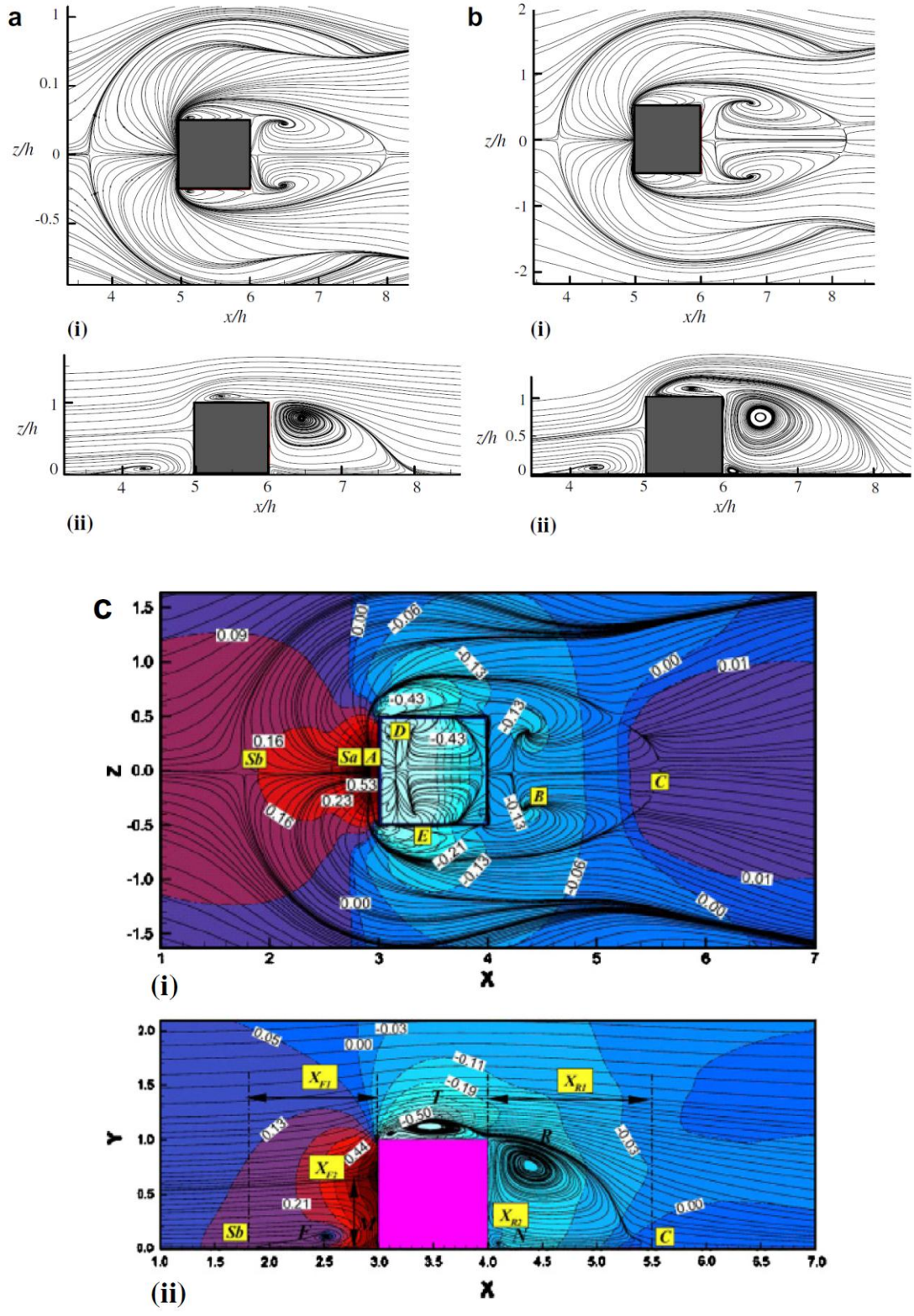

Figure 4.14 Comparison of the time averaged vertical and horizontal streamlines for the non-linear k-ε (a), improved k-ω (b) and DNS (c) (Seeta Ratnam and Vengadesan, 2008).

The flow is considered a turbulent flow since the Re number is 5610 based on channel height H and the Re number is 1870 based on cube edge length, both numbers are greater than 1000 and it is reported in Versteeg and Malalasekera

(2007) that the flow is turbulent for Re > 1000 based on cube size and bulk velocity. The basic equations used were incompressible three-dimensional, time dependent; Reynolds averaged Navier–Stokes equations and energy equation. The pre-processor GAMBIT 2.2.30 was used to build the geometry and construct the computational mesh while FLUENT 6.2.16 was the solver used to solve the governing equations.

Figure 4.14 shows the comparison between the results of the non-linear *k-ε* (a), improved *k-ω* (b) and DNS (c) for the average streamlines in the central vertical plan and the horizontal plan on the first grid point from the bottom wall. It was noticed the agreement between the three simulations; the horseshoe vortex was formed in front of the cube and recirculation areas on top (marked as T) and behind the cube (marked as R); all the vortices look similar to those in the DNS simulation. The flow separates in front of the cube at the point (Sb) which is called the saddle point and an attachment point is observed in front of the cube which is called nodal point (Sa).

In the leeward direction of the cube, the reattachment occurs at a distance downstream of the leeward façade marked as C. The lengths of front recirculation length (X_{F1}), top recirculation (X_t), reattachment length (X_{R1}) and secondary recirculation lengths (X_{F2}), and (X_{R2}) are given in Table 4.3 (Seeta Ratnam and Vengadesan, 2008). Comparing the results with the flow patterns described by Martinuzzi and Tropea (1993) in Figure 4.1 one can notice the agreement in the main flow features. These results are then compared to the results obtained from the CFD simulation in this work to assess its consistency.

In a research by Yang (2004a), CFD was used to simulate the coupled external and internal flow field around a 6m cubic building with two small openings. The commercial CFD code CFX5 was used and the simulation results were compared to the published Computational Wind Engineering 2000 Conference (CWE2000) competition data which implemented a detailed set of full-scale measurements for a cube structure with well-defined boundary conditions.

Table 4.3 Summary of separation (XF1 and XF2), reattachment (XR1 and XR2) and top recirculation length (Xt) for a wall mounted cubed by different turbulence models (Seeta Ratnam and Vengadesan, 2008).

Turbulence model	Front recirculation length (X_{F1})	Top recirculation (X_t)	Reattachment length (X_{R1})	Secondary recirculation length (X_{F2})	Secondary recirculation length (X_{R2})
DNS	1.2	0.5	1.5	0.6	0.15
Standard *k-ε*	0.8	0.4	2.2	0.58	0.18
Low Re *k-ε*	1.58	0.6	2.3	0.6	0.15
Non-linear *k-ε*	1.5	0.55	2.0	0.6	0.13
Standard *k-ω*	1.4	0.3	2.2	0.55	0.2
Improved *k-ω*	1.29	0.5	2.2	0.6	0.15

For the inlet profile Yang (2004a) used an empirical log-law profile with specified turbulent kinetic energy (k) and dissipation rate (ε), the outlet was assigned a relative static pressure equal to zero, the ground was a non-slip rough wall with roughness length (z_0) = 0.01m, the top and side boundary conditions were symmetry boundary conditions, the wind direction was perpendicular to the calculation domain with reference wind velocity 10 m/sec at a reference height of 6m. Second order discretisation scheme in CFX5 was used and the convergence criterion was set to 10^{-6} for all flow variables (Yang, 2004a). The domain dimensions are illustrated in Figure 4.15. The dimensions are 96 m × 66 m × 36 m which corresponds to 5H (H=building height) upstream and 10H downstream, and 5H away from each side and above the roof of the cube.

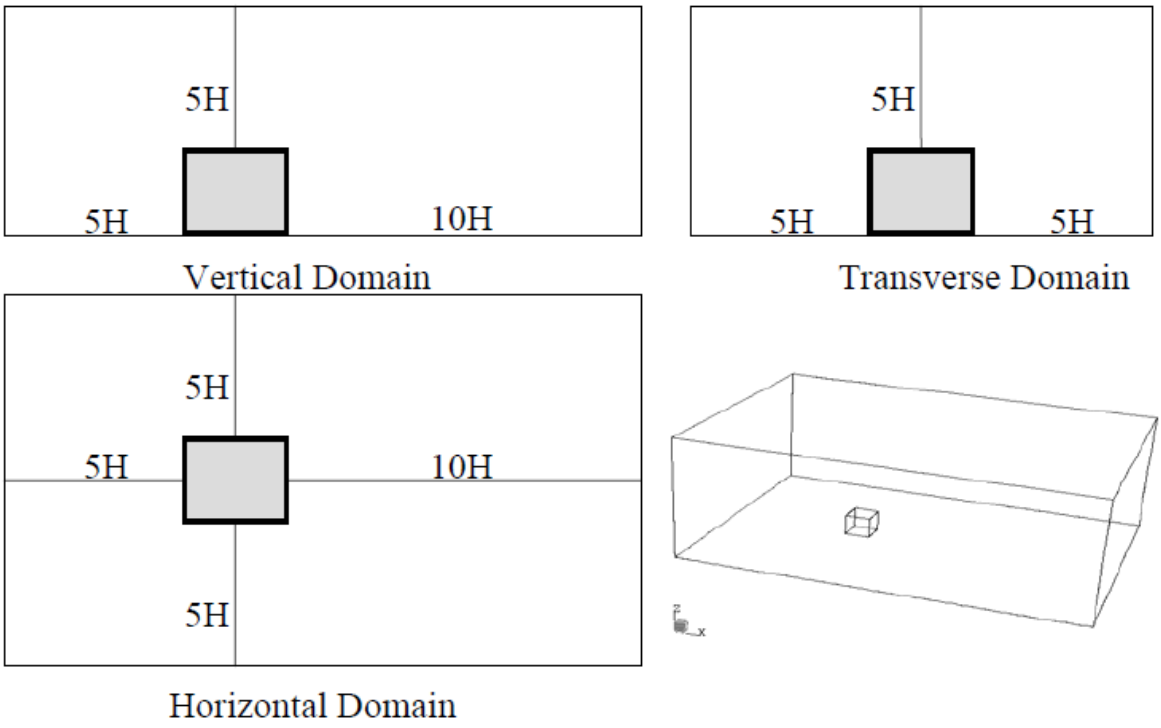

Figure 4.15 CFD simulation domain for a 6m cube (Yang, 2004a).

Figure 4.16 shows the comparison between the results of the CFX5 simulations for the standard k-ε and the RNG model compared to the full scale measurements of the Silsoe cube and the results from the CWE2000 competition. The distribution of pressure along the windward façade is similar in all the cases. However, in terms of the stagnation point, all the models except the CWE2000 MMK model predicted a higher stagnation position than measured. On the leeward façade, both CFX5 models showed similar negative pressures near the ground but the RNG model gave results closer to the field measurements. Near the roof windward edge all models significantly over-predicted the negative peak pressure which gradually decreased from the windward edge towards the leeward edge. However, numerical results are all lower than the full-scale measurements elsewhere on the roof. But when comparing the results with the Silsoe full-scale data and 15 individual wind tunnel tests along with the average of the 15 tests (Figure 4.17), Yang (2004a) considered that there is good agreement on the windward and leeward facades but none of the computational models predicted the flow trends correctly on the roof since all of them under predicted the pressure coefficient compared to the full-scale measurements.

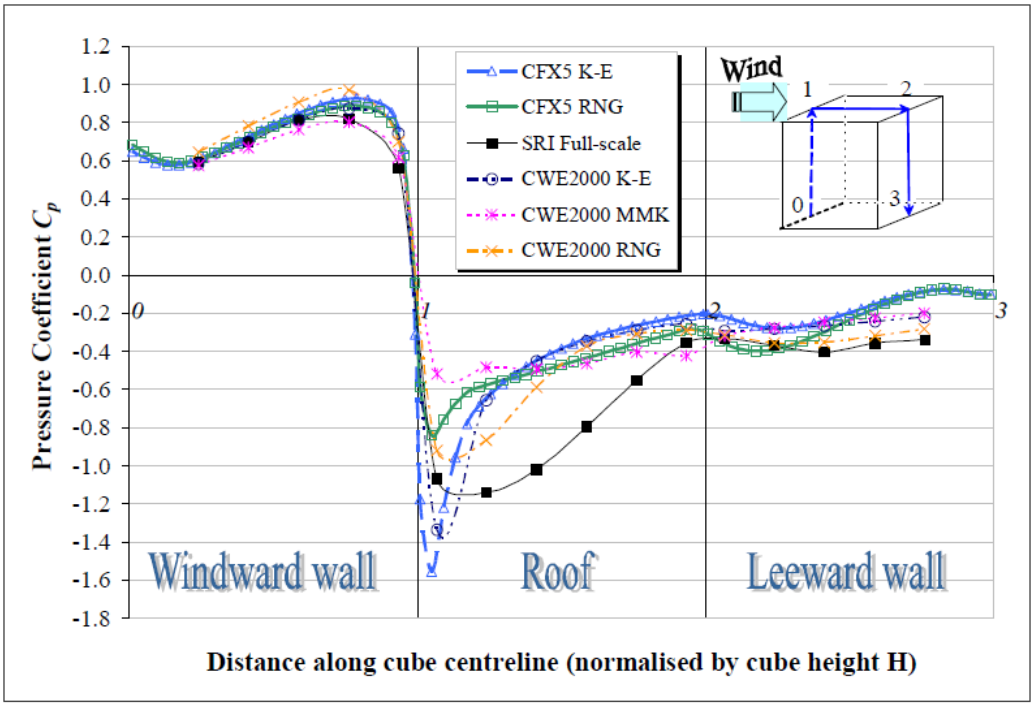

Figure 4.16 Pressure coefficients comparison for the cube through the streamwise vertical centreline section with the wind perpendicular to the windward façade (Yang, 2004a).

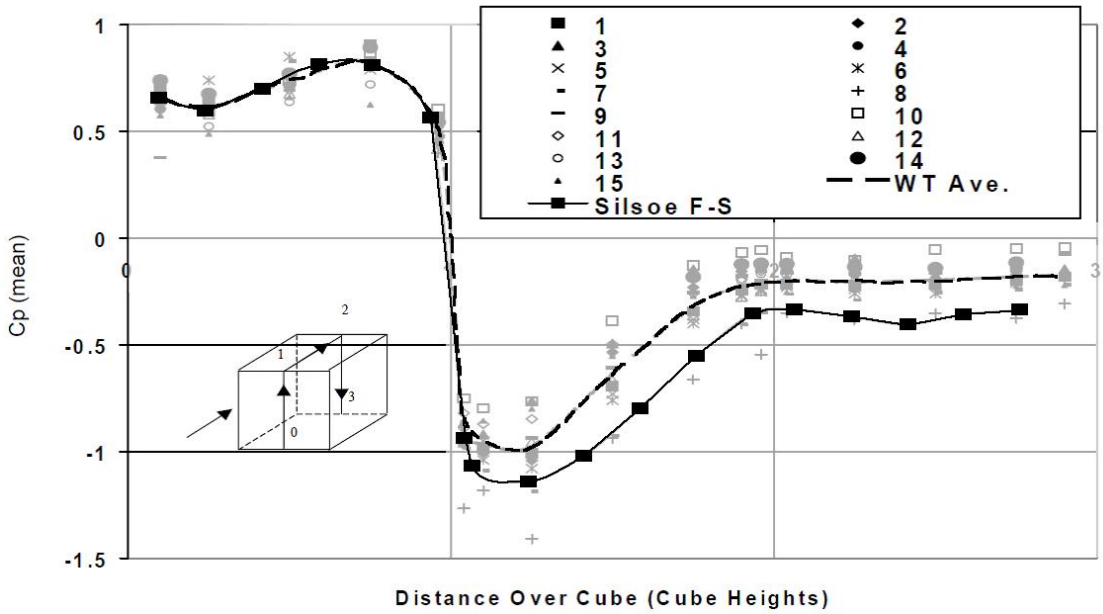

Figure 4.17 Vertical central section mean pressure coefficients with wind normal to one face (0^0) from the Windtechnologische Gesellschaft comparative wind-tunnel testing program, including the Silsoe full-scale test (Hölscher and Niemann, 1998).

Looking at the results of the reviewed in-situ measurements, wind tunnel tests and validated CFD simulations, it can be argued that all these wind assessment tools were able to capture the flow features qualitatively in terms of the presence of recirculation areas, stagnation point, separation and reattachment.

However, quantitatively, there were some discrepancies in locations of main flow feature and pressure coefficients along the surfaces of the cube. These discrepancies were mostly observed on the roof of the cube and at the leeward façade. The CFD tool under predicted the pressure coefficient compared to the other tools. Thus, for the purpose of roof mounting wind turbines, CFD should be used for comparing alternatives for specifying the optimum mounting locations, as for estimating the energy yield of the proposed wind turbine, it is preferable to count on in-situ measurements.

4.3 CFD simulation of wind flow around a cube in a turbulent channel flow

As mentioned earlier, the case of a cube immersed in a turbulent channel flow is the most widely studied flow problem in wind engineering since the cube exhibits most of the flow phenomena for wind flow around a bluff body. Thus, the cube case has been chosen for the validation study in this research. However, to have a reliable start point for a CFD simulation, literature on CFD has been reviewed in the previous chapter and best practice guidelines for simulation variables have been extracted to be a start point for the simulation work in this research.

Other simulation variables needed more investigation, which is included in the following sections, such as the horizontal homogeneity of the atmospheric boundary layer profile (ABL) and running mesh independence test. Accordingly, the simulation variables are specified and used for simulating wind flow around a surface mounted cube in a turbulent channel flow. Then, the yielded results are presented and compared to the previously mentioned in-situ measurements, wind tunnel tests and validated CFD simulations to assess the quality of the CFD simulation and use the simulation variables in further simulations.

4.3.1 *Best practice guidelines for CFD simulation variables*

Although Franke *et al.* (2004) asserted the importance of using wind tunnel tests for validating CFD simulations, Van Hooff *et al.* (2011) and Lu and Ip (2009) suggested that using the CFD code with a certain combination of computational settings and parameters would lead to accurate CFD simulations. This can be considered true to some extent provided that those settings and

parameters would have been implemented for similar flow problems and validated with one of the other wind assessment tools. Van Hooff *et al.* (2011) acknowledged that for flow simulations, these conditions are: a computational domain that is large enough, a computational grid based on grid-sensitivity analysis, steady RANS simulations with the realizable k-ε model, standard or non-equilibrium wall functions modified for roughness, second order discretisation schemes and the SIMPLE algorithm for pressure-velocity coupling. These conditions and other recommendations found in literature are considered for the CFD simulations in this research. However, it can be argued that these conditions are case specific and can differ from one flow problem to another. Thus a comparison with other tools is still needed.

Different techniques can be used in CFD simulations such as Steady Reynolds Averaged Navier Stokes (RANS), Unsteady Reynolds Averaged Navier Stokes (URANS), Large Eddy Simulation (LES) or Direct Numerical Simulation (DNS). Choosing which technique to use is highly dependent on the required details of the flow and the available computational power. Although the URNAS, LES and DNS techniques yield more reliable results, their implementation in studying air flow around buildings is few when compared to Steady RANS models. Accordingly, there is a lack in literature for detailed validation and sensitivity studies for these methods. This is not the case for RANS models where guidelines and best practice documents can be found in literature.

The availability of these guidelines stemmed from the uncertainties about CFD simulations. Accordingly, Sørensen and Nielsen (2003), Chen and Zhai (2004), Franke *et al.* (2004), Wit (2004), Franke *et al.* (2007), Blocken *et al.* (2011) and others addressed the issues of quality control and best practice guidelines for CFD modelling in their researches. According to those publications, the minimum requirements for carrying out a consistent CFD simulation can be summarised in the following points:

- Second order Schemes or above should be used for solving the algebraic equations.
- The scaled residuals should be in the range of 10^{-4} to 10^{-6}.

- Multi-block structured meshes are preferable and carrying out sensitivity analysis with three levels of refinements where the ratio of cells for two consecutive grids should be at least 3.4.
- Mesh cells to be equidistant while refining the mesh in areas of complex flow phenomena.
- If cells are stretched, a ratio not exceeding 1.3 between two consecutive cells should be maintained.
- For flows around isolated buildings, the realizable k-ε turbulence model is preferred.
- Accuracy of the studied buildings should include details of dimension equal to or more than 1 m.
- If H is the height of the highest building the lateral dimension = 2H + Building width, Flow direction dimension = 20H + Building dimension in flow direction and Vertical Direction = 6H while maintaining a blockage ratio below 3%.
- For the boundary conditions, the bottom would be a non-slip wall with standard wall functions, top and side would be symmetry, outflow would be pressure outlet and inflow would be a log law atmospheric boundary layer profile which should be maintained throughout the length of the domain when it is empty.
- Horizontal homogeneity of ABL profile throughout the computational domain.

One of the main factors affecting the consistency of the CFD simulation results is the last requirement which is the horizontal homogeneity of the atmospheric boundary layer (ABL) profile throughout the computational domain which means no streamwise gradients in the flow variables in the flow direction from the inlet boundary throughout the domain to the outlet boundary.

4.3.2 *Horizontal homogeneity of the atmospheric boundary layer (ABL) profile*

Yang (2004a) asserted the importance of correctly reproducing the atmospheric boundary layer (ABL) profile in CFD simulations in addition to maintaining the profile throughout the streamwise direction of the computational domain. Richards and Hoxey (1993) also stated that all simulation variables, especially the boundary conditions should be adjusted to produce a horizontally

homogenous boundary layer flow in the absence of any obstructions. For achieving this, they suggested using the standard *k*-ε turbulence model, and the inflow profile would be expressed in terms of velocity profile (u), turbulent kinetic energy (k) and its dissipation rate (ε) through the equations below:

$$\boldsymbol{u = \frac{u^*}{\kappa} ln\left(\frac{z+z_0}{z_0}\right)} \qquad \textbf{Equation 4.1}$$

$$\boldsymbol{k = \frac{{u^*}^2}{\sqrt{C_\mu}}} \qquad \textbf{Equation 4.2}$$

$$\boldsymbol{\varepsilon = \frac{{u^*}^3}{\kappa(z+z_0)}} \qquad \textbf{Equation 4.3}$$

where u^* is the friction velocity, κ is the von Karman constant, z_0 is the aerodynamic roughness length and C_μ is the turbulence model constant.

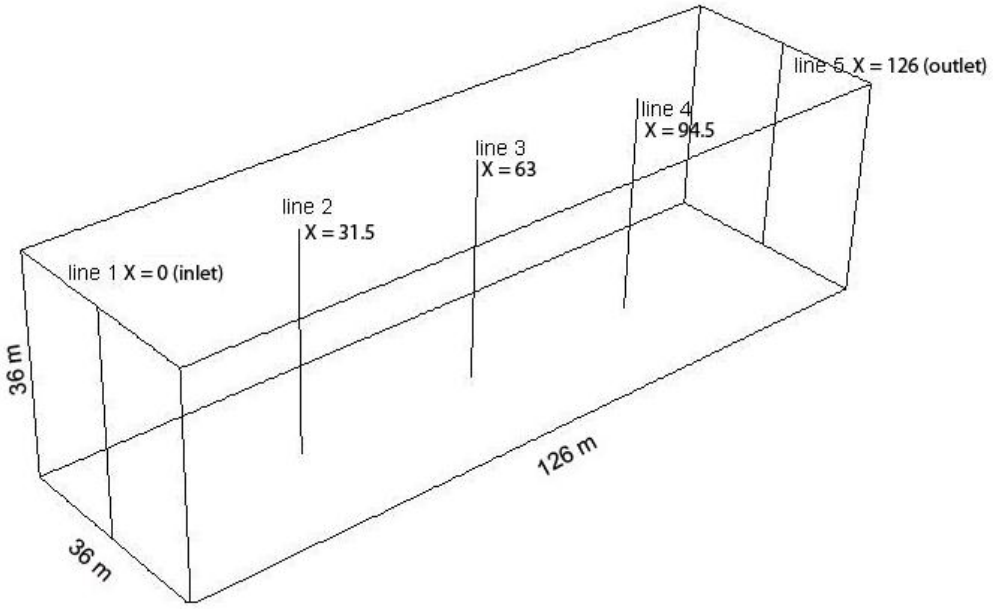

Figure 4.18 Computational domain dimensions and positions of lines 1, 2, 3, 4 and 5

In this work modelling an equilibrium ABL in a 3D empty computational domain of dimensions X x Y x Z = 126m x 36m x 36m was carried out (Figure 4.18). The mesh used is an equidistant structured mesh with spacing of 0.5 m in X, Y and Z directions giving 1306368 hexahedral cells. It should be noted here that Hargreaves and Wright (2007) and Yang et al. (2009) asserted that the horizontal homogeneity of the ABL profile is independent of mesh resolution. The simulation was performed using the commercial CFD code Fluent 12.1.

The inlet boundary condition was specified using a user defined function (UDF) satisfying equations 4.1, 4.2 and 4.3 for the velocity (u), turbulent kinetic energy (k) and turbulent dissipation rate (ε) respectively as mentioned in Richards and Hoxey (1993).

The bottom boundary condition was specified as a rough wall and standard wall functions were used, the roughness height (k_s) and roughness constant (C_s) were determined according to the relationship between k_s, C_s and z_0 derived by Blocken *et al.* (2007b) satisfying equation 4.4. In addition, a wall shear stress of 0.58Pa was assigned for the bottom boundary satisfying equation 4.5 for the shear stress (τ_w). According to Blocken *et al.* (2007b), specifying a wall shear stress at the bottom of the computational domain associated with the ABL profiles satisfying equations 4.1, 4.2 and 4.3 would result in a good homogeneity for both wind speed and turbulence profiles. The top and side boundary conditions were specified as symmetry while the outlet boundary condition was specified as pressure outlet.

$$\boldsymbol{k_s = \frac{9.793 z_0}{C_s}} \qquad \textbf{Equation 4.4}$$

$$\boldsymbol{\tau_w = \rho u^{*^2}} \qquad \textbf{Equation 4.5}$$

The realizable *k-*ε turbulence model was used for the closure of the transport equations. The SIMPLE algorithm scheme was used for the pressure-velocity coupling. Pressure interpolation is second order and second-order discretisation schemes were used for both the convection and the viscous terms of the governing equations. The solution was initialised by the values of the inlet boundary conditions. The chosen convergence criterion was specified so that the residuals decrease to 10^{-6} for all the equations. The solution was initialized with the values at the inlet boundary condition and it converged after 499 iterations (Figure 4.19) and velocity, turbulent dissipation rate (TDR) and turbulent kinetic energy (TKE) were plotted along five equidistant vertical lines in the streamwise direction of the domain (X= 0, 31.5, 63, 94.5 and 126m) (Figure 4.18).

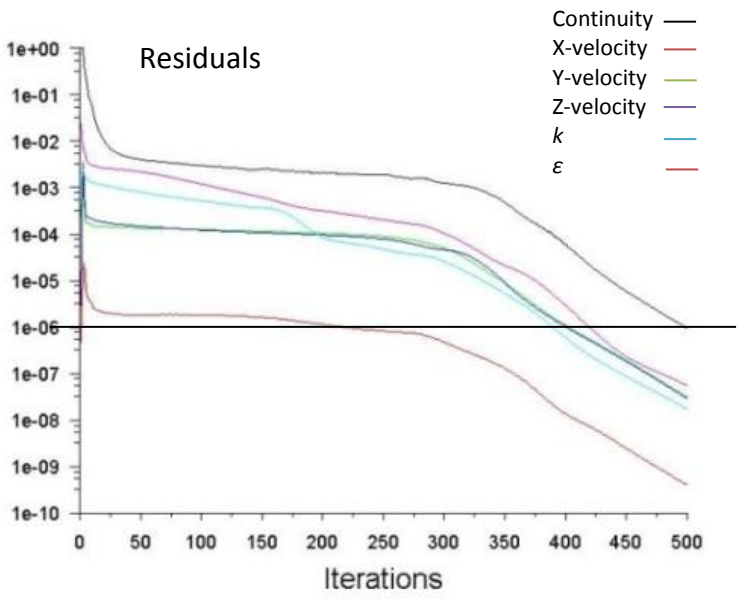

Figure 4.19 Scaled residuals reaching 10^{-6} after 499 iterations.

Horizontal homogeneity of the ABL means that the plots of velocity, TDR and TKE should coincide along lines 1, 2, 3, 4 and 5 (Figure 4.18). Horizontal homogeneity was achieved for both velocity (Figure 4.20) and TDR (Figure 4.21). As for TKE, Figure 4.22 shows streamwise gradients in the vertical TKE profile which means that horizontal homogeneity was not achieved.

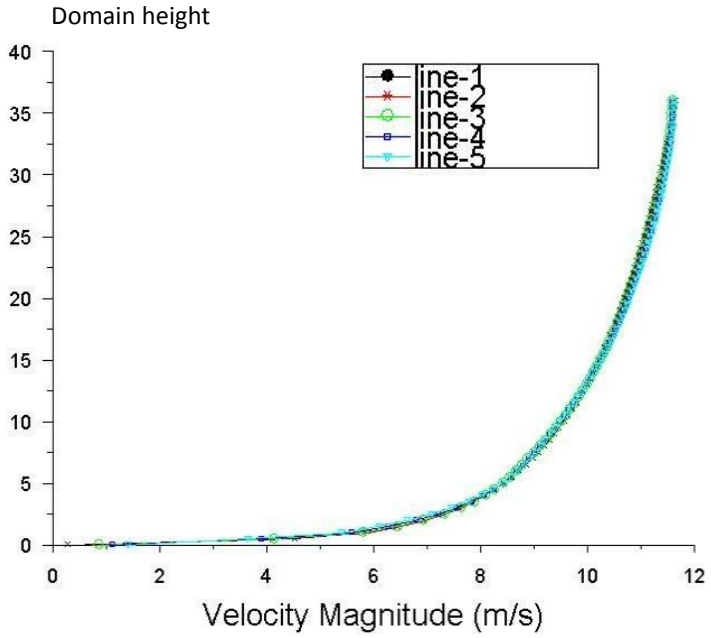

Figure 4.20 Velocity magnitude graph showing the horizontal homogeneity of the velocity profile.

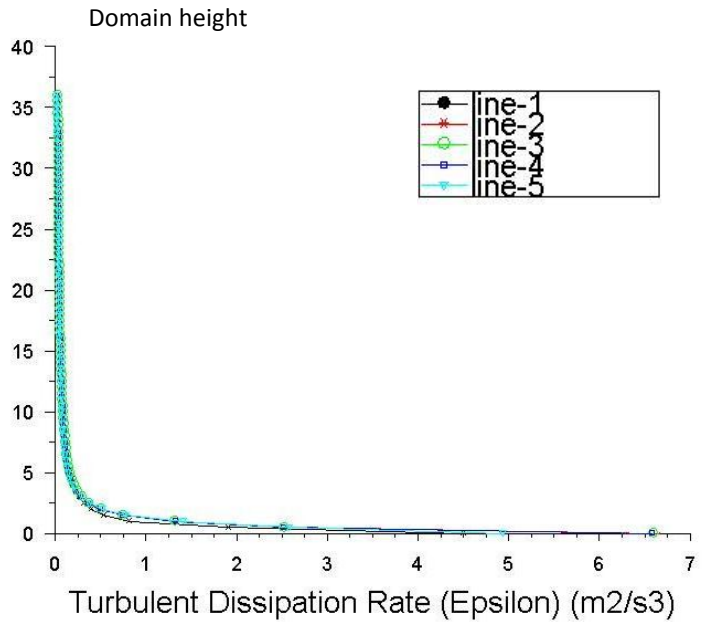

Figure 4.21 TDR graph showing the horizontal homogeneity of the TDR profile.

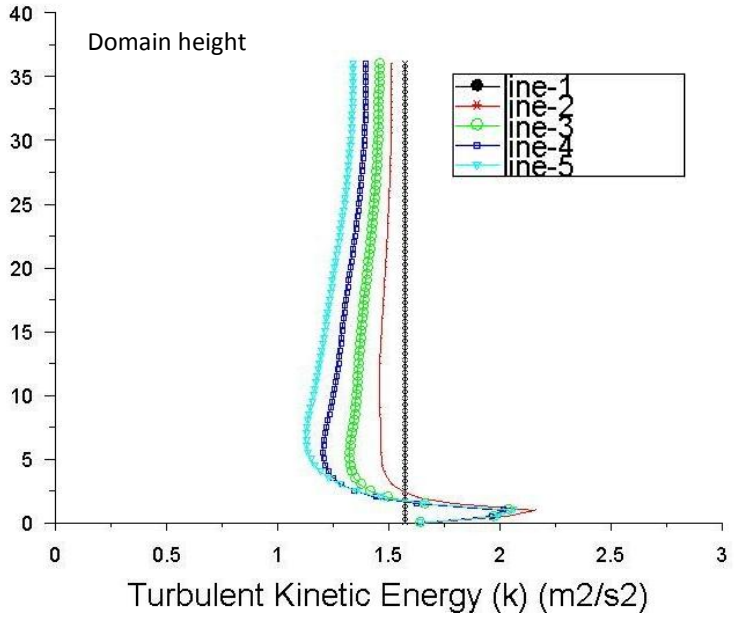

Figure 4.22 TKE graph showing the streamwise gradients in the vertical TKE profile.

According to Yang *et al.* (2009), the measures taken by Blocken *et al.* (2007b) improved the level of horizontal homogeneity to some extent. However, Yang *et al.* (2009) argued that better results can be achieved if the mean velocity profile is represented by the logarithmic law (Equation 4.1), turbulent kinetic energy (k) and turbulent dissipation rate(ε) represented by equations 4.6 and 4.7 respectively.

$$k = \frac{u^{*2}}{\sqrt{C_\mu}} \sqrt{C_1 . ln(\frac{z+z_o}{z_o}) + C_2} \qquad \text{Equation 4.6}$$

$$\varepsilon = \frac{u^{*3}}{\kappa(z+z_0)} \sqrt{C_1 . ln(\frac{z+z_o}{z_o}) + C_2} \qquad \text{Equation 4.7}$$

where C_1 and C_2 are constants obtained from fitted curve of the k profile from wind tunnel tests and equal to -0.17 and 1.62 respectively. All other simulation parameters were the same as those in Blocken *et al.* (2007b) except that the ground boundary condition was set as a non-slip wall with roughness height equal to 0.4m and roughness constant equal to 0.75 satisfying equation 4.4. The solution converged after 687 iterations. Both the velocity and TDR showed very good homogeneity in the streamwise direction of the domain (Figure 4.23 and Figure 4.24), as for the TKE the results were improved largely. However, small streamwise gradients in the vertical TKE profile were noticed near the ground (Figure 4.25).

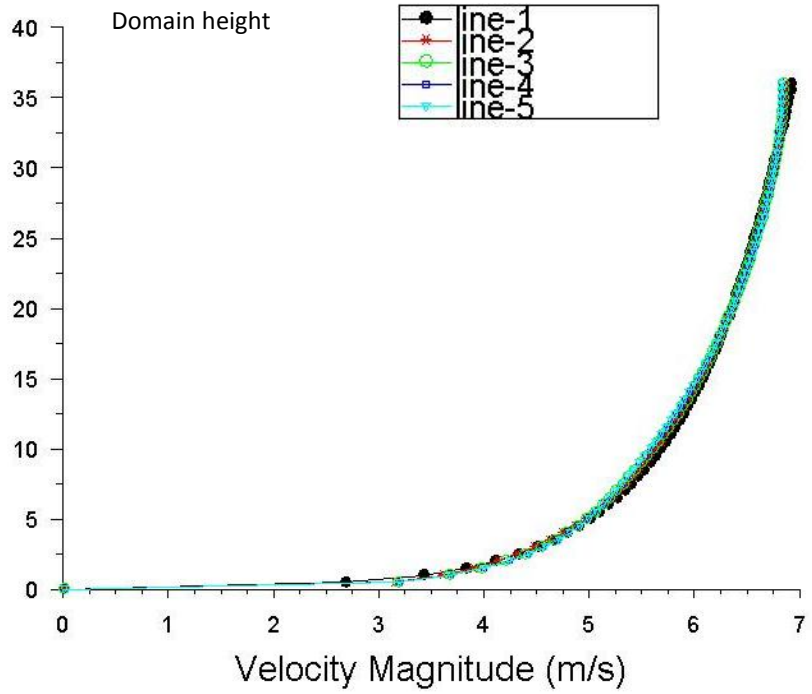

Figure 4.23 Velocity magnitude graph showing the horizontal homogeneity of the velocity profile.

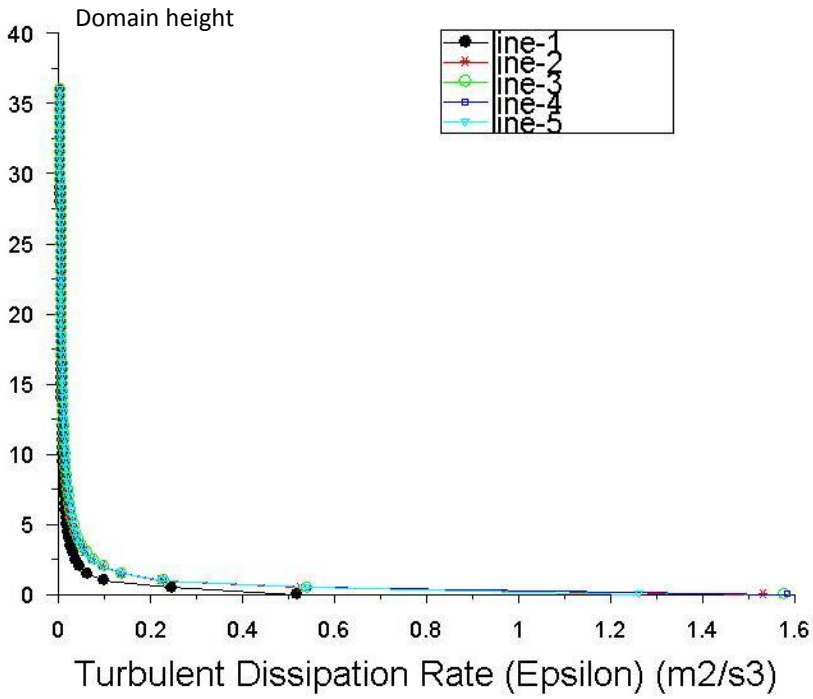

Figure 4.24 TDR graph showing the horizontal homogeneity of the TDR profile.

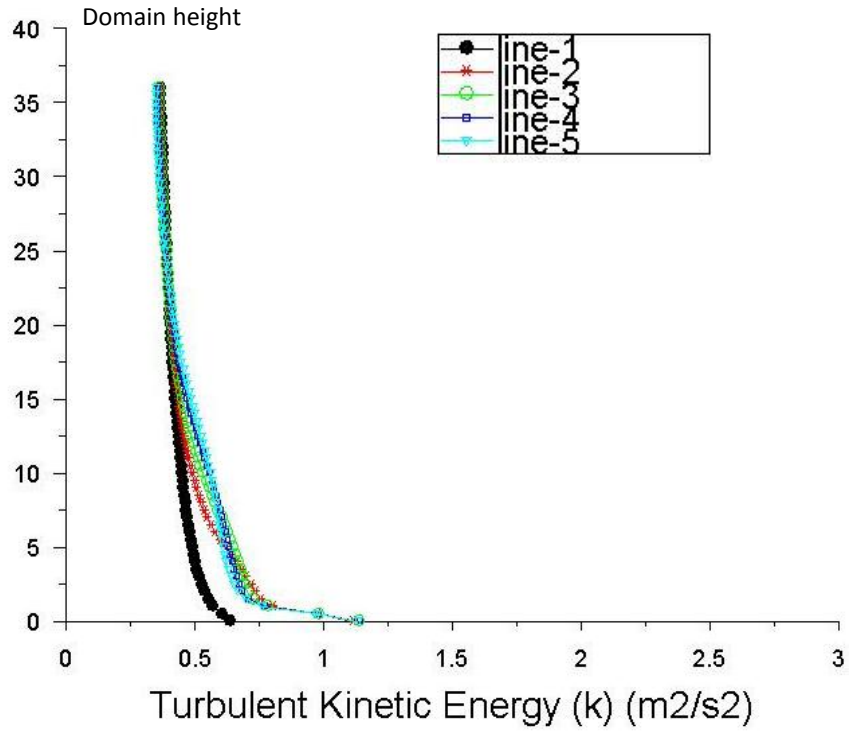

Figure 4.25 TKE graph showing the near ground streamwise gradients in the vertical TKE profile.

According to Blocken *et al.* (2007b) and Hargreaves and Wright (2007), these near ground streamwise gradients can be eliminated if the outlet profile of a similar simulation in a longer domain (10000m and 5000m respectively) is used

as the inlet profile of the same domain. However, for limited computational power available, simulation was run for the same domain but with double the length in the streamwise direction leading to a domain of dimensions 252m x 36m x 36m. When comparing the results with the results from the previous two simulations, it was noticed that horizontal homogeneity for velocity, TDR and TKE profiles were achieved throughout the computational domain (Figure 4.26, Figure 4.27 and Figure 4.28). The outlet profile was written to be used as the inlet profile for the rest of the simulations in this research.

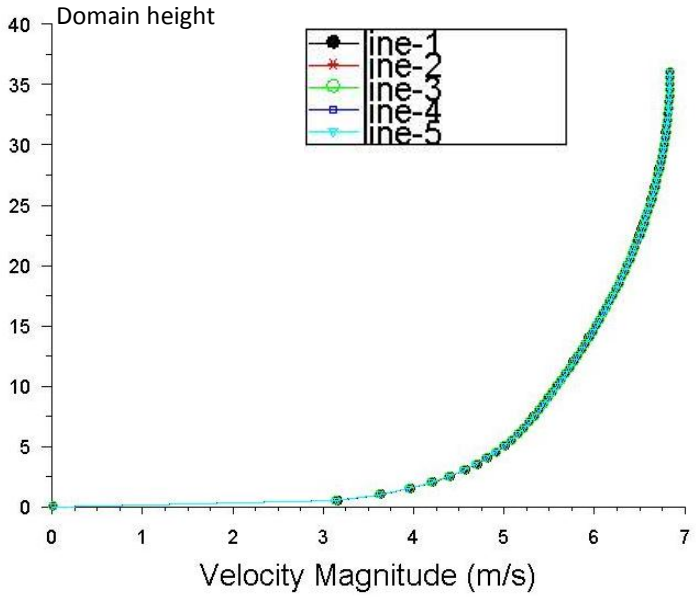

Figure 4.26 Velocity magnitude graph showing the horizontal homogeneity of the velocity profile.

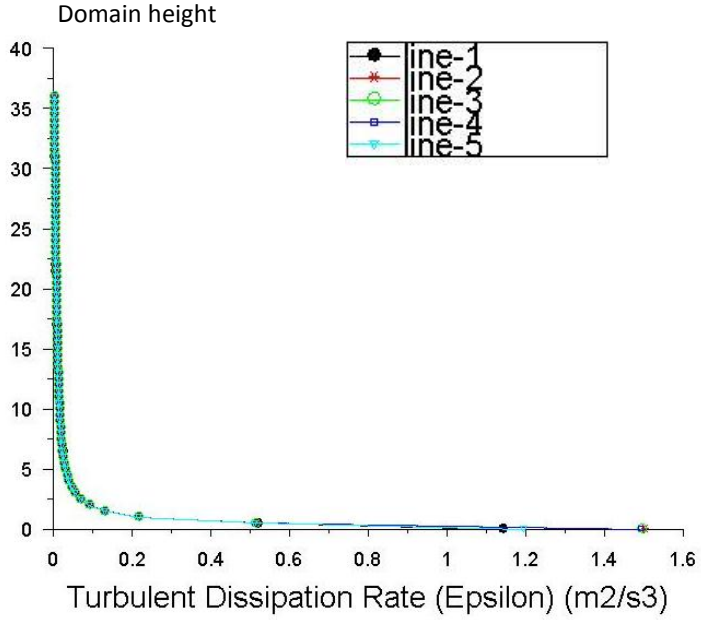

Figure 4.27 TDR graph showing the horizontal homogeneity of the TDR profile.

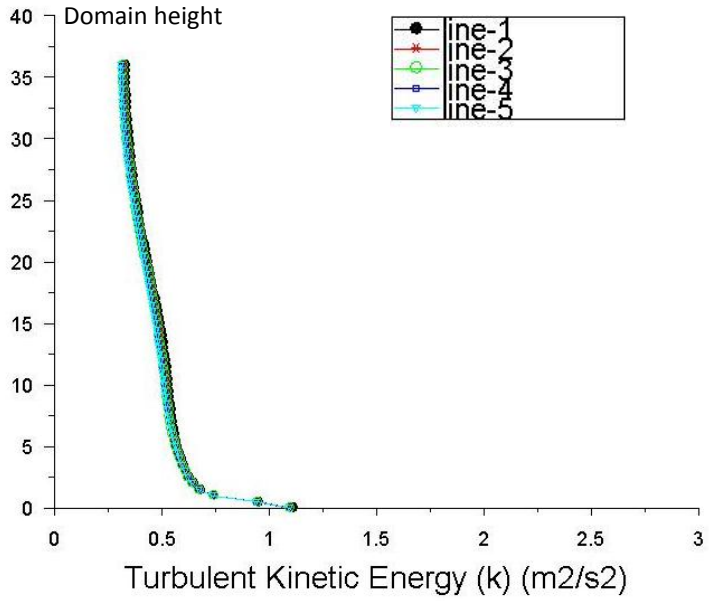

Figure 4.28 TKE graph showing the horizontal homogeneity of the TKE profile.

4.3.3 *Computational mesh*

The same simulation conditions used for achieving a horizontally homogeneous ABL profile were used for the following simulations. The flat roof case (the cube) was used for the validation and mesh independence test. Due to the limited computational power available, the mesh had to be coarsened in areas away from the cube and refined in areas close to the cube. In order to determine the dimensions of the refinement area, the velocity pathlines in the vertical central plan and at ground level were plotted for an 0.3 m spacing mesh to determine the area of influence of the cube on the flow. It was found that this area extends 9m in the windward direction, the sides and above the cube. In the leeward direction of the cube this area extends to 18m (Figure 4.29).

A new multi- block mesh was constructed where the area around the cube extending 18 m in the leeward direction and 9m in the windward direction, sides and above the cube were assigned a resolution of 0.3m in the X, Y and Z directions. As for the rest of the computational domain the mesh resolution was set to 1.2m in the X, Y and Z directions.

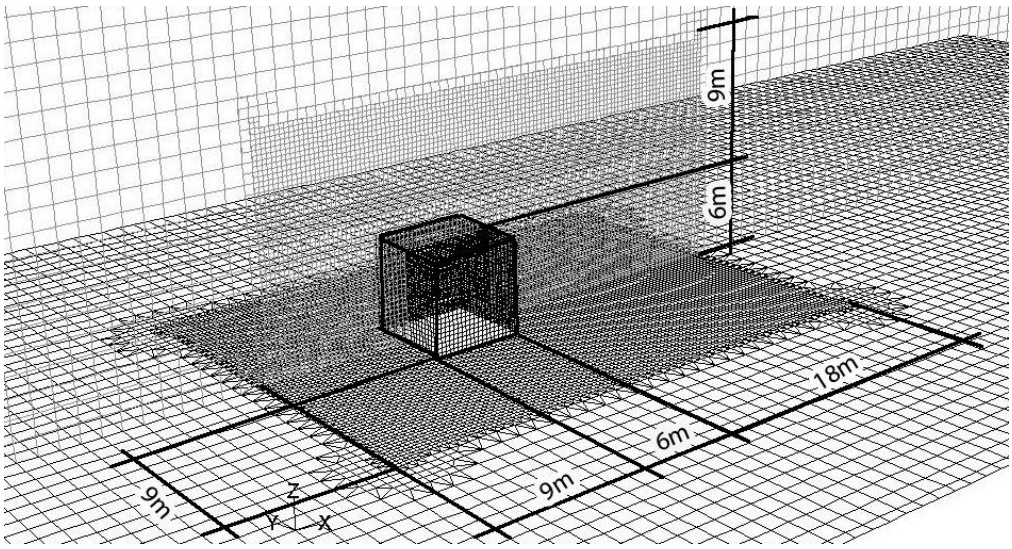

Figure 4.29 Mesh refinement areas around the cube.

To assess the effect of the newly constructed mesh on the accuracy of the simulation, the results from the multi-block mesh were compared to those from the single block mesh. Vertical velocity pathlines, horizontal velocity pathlines and pressure coefficients along the centreline of the windward facade, roof and leeward facade were plotted. It was noticed that coarsening the mesh in areas away from the cube did not affect the accuracy of the results quantitatively or qualitatively. Both the vertical and horizontal velocity pathlines were identical for the multi-block mesh and the single block mesh. The same results were observed for the values of the pressure coefficients along the centreline of the cube in the flow direction.

A mesh independence study was carried out to determine the dependence of the flow field on the refinement of the mesh. Two other meshes were used; the first mesh had a resolution of 0.2m around the cube and 0.8m throughout the rest of the computational domain. The second mesh had a resolution of 0.1m around the cube and 0.8m throughout the rest of the computational domain.

Figure 4.30 shows a comparison between the three meshes; the main flow features which were exhibited in the velocity pathlines plots for the 0.3m mesh are the same as in the 0.2m and the 0.1m mesh. All three meshes were able to capture the main flow features around a cube in a turbulent channel flow. Thus, it can be concluded that the 0.3m mesh is sufficient for running a mesh independent simulation.

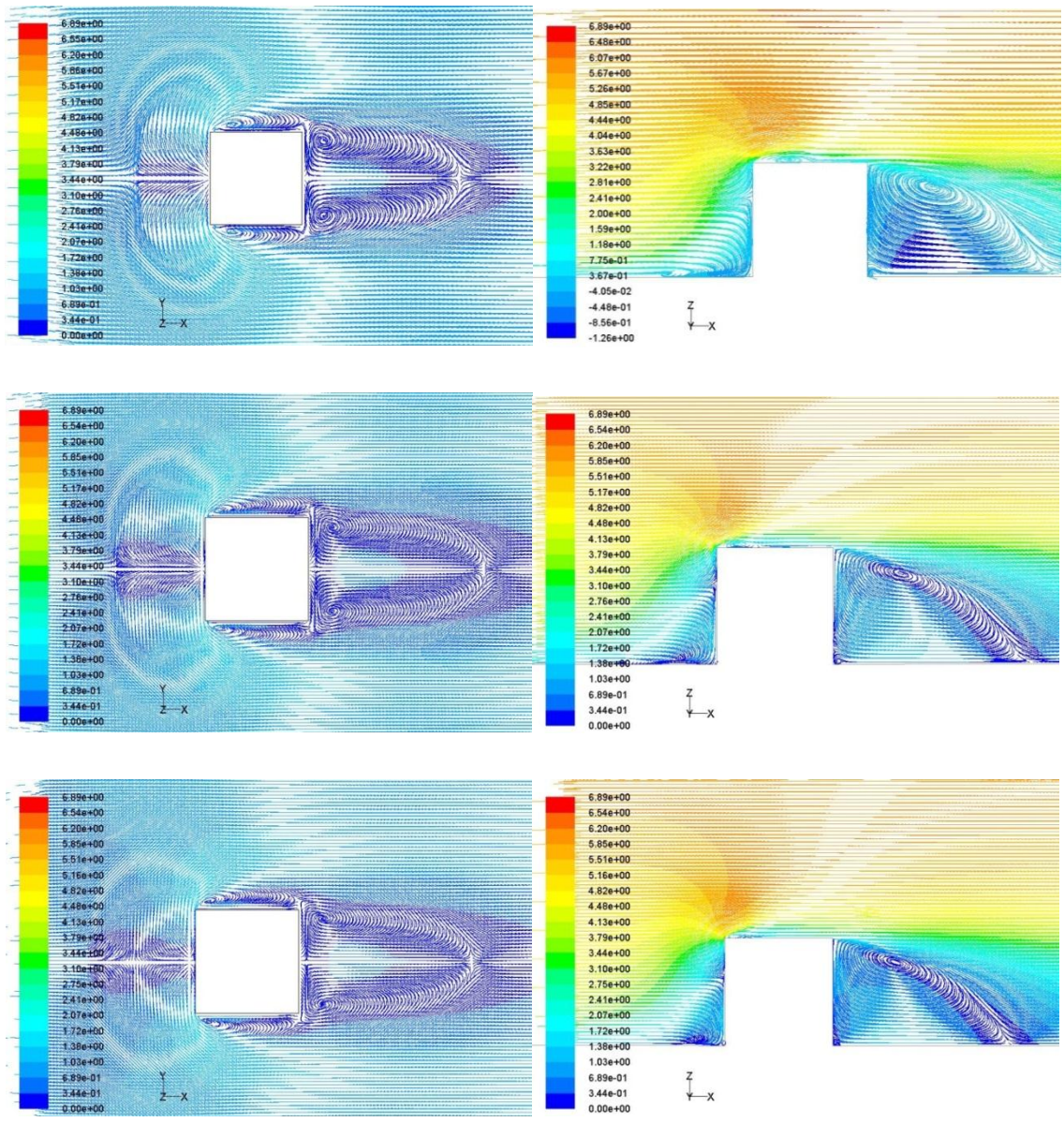

Figure 4.30 Streamwise velocity pathlines for different mesh resolutions. From top to bottom, left: velocity pathlines at ground level for the 0.3m, 0.2m and 0.1m grids, right: centreline velocity pathlines for the 0.3m, 0.2m, and 0.1m grids.

4.3.4 *Simulation results*

Comparing the flow field in the CFD simulation with the previously mentioned wind tunnel tests, in-situ measurements and validated CFD simulations, it was noticed that, qualitatively, the flow features around a cube in a turbulent channel flow were captured in the CFD simulation (Figure 4.31 and Figure 4.32); the horseshoe vortex started to form in the windward direction of the cube and extended along its sides (V1), the division of the main flow into four main streams was noticed, the first stream deviated downwards the windward façade (S1), the second stream deviated above the cube roof (S2) and the other two

streams deviated to the sides of the cube (S3), the deviation from the main stream happened at the point of maximum pressure on the windward façade of the cube at the stagnation point which was clearly visible (St). Due to the presence of the cube, the flow separated but reattached again in the leeward direction of the cube (Rx1).

Also, the flow separated on hitting the windward edge of the cube but reattached again on top of the roof (Rx2). Due to separation and reattachment of the flow, recirculation areas, or vortices, were formed at the same locations as those in the reviewed flow problems. The standing vortex in front of the windward façade was formed (V2) in addition to the two side vortices (V3) and the two leeward vortices (V4), also the recirculation area on top of the roof was captured (V5). The high velocity gradients areas between the vortices and the corner streams were also observed. Qualitatively, the flow results of the CFD simulation compare favourably with the wind tunnel tests and the in-situ measurements as the CFD simulation has captured all the flow features exhibited using those tools.

However, in order to assess the consistency of the CFD simulation, the locations of the front separation on the windward façade (stagnation point), the location of the front separation on the ground in front of the cube (the saddle point), the reattachment length on top of the roof, the reattachment length in the leeward direction of the cube, ground front separation and pressure distribution along the vertical centreline of the windward façade, roof and leeward façade were investigated.

Results showed that the saddle point (Sp) occurred at a distance 0.80h (h is the cube height) from the windward facade, stagnation point (St) occurred at a height of 0.80h from the ground, the roof reattachment length (Rx2) occurred at a distance 0.32h from the windward roof edge, the reattachment length in the leeward direction of the cube (Rx1) occurred at a distance 1.60h from the leeward façade of the cube.

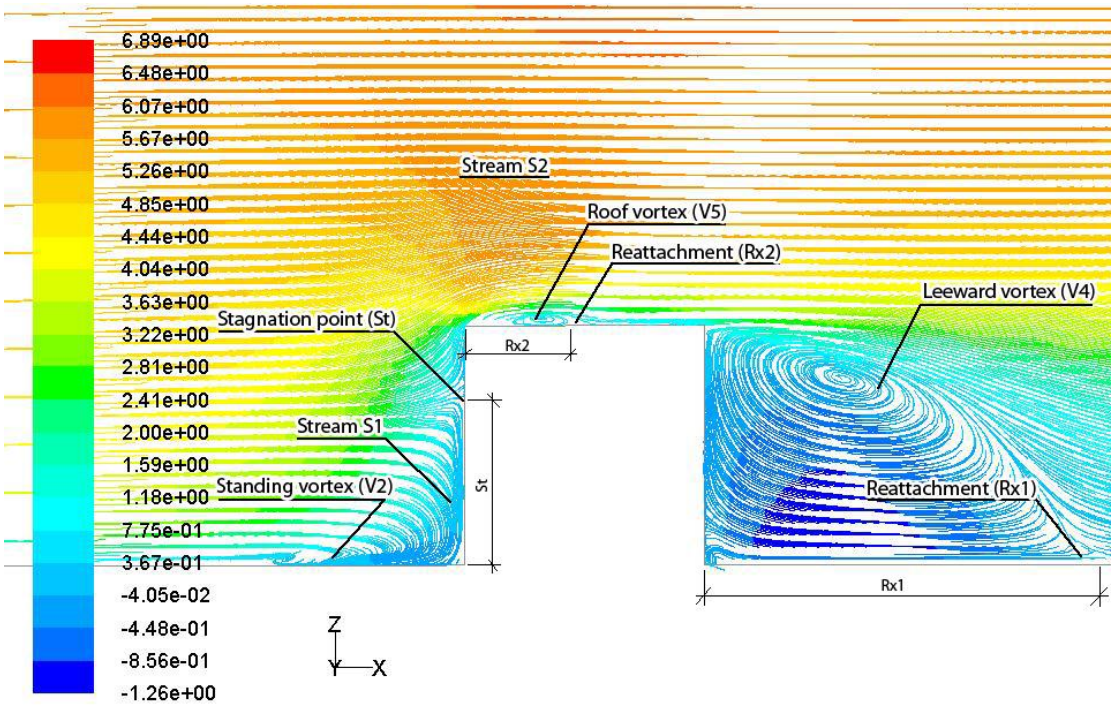

Figure 4.31 Vertical streamwise velocity pathlines along the central plan passing through the cube showing the main flow features and their locations.

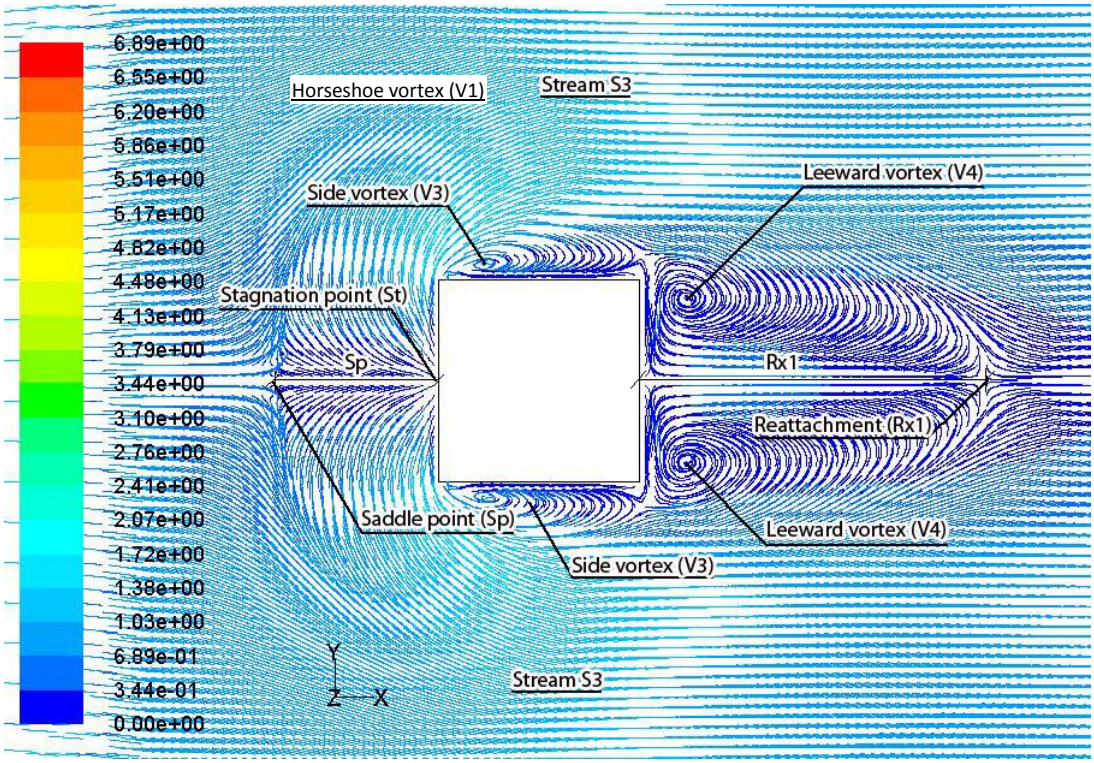

Figure 4.32 Ground streamwise velocity pathlines showing the main flow features around the cube and their locations.

As for the pressure distribution along the vertical centreline of the windward façade, the roof and the leeward façade (Figure 4.33), it was noticed that the

location of maximum positive pressure coefficient (CpW) was at a distance 0.8h from the ground which is the stagnation point and the registered value was 0.81, on top of the roof the maximum negative pressure (CpR) occurred at location 0.05h from the windward edge of the roof and the registered value was -0.97, as for the leeward façade the maximum negative pressure (CpL) occurred at location 0.85h from the ground and the registered value was -0.17.

To put these results in context, they were compared to the results of the previously mentioned in-situ measurements, wind tunnel tests and validated CFD simulations[5]. In addition Figure 4.33 shows a complete pressure coefficients distribution along the centreline of the windward façade, roof and leeward façade in comparison with the 15 wind tunnel tests, their average (Hölscher and Niemann, 1998) and the Silsoe cube full-scale measurements (Richards *et al.*, 2001).

Looking further into the CFD simulation results in this study in comparison with the results from other tools and validated CFD simulations, the results are consistent and fall within the ranges of the reviewed results. For the saddle point (Sp), the point occurred at 0.8h which falls within the range of the validated CFD simulations results which was between 0.64h and 1.58, also that value is almost the same as that from the simulation of Rodi (1997) (0.81h) who used LES which is considered more consistent than any other RANS model.

The stagnation point occurred at 0.80h which is so close to the in situ measurement results (0.81h), falls within the range of the wind tunnel test (0.64h to 0.85h) as well as the range of the validated CFD simulation results (0.60h to 0.85h). The best agreement was with the validated CFD simulation of Yang (2004) using the RNG models in CFX5 (0.80h), then with the in-situ measurements by Richards and Hoxey (2006) and Richards *et al.* (2001) (0.81h) and then with the wind tunnel test by Richards *et al.* (2007) (0.81h).

[5] A table comparing the obtained CFD results in this work compared to the reviewed results from in-situ measurements, wind tunnel tests and validated CFD simulations is included in appendix 1.

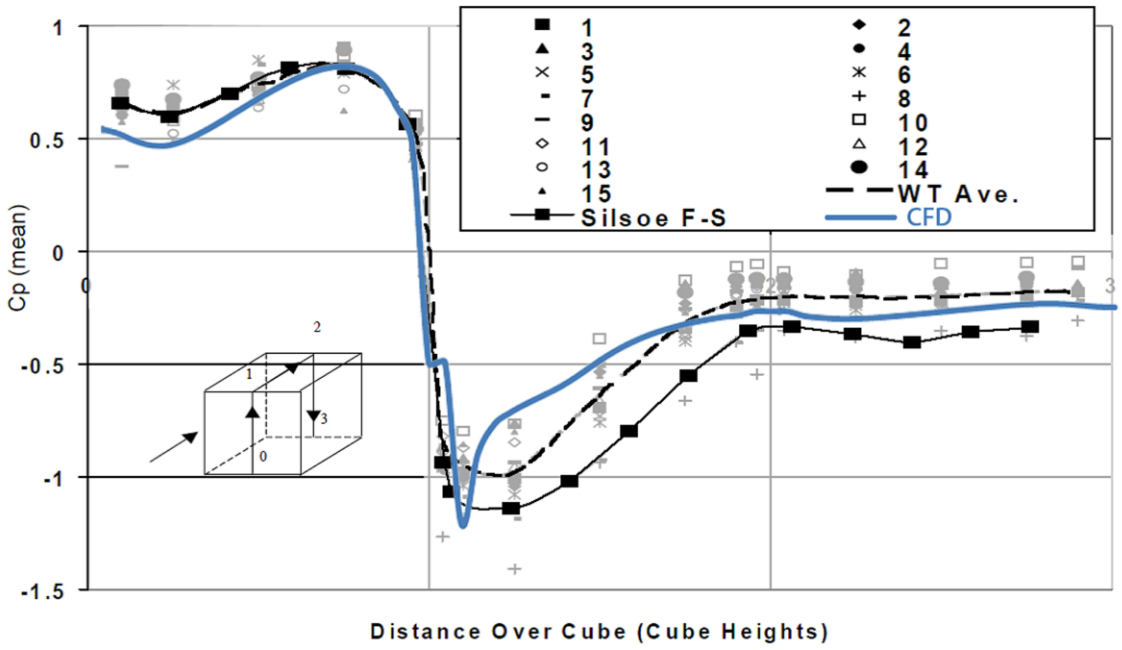

Figure 4.33 Pressure coefficients along the centreline of the windward façade, roof and leeward façade in comparison with the 15 wind tunnel tests from Hölscher and Niemann (1998) and the Silsoe 6m cube full scale measurement from Richards et al. (2001).

The simulation results in this study shows that the flow reattached on top of the roof at a distance of 0.32h which falls within the range of all the reviewed results (0.30h to 0.84h). Although there were some discrepancies throughout the whole results, the CFD simulation results agreed well with the wind tunnel test by Castro and Robins (1977) (0.3h) and the validated CFD simulation results by Seeta Ratnam and Vengadesan (2008) using the standard *k- ω* model (0.30h). As for the reattachment length in the leeward direction of the cube, although the obtained simulation results in this work (1.60h) was slightly higher than the maximum recorded wind tunnel test results for the CEDVAL cube (Vardoulakis *et al.*, 2011) (1.50h), the result was within the range of the validated CFD simulations and it was closest to the results of Seeta Ratnam and Vengadesan (2008) (1.50h) using DNS which is considered one of the most consistent techniques in CFD simulations. However, it should be noted that all the reviewed validated CFD simulation results over predicted the recirculation area in the leeward direction of the cube and the reported results are considered the closest to the wind tunnel tests in terms of not over predicting the reattachment length leeward the cube.

The maximum recorded positive pressure coefficient along the centreline for the windward façade (0.81) was within the range of the wind tunnel results (0.75 to 0.87) but was less than the lowest recorded value for the validated CFD simulations (0.89) as for the in-situ measurements it was 0.86 which is relatively close to the obtained results. However, it should be noted that all the reviewed validated CFD simulations over predicated the maximum recorded positive pressure coefficient along the centreline for the windward façade compared to the wind tunnel tests and the in-situ measurements.

Although the maximum negative pressure coefficient on the roof (-0.97) was within the range of the validated CFD simulations (-0.85 to -1.56) and it compared favourably with the in-situ measurements (-0.90) and the wind tunnel tests range (-0.90 to -1.10), the same over prediction was observed for most of the reviewed validated CFD simulations especially the results from Paterson and Apelt (1989) and Yang (2004a) using the k-ε turbulence model in CFX5. On the leeward façade, although all the reviewed results for the maximum negative pressure coefficients (-0.10 to -0.40) compared favourably with the reported result (-0.17), it was noticed again that the highest values were recorded for the validated CFD simulation results.

4.4 Conclusion

This chapter has demonstrated that validation studies are needed to give confidence in CFD simulations. This chapter started by discussing the reasons behind the need to validate CFD simulations and the rationale behind choosing the flow problem of air flow around a cube in a turbulent channel flow as the validation case. Results from other tools such as in-situ measurements, wind tunnel tests and validated CFD simulations were reviewed from literature for the purpose of comparing the reviewed results with the results of the CFD simulation undertaken in this study for the same flow problem.

However, discrepancies exist between the results of different tools and between the results of different researchers using the same tool. This demonstrates the importance of running validation studies and not only relying on best practice guidelines or previous recommendations for simulation conditions. However, using these best practice guidelines can be a start point for running a consistent CFD simulation. One of the main recommendations is to achieve a horizontally

homogeneous atmospheric boundary layer (ABL) profile which was successfully achieved in this work. In addition, a grid impendence study was carried out and a mesh resolution was reached which yielded a mesh independent simulation.

Simulation was run and results were obtained and compared to the reviewed results using different tools for assessing similar wind flow problems. It can be concluded that the results are consistent and compares favourably with other reviewed results as all the flow features were captured in the CFD simulation. In addition, all the values of the specific lengths of the flow were within the ranges of the reviewed results. The obtained results are closest to the wind tunnel results from Castro and Robins (1977) which is another indication of the consistency of the obtained results in this work as it was mentioned earlier that the results from Castro and Robins (1977) are considered in literature as reliable results for comparison and validation purposes.

The highest discrepancies were found on the roof in terms of the distribution of maximum pressure coefficients although the values were acceptable and the locations were also acceptable. But for the values near the windward edge of the roof, discrepancies were observed. However, these discrepancies where consistently reported in similar published CFD simulations (Baskaran and Stathopoulos, 1994; Yang, 2004a; Franke, 2007; Cóstola *et al.*, 2009) which suggests that the source of the error might be the way in which the code solves the flow in these areas. It was noticed that none of the reviewed results matched the results from the in-situ measurements which is argued to be the most accurate results, the same occurred with the obtained CFD results especially on the roof but it should be noted that the obtained results are closer to the reviewed wind tunnel tests results. However, when comparing the obtained results with the reviewed validated CFD simulations results and other wind assessment tools results, the obtained results compare more favourably than the reviewed CFD simulations results. Accordingly, the used simulations variables can be used with confidence for simulating wind flow in further simulations in this research.

Chapter Five

Roof Shape, Wind direction, Building Height and Urban Context Effect on the Energy Yield and Positioning of Roof Mounted Wind Turbines

Chapter Structure

5.1 Introduction

5.2 Roof mounted wind turbines

5.3 Flow problems settings

5.4 Results analysis

5.5 Conclusion

Chapter 5: Roof Shape, Wind direction, Building Height and Urban Context Effect on the Energy Yield and Positioning of Roof Mounted Wind Turbines

5.1 Introduction

It was concluded in the previous chapter that using CFD simulations with the previously mentioned set of simulation variables is a valid tool for studying urban wind flow for different applications. One of these applications is sitting wind turbines within urban areas or on top of buildings' roofs which, according to Stankovic et al. (2009), is one of the potentially low-cost renewable sources of energy. However, in order to specify the optimum mounting location of a wind turbine, an investigation of the wind resources and the wind flow around the proposed mounting location is required. Thus, this chapter focuses on investigating the effect of roof shape, wind direction, building height and surrounding urban configuration on the energy yield and positioning of roof mounted wind turbines.

This chapter is divided into three main sections; the first section (5.2) gives an overview of roof mounting wind turbines; the second section (5.3) reports the wind flow problems settings in terms of simulations variables, roof shapes, buildings' dimensions, wind directions and urban configurations; the third section (5.4) reports the investigated flow variables for the investigated flow problems and is further divided into three subsections; the first subsection reports the results of different wind directions for the investigated roof shapes; the second subsection reports the results of varying the height of the chosen optimum roof shape and the last subsection reports the results of varying the height of the optimum roof shape when placed within different urban configurations. This chapter concludes by comparing the results and reporting the optimum mounting location for each of the investigated roof shapes, the optimum roof shape for mounting wind turbines, the effect of height on wind flow above the roof and the effect of different urban configurations on wind flow above the optimum roof shape for roof mounting wind turbines.

5.2 The case of roof mounted wind turbines

Sievert (2009) asserted that one of the main factors affecting the success of roof mounted wind turbines is the roof shape of the building where a wind

turbine is to be mounted. Rafailidis (1997) demonstrated that the wind flow and turbulence intensity at the roof level are strongly dependant on the roof shape. The WINEUR (2007) report stated that the shape of the roof affects wind flow around the mounted wind turbine and buildings have a speed up effect on wind. Accordingly, Dutton *et al.* (2005) recommended the investigation of the locations where the speed-up effects take place over different roof shapes to take advantage of the increased wind speed.

Although Blackmore (2008) acknowledged the importance of roof shapes in the performance of roof mounted wind turbines, there have been limited previous studies in the field. Sara Louise (2011) confirmed Blackmore's (2008) assertion and added that very little CFD work has been undertaken to study wind flow close to buildings' roofs for applications of roof mounted wind turbines. Kindangen *et al.* (1997) studied flat , gabled, pyramidal, wedged and vaulted roof shapes effect on indoor air speed distributions under five wind directions (0, 30, 45, 60 and 90 degrees). Asfour and Gadi (2008) investigated natural ventilation performance of two equivalent domed and vaulted roofs. Huang *et al.* (2009) investigated the effect of wedge-shaped roofs on wind flow and pollutant dispersion in a street canyon within an urban environment. And Ayata (2009) investigated the different effects of flat and gabled roofs on reducing the wind effect on the detached houses.

On the other hand, for the purpose of roof mounting wind turbines, Ledo *et al.* (2011) studied wind flow around pitched, pyramidal and flat roofs under three wind directions (0, 45 & 90 degrees), they concluded that the power density above the flat roof is greater and more consistent than above the other roof types[1] and they recommended extending the investigation to include other roof shapes. Phillips (2007) investigated the mounting location for a single wind direction for a gabled roof and recommended extending the investigation to include more roof types and more locations with different wind directions. Mertens (2006) analysed flow over a flat roof with a view to developing a small wind turbine siting guidelines focusing on the mounting height.

[1] For the pitched (gabled), pyramidal, and flat roofs, the obtained results in this work are in accordance with the results from Ledo et al. (2001).

Slowe (2006) acknowledged that wind speeds over roof tops are not sufficiently well understood to enable accurate predictions of energy outputs, accordingly, some established manufacturers of micro-wind turbines are cautious about putting their products on buildings and currently install the vast majority of their products on free-standing poles rather than on buildings. It was added that a variety of factors influence the energy yield of roof mounted wind turbines; these include the influence of the roof shape on wind flow over the building; how high above the roof and where above the roof the turbine is sited. Understanding how wind flows around different roof shapes will help determine areas of high turbulence intensities, to be avoided, since high levels of turbulence could cause early fatigue failure of the turbine blades, also areas of substantial flow separation zone will make the turbine subject to very low wind speed, thus it is preferable to mount wind turbines where wind speed is maximum and turbulence intensity is minimum (Lu and Ip, 2009). Thus, these are the two main quantitative flow variables to be investigated in this work in addition to qualitatively investigating the flow patterns around the investigated roof shapes.

5.3 Flow problems settings

In order to specify the optimum roof shape for mounting wind turbines, the CFD commercial code Fluent 12.1 is used, implementing the simulation variables previously mentioned in chapter four in the validation study, to simulate wind flow above six different roof shapes covering a cubic building whose edge height is six meters. These roof shapes are flat, domed, gabled, pyramidal, barrel vaulted and wedged roofs which represent the basic shapes of most commonly used roof shapes in urban areas (Figure 5.1).

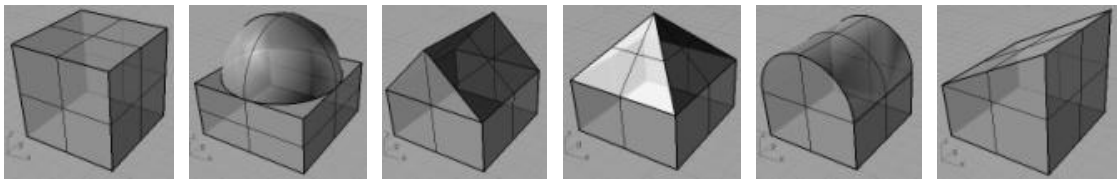

Figure 5.1 From left to right: flat, domed, gabled, pyramidal, vaulted and wedged roofs.

To investigate the effect of wind direction, simulations were run with different wind directions (Figure 5.2). To understand the effect of each roof shape on wind flow around the mounted wind turbine, streamwise velocity pathlines are plotted along the central plan parallel to the wind direction (Figure 5.3) and to

determine the optimum location for mounting a wind turbine on top of each roof, both the turbulence intensity and streamwise velocity are plotted along different locations above each roof extending from directly above roof to a height of 2.5H above ground level (H = Height of the of the 6m cube) (Figure 5.4). All roof shapes cover a building of square cross section 6m x 6m. Accordingly, the optimum mounting location for each roof type under different wind directions is specified and the results are compared to each other to determine the optimum roof shape for mounting wind turbines.

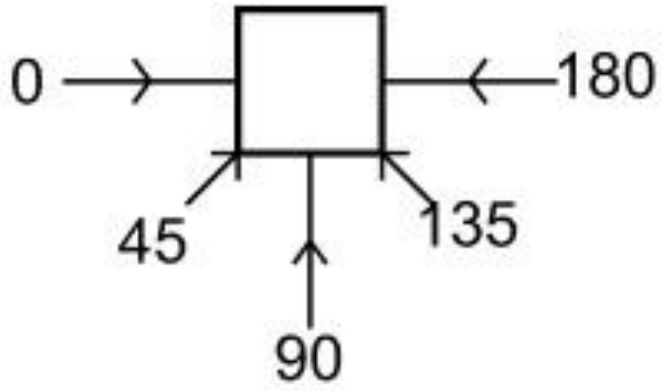

Figure 5.2 investigated wind directions.

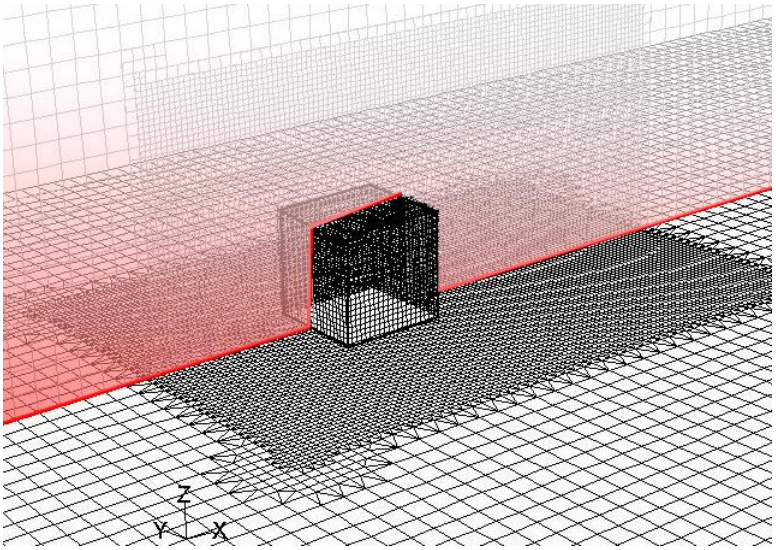

Figure 5.3 Central plan parallel to the wind direction where the streamwise velocity pathlines are plotted.

In order to investigate the effect of building height on wind flow above the building, the optimum roof shape is used to cover the same building but after increasing the height to reach 12m then 24m respectively. Then, the three

cases (6m, 12m and 24m) are compared to each other in terms of flow patterns, turbulence intensity and streamwise velocity, thus the effect of height is identified. For investigating the effect of urban configuration and height on wind flow above the roof of a building, the optimum roof shape is used to cover a 4.5m, 6m, 12m and 24m buildings placed in an array of cubic buildings whose edge height is 6m, the cubes are arranged in an urban canyon configuration and in a staggered urban configuration. Simulations are run and the results are analysed to identify the effect of both configurations on the energy yield and positioning of the proposed wind turbines

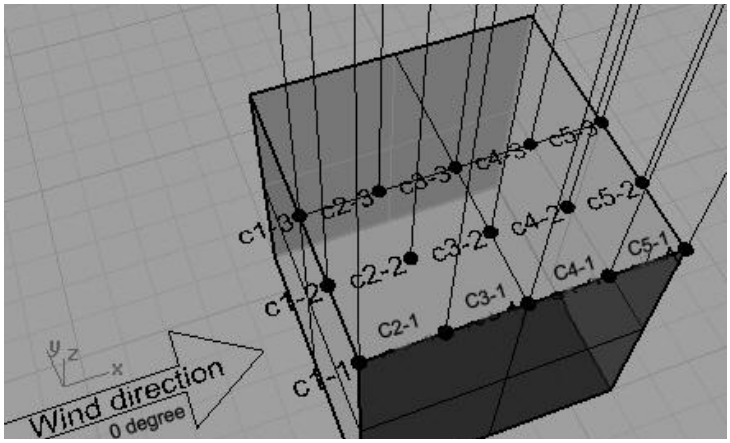

Figure 5.4 Measurements locations on top of the flat roof.

5.4 Results analysis

Since all roof shapes are at least symmetrical along one axis, measurements were taken from either all the roof at 30 different measurements locations or half the roof at 15 different measurements locations, the points are spaced evenly from the windward edge to the leeward edge in an array of 5 points in the streamwise direction and 5 points perpendicular to the streamwise direction, the spacing between the points is 1.5m.

The measurements locations extend vertically above the roof to a distance equal to 9m and the measurements are recorded at the nodes of the computational mesh, i.e. every 0.3m which resulted in 30 vertical measurements locations along the vertical line (Figure 5.4). Flow patterns are visualised along the vertical streamwise central plan, turbulence intensities and streamwise velocities are recorded along the vertical measurements locations. In order to identify the accelerating effect of the roof shape, the streamwise

velocity and the turbulence intensity are normalised against the streamwise velocity and the turbulence intensity at the same locations under the same flow conditions without the building being there (an empty domain).

5.4.1 *Effect of roof shape and wind direction*

The investigated roof shapes are subjected to different wind directions namely: 0^0, 45^0, 90^0, 135^0 and 180^0 (Figure 5.2). Since all roof shapes are at least symmetrical along one axis, no further angles were studied. According to the degree of symmetry of the roof shape, the number of incident wind directions is determined.

5.4.1.1 0^0 Wind direction

The 0^0 wind direction applies to all the investigated roof shapes. Positioning roof mounted wind turbines requires understanding wind flow characteristics such as flow patterns, turbulence intensity and wind velocity around different roof shapes. Visualizing the flow pattern around each roof shape helps in determining the recirculation areas, stagnation points, flow separation and reattachment. This gives a qualitative assessment of the potential places on top of the roof where a wind turbine can be mounted. However, in order to determine the exact location for mounting a wind turbine, both the turbulence intensity and streamwise velocity are measured. A rule of thumb is to avoid locations of high turbulence intensity and low mean wind speed to maximise the energy yield and reduce the wearing of the wind turbine.

In order to study wind flow characteristics around different roof shapes, streamwise velocity pathlines were plotted along the vertical central plan passing through the building, turbulence intensity and streamwise velocity were plotted at 15 different locations above the roof staring at 6m high (1H) up to 9m high (1.5H) above the highest point of the roof. To be able to identify the accelerating effect different roof shapes have on local air flow, all plotted values were normalized against the values at the same locations in an empty domain. Figure 5.5 (a, b, c, d, e and f) shows the main features of the flow above the investigated roof shapes through plotting the streamwise velocity pathlines along the vertical central streamwise plan.

Flow pattern

For the flat roof it was noticed that corner streams and flow separation areas are formed above the building due to the formation of a small vortex above the roof, the corner streams subsequently merge into the general flow around the corner.

The recirculation area above the building is located at the windward half of the roof and the area above is characterised with high streamwise velocities which make it a potential area for mounting a wind turbine if the recirculation area is avoided due to the high levels of turbulence in this area. More detailed analysis of the flow above the flat roof case was included in chapter four when studying the flow around a cube in a turbulent channel flow for validation purposes.

For the domed and the barrel vaulted roofs, unlike the flat roof case, it was noticed that the flow was strongly attached to both roofs and no recirculation areas were formed above the roof. In addition, the area of maximum streamwise velocity was noticed to be directly above the highest point of the two roofs. For the gabled and the pyramidal roofs, the flow was strongly attached to the windward parts of the roofs but large recirculation areas were formed at the leeward part of the roof.

The centre of the recirculation area of the gabbled roof was formed at the same height of the ridge of the roof, for the pyramidal roof it was between the roof's peak point and eave. The areas of maximum streamwise velocities for both cases were both located at the leeward parts of the roofs. As for the wedged roof the flow was attached to the roof and no recirculation area was formed on top of the roof and the area of maximum streamwise velocities was formed beyond the roof on top of the recirculation area at the leeward direction of the building.

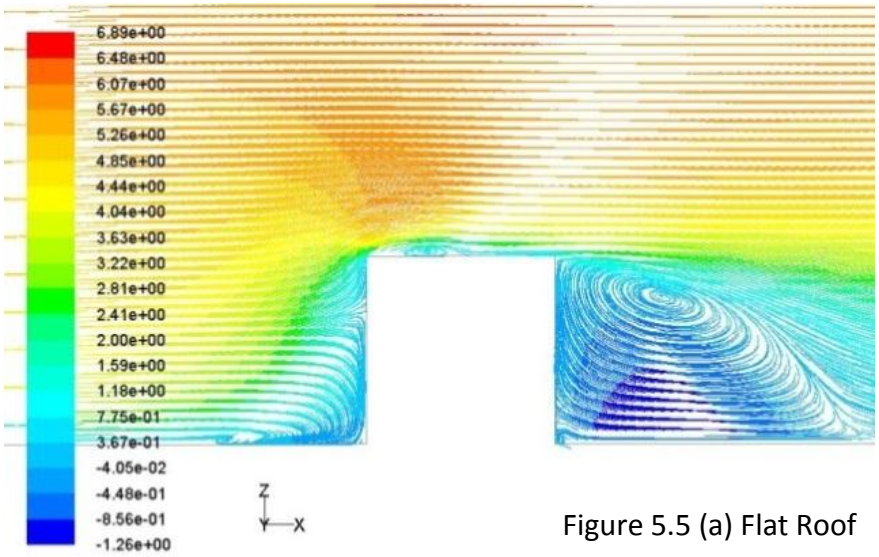

Figure 5.5 (a) Flat Roof

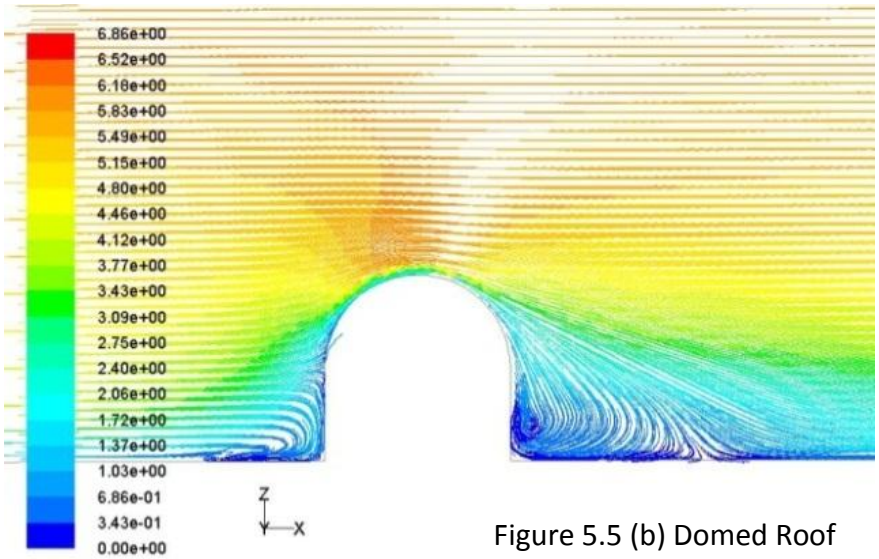

Figure 5.5 (b) Domed Roof

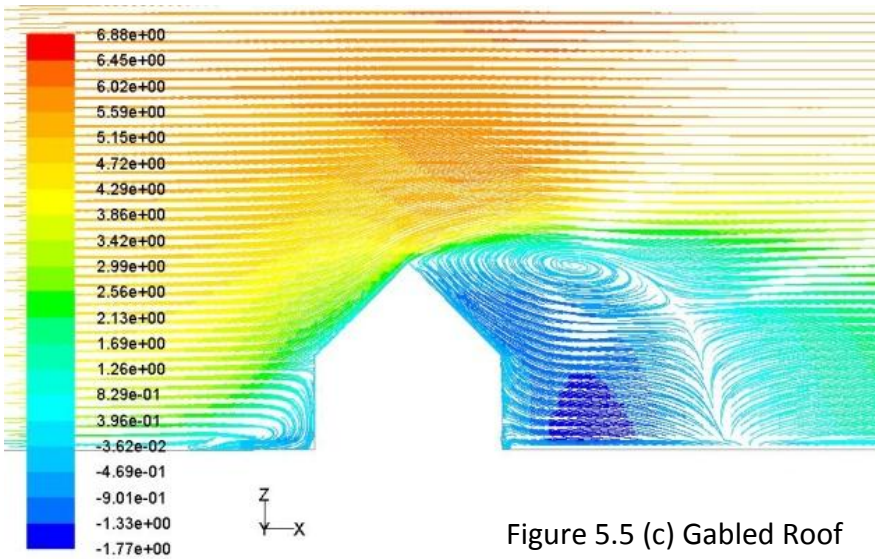

Figure 5.5 (c) Gabled Roof

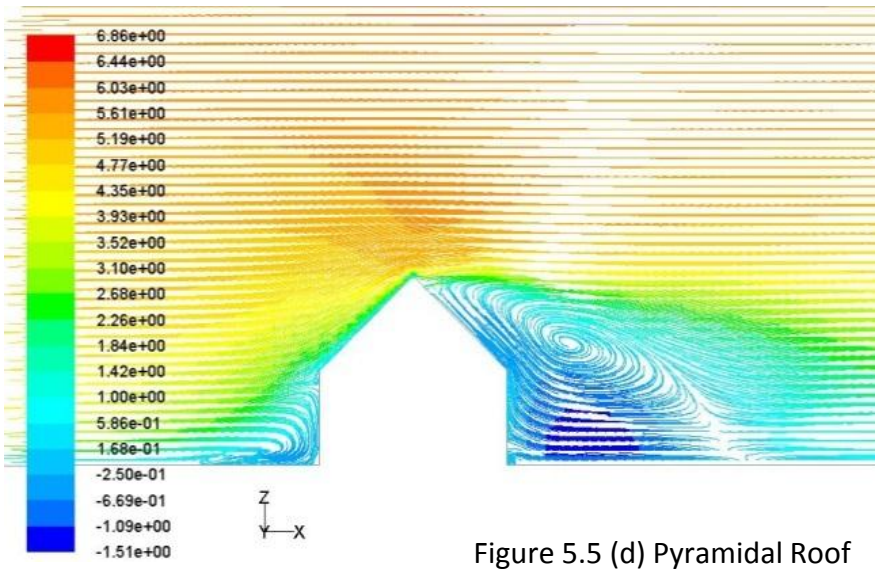

Figure 5.5 (d) Pyramidal Roof

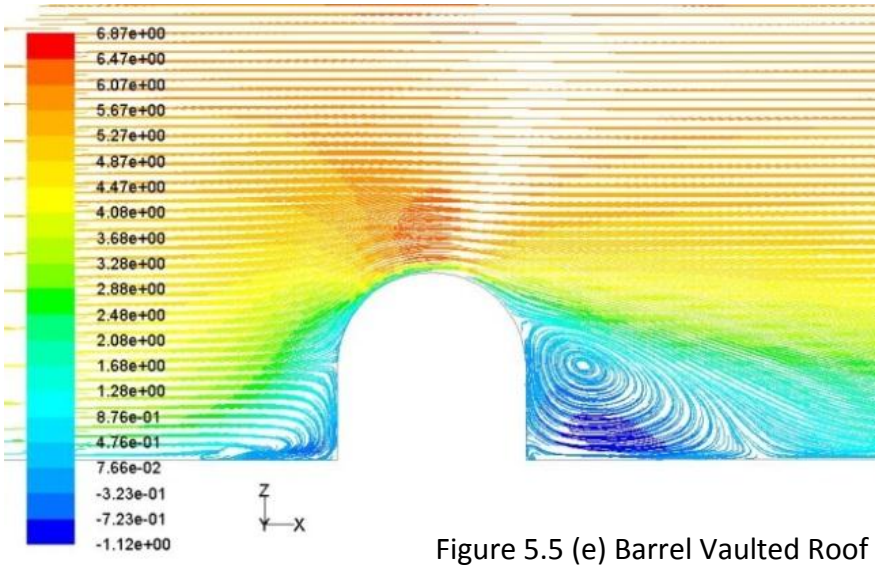

Figure 5.5 (e) Barrel Vaulted Roof

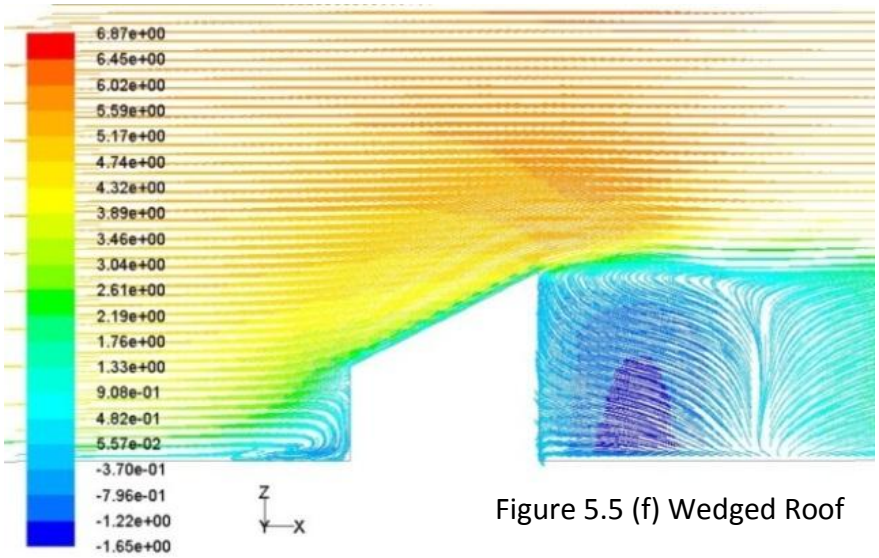

Figure 5.5 (f) Wedged Roof

Figure 5.5 Streamwise velocity pathlines along the vertical central streamwise plan for the investigated roof shapes, (a) flat, (b) domed, (c) gabled, (d) pyramidal, (e) barrel vaulted and (f) wedged roofs.

Turbulence intensity (TI)[2]

The presence of a building in a free stream affects the turbulence intensity in its vicinity. The shape of the building is one of the main factors affecting how much the turbulence intensity increases due to the interaction between the flow and the building. Accordingly, the roof shape plays an important role in how much turbulence the roof mounted wind turbine would be subjected to. The turbulence intensities above the six roofs were measured and normalised to determine where are the areas of maximum turbulence intensities to be avoided when mounting wind turbines on top of the investigated roofs. According to Ledo *et al.* (2011) for roofs with inclined surfaces, the turbulence intensity rises to 40%, which means that it is not acceptable to mount a turbine below the ridge level. Beyond the roof peak, the turbulence level decreases with height. Accordingly, the normalised turbulence intensities where plotted at 15 different locations above the roof starting from 6m above ground level to 15m above ground level.

Table 5.1 shows the range of maximum increase in TIs, and the location of maximum recorded turbulence intensity for each roof. All roof shapes resulted in an increase in turbulence intensities above them. The minimum increase in turbulence intensity was recorded on top of the wedged roof which reached 1.15 TI[3] at location W1-1 (windward corner) at height H and the maximum increase in turbulence intensity was recorded on top of the flat roof which reached 2.8TI at location C1-3 (midpoint of the windward roof edge) at height 1.1H.

The obtained results in this work shows that after 1.2H with the increase in height above the roof the turbulence intensity decreases as well as the wind velocity. Thus, in order to take advantage of the accelerating effect of the roof while avoiding high turbulent areas, a compromise between mounting location, wind velocity and turbulence intensity should be reached. For all investigated roofs, it was noticed that the region of maximum turbulence intensity ranged between directly above the roof to a distance of 1.2H. This area should be

[2] A complete plot of the turbulence intensities along different measurements point for all roofs is included in appendix 2.

[3] TI is the turbulence intensity at the same location, under the same flow conditions in an empty domain.

avoided when mounting wind turbines on top of buildings. According to the Encraft Warwick Wind Trials Project (Encraft, 2009), the lowest position of the rotor should be at least 30% of the building height above the roof level, and according to the recommendations of the WINEUR (2007) report, a roof mounted wind turbine on top of a flat roof should be positioned at a height from 35% to 50% of the building height. In addition to that, the roof mounted wind turbine should be mounted at a height where there is clearance between the rotating blades and the roof. Accordingly, in this work, the vertical range extending from directly above the roof (H) to 1.3H will be avoided when roof mounting wind turbines for practical reasons and due to expected high levels of turbulence.

Table 5.1 Turbulence intensities values and locations for different roof shapes.

Turbulence Intensity (TI)	Flat (Cube)	Domed	Gabled	Pyramidal	Barrel Vaulted	Wedged
Range of maximum increase in TIs values	1.8TI to 2.8TI	1.2TI to 2.2TI	1.7TI to 2.7TI	1.2TI to 2.35TI	1.7TI to 2.3TI	1.15TI to 2TI
Vertical range of maximum TIs locations	H to 1.15H	H to 1.15H	H to 1.2H	H to 1.2H	H to 1.15H	H to 1.15H
Location of maximum recorded TI value	C1-3 at 1.1H	D2-3 at 1.1H	G3-1 at 1.1H	P3-3 at 1.1H	V2-2 at 1.1H	W5-1at 1.15H

C refers to a location above the cube, D above the domed, G above the gabled, etc.

Streamwise velocity[4]

The main factor affecting the energy yield of a wind turbine is the wind velocity. The importance of the speed of the wind is that the energy yield is directly proportional to cube the wind speed (Equation 2.1, Chapter 2). This means that if the wind speed doubles the energy yield will increase eight times. Thus, one

[4] A complete plot of the streamwise velocities along different measurements point is included in appendix 3.

of the main factors affecting the economic potential of urban wind turbines is the average wind speed (Joselin Herbert *et al.*, 2007; Blackmore, 2008; Eriksson *et al.*, 2008; Stankovic *et al.*, 2009).

Table 5.2 Streamwise velocities values and locations for different roof shapes.

Streamwise velocity (U)	Flat	Domed	Gabled	Pyramidal	Barrel Vaulted	Wedged
Range of maximum increase in Us values	1.05U to 1.1U	1.02U to 1.18U	1.0U to 1.06U	1.01U to 1.07U	1.03U to 1.24U	1.0U to 1.03U
Vertical range of maximum Us locations	1.3H to 1.85H	1.3H to 1.6H	1.6H to 2.5H	H to 1.45H	1.1H to 1.6H	1.4H to 2.5H
Location of maximum recorded U value	C2-3 at 1.45H	D3-3 at 1.1H	G5-1 at 1.6H	P3-2 at 1.15H	V3-3 at 1.1H	W5-1 at 1.45H
Maximum recorded U value above maximum turbulence area (> or equal to 1.3H)	1.095U at C2-3 at 1.45H	1.12U at D3-3 at 1.3H	1.05U at G5-1 at 1.6H	1.05U at P4-2 at 1.3H	1.16U at V3-3 at 1.3H	1.03U at W5-1 at 1.45H

Table 5.2 shows the range of maximum increase in streamwise velocities, and the location of maximum recorded streamwise velocities for each roof, in addition to the maximum recorded streamwise velocities above the area of maximum turbulence intensities (> or equal to 1.3H). As in the turbulence intensity, all roof shapes had an accelerating effect on the wind speed above them. This speed up effect was reported by Mertens (2006) for flat roofs. The same thing applies for the investigated cases in this research. The maximum increase in streamwise velocity varied at different locations between negligible acceleration on top of the gabled and the wedged roof to 1.24U[5] above the vaulted roof, the maximum streamwise velocities were mostly observed at heights between 1.0H and 1.85H then it decreased gradually until the presence of the building had no effect at a height more than or equal 2.5H. The maximum

[5] U is the streamwise velocity at the same location under the same flow conditions in an empty domain.

streamwise velocity was observed above the barrel vaulted roof at location V3-3 at a height of 1.1H.

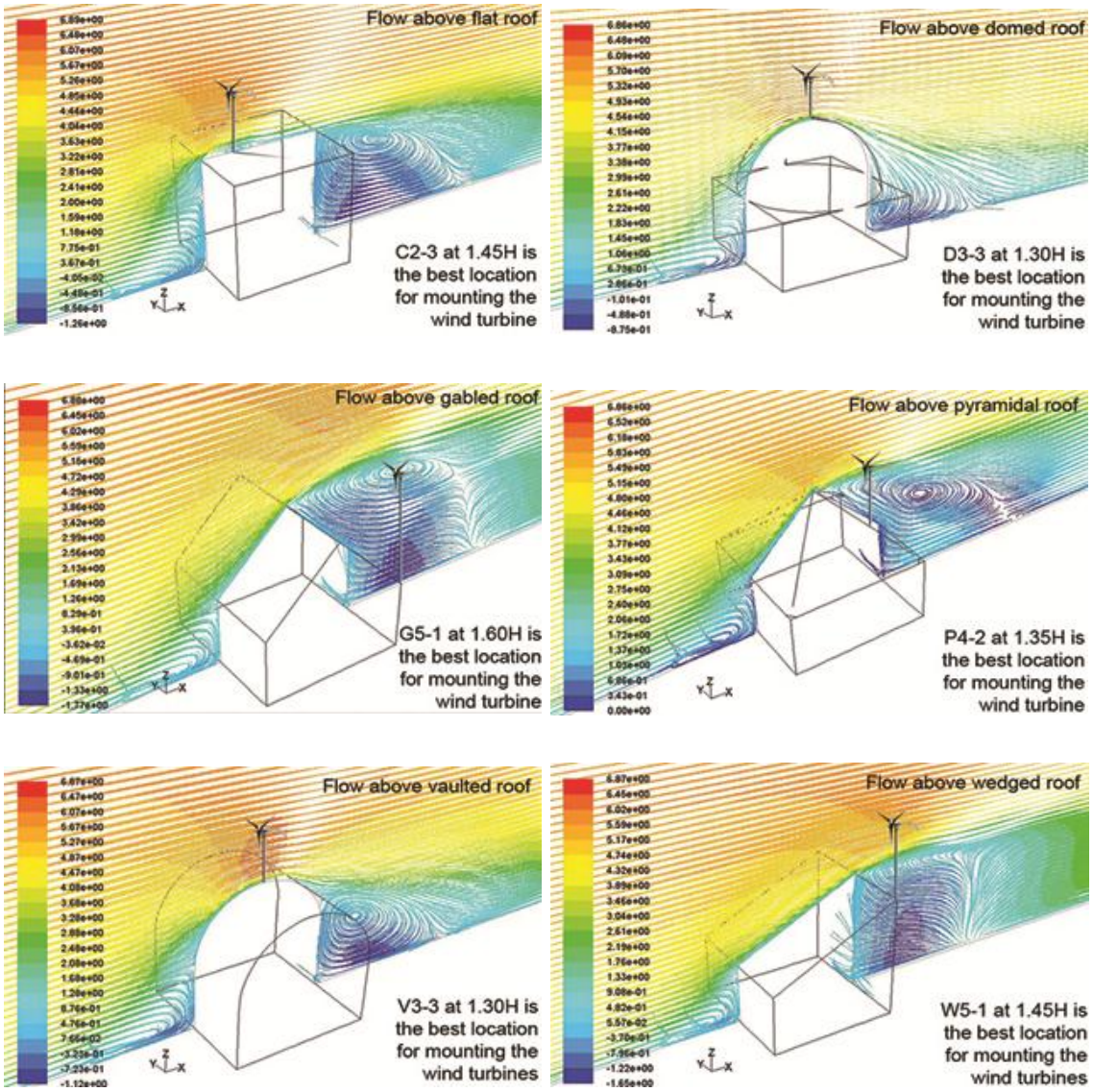

Figure 5.6 Optimum mounting location for different investigated roof shapes under 0^0 wind direction.

Keeping in mind these results and the recommendations from both the WINEUR (2007) report and the Encraft Warwick Wind Trials Project (Encraft, 2009), when analysing the streamwise velocities plots, even if the maximum acceleration occurs in the area from directly above the roof to 1.3H, it should be ignored and the acceleration in the area above or equal to 1.3H should only be counted for. Thus, Table 5.3 shows that the optimum location for mounting a micro-wind turbine on top of a flat roof is at height of 1.45H at location C2-3 (between the roof windward edged and the middle of the roof), for the domed roof: D3-3 (midpoint of the roof) at 1.3H, for the gabled roof: G5-1 (the leeward

corner of the roof) at 1.6H, for the pyramidal roof: P4-2 (leeward hip, midway between the middle of the roof and the leeward roof edge) at 1.35H, for the barrel vaulted roof: V3-3 (midpoint of the roof) at 1.3H and for the wedged roof: W5-1 (the leeward corner of the roof) at 1.45H (Figure 5.6).

Figure 5.7 shows a comparison between the recorded streamwise velocities at the optimum mounting locations above each roof shape, it is noticed that the highest maximum increase in velocity occurred on top of the vaulted roof at location V3-3 (midpoint of the roof) at height of 1.3H and the velocity at that point reached 1.16 times the velocity at the same location in an empty domain. Since the energy yield of a wind turbine is directly proportional to cube the wind velocity, therefore mounting a wind turbine on top of a vaulted roof at that particular location, would yield 56.1% more power than a free standing wind turbine at the same location under the same flow conditions.

Table 5.3 Maximum normalised velocities and locations for 0^0 wind direction.

Roof shape	Maximum normalized velocity	Location
Flat	1.095	2-3 at 1.45H
Domed	1.12	3-3 at 1.3H
Gabled	1.05	5-1 at 1.6H
Pyramidal	1.05	4-2 at 1.3H
Barrel Vaulted	1.16	3-3 at 1.3H
Wedged	1.03	5-1 at 1.45H

On the other hand, the lowest maximum increase in streamwise velocity occurred on top of the wedged roof at location W5-1 (the leeward corner of the roof) at height of 1.45H and the velocity at that point reached 1.03 times the

velocity at the same location in an empty domain which means that mounting a wind turbine on top of a wedged roof would yield only 9% more power than a free standing wind turbine at the same location under the same flow conditions. However, the accelerating effect of a wedged roof is more pronounced in a region at the leeward direction of the building, which makes a free standing wind turbine at the leeward direction of a wedged roof building (not on top of the roof) more feasible in terms of taking advantage of the accelerating effect of the building.

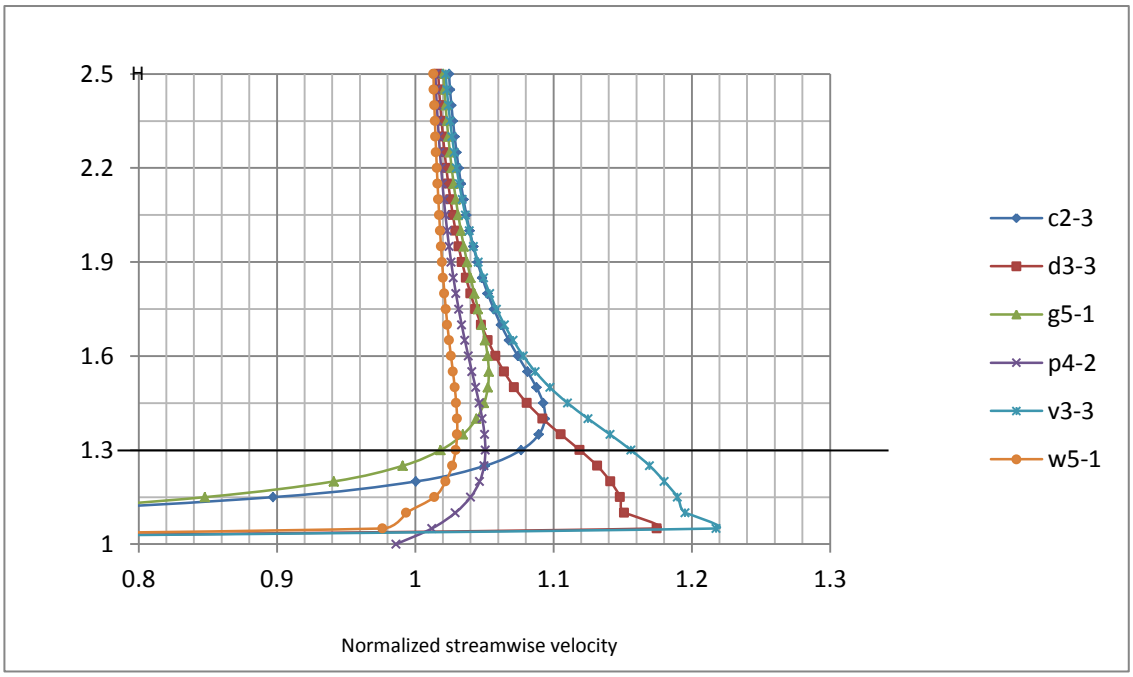

Figure 5.7 Comparison between normalized maximum recorded streamwise velocities above all roof shapes for the 0 degree wind direction.

5.4.1.2 45^0 Wind direction

When rotating all the investigated cases 45^0 or assuming that the wind direction is inclined by 45^0 from the windward façade and due to the different geometry and symmetry features of the investigated roof shapes, more measurements points are needed to include all the roof for asymmetrical shapes along the streamwise wind direction axis, these roofs are the barrel vaulted, wedged and gabled roofs, as for the flat, domed and pyramidal roofs, half the measurement points on top of the roof are only needed (Figure 5.8).

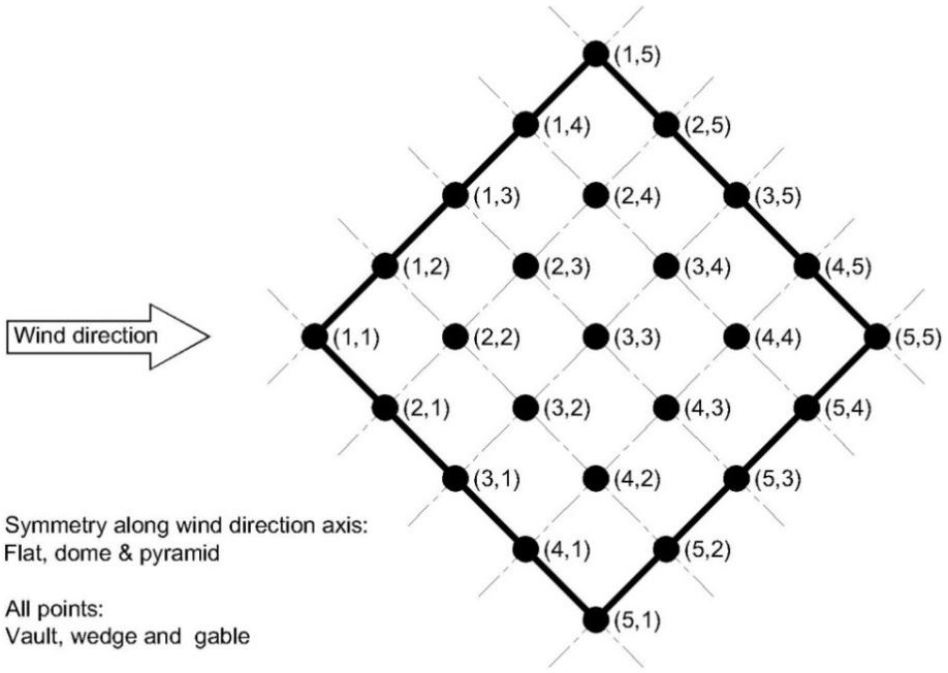

Figure 5.8 45^0 wind direction and the different measurements points on the roofs.

Flow pattern

Figure 5.9 (a-f) shows the streamwise velocity pathlines along the vertical central streamwise plan for the investigated roof shapes with the wind direction inclined 45^0 from the windward façade. For the flat roof, the main flow features which were exhibited in the 0^0 wind direction case were the same in this case in terms of the division of the flow into four main streams, the first stream deviated on top of the roof, the second downward on the windward façade and the two other streams to the sides of the cube.

Stagnation point was formed at a lower location near to the ground compared to the previous case. For the recirculation areas (standing vortex, side and leeward vortices) they were visible, however, the recirculation area on top of the roof was very small since the flow has barely separated from the roof. Thus, it is assumed that levels of turbulence on top of the roof would be less than the previous case which suggests more potential locations for mounting wind turbines.

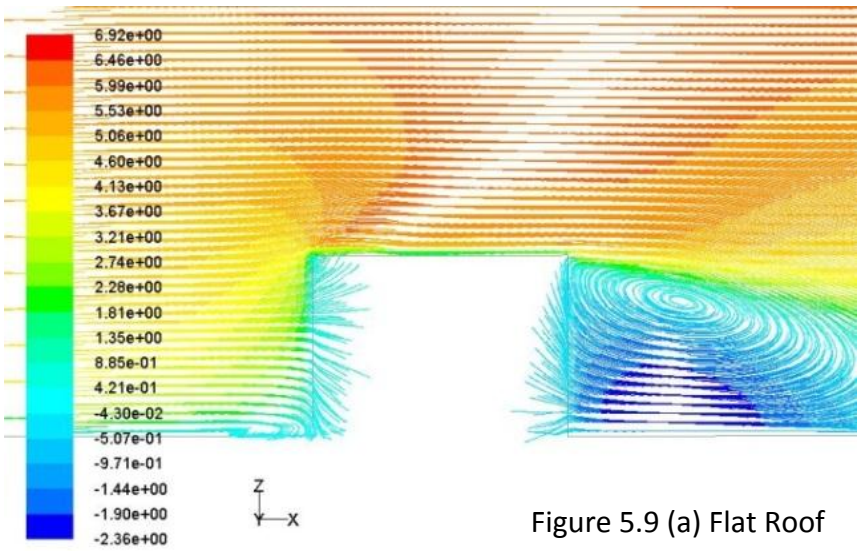

Figure 5.9 (a) Flat Roof

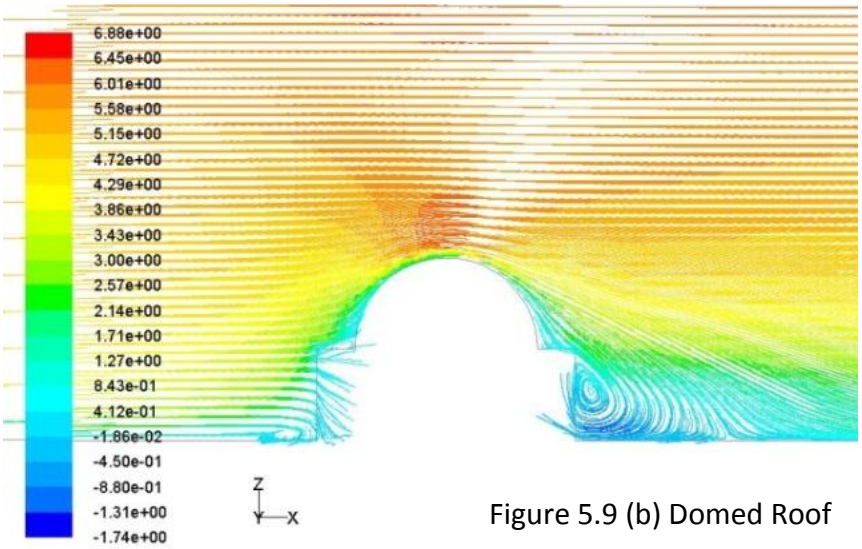

Figure 5.9 (b) Domed Roof

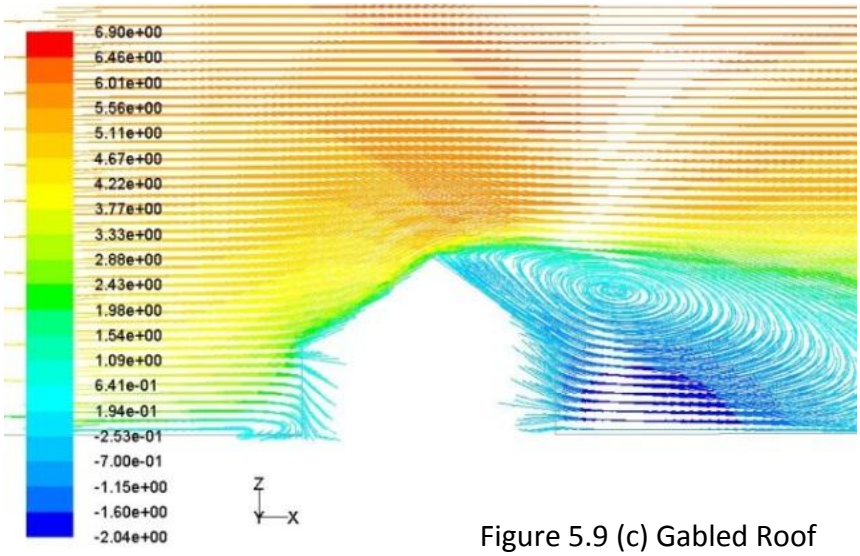

Figure 5.9 (c) Gabled Roof

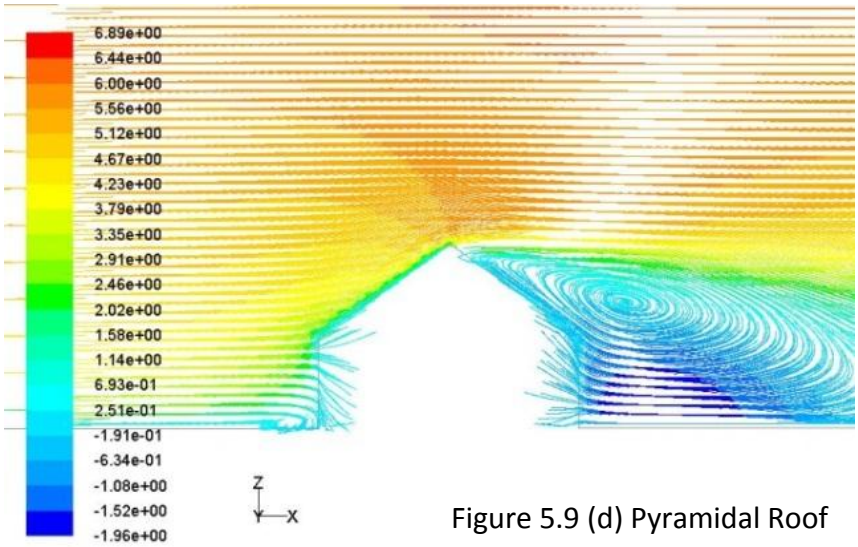

Figure 5.9 (d) Pyramidal Roof

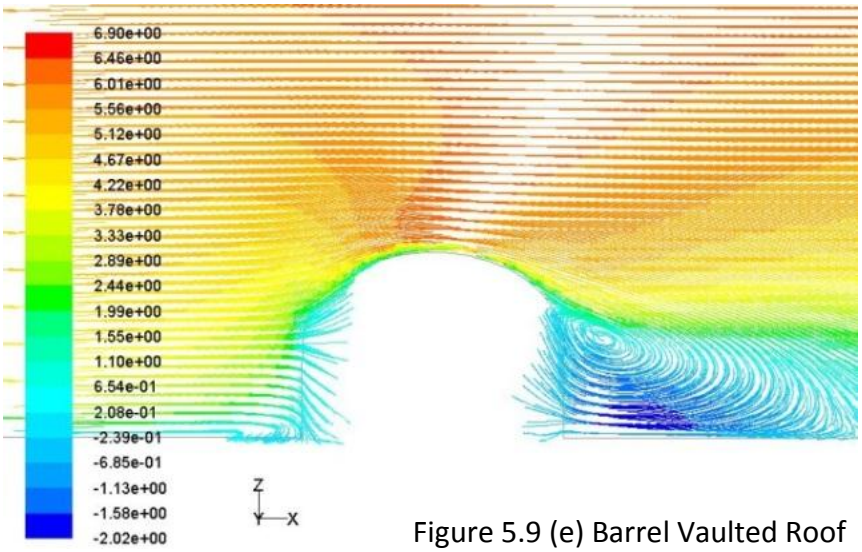

Figure 5.9 (e) Barrel Vaulted Roof

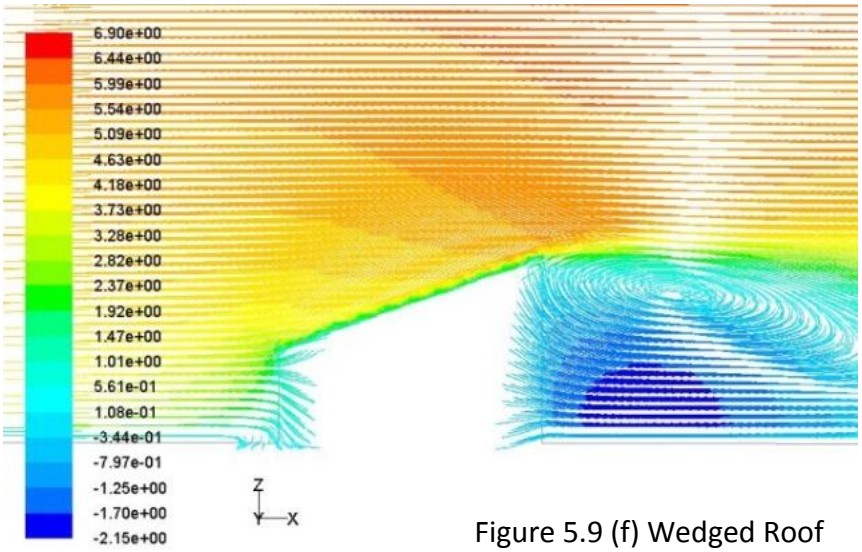

Figure 5.9 (f) Wedged Roof

Figure 5.9 Streamwise velocity pathlines along the vertical central streamwise plan for the investigated roof shapes, (a) flat, (b) domed, (c) gabled, (d) pyramidal, (e) barrel vaulted and (f) wedged roofs with 45^0 wind direction.

The flow above the domed and the vaulted roofs are similar in terms of the attachment of the flow to both surfaces. As in the previous cases, the area of maximum acceleration occurred on top of the highest points above both roofs (midpoint of the roof). For the gabled and the pyramidal roofs, the flow patterns are the same as in the previous cases except that for the gabled roof, in this case, the centre of the recirculation area in the leeward direction of the building is closer to the ground and the leeward part of the roof, which suggests that the levels of turbulence might be higher than previous cases and the potential mounting locations might be less. The same phenomenon happened with the wedged roof; the area of maximum acceleration was found to be beyond the roof on top of the recirculation area. Above the roof, the flow did not separate and the roof accelerating effect was not pronounced.

Turbulence intensity (TI)[6]

As seen in the flow pattern around the flat roof case with the wind direction inclined 45^0 from the windward façade, the recirculation area above the roof was minimum and the flow barely separated from the roof, which indicates lower levels of turbulence in that particular location, this can be attributed to the lower pressure difference between the roof and the windward façade which is due to the building vertical edge facing the windward direction which resulted in less suction at the sides and the roof of the building leading to more attachment of the flow to the buildings' surfaces. The same phenomenon occurred for the other five cases and this can be confirmed by the location of the standing vortices in front of the buildings which were formed in closer location to the vertical edge facing the wind than the cases of the wind perpendicular to the windward façade.

Table 5.4 shows the range of maximum increase in TIs, and the location of maximum recorded turbulence intensity for each roof. All roof shapes, once again, resulted in an increase in turbulence intensities above them. The minimum increase in turbulence intensity was recorded on top of the wedged roof which reached 1.14TI at location W1-1 (windward corner) at height H, and

[6] A complete plot of the turbulence intensities along different measurements point is included in appendix 4.

the maximum increase in turbulence intensity was recorded on top of the flat roof which reached 2.42TI at location C5-1 (right corner) at height 1.1H.

The quantitative results of the turbulence intensities confirms the interpretations of the qualitative results of the previously discussed flow patterns since all the recorded values of the turbulence intensities in the 45^0 cases are either lower or equal to the recorded values in the 0^0 cases, also the vertical range of maximum recorded turbulence intensities is lower in these cases than the previously discussed cases which suggests that a wind inclined 45^0 to similar buildings with similar geometries would encounter less turbulence levels on top of the roof than when the wind is perpendicular to one of the building's facades.

Table 5.4 Turbulence intensities values and locations for different roof shapes with wind direction 45^0.

Turbulence Intensity (TI)	Flat (Cube)	Domed	Gabled	Pyramidal	Barrel Vaulted	Wedged
Range of maximum increase in TIs values	1.66TI to 2.42TI	1.22TI to 2.14TI	1.22TI to 2.12TI	1.16TI to 1.96TI	1.3TI to 2.35TI	1.14TI to 2.07TI
Vertical range of maximum TIs locations	H to 1.15H	H to 1.13H	H to 1.15H	H to 1.1H	H to 1.15H	H to 1.15H
Location of maximum recorded TI value	C5-1 at 1.1H	D2-2 at 1.0H	G5-5 at 1.1H	P3-3 at 1.1H	V5-2 at 1.0H	W1-5 at 1.0H

Streamwise velocity[7]

Table 5.5 shows that all roof shapes had an accelerating effect on wind flow above them. When comparing these cases with the previous cases it can be noticed that the minimum accelerating effect for the 45^0 wind direction cases is higher than or equal to those of the 0^0 wind direction for all the roof cases except for the barrel vault case, as for the maximum increase in the

[7] A complete plot of the streamwise velocity along different measurements point is included in appendix 5.

accelerating effect, all the cases of the 45^0 recorded higher values than the 0^0 except also for the barrel vault case which can be attributed to the aerodynamic properties of the vault which is different from the other cases.

Table 5.5 Streamwise velocities values and locations for different roof shapes with wind direction 45^0.

Streamwise velocity (U)	Flat (Cube)	Domed	Gabled	Pyramidal	Barrel Vaulted	Wedged
Range of maximum increase in Us values	1.02U to 1.15U	1.01U to 1.21U	1.01U to 1.09U	1.01U to 1.08U	1.01U to 1.18U	1.0U to 1.07U
Vertical range of maximum Us locations	1.75H to 1.2H	1.1H to 1.9H	1.15H to 2.5H	1.05H to 2.5H	1.05H to 2.5H	1.3H to 2.5H
Location of maximum recorded U value	C2-2 at 1.1H	D3-3 at 1.1H	G2-5 at 1.25H	P3-3 at 1.05H	V3-3 at 1.05H	W5-5 at 1.3H
Maximum recorded U value above maximum turbulence area (> or equal to 1.3H)	1.12U at C2-2 at 1.3H	1.14U at D3-3 at 1.3H	1.09U at G3-5 at 1.4H	1.08U at P4-4 at 1.3H	1.14U at V3-3 at 1.3H	1.07U atW5-5 at 1.3H

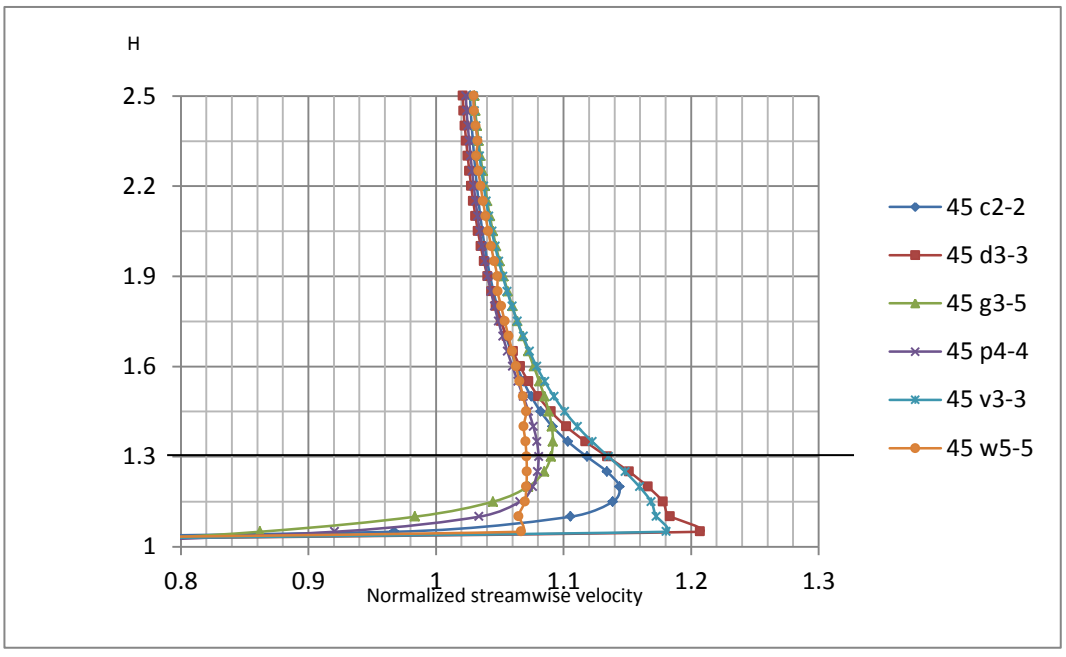

Figure 5.10 Maximum streamwise velocity for the 45 direction.

The maximum streamwise velocities were mostly observed at heights between 1.05H and 2.50H. The maximum streamwise velocity was observed above the domed and vaulted roofs at locations D3-3 and V3-3 (midpoints of the two roofs) respectively at the same height of 1.30H. Figure 5.10 shows a comparison between the maximum recorded streamwise velocities on top of each of the roof shapes when the wind is at an angle of 45^0.

5.4.1.3 90^0 Wind direction

The case when the wind is flowing perpendicular to the roof profile (90^0) applies only to the gabled, barrel vaulted and the wedged roofs, the rest of the roof shapes are the same as the 0^0 wind direction due to the symmetry of the geometries. All the points above the wedged roof needs to be investigated since the wedged roof is not symmetrical along the streamwise wind direction axis, as for gabled and barrel vaulted roofs, due to symmetry conditions, only half of the roof can represent the whole roof (Figure 5.11).

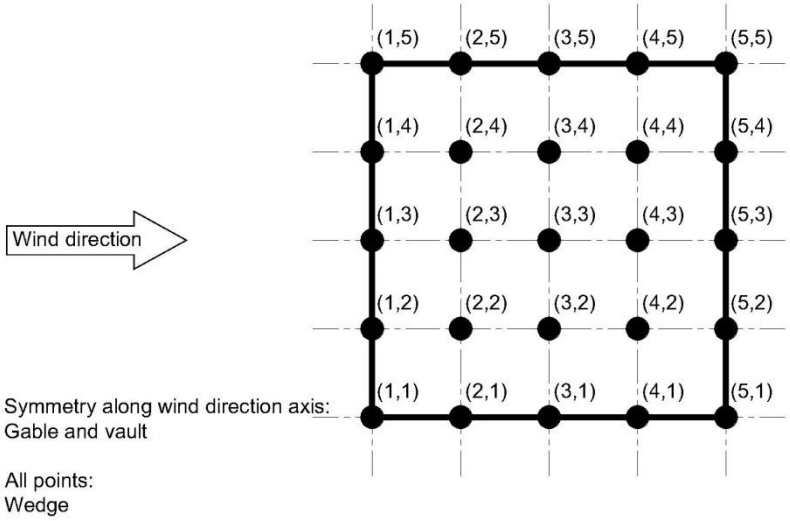

Figure 5.11 90^0 wind direction and the different measurements points on the roofs.

Flow pattern

Figure 5.12 shows the streamwise velocity pathlines along the vertical central streamwise plan for the gabled, barrel vaulted and wedged roofs with wind direction perpendicular to roof profile. The main flow features around the three buildings are the same in terms of the division of the main flow stream into 4 streams; above, to the sides and down the windward façade. The stagnation

points and the recirculation areas, in the leeward direction and windward direction of the buildings are formed at the same locations.

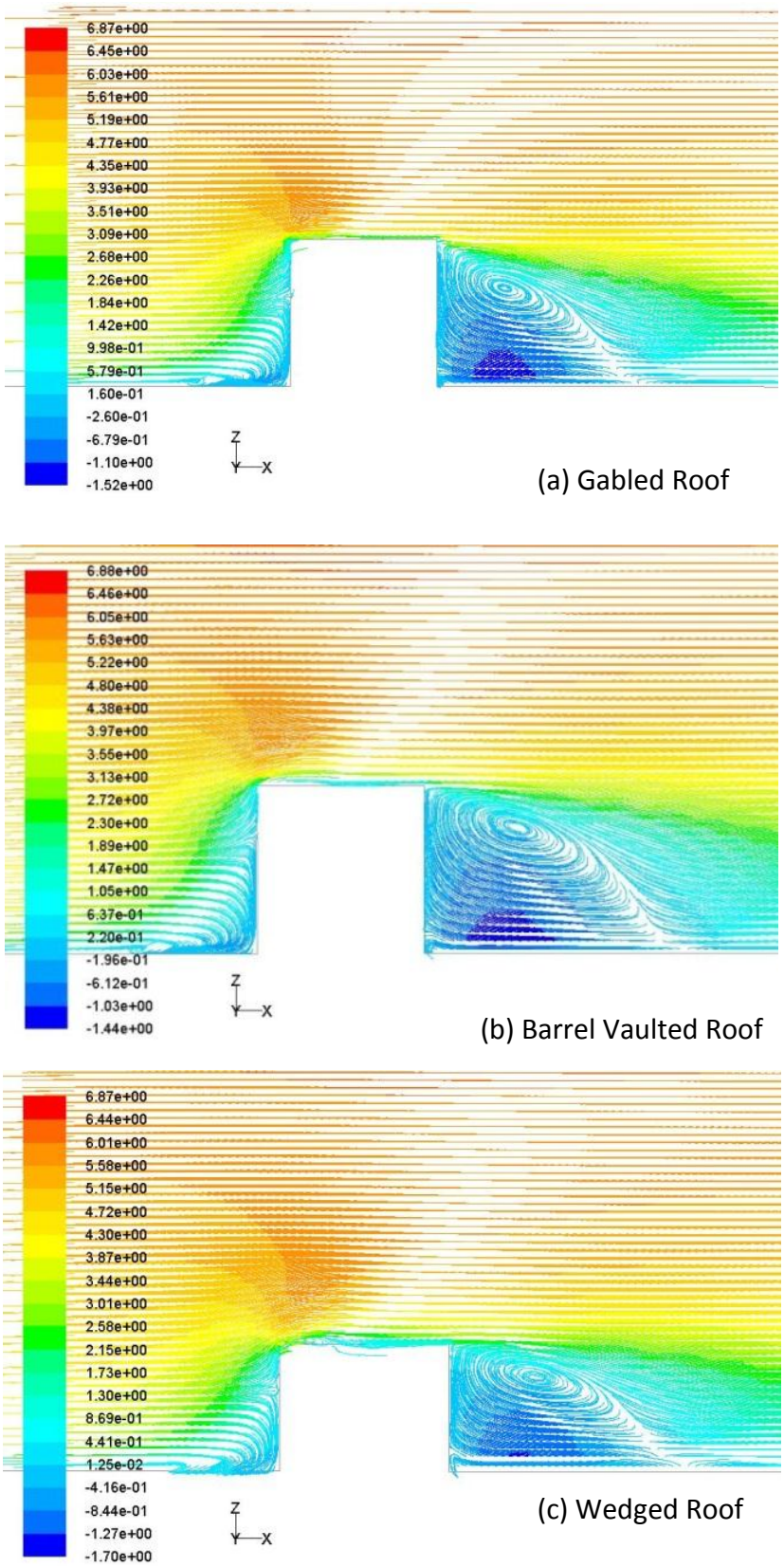

Figure 5.12 Streamwise velocity pathlines along the vertical central plan passing through the (a) gabled roof, (b) barrel vaulted roof and (c) wedged roof with 90^0 wind direction.

The main difference between the flow patterns for the three cases is the recirculation area on top of the roofs. For the gabled roof the flow is attached to the roof and no recirculation area is formed. As for the barrel vaulted and wedged roofs, a small recirculation area is formed near the windward edge of the roof. The flow reattached in both cases above the roof near the midpoint of the roof. The accelerating effect for the three cases is noticed in the area closer to the windward edge of the roof which is due to the interaction between the wind and the edges of the three buildings. However, since the flow is perpendicular to the roof profile, the turbulence intensities and the accelerating effects are not expected to be higher than the previous cases for the same roof shapes when the flow was either parallel or inclined to the roof profile.

Turbulence intensity (TI)[8]

According to the results reported in Table 5.6, it is noticed that the highest levels of turbulence were recorded very close to the roof (from H to 1.15H). All cases resulted in an increase in turbulence intensities above the roofs but the lowest increase in turbulence intensity was recorded above the wedged roof which reached 1.2TI at location W1-1 (windward right corner) at height H, and the maximum increase in turbulence intensity was recorded on top of the barrel vaulted roof which reached 3.28TI at location V1-2 (on the windward edge midway between the roof streamwise axis and the right corner) at height H.

It can be noticed that for the three cases that the maximum recorded increase in turbulence intensities occurred exactly at the windward edge of the roof and the vertical range of maximum increase in turbulence intensities reached 1.1H for both the gabled and barrel vaulted roofs and reached 1.15H for the wedged roof which confirms the interpretations of the qualitative results of the flow patterns around the investigated cases. Thus, it can be argued that when the flow is perpendicular to the roof profile, the wind turbine on top of the roof will suffer from less levels of turbulence even when placed close to the roof surface.

[8] A complete plot of the turbulence intensity along different measurements point is included in appendix 6.

Table 5.6 Turbulence intensities values and locations for different roof shapes with wind direction 90^0.

Turbulence Intensity (TI)	Gabled	Barrel Vaulted	Wedged
Range of maximum increase in TIs values	1.32TI to 2.56TI	2.04TI to 3.28TI	1.2TI to 2.4TI
Vertical range of maximum TIs locations	H to 1.1H	H to 1.1H	H to 1.15H
Location of maximum recorded TI value	G1-3 at 1.0H	V1-2 at 1.0H	W1-5 at 1.0H

Streamwise velocity[9]

In this case, the accelerating effect for the three cases occurred at locations nearer to the roof than the previous cases. For both the gabled and wedged roofs, the maximum accelerating effect occurred directly at height H and registered 1.09U for both cases while for the barrel vaulted roof, it occurred at a height of 1.2H but the value was the same as in the previous two cases (Table 5.7). Thus, the maximum accelerating effect was the same above the three roof shapes when the wind is perpendicular to the roof profile.

However, above 1.3H the barrel vaulted roof registered the highest acceleration which reached 1.083U at location V2-2 (midpoint between the windward roof edge and the centre of the roof) at height 1.35H. Both the gabled and the wedged roofs registered the same acceleration of 1.075U at 1.3H but at location G2-3 (between the roof windward edged and the middle of the roof) for the gabled roof and location W2-4 (on the left half of the roof midpoint between the windward roof edge and the centre of the roof) for the wedged roof. Figure 5.13 shows a comparison between the maximum recorded streamwise velocities on top of the three investigated roofs when the wind is perpendicular to the roof profile.

[9] A complete plot of the streamwise velocity along different measurements point is included in appendix 7.

Table 5.7 Streamwise velocities values and locations for different roof shapes with wind direction 90^0.

Streamwise velocity (U)	Gabled	Barrel Vaulted	Wedged
Range of maximum increase in Us values	1.04U to 1.09U	1.04U to 1.09U	1.04U to 1.09U
Vertical range of maximum Us locations	1.0H to 1.6H	1.2H to 1.75H	1.0H to 1.6H
Location of maximum recorded U value	G2-1 at 1.0H	V2-1 at 1.2H	W2-2 at 1.0H
Maximum recorded U value above maximum turbulence area (> or equal to 1.3H)	1.075U at G2-3 at 1.3H	1.083U at V2-2 at 1.35H	1.075U at W2-4 at 1.3H

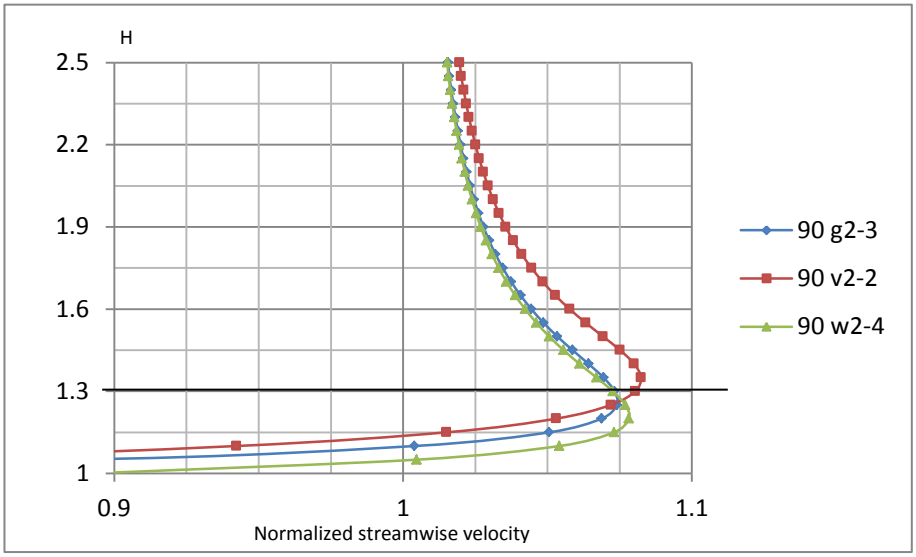

Figure 5.13 Maximum recorded normalized streamwise wind velocity for different roof shapes with wind direction 90^0.

5.4.1.4 135^0 Wind direction

The case of the 135^0 wind direction only applies to the wedged roof shape and registering the flow variables along the whole roof is necessary for understanding wind flow above the wedged roof when the wind is blowing at a 135^0 angle (Figure 5.14).

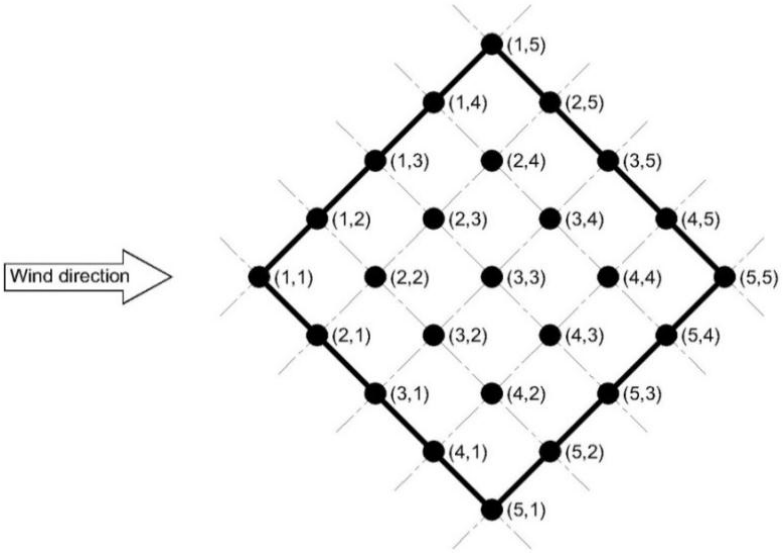

Figure 5.14 135^0 wind direction and the different measurements points on above the wedged roof.

Flow pattern

The flow is divided into the 4 main streams; above the roof, down the windward façade and two streams to the two sides of the building. No recirculation area was formed above the roof, the flow remained attached to the roof but with very low velocity until the leeward vertical edge where the pressure is minimum and the pressure difference between the windward vertical edge and the leeward vertical edge is maximum which resulted in the formation of a recirculation area leeward the building and the centre was close to the leeward edges of the roof (Figure 5.15).

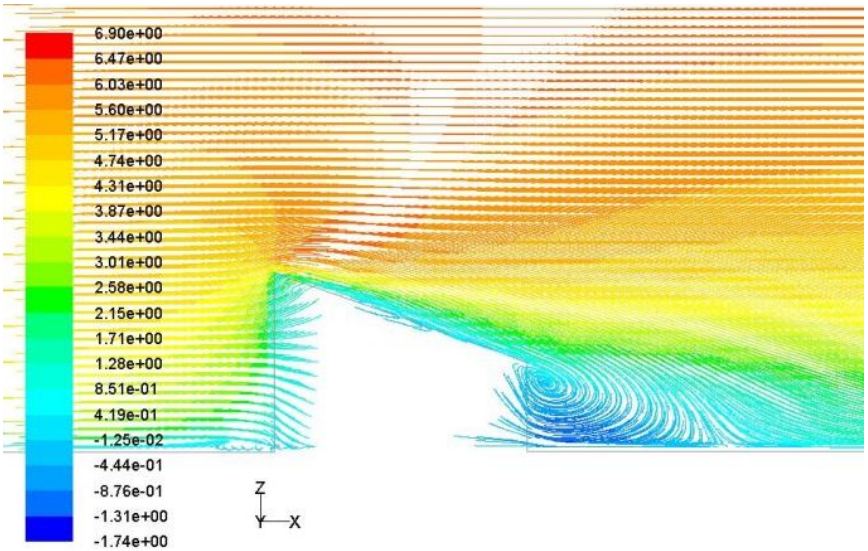

Figure 5.15 Streamwise velocity pathlines along the vertical central plan passing through the wedged roof when the wind is at a 135^0 angle.

Contrary to the case when the roof was facing the windward direction, the area of maximum acceleration was on top of the roof covering an area extending above the windward half of the roof, as for the previously mentioned case, the acceleration occurred leeward the building. Thus, it is expected in this case to find locations on top of the roof where wind turbines can be mounted to take advantage of the accelerating effect of the roof.

Turbulence intensity (TI)[10]

In terms of turbulence intensity above the wedged roof when one of the tall vertical edges is facing the wind (135^0), it was noticed that the range of maximum increase in turbulence intensity ranged between 1.4TI at W1-5 (windward lower corner) at a height of H from the ground to 2.6TI at W5-2 (on the leeward inclined edge midpoint between horizontal windward roof edge and the parallel roof centreline) at 1.14H. The vertical range of maximum recorded turbulence intensities ranged between H and 1.15H (Table 5.8). It was noticed that among all the investigated wedged roof cases, this case recorded the highest increase in turbulence intensity.

Table 5.8 Turbulence intensities values and locations for the wedged roof with wind direction 135^0.

Turbulence Intensity (TI)	Wedged
Range of maximum increase in TIs values	1.4TI to 2.6TI
Vertical range of maximum TIs locations	H to 1.15H
Location of maximum recorded TI value	W5-2 at 1.14H

Streamwise velocity[11]

Although the maximum acceleration reached 1.18U at location W2-2 (midpoint between the windward corner and the midpoint of the roof) at height 1.15H, this

[10] A complete plot of the turbulence intensity along different measurements point is included in appendix 8.

[11] A complete plot of the streamwise velocity along different measurements point is included in appendix 9.

area is characterised by high levels of turbulence, thus it is not preferable to mount wind turbines in this area. According to the reported results in Table 5.9, the range of maximum increase in streamwise velocities ranged between 1.07U at W5-1 (right corner) at 1.35H to 1.18U at W2-2 (midpoint between the windward corner and the midpoint of the roof) at 1.15H and the vertical range of maximum recorded streamwise velocities ranged between 1.15H and 1.3H. Thus, the potential mounting location is at W3-2 (midpoint between the midpoint of the horizontal windward edge and the midpoint of the roof) at 1.3H where the streamwise velocity reaches 1.14U.

Table 5.9 Streamwise velocities values and locations for the wedged roof with wind direction 135^0.

Streamwise velocity (U)	Wedged
Range of maximum increase in Us values	1.07U to 1.18U
Vertical range of maximum Us locations	1.15H to 1.3H
Location of maximum recorded U value	W2-2 at 1.15H
Maximum recorded U value above maximum turbulence area (> or equal to 1.3H)	1.14U at W3-2 at 1.3H

5.4.1.5 180^0 Wind direction

The case of the 180^0 (Figure 5.16) wind direction only applies to the wedged roof shape but since the roof shape is symmetrical along the streamwise direction axis, only measurements points on half the roof can represent the whole flow above the roof.

Apart from the main flow features that were discussed earlier and was pronounced in this case such as the division of the flow into 4 main streams, the stagnation point, the standing vortex and the leeward vortex. Figure 5.17 shows that the main feature that distinguishes this case form the previous cases is that the flow separated on top of the roof and at the leeward direction of the building resulting in the formation of a relatively big recirculation area extending from above the roof to the leeward façade of the building.

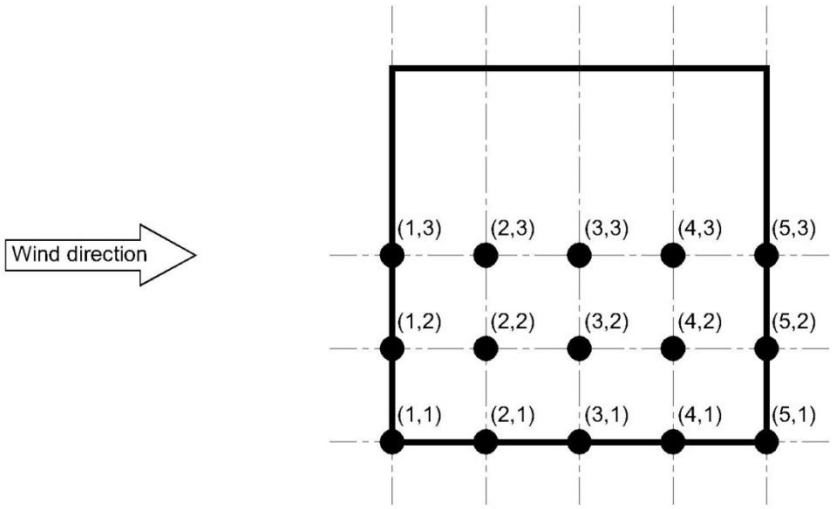

Figure 5.16 180^0 wind direction and the different measurements points on above the wedged roof.

Flow pattern

In previous cases two vortices were formed; the first one above the roof and the second one at the leeward direction of the building. In this case, these two vortices merged together to form a big vortex on top of the roof and behind the building due to the pressure difference between the roof, leeward façade and the windward façade. However, the maximum acceleration is noticed to be in the same location as the previous case above the roof in the area near the windward roof edge but higher than the previous cases, but it should be noted that due to the large recirculation area on top of the roof, a roof mounted wind turbine would suffer from high levels of turbulence.

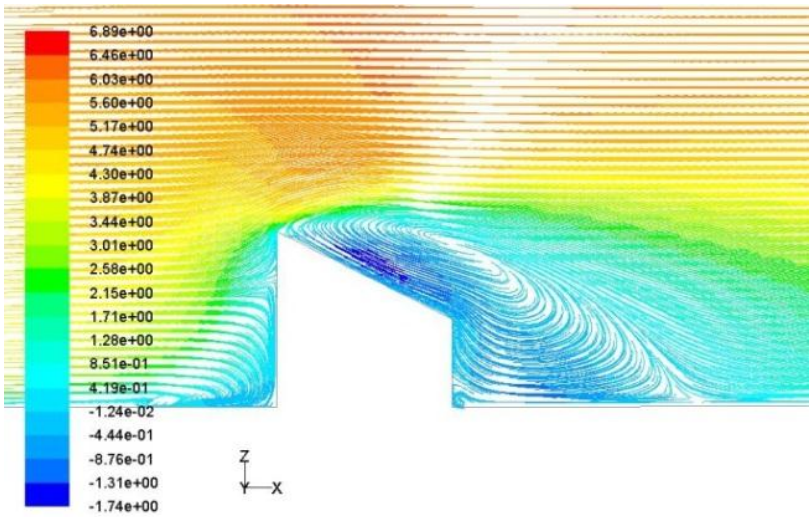

Figure 5.17 Streamwise velocity pathlines along the vertical central plan passing through the wedged roof when the wind is at a 180^0 angle.

Turbulence intensity (TI)[12]

As seen from the streamwise velocity pathlines, a large recirculation area existed above the roof and merged with the vortex in the leeward direction of the building, which indicates the existence of high levels of turbulence above the investigated roof. Table 5.10 demonstrates that among all the investigated wedge cases, this case has recorded the highest levels of turbulence whether as minimum value or maximum value. The range of maximum increase in turbulence intensities ranged between 2.24TI at W5-1 (leeward corner) at height H to 3.04TI at W4-3 (midway between roof midpoint and leeward edge midpoint) at height 1.15H, which is the same vertical range of maximum turbulence intensities locations.

Table 5.10 Turbulence intensities values and locations for the wedged roof with wind direction 180^0.

Turbulence Intensity (TI)	Wedged
Range of maximum increase in TIs values	2.24TI to 3.04TI
Vertical range of maximum TIs locations	H to 1.15H
Location of maximum recorded TI value	W4-3 at 1.15H

Streamwise velocity[13]

According to the observations from the streamwise velocity pathlines it was assumed that the maximum levels of wind acceleration would exist away from the roof. Comparing the results in Table 5.11 with the previous results for all wedged roofs cases, this is true since the vertical range of maximum streamwise velocity falls between 1.4H and 1.75H. As for the accelerating effect, it ranged between1.03U at W1-3 (midpoint of the windward edge) at

[12] A complete plot of the turbulence intensity along different measurements point is included in appendix 10.

[13] A complete plot of the streamwise velocity along different measurements point is included in appendix 11.

1.75H to 1.08U at W2-1 (midway between the windward corner and the midpoint of the inclined edge) at 1.4H.

Table 5.11 Streamwise velocities values and locations for the wedged roof with wind direction 180^0.

Streamwise velocity (U)	Wedged
Range of maximum increase in Us values	1.03U to 1.08U
Vertical range of maximum Us locations	1.4H to 1.75H
Location of maximum recorded U value	W2-1 at 1.4H
Maximum recorded U value above maximum turbulence area (> or equal to 1.3H)	1.08U at W2-1 at 1.4H

Table 5.12 shows a comparison between different roof cases under different wind directions. When analysing the results in the horizontal direction of the table, it can be noticed that for the flat roof, only two cases represent the five incident wind directions, these are the 0^0 wind direction and the 45^0 wind direction, among all the cases the 45^0 wind direction registered the highest acceleration of wind which would result in an increase in the energy yield of the mounted wind turbine at that location by 40.5 % more power than a free standing wind turbine at the same location under the same flow conditions. The optimum mounting locations above the flat roof was between locations C2-3 (between the roof windward edged and the middle of the roof) (0^0) and C2-2 (midpoint between the windward roof edge and the centre of the roof) (45^0). Thus it can be assumed that areas near the middle of the roof above 1.3H would be potential mounting locations for wind turbines.

As in the case of the flat roof, all five wind directions are represented by the 0^0 wind direction and the 45^0 wind direction for the domed roof. However in this case, all maximum acceleration under different wind directions occurred at one location which is exactly above the highest point of the dome (D3-3: midpoint of the roof) at a height of 1.3H, the increase in power ranged between 40.5% and 48.2% but the maximum acceleration occurred when the wind was at a 45^0 direction. Thus, for a domed roof covering a cubicle building the optimum

mounting location for a wind turbine is exactly at the middle of the roof at a height of 1.3H under any wind direction.

Table 5.12 Comparison between different roof cases with different wind directions[14].

Wind direction	0^0	45^0	90^0	135^0	180^0
Flat Roof			0^0	45^0	0^0
Location of maximum recorded U value above 1.3H	C2-3	C2-2	C2-3	C2-2	C2-3
Vertical location	1.45H	1.3H	1.45H	1.3H	1.45H
Maximum recorded U value above 1.3H	1.095U	1.12U	1.095U	1.12U	1.095U
Percentage of increase in power	31.3%	40.5%	31.3%	40.5%	31.3%
Domed Roof			0^0	45^0	0^0
Location of maximum recorded U value above 1.3H	D3-3	D3-3	D3-3	D3-3	D3-3
Vertical location	1.3H	1.3H	1.3H	1.3H	1.3H
Maximum recorded U value above 1.3H	1.12U	1.14U	1.12U	1.14U	1.12U
Percentage of increase in power	40.5%	48.2%	40.5%	48.2%	40.5%
Gabled Roof				45^0	0^0
Location of maximum recorded U value above 1.3H	G5-1	G3-5	G2-3	G3-5	G5-1
Vertical location	1.6H	1.4H	1.3H	1.4H	1.6H
Maximum recorded U value above 1.3H	1.05U	1.09U	1.075U	1.09U	1.05U

[14] Shaded black is the maximum recorded value and shaded dark grey is the minimum recorded value.

Wind direction	**0^0**	**45^0**	**90^0**	**135^0**	**180^0**
Percentage of increase in power	15.8%	29.5%	24.2%	29.5%	15.8%
Pyramidal Roof			0^0	45^0	0^0
Location of maximum recorded U value above 1.3H	P4-2	P4-4	P4-2	P4-4	P4-2
Vertical location	1.3H	1.3H	1.3H	1.3H	1.3H
Maximum recorded U value above 1.3H	1.05U	1.08U	1.05U	1.08U	1.05U
Percentage of increase in power	15.8%	26%	15.8%	26%	15.8%
Barrel vaulted Roof				45^0	0^0
Location of maximum recorded U value above 1.3H	V3-3	V3-3	V2-2	V3-3	V3-3
Vertical location	1.3H	1.3H	1.35H	1.3H	1.3H
Maximum recorded U value above 1.3H	1.16U	1.14U	1.083U	1.14U	1.16U
Percentage of increase in power	56.1%	48.2%	27%	48.2%	56.1%
Wedged Roof					
Location of maximum recorded U value above 1.3H	W5-1	W5-5	W2-4	W3-2	W2-1
Vertical location	1.45H	1.3H	1.3H	1.3H	1.4H
Maximum recorded U value above 1.3H	1.03U	1.07U	1.075U	1.14U	1.08H
Percentage of increase in power	9.3%	22.5%	24.2%	48.2%	26%

For the gabled roof case, the 0^0, 45^0 and 90^0 cases represent all the five wind directions as the 135^0 and the 180^0 wind directions are represented by the 45^0

and the 0^0 wind directions respectively. Among all the cases, the maximum accelerating effect occurred when the wind was at 45^0 wind direction and the expected increase in energy yield would reach 29.5% more power than a free standing wind turbine at the same location under the same flow conditions, the optimum mounting location is at location G3-5 (midpoint along the leeward inclined edge) at a height of 1.4H. It was noticed that the optimum mounting location changes over the gabled roof with the change in wind direction as well as the accelerating effect. More potential mounting locations are found near the edges of the building.

The pyramidal roof is the least among all investigated roof shapes in terms of accelerating wind under different wind directions since the maximum expected increase in power would reach 26% which is the least increase in power among all the investigated cases. This value was registered at location P4-4 (on the roof streamwise axis between the midpoint of the roof and the leeward corner) at a height of 1.3H when the wind was at an angle of 45^0. This case and the 0^0 case represent all five wind directions for the pyramidal roof as in the flat and domed roofs cases. It is noticed that for all cases, the optimum mounting location for a wind turbine on top of a pyramidal roof is near the leeward edge of the roof at height of 1.3H.

As in the case of the gabled roof, the case of the barrel vaulted roof, the 0^0, 45^0 and 90^0 cases represent all the five wind directions as the 135^0 and the 180^0 wind directions are represented by the 45^0 and the 0^0 wind directions respectively. But contrary to the case of the gabled roof, potential mounting locations on top of the barrel vaulted roof is consistent throughout all wind directions as the optimum mounting location is at location V3-3 (midpoint of the roof) at 1.3H for all cases except for the 90^0 wind direction where the optimum mounting location occurred at V2-2 (midpoint between the windward roof edge and the centre of the roof) at height 1.35H which also can be considered within the middle area above the vaulted roof. However, the maximum accelerating effect registered when the wind was parallel to the roof profile (0^0) as the expected increase in energy yield reached 56.1% more than a free standing wind turbine at the same location under the same flow conditions. Among all the barrel vaulted roof cases, the 90^0 case registered the lowest accelerating effect

corresponding to only 27% more power. Thus, when wind is perpendicular to an isolated vaulted building, it is not expected to cause the wind to be accelerated as in the cases of other wind directions.

The wedged roof is the only case where all wind directions needed to be investigated as each wind direction represents a unique interaction between the wind and the geometry of the building. It was noticed that for each wind direction, the maximum acceleration and accordingly the potential optimum mounting location differed from one direction to another. However, it was noticed that for all cases except the 135^0 case, the accelerating effect was low compared to other roof cases which, when looking at the streamwise velocity pathlines, can be attributed to the fact that the maximum accelerating effect occurs leeward of the building. As for the 135^0 case, the maximum accelerating effect occurred at location W3-2 (midpoint between the midpoint of the horizontal windward edge and the midpoint of the roof) at height 1.3H and the wind turbine to be mounted at that location would yield 48.2% more power than a free standing wind turbine at the same location under the same flow conditions. Thus, since the case of the 135^0 is the only case where the wind is accelerated above the roof, it can be argued that only when the wind is flowing at an angle of 135^0 to a gabled roof isolated building, a roof mounted wind turbine can considerably benefit from the accelerating effect of the building. Otherwise, when wind is flowing at other wind directions, free standing ground mounted wind turbine higher than the gabled roof located at the leeward direction of the building might benefit from the accelerating effect of the gabled roof.

5.4.2 *Optimum roof shape and building height*

Since the simulation results has shown that the barrel vaulted roof shape is the optimum roof shape for roof mounting wind turbines under a wind direction which is parallel to the roof profile (0^0), both the barrel vault and the 0^0 wind direction were chosen for investigating other variables affecting wind flow above the roof. The other variables are the building height and the surrounding urban configuration. In this section wind flow around a 12m and 24m barrel vaulted buildings are investigated and compared to the 6m high case to identify the effect of varying the height of the building on the turbulence intensity and the

streamwise velocity on top of the barrel vaulted roof and its effect on specifying the mounting location of the wind turbine and accordingly the increase in its power output compared to a free standing wind turbine at the same location under the same flow conditions.

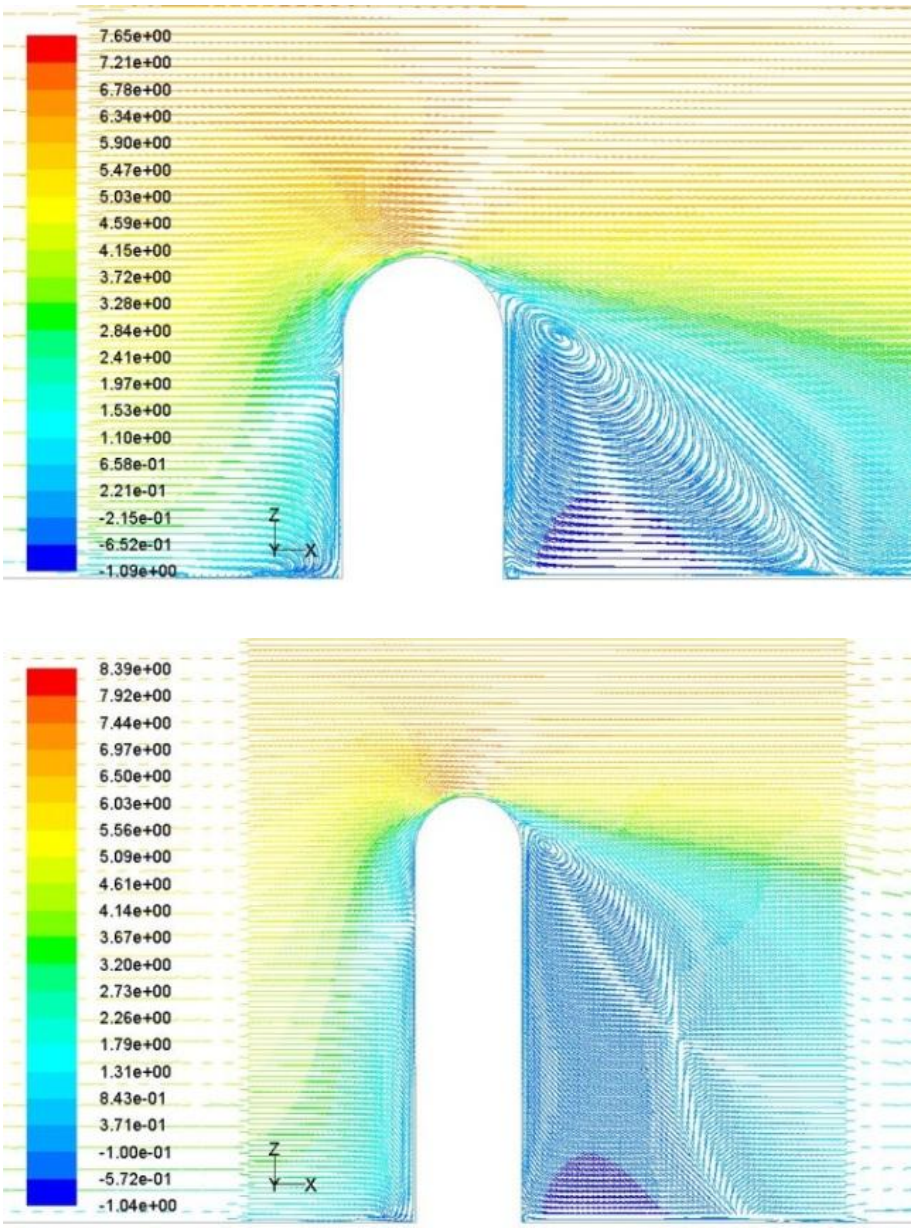

Figure 5.18 Streamline velocity pathlines along the central vertical axis for the 12m vaulted buildings (top) and the 24m vaulted building (bottom).

In the 12m barrel vaulted building case a domain whose dimensions 315 x 132 x 72m is used to simulate wind flow around the studied case which resulted in a blockage ratio of 0.3% which is less the than the maximum recommended

blockage ratio[15]. In the 24m barrel vaulted building case a domain with dimensions 504 x 264 x 144 is used to simulate wind flow around the studied case which resulted in a blockage ratio of 0.1% which is also less than the maximum recommended blockage ratio of 3%. The flow variables are measured from directly above the roof to a distance of 9m (the vertical distance where the building has an effect on the wind flow field above it).

Figure 5.18 shows the streamwise velocity pathlines for both cases, where the main flow features are similar to each other and the 6m vaulted roof case. The flow was attached to the roofs surfaces and only separated at the leeward direction of the building, the stagnation point was formed at the same location at a height of 2/3 of the building height in all cases and the standing vortex in front of the windward façade was formed at the same location for all three cases. As for the vortex leeward the building, both the 6m case and the 12m exhibit the same pattern except for the reattachment length which is larger for the 12m case than the 6m case which suggests that there is a relation between the building height and the reattachment length leeward the building. For the 12m case the leeward vortex was formed at the same location with respect to the building roof, however the recirculation area did not reach the ground as it interfered with another backflow area which was formed near the ground due to the pressure difference between the leeward and the windward areas of the building. But it can be argued that this behaviour did not affect the flow pattern on top of the roof.

Plotting both the turbulence intensities and the streamwise velocities along the 15 measurements points along the roof for the 12m and 24m barrel vaulted buildings[16], it was noticed that the same flow patterns were consistent among both cases and when compared to the 6m case since the maximum turbulence intensity occurred at the same location of V2-3 (between the roof windward edged and the middle of the roof) and the maximum streamwise velocity occurred at the same location of V3-3 (midpoint of the roof). However, when comparing the values at both locations for the three cases, Figure 5.19 shows

[15] Refer to chapter three for the recommendations on the computational domain dimensions.

[16] Refer to appendences 12, 13, 14 and 15 for a complete set of plots for the turbulence intensities and streamwise velocities for both cases.

that there was an increase in the turbulence intensity with the increase in the height of the building which suggests that there is a relationship between the building height and the turbulence intensity. Which is confirmed by Jha (2010) who noted that turbulence within the built environment is highly dependent on buildings heights, the higher the building height the more turbulence will be generated.

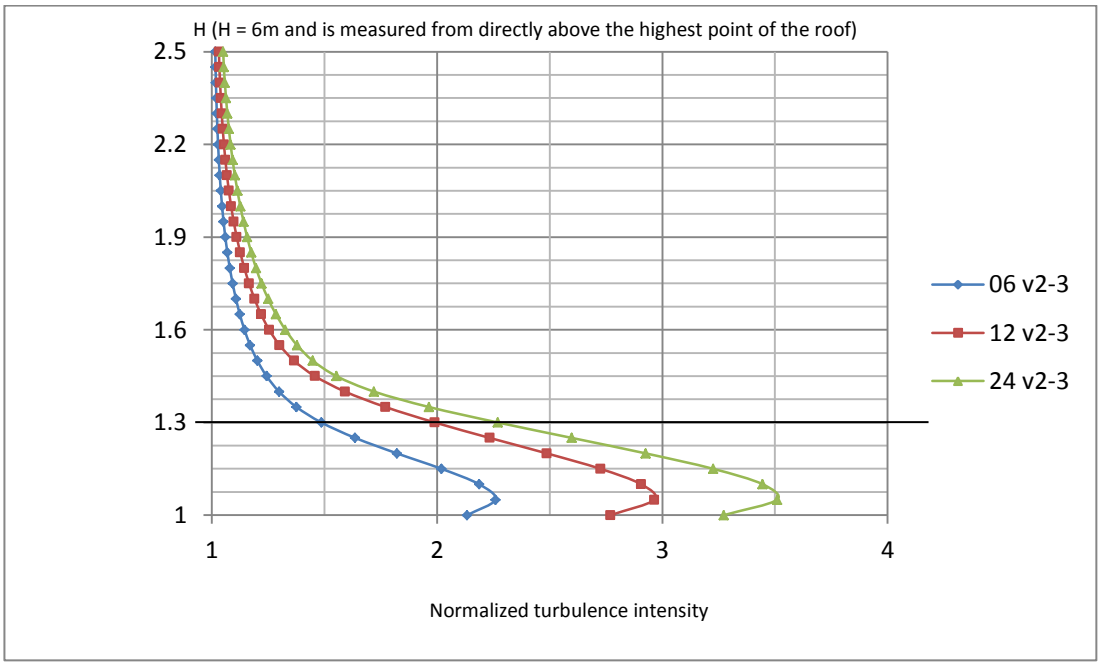

Figure 5.19 Comparison between the maximum recorded turbulence intensities at location v2-3 for the 3 heights.

However, it was noticed that the locations of the maximum recorded turbulence intensities were consistent across the three investigated heights; for the three cases, the maximum recorded turbulence intensities occurred at the midpoint of the barrel vaulted roof at a height of 0.3m above the highest point of the roof which suggests that location of maximum turbulence intensity above an isolated barrel vaulted roof building is independent of the building height. Other variables might affect the location of the maximum recorded turbulence intensity such as the width and the length of the roof. It should be noted that the recommendations from the Encraft Warwick Wind Trials Project (Encraft, 2009) and the WINEUR (2007) report relates the position of maximum turbulence areas with the building height (30% and 35% - 50% of the building height respectively). However, both projects depended on in-situ measurements for assessing wind resources at locations of urban wind turbines, but, there was no

clear information about how the turbulence data was collected, especially when the anemometers used are conventional cub anemometers known for their limitations in capturing turbulence; ultrasonic anemometers are required for registering turbulence. Thus, research is needed in this area to identify whether or not this relationship exists. In light of the obtained results in this work, building height affects the value of turbulence above the roof (with the increase in building height, turbulence intensity increase) while it does not affect the location where the turbulence occurs.

As for the streamwise velocity, Figure 5.20 shows that the accelerating effect of the building was consistent among the three cases above the height of 1.2H where the acceleration increased with the increase in height, but from the highest point of the roof to that height the same pattern applied to the 12m and the 24m cases but for the 6m case the pattern was different, which suggests that the ground roughness had an effect on the streamwise velocity. The used roughness length in all three cases was equal to 0.03m which corresponds to nearly flat or gently undulating countryside.

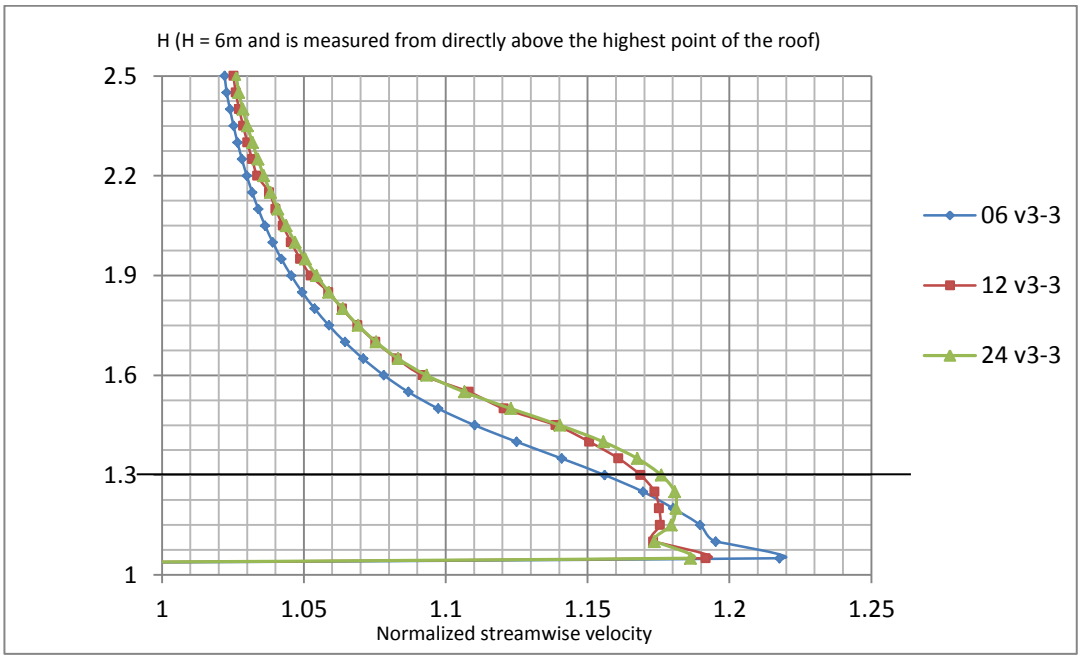

Figure 5.20 Comparison between the maximum recorded velocities at location v3-3 for the 3 heights.

Although this is considered low roughness, Figure 5.20 shows that it had an effect on the accelerating effect above the 6m barrel vaulted building and this effect decreased with the increase of the building height. For all three cases, the

maximum streamwise velocity occurred at the same location (V3-3: roof midpoint at height 1.3H), the 6m case registered a maximum streamwise velocity of 1.16U which corresponds to an increase in energy yield of 56.1%, the 12m case registered 1.17U which corresponds to an increase in energy yield of 60.1%, as for the 24m case, it registered 1.17U which correspond to an increase in energy yield of 64.3%. Thus, it can be argued that a roof mounted wind turbine on top of higher buildings will be introduced to more wind acceleration and accordingly would capture more power from the wind.

These results were in accordance with those from Reiter (2010) who found that the accelerating effect above the building is highly dependent on the building height and independent of building length. Several simulations were carried out with different buildings heights and constant length and width and it was noticed that the acceleration effect increases with the increase in the building height. Other simulations were carried out varying building's length and fixing building height and the results were not changing. Thus, it was confirmed that building height is a key parameter influencing the accelerating effect around a single building: the higher the building, the more the accelerating effect.

5.4.3 *Different urban configurations and different building's height*

Although the isolated building case can be encountered in rural areas and non-urban environments, the most common case is the building where a roof mounted wind turbine is proposed is to be within an urban context. The wind flow around a roof mounted wind turbine within an urban environment will be affected by the variables within the built environment. One of these variables is the urban configuration surrounding the building to be integrating a roof mounted wind turbine.

In this section, two urban configurations are used to examine the effect of urban configuration on the energy yield and positioning of a roof mounted wind turbine. These configurations are a street canyon urban configuration and a staggered urban configuration whose buildings heights are 6m and the spacing between the buildings are 6m in all directions. The barrel vaulted roof case with wind direction parallel to the roof profile was chosen as the study case in this section since it has proven to be the optimum roof shape for mounting wind turbines.

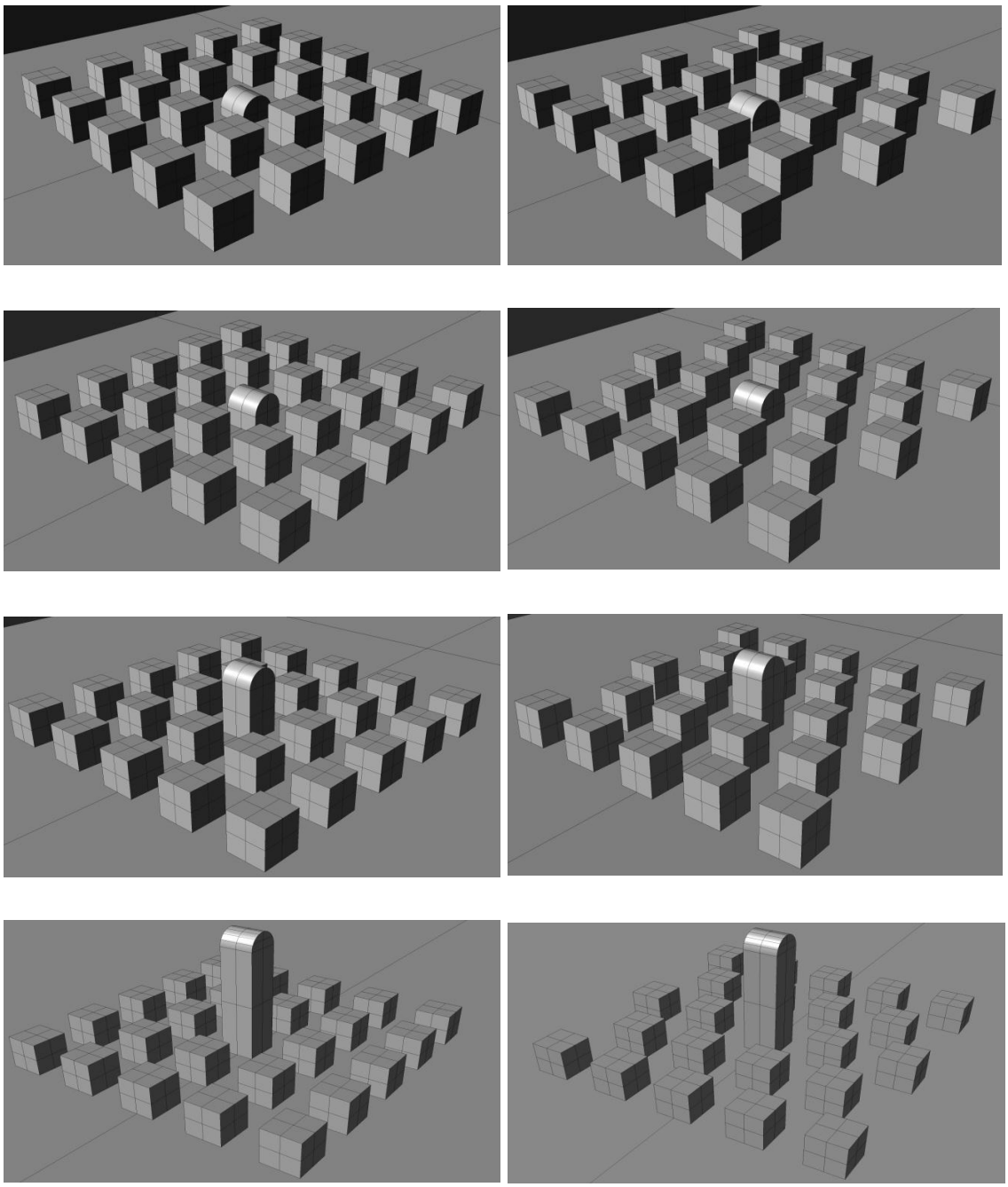

Figure 5.21 Perspectives of the investigated cases varying building height (4.5, 6, 12 & 24m from up to down) with urban canyon configuration (left) and staggered urban configuration (right).

As seen in the previous section the height of the building had an effect on wind flow above the investigated roof, thus four different heights were chosen for the barrel vaulted building to be placed within the proposed urban configurations. For the first case, the building height is less than the surrounding urban context (4.5m), the second case the building height is the same as the surrounding urban context (6m), the third and the fourth cases the buildings heights are higher than the surrounding urban context (12m and 24m respectively) (Figure 5.21).

In constructing the computational mesh, the same rules of thumb which was used and previously mentioned in earlier simulations were used maintaining a distance between the extents of the studied urban configuration and the front, the side and top boundaries which is equal to five times the height of the highest building and a distance from the leeward building in the urban configuration which is 15 times the height of the tallest building, the obtained blockage ratios for the 24m, 12m, 6m, 4.5m cases are 0.7%, 1.7%, 4.3% and 4.3% respectively. Since the blockage ratios for the 4.5m and 6m cases exceeded 3%, the domain size of the 24m case was used for all the cases to maintain a blockage ratio less than 3%.

The mesh is the same as in the 6m barrel vault case; 1.2 m spacing in the x, y and z directions away from the urban configuration and 0.3 m spacing in the x, y and z directions close to the urban configuration, except for the 24 m cases where the mesh away from the urban configuration has a resolution of 2.4 m in the x, y and z directions and the same resolution of 0.3m close to the urban configuration, this is due to the limited computational power which did not enable having a finer mesh away from the urban configuration. In order to assess the effect of coarsening the mesh away from the studied urban configuration, the mesh for the 6m vaulted building within a street canyon urban configuration was coarsened to reach 2.4m and the simulation was run and the results were compared to the fine mesh and no differences were observed. Thus, the results for the coarsened mesh away from the urban configuration in the 24m barrel vaulted building within different urban configurations were accepted.

5.4.3.1 Flow pattern

Figures 5.22 – 5.29 show the streamwise velocity pathlines for all eight investigated cases where a barrel vaulted building whose height varies between, 4.5m, 6m, 12m and 24m is placed within a street canyon urban configuration and a staggered urban configuration.

In the first case where the 4.5m vaulted building was placed within the street canyon configuration (Figure 5.22), it was noticed that flow patterns around the building differed from the case of the 6m isolated building since the standing vortex in front of the windward façade was not formed, no reattachment was

observed leeward the building but a large rotating vortex was formed whose centre was at a height of 3m from the ground, as for the stagnation point it was visible but was formed on the surface of the vault at a height of 3.75m contrary to the isolated building case where the stagnation point was located on the windward façade.

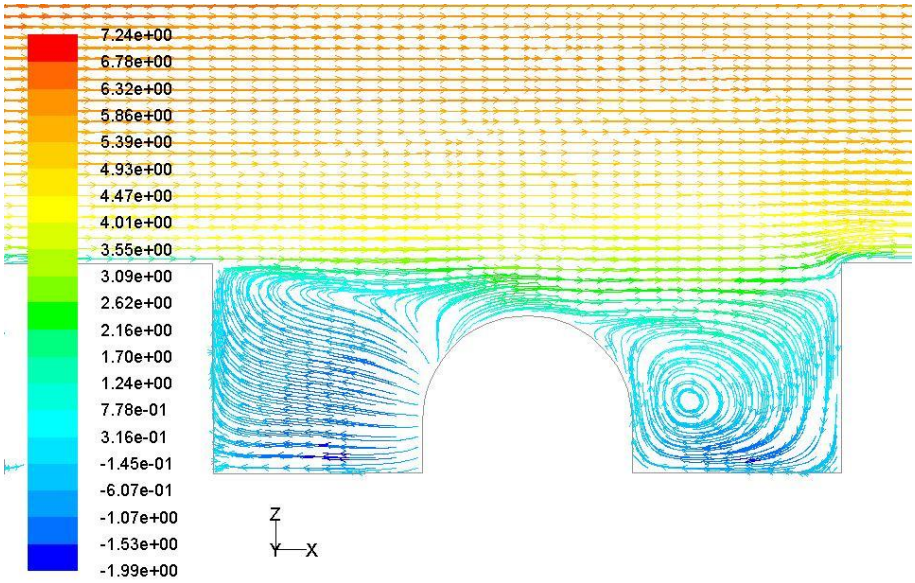

Figure 5.22 Streamwise velocity pathlines along the vertical central plan passing through the 4.5m barrel vaulted building in an urban canyon configuration.

Looking into the flow pattern above the building it can be noticed that the flow was not disturbed by the presence of the barrel vaulted roof which had a negligible effect in terms of accelerating the wind above it. The behaviour of wind in this case can be attributed to the compactness of the urban configuration as the distance between the cubes is 6m which prevents the flow from developing the usual flow patterns.

However, for the same building placed within a staggered configuration (Figure 5.23) more space (12m) is available in front of the building for the flow to develop flow patterns similar to those around an isolated building. It can be noticed that the stagnation point was formed at the same location of the isolated building at the point of intersection between the windward façade and the curvature of the roof at a height of 3m above ground. The standing vortex was clearly visible in front of the windward façade. In the leeward direction of the building a recirculation area started to develop but did not completely develop

into a rotating vortex. As for the flow above the roof, it was similar to that of the isolated building but no significant acceleration was observed.

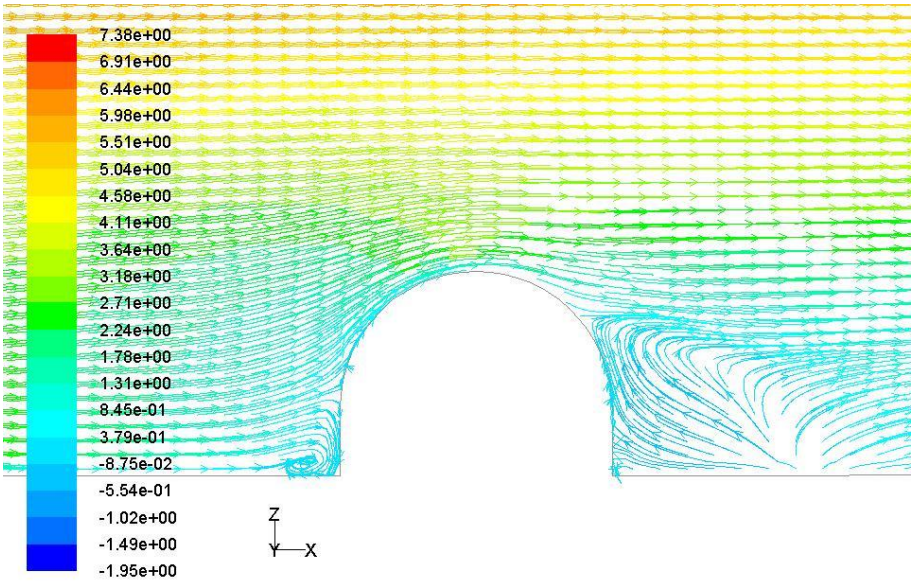

Figure 5.23 Streamwise velocity pathlines along the vertical central plan passing through the 4.5m barrel vaulted building in a staggered urban configuration.

In the case of the 6m barrel vaulted building within a street canyon urban configuration (Figure 5.24), a slight accelerating effect was noticed above the roof, which indicates that the roof had an effect on the flow above it when the building height was the same as the surrounding buildings, but this effect might not be that significant when roof mounting wind turbines, this will be determined in later section when investigating the values of streamwise velocities above each of the investigated cases.

For the rest of the flow patterns, it was noticed that the flow is similar to the 4.5m case within street urban canyon as the stagnation point was formed at the same location but at height of 5.2m above ground. At the leeward direction of the building a similar vortex was formed whose centre was at a height of 2.25m from the ground and the standing vortex was also not visible in front of the windward façade. However, the main difference was that in front of the windward façade a large recirculation area was formed which developed into a complete large vortex whose centre is at the same height of the stagnation point.

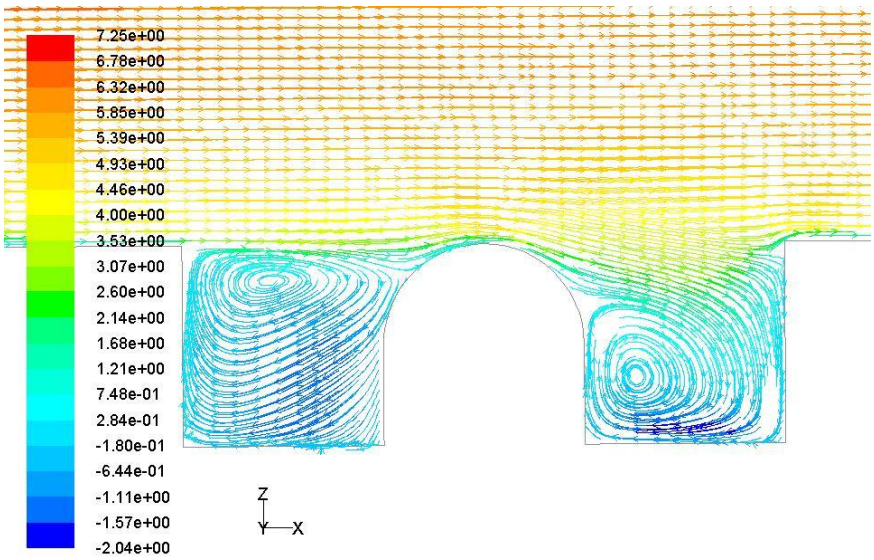

Figure 5.24 Streamwise velocity pathlines along the vertical central plan passing through the 6m barrel vaulted building in an urban canyon configuration.

As for the case of the 6m barrel vaulted building within a staggered urban configuration (Figure 5.25), the flow pattern is similar to the 4.5m barrel vaulted building placed within a staggered urban configuration case and the stagnation point is formed at the same location of the intersection between the curvature of the barrel vault and the vertical part of the building at a height of 4.5m above ground which is the same as the case of the isolated 6m barrel vaulted building. In front of the windward façade a satnding vortex fromed which is similar to the one formed in the cases of the isolated building and the 4.5m bulding within a staggered urban configuration.

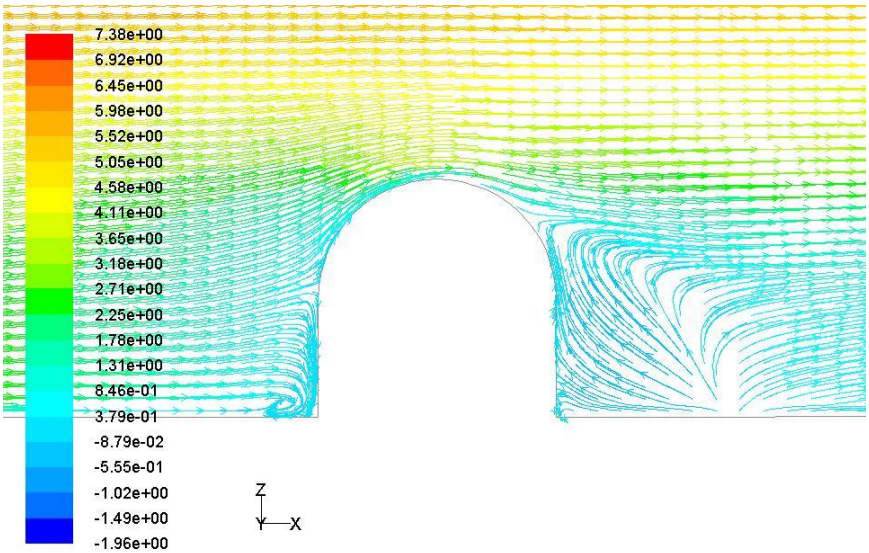

Figure 5.25 Streamwise velocity pathlines along the vertical central plan passing through the 6m barrel vaulted building in a staggered urban configuration.

As the height of the building increases the flow pattern gets closer to the case of the isolated building but not identical. This was evident in the 12m vaulted building placed within an urban canyon configuration (Figure 5.26), especially in terms of accelerating the wind above the vaulted roof as the flow was accelerated above the roof and the stagnation point was formed on the windward façade of the building but was shifted upwards to the point of intersection between the windward façade and the curvature of the vault which is at a height of 10.5m. Leeward the building, an area of back flow was formed due to the pressure difference between the windward façade and leeward façade which did not develop into a complete vortex similar to what happened in the 4.5m and 6.0m barrel vaulted buildings placed within a staggered urban configuration.

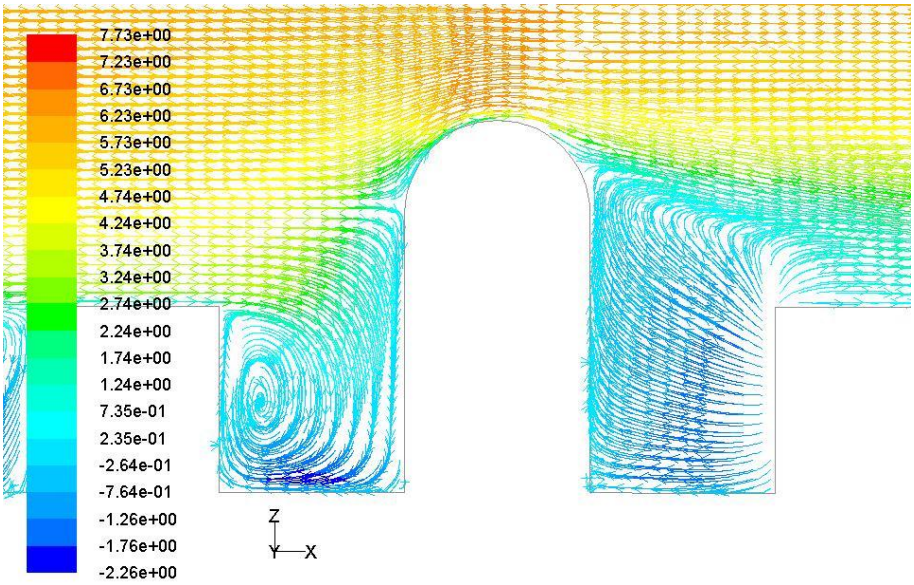

Figure 5.26 Streamwise velocity pathlines along the vertical central plan passing through the 12m barrel vaulted building in an urban canyon configuration.

For the12m barrel vaulted building placed within a staggered urban configuration (Figure 5.27), the flow pattern was similar to the case of the 12m case placed within an urban canyon configuration in terms of locations of stagnation point, recirculation area and the attachment of the flow to the surface of the barrel vaulted roof. The only difference is the formation of the standing vortex in front of the windward façade of the building due to the available space in front of the building similar to the previous staggered urban configurations cases.

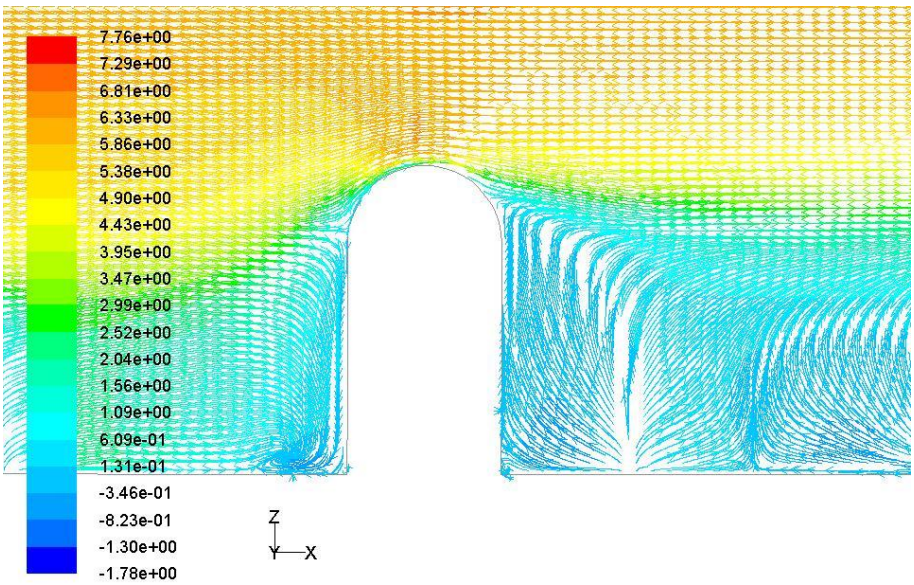

Figure 5.27 Streamwise velocity pathlines along the vertical central plan passing through the 12m barrel vaulted building in a staggered urban configuration.

The 24m cases are the closest to the isolated buildings cases in terms of the accelerating effect the barrel vaulted roofs have on the flow above them. For the 24m barrel vaulted building placed within an urban canyon configuration (Figure 5.28) the stagnation point was formed on the windward façade at a height of 18m above ground which is 2m higher than the stagnation point of the isolated building case. In addition, at the leeward direction of the building the recirculation area developed to a complete rotating vortex similar to the isolated building case, its centre was located at the same height but shifted away from the leeward façade for a distance of 4m.

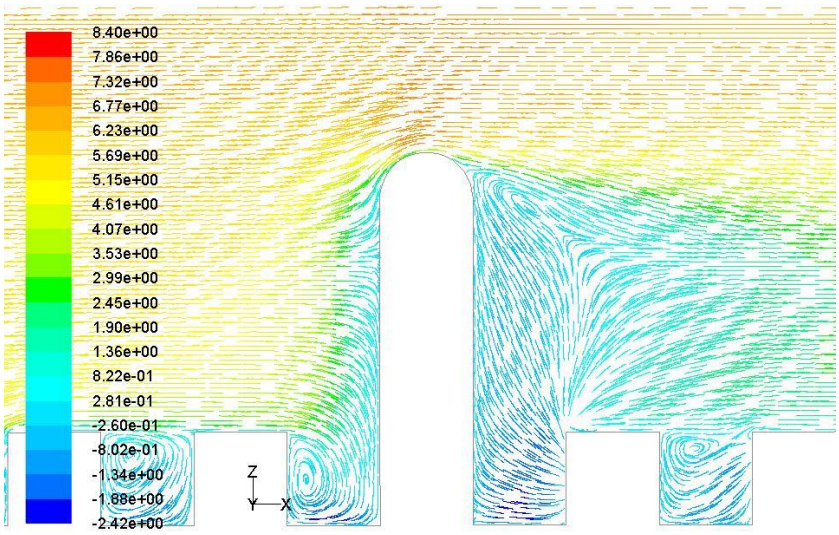

Figure 5.28 Streamwise velocity pathlines along the vertical central plan passing through the 24m barrel vaulted building in an urban canyon configuration.

The main difference was the absence of the standing vortex in front of the windward façade, instead a big vortex was formed next to the adjacent windward building similar to the ones formed in the previous 6m and 12m barrel vaulted building placed within urban canyons configurations cases. As for the 24m barrel vaulted building placed within a staggered urban configuration (Figure 5.29), all the flow features were the same as the 24m urban canyon case except for the backward flow in the leeward direction of the building which did not develop into a complete vortex.

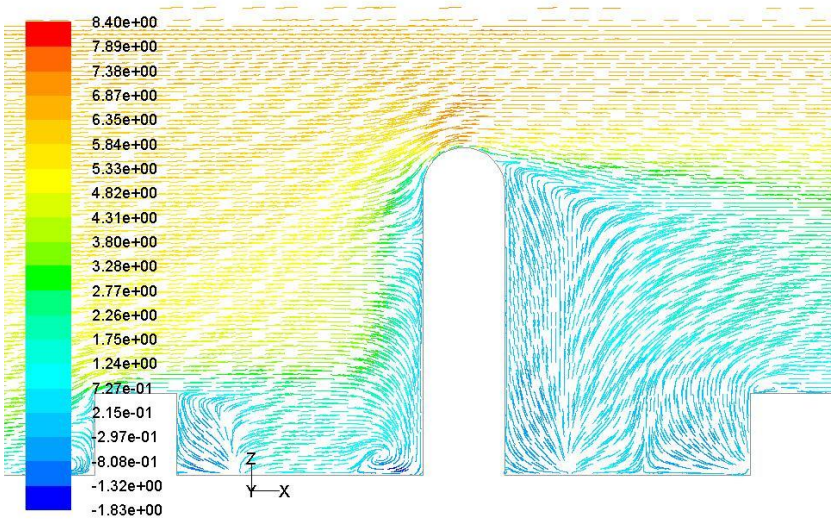

Figure 5.29 Streamwise velocity pathlines along the vertical central plan passing through the 24m barrel vaulted building in a staggered urban configuration.

5.4.3.2 Turbulence intensity[17]

Table 5.13 reports different values of increase in turbulence intensities above the investigated barrel vaulted buildings with heights 4.5m, 6m, 12m and 24m placed within both street urban canyon configuration and staggered urban configuration. It is noticed that with the increase in building height, whether placed within an urban canyon configuration or a staggered urban configuration, the turbulence intensity increases. The only case which is outside this pattern is the 4.5m canyon case (2.02TI), however it is still very close to the 4.5m staggered case (1.94TI) and the 6m canyon case (1.95TI).

For all the heights, except the 4.5m height, the staggered urban configuration caused more turbulence above the investigated roofs than the street urban

[17] For a complete set of plots for the turbulence intensities, refer to appendences 16 to 23.

canyon configuration. For the 4.5m and the 6m cases the high turbulence areas extended to a height of 1.36H as for the 12m and 24m cases the highest turbulence areas did not exceed the height of 1.15H and in all cases the location of maximum turbulence intensity was near the middle of the roof (V2-3 or V2-2) except for the 4.5m staggered case where that location was at V1-3 (midpoint of the windward edge).

Table 5.13 Different turbulence intensities on top of the barrel vaulted building with heights 4.5m, 6m, 12m and 24m placed within both street urban canyon configuration and staggered urban configuration.

Turbulence Intensity (TI)	4.5m Canyon	4.5m Staggered	6m Canyon	6m Staggered	12m Canyon	12m Staggered	24m Canyon	24m Staggered
Range of maximum increase in TIs values	1.42TI to 2.02TI	1.83TI to 1.94TI	1.48TI to 1.95TI	1.92TI to 2.12TI	2.05TI to 2.72TI	2.11TI to 2.74TI	2.58TI to 3.50TI	2.60TI to 3.50TI
Vertical range of maximum TIs locations	H to 1.36H	1.25H to 1.35H	1.05H to 1.30H	H to 1.30H	H to 1.15H	H to 1.10H	H to 1.15H	H to 1.15H
Location of maximum recorded TI value	V2-3 at H	V1-3 at 1.25H	V2-3 at 1.05H	V2-3 at 1.10H	V2-2 at 1.10H	V2-2 at 1.05H	V2-3 at 1.05H	V2-3 at 1.05H

Comparing the results for each building height with the isolated building case, the building placed within an urban canyon configuration and the building placed within a staggered urban configuration, the effect of the urban configuration on the turbulence intensity above the barrel vaulted roof can be identified.

Figure 5.30 shows the normalised turbulence intensity at the locations of maximum recorded turbulence intensities for both the urban canyon case and the staggered urban case for the 4.5m barrel vaulted building. It is noticed that the location of the maximum increase in TI is different for both cases which

indicates that the surrounding urban configuration had an effect on wind flow above the barrel vaulted roof when it is lower than the surrounding urban context which overcame the roof shape effect on turbulence intensity. It is also noticed that the two curves do not follow the same pattern in the region close to the barrel vaulted roof which indicates that the turbulence produced by the two urban configurations are different in the vicinity of the buildings.

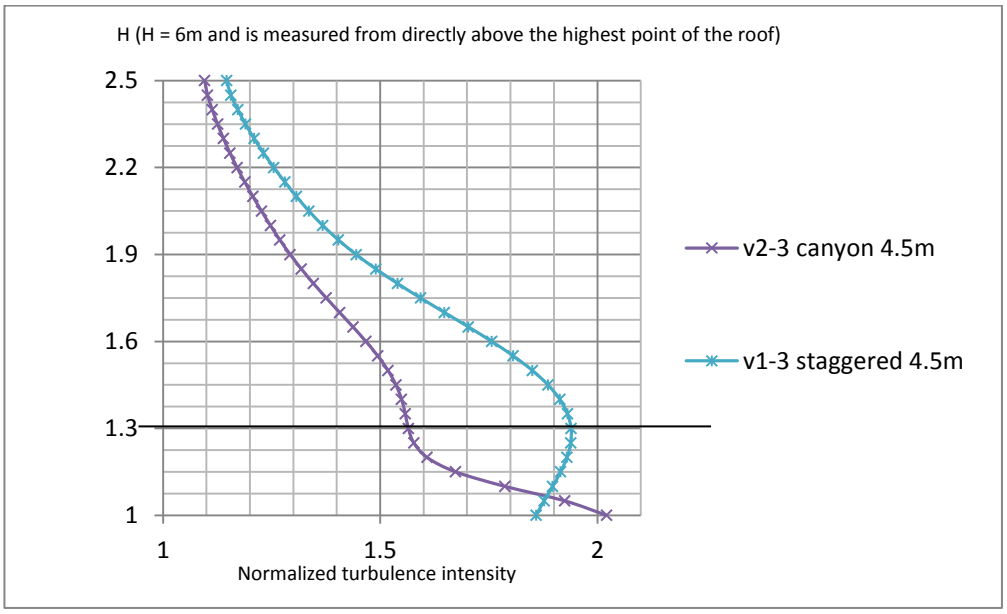

Figure 5.30 Maximum normalized turbulence intensity above the 4.5m vaulted building within an urban canyon configuration and a staggered urban configuration.

For the case of the 6m barrel vaulted building, it can be noticed from Figure 5.31 that the three curves for the isolated 6m barrel vaulted building case, the 6m barrel vaulted building within an urban canyon configuration and the 6m vaulted building within a staggered urban configuration, the three cases do not follow the same pattern near the roof. It is also noteworthy to mention that the location for maximum recorded turbulence intensity was the same for both urban configurations but differed from the isolated building case which indicates that both configurations had an effect on the wind flow above the building but not a significant effect since all locations are near the middle of the roof.

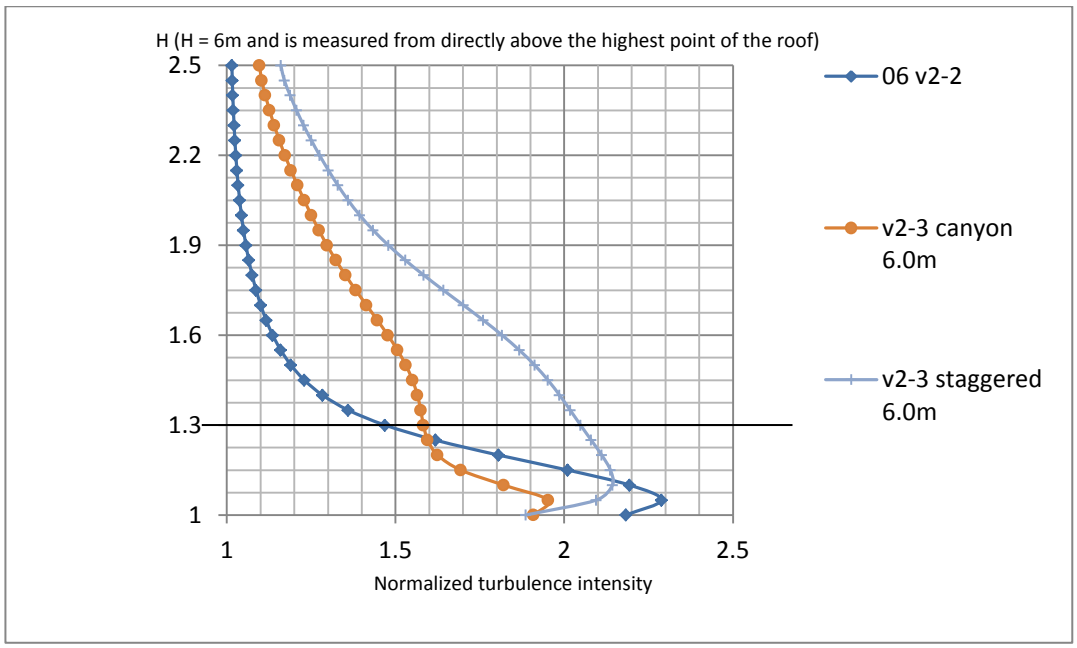

Figure 5.31 Maximum normalized turbulence intensity above the 6m vaulted building for the isolated building, within an urban canyon configuration and a staggered urban configuration.

In the 12m barrel vaulted building case for the three cases, Figure 5.32 shows more consistency in the pattern of the normalized turbulence intensities curves, both the staggered and the urban canyon configurations are almost identical, in terms of values and location, which means that the urban configuration had a negligible effect on the TI above the barrel vaulted 12m building. However, when comparing both cases with the isolated building case it was noticed that the pattern of increase in TI is similar in the three cases but the increase in TI above the isolated building is more than in the urban configuration cases.

This might be attributed to the ground roughness surrounding the studied building. Also, the locations differed between the urban cases and the isolated building case, although all locations were within the middle area of the roof. Thus, it can be argued that the surrounding urban context had an effect on the TI above the barrel vaulted building but this effect cannot be linked with the type of urban configuration surrounding the studied building of height 12m.

As for the case of the 24m barrel vaulted building for the three cases, Figure 5.33 shows that the three cases are almost the same in terms of values and locations for the normalized turbulence intensities. All TIs reached their maximum at a height of 1.05H at location V1-3 (midpoint of the windward edge)

which indicates that the urban context of a 24m barrel vaulted roof building has almost a negligible effect on TI above it.

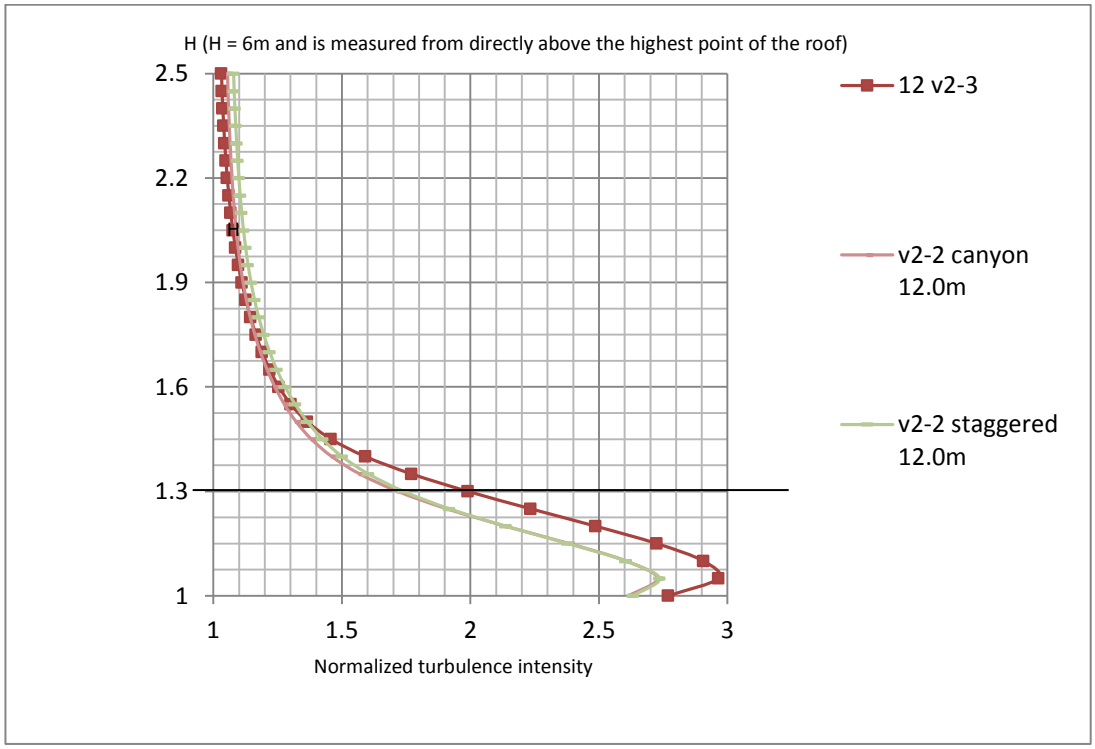

Figure 5.32 Maximum normalized turbulence intensity above the 12m vaulted building for the isolated building, within an urban canyon configuration and a staggered urban configuration.

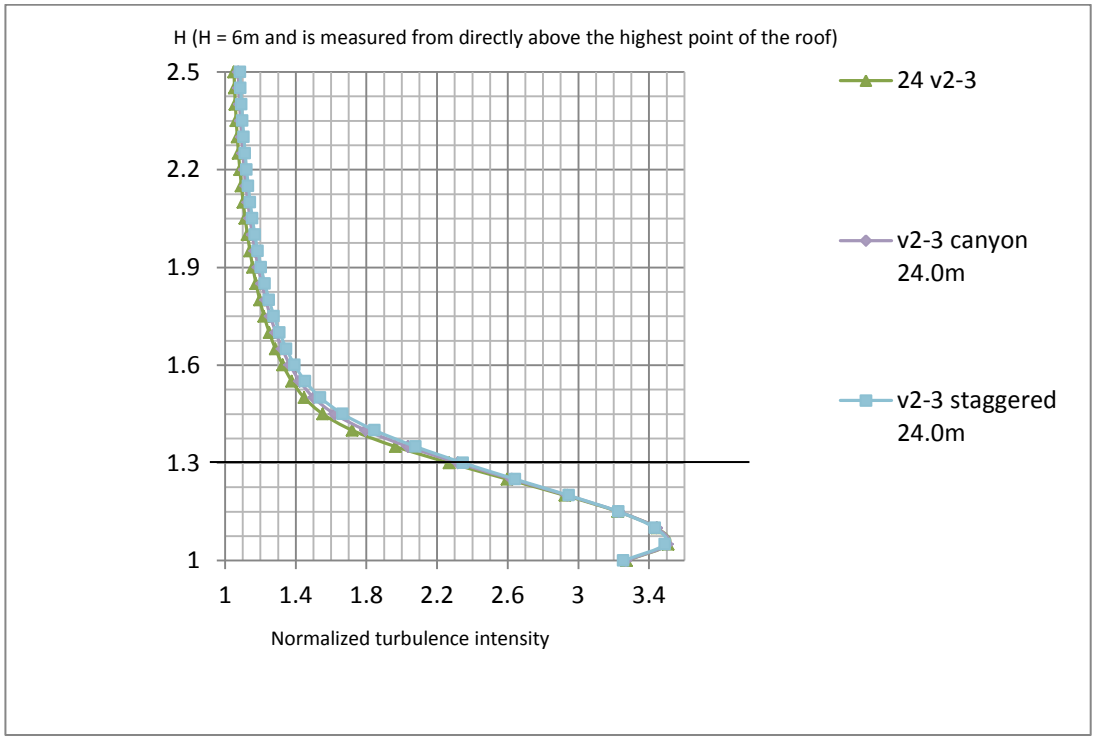

Figure 5.33 Maximum normalized turbulence intensity above the 12m vaulted building for the isolated building, within an urban canyon configuration and a staggered urban configuration.

5.4.3.3 Streamwise velocity[18]

Table 5.14 reports the results of the normalized streamwise velocities at different locations for the 4.5m, 6m, 12m and 24m barrel vaulted building placed within both street urban canyon configuration and staggered urban configuration. It can be noticed a consistency in results for two groups of cases; the first group is the 4.5m and 6m cases and the second group is the 12m and the 24m cases.

For the first group, the increase in streamwise velocity was kept to a minimum as it ranged between no acceleration to 1.09U and both the urban canyon and staggered urban configurations registered very close values at the same measurement points in terms of height and locations. For the second group (12m and the 24m cases), the location of maximum recorded streamwise velocity above 1.3H was recorded at the same location (V3-3: midpoint of the roof) at 1.3H but the values changed between the two cases as the 12m vaulted building within an urban canyon case registered 1.13U while the 24m case registered 1.15U. For the staggered configuration cases the same pattern was recorded in terms of lower recorded streamwise velocity for the 12m case (1.10U) compared to the 24m case which registered 1.13U.

Comparing the results of the acceleration on top of the investigated roof case within a staggered urban configuration to the investigated roof case within an urban canyon configuration it was noticed that the staggered configuration case registered lower acceleration (1.10U and 1.13U) than the urban canyon configuration cases (1.13U and 1.15U) for both the 12m and the 24m barrel vaulted building. Both the 24m two cases have registered higher values (1.15U and 1.13U) than the 12m two cases (1.13U and 1.10U), which indicates that with the increase in height the accelerating effect is more pronounced.

Comparing the results for each building height for the isolated building case, the building placed within an urban canyon configuration and the building placed within a staggered urban configuration, the effect of the urban configuration on the streamwise velocity above the barrel vaulted roof can be identified. Figure 5.34 shows the normalised streamwise velocities at the locations of maximum

[18] Refer to appendences 24 to 31 for a complete set of plots for the streamwise velocities.

recorded streamwise velocities for both the urban canyon case and the staggered urban case for the 4.5m barrel vaulted building in comparison with the 6m vaulted isolated building case.

Table 5.14 Different streamwise velocities on top of the barrel vaulted building with heights 4.5m, 6m, 12m and 24m placed within both street urban canyon configuration (Cany.) and staggered urban configuration (Stag.).

Streamwise velocity	4.5m Canyon	4.5m Staggered	6m Canyon	6m Staggered	12m Canyon	12m Staggered	24m Canyon	24m Staggered
Range of maximum increase in Us	1.0U[19] to 1.07U	1.00U to 1.09U	1.00U to 1.07U	1.00U to 1.09U	1.02U to 1.17U	1.03U to 1.12U	1.02U to 1.15U	1.02U to 1.14U
Vertical range of maximum Us	1.55H to 2.50H	1.75H to 2.50H	1.50H to 2.50H	1.75H to 2.50H	1.05H to 2.0H	1.05H to 2.0H	1.25H to 1.60H	1.25H to 1.60H
Location of maximum recorded U	Same at all locations 1.07U 2.5H	Same at all locations 1.09U 2.5H	Same at all locations 1.07U 2.5H	Same at all locations 1.09U 2.5H	V3-3 1.05H	V3-3 1.05H	V3-3 1.25H	V3-3 1.25H
Maximum recorded U above maximum turbulence area	Same at all locations 1.07U 2.5H	Same at all locations 1.09U 2.5H	Same at all locations 1.07U 2.5H	Same at all locations 1.09U 2.5H	1.13U at V3-3 1.3H	1.10U at V3-3 1.3H	1.15U at V3-3 1.3H	1.13U at V3-3 1.3H

[19] U is the streamwise velocity.

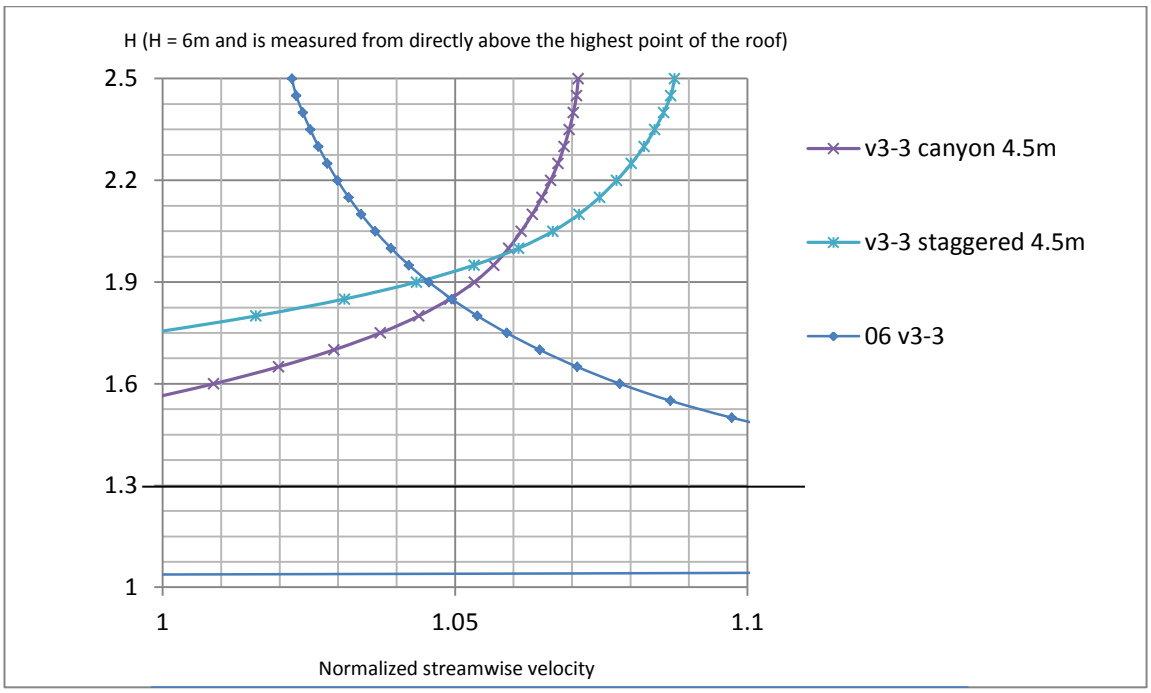

Figure 5.34 Maximum normalized streamwise velocity above the 4.5 vaulted building within an urban canyon configuration and a staggered urban configuration in comparison with the isolated 6m vaulted building case.

It is noticed that the increase in streamwise velocity is very low in both cases compared to the isolated 6m barrel vaulted building which means that both staggered and urban configurations reduced the accelerating effect of the barrel vaulted roof shape. The maximum streamwise velocity for both cases were recorded at the same location (middle of the roof at V3-3) which might be attributed to the symmetry of both configurations and not necessarily due to the roof effect of the vault since the locations of maximum recorded turbulence intensities were different for both cases.

For the 6m barrel vaulted building case, Figure 5.35 shows a comparison between the three cases; the isolated building case, the building within an urban canyon configuration and the building within a staggered urban configuration. It was noticed again that all maximum values occurred at the same location (middle of the roof at V3-3). However the three patterns were different from each other; both the urban canyon and the staggered urban configurations were similar to the previous two cases of the 4.5m but the pattern of the isolated 6m building case is different from both cases which suggests that the placement of the building within an urban configuration would have an effect on the streamwise velocity above the roof when the building height is the same as the

surrounding urban context. The maximum recorded streamwise velocity for the urban canyon case and the staggered urban configuration case were 1.07U and 1.09U respectively corresponding to 22.5% and 29.5% increase in power respectively, while for the isolated building case, it reached 1.16U which corresponds to 56.1% increase in power.

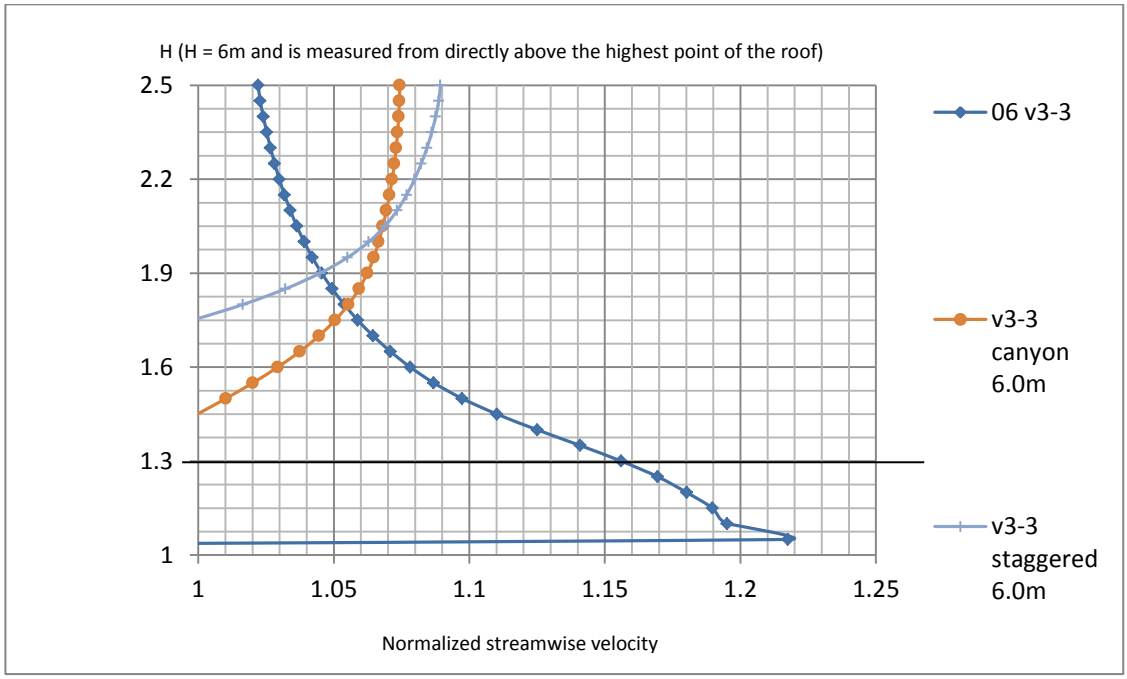

Figure 5.35 Maximum normalized streamwise velocity above the 6m vaulted building for the isolated building, within an urban canyon configuration and a staggered urban configuration.

Increasing the height to 12m, Figure 5.36 shows that all three cases benefited from the accelerating effect of the barrel vaulted roof shape. Above 1.3H, the isolated building recorded the maximum increase in streamwise velocity (1.15U) which corresponds to 52% increase in power then the barrel vaulted building within urban canyon configuration (1.13U) which corresponds to 44% increase in power and then the barrel vaulted building within staggered urban configuration (1.10U) which corresponds to 33% increase in power. The location of the maximum increase in streamwise velocities is the same for all cases but the values are different. This means that the surrounding urban configuration affected wind acceleration above the 12m barrel vaulted roof. However, when comparing the effect of the surrounding urban configuration on a 12m vaulted building to the effect on the 4.5m and the 6m vaulted buildings, it can be noticed that the effect decreased with the increase in the building height.

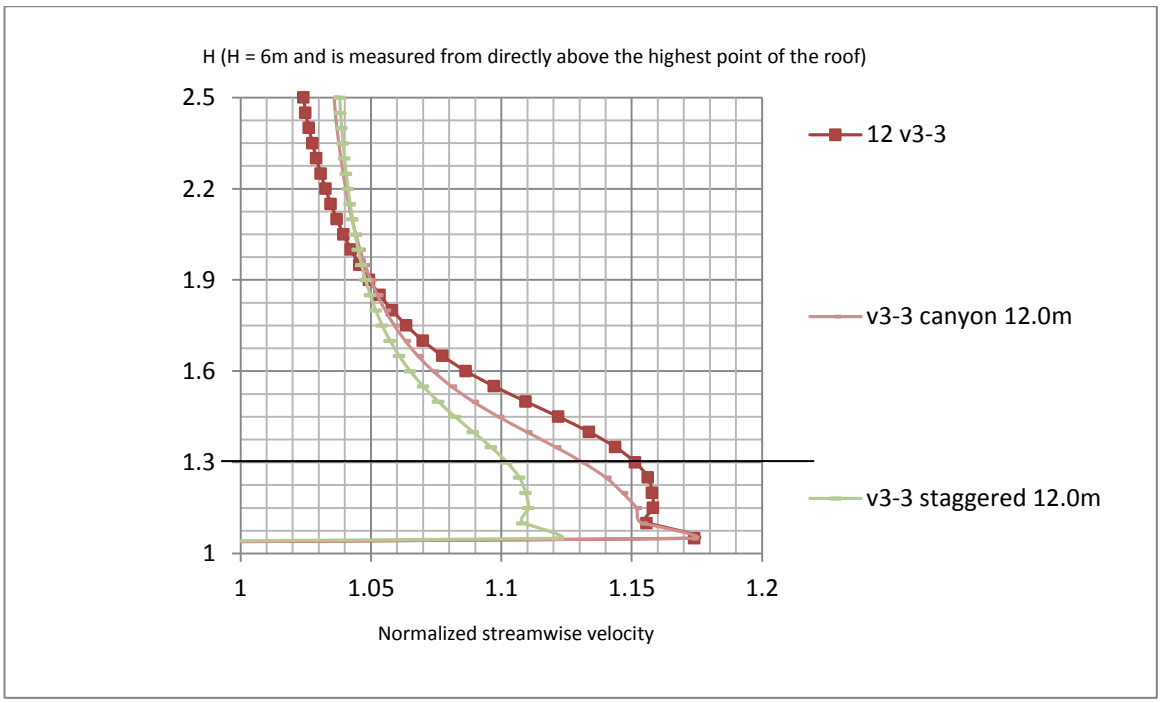

Figure 5.36 Maximum normalized streamwise velocity above the 12m vaulted building for the isolated building, within an urban canyon configuration and a staggered urban configuration.

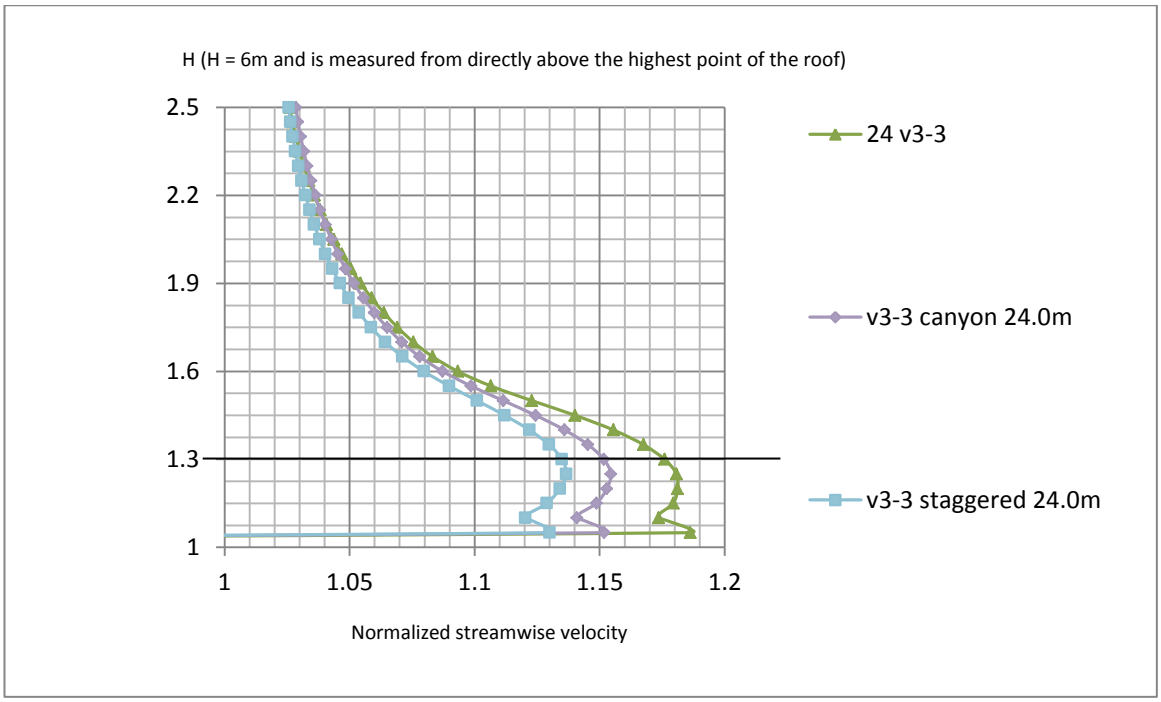

Figure 5.37 Maximum normalized streamwise velocity above the 24m vaulted building for the isolated building, within an urban canyon configuration and a staggered urban configuration.

Increasing the height to 24m, Figure 5.37 shows that the three curves had the same pattern and the maximum recorded values were recorded at the same location (V3-3: midpoint of the roof). However, there were small differences

between the values recorded for the three cases. Above 1.3H, the isolated building recorded a maximum of 1.18U which corresponds to 64.3% increase in power then the building within an urban canyon configuration recorded 1.15U which corresponds to 52% increase in power and then the building within the staggered urban configuration recorded 1.13U which corresponds to 44% increase in power.

5.5 Conclusion

In this chapter, the effect of the roof shape, wind direction, building height and surrounding urban configurations on wind flow above the roof were investigated to determine their effect on specifying the optimum mounting location in light of the accelerating effect that occurs on top of the investigated roof shapes. Different effects of different roof shapes were observed through the flow characteristics in terms of wind flow patterns, turbulence intensities and streamwise velocities. Based on the investigation, the best location for mounting the wind turbine on top of each roof was determined.

For the isolated 6m high building cases with different roof shapes subjected to 0^0 wind direction (Figure 5.6), it can be concluded that the best location for mounting a wind turbine on top of a flat roof is at height of 1.45H at location C2-3 (between the roof windward edged and the middle of the roof), for the domed roof: D3-3 (midpoint of the roof) at 1.3H, for the gabled roof: G5-1 (the leeward corner of the roof) at 1.6H, for the pyramidal roof: P4-2 (on the leeward hip, midway between the middle of the roof and the leeward roof edge) at 1.35H, for the barrel vaulted roof: V3-3 (midpoint of the roof) at 1.3H and for the wedged roof: W5-1 (the leeward corner of the roof) at 1.45H. These locations are where the streamwise wind velocities reached their maximum which is greater than the streamwise velocity at same location without the building in the flow field. This means that all investigated roof shapes have an accelerating effect on wind. However, this accelerating effect differs from one roof shape to another.

When comparing those six positions to each other it can be noticed that the highest maximum increase in streamwise velocity occurred on top of the barrel vaulted roof at location V3-3 (midpoint of the roof, Figure 5.6) at height of 1.3H and the velocity at that point reached 1.16 times the velocity at the same location in an empty domain under the same flow conditions. Since the energy

yield of a wind turbine is directly proportional to cube the wind velocity, therefore mounting a wind turbine on top of a vaulted roof would yield 56.1% more power than a free standing wind turbine at the same location under the same flow conditions.

On the other hand the lowest maximum wind velocity acceleration occurred on top of the wedged roof at location W5-1 (the leeward corner of the roof) at height of 1.45H (Figure 5.6) and the velocity at that point reached 1.03 times the velocity at the same position in an empty domain, which means that mounting a wind turbine on top of a wedged roof would yield only 9% more electricity than a free standing wind turbine at the same location under the same flow conditions. However, the accelerating effect of a wedged roof is more pronounced in a region at the leeward direction of the building, which makes a free standing wind turbine at the leeward direction of a wedged roof isolated building more feasible in terms of taking advantage of the accelerating effect of the building.

As for the wind direction 45^0 (Figure 5.8), it was found that the optimum location for mounting a wind turbine on top of a flat roof is at a height of 1.30H at location C2-2 (midpoint between the windward roof edge and the centre of the roof), for the domed roof: D3-3 (midpoint of the roof) at 1.3H, for the gabled roof: G3-5 (midpoint along the leeward inclined edge) at 1.4H, for the barrel vaulted roof: V3-3 (midpoint of the roof) at 1.3H and for the wedged roof: W5-5 (leeward corner) at 1.3H. The maximum acceleration occurred on top of the domed and the vaulted roofs and reached 1.14U which corresponds to 48% more power than a free standing wind turbine at the same location under the same flow conditions. The minimum acceleration occurred on top of the wedged roof and reached 1.07U which corresponds to 22.5% more power than a free standing wind turbine at the same location under the same flow conditions.

For the 90^0 (Figure 5.11) cases the optimum roof shape for roof mounted wind turbines is the domed roof where a wind turbine mounted at location D3-3 (midpoint of the roof) at height of 1.3H can yield 40.5% more power than a free standing wind turbine at the same location under the same flow conditions, as for the wind turbine to be mounted on top of the gabled and the wedged roof at the optimum location, each would yield 24.2% more electricity than a free standing wind turbine at the same location under the same flow conditions. This

angel is the least in terms of accelerating wind on top of the barrel vaulted roof since the roof mounted wind turbine at the optimum location would yield 27% more power. For all the cases the least acceleration occurred on top of the pyramidal roof which would yield 15.8% more power.

For the 135^0 case (Figure 5.14), which only applies to the wedged roof, the optimum location for mounting a wind turbine is at W3-2 (midpoint between the centreline and the windward horizontal edge) at height 1.3H where the wind acceleration reached 1.14U which means that a wind turbine mounted at that location would yield 48% more power than a free standing wind turbine at the same location under the same flow conditions. The 180^0 case (Figure 5.16) also applies only to the wedged roof case and a wind turbine mounted at location W1-2 (midway on the windward inclined edge between windward horizontal edge and the centreline) at height 1.4H would yield 26% more power than a free standing wind turbine at the same location under the same flow conditions.

Thus, when comparing the results to each other, it can be noticed that for the 0^0 wind direction, the barrel vaulted roof is the optimum roof shape for roof mounting wind turbines then the domed roof, the flat roof, the gabled and the pyramidal roofs, and then the wedged roof. For the 45^0 wind direction, the domed and the barrel vaulted roofs come first then the flat roof, gabled roof, pyramidal roof then the wedged roof. For the 90^0 wind direction, the domed roof comes first, then the flat roof, the barrel vaulted roof then the gabled and the wedged roofs together. For the 135^0 wind direction, the domed, barrel vaulted and the wedged roofs come first then the flat roof, the gabled roof and then the pyramidal roof. However, when looking at the overall results, it can be argued that the optimum roof shape for mounting wind turbines is the barrel vaulted roof when the wind direction is parallel to the roof profile. Thus, this case was chosen for investigating the effect of the building height and the surrounding urban configurations on the energy yield and positioning of roof mounted wind turbines.

For the building height variable, it can be argued that a roof mounted wind turbine has higher potentials if mounted on top of higher buildings than low rise buildings. However, it should be noted that a wind turbine mounted on top of higher buildings would also suffer from higher levels of turbulence which should

be kept in mind when choosing a specific wind turbine as it should be able to withstand the higher levels of turbulence.

When studying the effect of the surrounding urban configuration (urban canyon and staggered configurations) on wind flow above the barrel vaulted roof subjected to a 0^0 wind directions having different heights, it was noticed that the closer the building height to its surrounding, the more disturbance the flow will suffer from and the taller the building than the surrounding urban configuration, the less the effect on the flow around and above the building. This is attributed to the surrounding terrain roughness. In the case of the isolated building the roughness length was equal to 0.03 which corresponds to nearly flat or gently undulating countryside as for the other cases where the barrel vaulted building was placed within urban context, the roughness corresponds to that of domestic housing areas which affected the wind flow above the investigated cases.

When comparing the flow patterns of the urban canyon configuration to the staggered configuration, it was noticed that the staggered configuration had less effect on the flow patterns around the investigated buildings than the urban canyon configuration. This can be attributed to the larger distance in front of the studied building in the staggered configuration than the urban canyon configuration which gives the flow a chance to develop and exhibits similar features to those of the isolated buildings cases.

Thus, for roof mounting a wind turbine within an urban configuration, it can be recommended that the building should be higher than the surrounding buildings and for specifying the optimum location for mounting the wind turbine, both the turbulence intensity and the streamwise velocity should be assessed above the roof placed within the urban surrounding.

Accordingly, when looking at all the results for the turbulence intensity for the barrel vaulted roofed building with different heights whether isolated or within different urban configurations it can be concluded that when the building height is less than or the same as the surrounding urban context, the surrounding urban context will have an effect on the turbulence above the roof. However, not necessarily that the presence of the building within an urban configuration will contribute to increasing the turbulence intensity above its roof as the flow is

complicated and other factors such as the roof shape, the urban configuration, building geometry and any other elements within the urban context might affect the flow. As seen in the case of the 12m barrel vaulted building within both urban configurations, the isolated building case registered higher turbulence above the roof (2.98TI) than the building placed within different urban configurations (2.72TI for both urban configurations). Also it was noticed that with the increase in the height of the building whether isolated or placed within an urban area, the turbulence intensity increased which indicates the presence of a relationship between the building height and the turbulence it causes above its roof.

Figure 5.38 shows a comparison between the increase in the energy yield of the proposed wind turbine at the optimum mounting location for all investigated barrel vaulted roof cases under 0^0 wind direction. It is noticed that at the proposed optimum mounting location of a wind turbine above the investigated cases, the isolated building would introduce more acceleration to the wind than a building placed within an urban context. Comparing the cases of different barrel vaulted buildings with different heights within different urban configurations, one can notice the decrease in the difference between the recorded values with the increase in the height of the studied building. This suggests that with the increase in height, the effect of the surrounding urban context diminishes and other variables such as the roof shape and the height of the building affect the flow above the building roof.

It is noticed that when the building is higher than its surroundings the urban canyon introduces more acceleration above the investigated roof than the staggered configuration. However, when the building is lower than or the same height as the surrounding urban configuration, the staggered urban configuration introduces more acceleration above the investigated roof than the urban canyon configuration. The difference in patterns between the two cases might be attributed to the effect of ground roughness on wind flow above the investigated cases and how the CFD code solves the flow near to the ground. Thus, more research is required to investigate the reason behind this change in pattern and whether it is related to the effect of the geometry of the urban

setting or it is related to the way in which the CFD code solves the flow at lower altitudes.

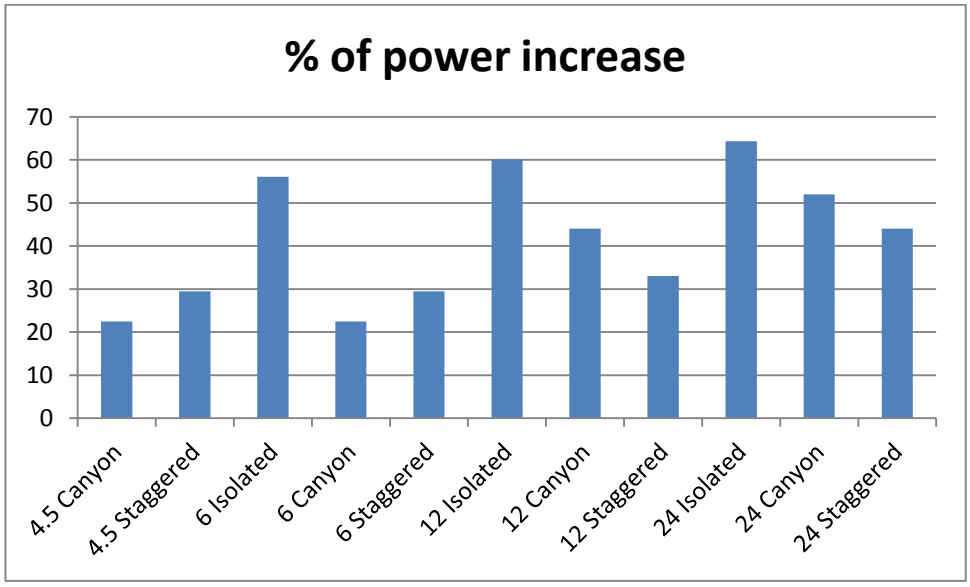

Figure 5.38 Comparison between the increase in the energy yield of the proposed wind turbine at the optimum mounting location for all investigated barrel vaulted roof cases under 0^0 wind direction.

Chapter Six

Conclusions and Recommendations for Future Work

Chapter Structure

6.1 Introduction

6.2 Summary

6.3 Conclusions

6.4 Recommendations for future work

Chapter 6: Conclusions and Recommendations for Future Work

6.1 Introduction

The conclusions on urban wind energy utilization and proposed future work in the field are outlined in this chapter. Thus, this chapter is divided into three main sections; the first section focuses on discussing the conclusions of this research which tackles four main points:

- Technology of urban wind turbines.
- CFD as a tool for assessing urban wind flow.
- Validating CFD results.
- Investigated independent variables.

The second section focuses on the recommendations for future work on urban wind turbines which focuses on CFD simulation, buildings, wind turbines and education. And the last part is the closing remarks of this thesis.

6.2 Summary

The main driver behind this research was the observed state of uncertainty regarding the viability and feasibility of urban wind turbines. The unfavourable wind conditions in urban areas due to the variation in the surface features are well established in research. On the other hand, the wind accelerating effect of buildings and the potentials of wind turbines taking advantage of the augmented wind presents itself as a potential for harnessing wind energy. Urban wind turbines send visual messages for tackling climate change which might encourage people on cutting down on their energy consumption while generating their own electrical power. On the other hand, the main idea behind urban wind turbines is to generate electricity where it is consumed, thus cutting down on the extra costs of infrastructure, cabling and power losses.

Accordingly, positioning roof mounted wind turbines at the optimum mounting location and the optimum roof shape for mounting wind turbines needed to be investigated. In addition, other factors such as wind direction, building height and surrounding urban configuration have an effect on the energy yield and positioning of roof mounted wind turbines, thus needed investigation.

However, urban wind turbines are subjected to lower mean wind speed and high levels of turbulence. Accordingly, specific technologies are required to cope with these conditions as demonstrated in chapter two. This work provided a scientific framework to assess wind flow around buildings for accurately positioning wind turbines to help in improving the energy yield of roof mounted wind turbines. Literature on the available and developing wind turbines technology has been reviewed to provide the underpinning knowledge required when installing wind turbines close to buildings.

Architects and planners who make the initial proposal on installing wind turbines close to buildings lack the knowledge of such technologies and even the basic systems of wind turbines due to the nature of their education. Thus, this part was covered by reviewing literature on the available and developing wind turbines technology to provide this knowledge, which leaded to specifying the required technologies when installing wind turbines close to buildings.

However, specifying the mounting location of a wind turbine within the built environment or close to buildings requires an understating of the nature of urban wind flow regimes. Accordingly, the available tools for assessing wind flow within the built environment were reviewed to specify the most relevant tool for assessing urban wind which, in this case, was the Computational Fluid Dynamics (CFD) simulations. Literature on CFD and its usage for assessing urban wind flow was reviewed in order to specify the best practice guidelines for using CFD in assessing urban wind flow. Based on the reviewed literature, the Realizable k-ε turbulence model was used. Reviewed research recommended running validation studies to assure the consistency of the yielded results.

Thus, a validation study was required to give confidence in the data entry of simulations variables in order to yield consistent results of the investigated flow problems. Despite the limitations of the used wind assessment tool, the results were consistent and compared favourably with the results from other published wind assessment tools such as wind tunnel tests and in-situ measurements as discussed in chapter three. Accordingly, the simulation conditions were used for investigating the main flow problems in this thesis to identify the optimum roof shape for mounting wind turbines, in addition to identifying the effect of wind direction, buildings height and surrounding urban configuration on the energy

yield and positioning for roof mounted wind turbines. The results can be summarized in the following points:

- Of the investigated roof shapes (flat, domed, gabled, pyramidal, barrel vaulted and wedged roofs), the barrel vaulted roof is the optimum roof shape for roof mounting wind turbines.
- Each roof shape has an optimum mounting location for wind turbines and wind flow above the roof should be accurately assessed to specify the optimum roof mounting location.
- For all investigated roof shapes, except for the domed roof, the optimum mounting locations changes with the change in the wind direction.
- Higher buildings introduce more acceleration to wind above the roof, thus roof mounted wind turbines are preferred to be mounted on high-rise buildings.
- When the building is lower or is of the same height as the surrounding urban configuration, the urban canyon configuration causes less acceleration than the staggered urban configuration above a barrel vaulted roofed building. While if the building is higher than the surrounding urban configuration, the urban canyon configuration causes more acceleration than the staggered urban configuration above a barrel vaulted roofed building. In all cases, the acceleration effect above the isolated building case is more pronounced than the building within an urban configuration.

More details on the obtained results and their implications in terms of the values of the expected increase in energy yield are highlighted in the following section.

6.3 Conclusions

With the development in urban wind turbines technologies and the governmental support of these technologies, in addition to the growing interest in urban wind turbines, there is a great need for ensuring the success of such systems through the following:

- Correctly assessing the wind resources at the installation site.
- Specifying to the highest degree of accuracy where to mount a wind turbine.

- Installing a wind turbine system that copes with the local wind flow conditions.

Integrating wind turbines within the built environment or in the vicinity of buildings requires the knowledge of the available wind turbines systems to use the most relevant turbine as the choice depends largely on wind flow conditions at the installation location.

6.3.1 *Technology of urban wind turbines*

Chapter two reviewed the available and developing technologies of wind turbines and their suitability for installation near buildings for the purpose of examining hypothesis one which stated that *'Wind regime around buildings is different from open fields and requires specific wind turbines technology. If existing literature on urban wind flow and developing wind turbines technology are reviewed, a set of criteria can be deduced which sets the guidelines for wind turbines technology to be used near to buildings'*. By examining this hypothesis, the context of integrating wind turbines within the built environment is identified.

It can be concluded that for a wind turbine to be installed in the vicinity of buildings, it is preferable to use vertical axis wind turbines with an induction, permanent magnet generator. If horizontal axis wind turbines are used, the counter rotating wind turbine system is preferable whose blades are implementing lift forces and is allowed to yaw to face the changing direction of wind using an active yaw system. In order to take advantage of the accelerating effect of buildings and avoid high levels of turbulence it is advised to mount the wind turbine on top of high rise buildings in areas with low roughness length. However, it is mandatory to assess the wind resources at the proposed installation site using one or more of the available wind assessment tools.

6.3.2 *CFD as a tool for assessing urban wind flow*

Chapter three reviewed the available wind assessment tools and their suitability for assessing urban wind flow or wind flow around isolated buildings for the purpose of examining hypothesis two which stated that *' For assessing wind flow around buildings, CFD simulations can be used to yield consistent results provided that best practice guidelines are followed and validation is carried out'*.

By examining this hypothesis, identifying the relevance of different tools for assessing wind flow around buildings is achieved.

It can be concluded that the CFD is the most relevant wind assessment tool for the purpose of integrating wind turbines within the built environment and assessing urban wind flow especially when the tool is used for comparing alternatives. However, CFD should be used vigilantly as it is embedded with errors and uncertainties. Thus, best practice guidelines should be consulted before using CFD as a simulation technique. However, it should be noted that these guidelines are not enough for having confidence in the yielded results. Accordingly running validation studies, as demonstrated in chapter four, through comparing the simulation results with the results from other wind assessment tools such as wind tunnel tests and in-situ measurements is mandatory for obtaining consistent results. In this research the 6m cube was chosen due to the availability of wind tunnel tests, in-situ measurements and validated CFD simulation results for that specific case which represents the flat roof case in this research.

6.3.3 *Validating CFD results*

The extracted best practice guidelines for CFD simulations, which chapter three concluded with, were used as the start point for the validation study in chapter four. The validation study in chapter four investigated wind flow around a cube in a turbulent channel flow and compared the obtained CFD results with in-situ measurements, wind tunnel tests results and validated CFD simulations results. It can be argued that the obtained CFD simulation results in this work compared favourably with the reviewed results. In addition, the obtained results in this work can be considered the closets results among the reviewed CFD simulation results to published wind tunnel tests and in-situ measurements. The obtained results contributed to examining hypothesis two. Thus, CFD simulation was considered a reliable wind assessment tool for yielding consistent results. In addition, the simulation variables used can be counted on for investigating the effect of roof shape, wind direction, building height and surrounding urban configuration on the energy yield and positioning of roof mounted wind turbines.

6.3.4 *Investigated independent variables*

Chapter five starts by addressing roof mounting wind turbines and the main factors affecting their performance, it was concluded that in order to assess the effect of roof shape, wind direction, building height and surrounding urban configuration on the energy yield and positioning of roof mounted wind turbines, two dependant variables should be investigated; these are the wind velocity and the turbulence intensity as they are the main variables affecting the performance of wind turbines.

In order to examine hypothesis three which stated *'One of the main reasons behind the low energy yield of urban wind turbines is the low mean wind speed. The presence of a building in wind flow field would increase the wind speed and turbulence intensity in the vicinity of the building and integrated wind turbines can take advantage of the accelerating effect that occurs',* the flow patterns around the investigated cases were plotted and the recorded wind velocity and turbulence intensities values above the studied buildings were normalized against the values at the same locations under the same flow conditions in an empty domain and the accelerating effect was identified. It can be concluded that:

- By examining hypothesis four which stated that *'Studying the variation in wind directions may or may not change the optimum mounting location of a roof mounted wind turbine'.* It was noticed that for all roof shapes except the domed roof, specifying the optimum roof mounting location for a wind turbine depends on the wind direction since the optimum location on top of each roof shape changed with the change in wind direction. Accordingly, identifying the effect of different wind directions on the optimum roof mounting location of a wind turbine is achieved.
- For the domed roof, the location of maximum acceleration under different wind direction was always the same (midpoint of the roof at location D3-3) and the increase in energy yield for an integrated wind turbine at that location would yield 40.5% to 48.2% more power based on the wind direction. The consistency in the location can be attributed to the symmetrical properties of the domed roof.

- As seen in Table 6.1 all roof shapes under different wind directions had an accelerating effect on wind above the roof. Maximum acceleration above flat, domed, gabled, pyramidal, barrel vaulted and wedged roofs reached 1.12U, 1.14U, 1.09U, 1.08U1.16U and 1.14U respectively, at wind directions 45^0, 45^0, 45^0, 45^0, 0^0 and 135^0 respectively.

Table 6.1 Maximum recorded streamwise velocities and their equivalent increase in energy yields under different wind directions for the investigated roof shapes.

	Flat	Domed	Gabled	Pyramidal	Barrel vaulted	Wedged
Maximum streamwise velocity (U)	1.12	1.14	1.09	1.08	1.16	1.14
Wind direction (degree)	45	45	45	45	0	135
Increase in energy yield (%)	40.5	48.2	29.5	26	56.1	48.2

- All roof shapes under different wind directions increased the turbulence intensity on top of the investigated roof shapes.
- By examining hypothesis five which stated that *'For each roof shape there is an optimum mounting location for wind turbines. Thus, if wind flow above each roof shape is assessed, the optimum mounting location can be identified and the performance of the integrated wind turbine can be improved'*, through comparing the results of the CFD simulations of wind flow around the investigated roof shapes, it was noticed that the location of maximum wind speed on top of each roof shape differed from one roof to another (Table 5.12). For the flat roof the increase in energy yield at different locations above the roof ranged between 31.3% (C2-3: between the roof windward edged and the middle of the roof) - 40.5% (C2-2: midpoint between the windward roof edge and he centre of the roof), for the domed roof: 40.5% (D3-3: roof midpoint) - 48.2% (D3-3: roof

midpoint), for the gabled roof: 15.8% (G5-1: the leeward corner of the roof) - 29.5% (G3-5: midpoint along the leeward inclined edge), for the pyramidal roof: 15.8% (P4-2: leeward hip, midway between the middle of the roof and the leeward roof edge) - 26% (P4-4: on the roof streamwise axis between the midpoint of the roof and the leeward corner), for the barrel vaulted roof: 27% (V2-2: midpoint between the windward roof edge and the centre of the roof) – 56.1% (V3-3: midpoint of the roof) and for the wedged roof: 9.3% (W5-1: the leeward corner of the roof) to 48.2% (W3-2: midpoint between the centreline and the windward horizontal edge). Thus, identifying the optimum roof mounting location for a wind turbine on top of the investigated roof shapes is achieved.

- By examining hypothesis six which stated that *'Different roof shapes have different effects on wind flow above them. If wind flow above different roof shapes is assessed, there would be a difference in the accelerating effect from one roof to another'* it was noticed that among all roof shapes, the barrel vaulted roof is the optimum roof shape for roof mounting wind turbines since it caused the highest acceleration which reached 1.16 times the wind velocity at the same location under the same flow conditions in an empty domain when the wind was flowing parallel to the roof profile, which means that a wind turbine mounted on top a vaulted roof would yield 56.1 % more power than a free standing wind turbine at the same location under the same flow conditions. Thus, this case was chosen for further investigations of other independent variables.
- On the other hand the lowest maximum acceleration occurred on top of the pyramidal roof since it reached only 1.08U which corresponds to an increase in the energy yield of the installed wind turbine by 26%.
- By examining hypothesis seven which stated that *'Another variable affecting wind flow above buildings' roofs is the building height. Thus, for a single roof shape, if the height of the building is changed, that would have an effect on the wind flow above it',* it can be concluded that changing the building height had no effect on the optimum mounting location of the wind turbine. However, it was noticed the increase in the accelerating effect above the roof with the increase in the building height. For the 6m case the increase in power reached 56.1%, the 12m case

caused acceleration in wind equivalent to an increase in power equal to 60.1%, as for the 24m case, the increase in power reached 64.3%. Accordingly, it can be concluded that high rise buildings are more preferable for mounting wind turbines rather than low rise buildings. Thus, identifying the effect of building height on wind flow above the roof is achieved.

- In order to examine hypothesis eight which stated that *'One of the main variables affecting urban wind flow is the urban setting. Thus, it is assumed that different urban configurations would have different effects on wind flow above buildings' roofs',* the height of the barrel vaulted roofed building was changed to identify the effect of varying the height within different urban configurations. It can be concluded that the closer the building to its surroundings the more the effect of the surroundings on the wind flow above the roof.
- In terms of the flow patterns, the staggered urban configuration had less effect on the flow above the investigated cases than the urban canyon configuration, this can be attributed to the bigger streamwise space in front of the investigated building when compared to the urban canyon configuration.
- In terms of the effect of the urban configuration on the accelerating effect above the investigated cases, two patterns were observed; the first applies to the cases where the building height is the same as or less than the surrounding urban configuration. And the second applies to the cases where the building height is larger than the surrounding urban configuration. In the first group, the urban canyon configuration had less accelerating effect than the staggered urban configuration since the acceleration above the barrel vaulted roof reached 1.07U which corresponds to an increase in power of 22.5% while for the staggered configuration it reached 1.09U which correspond to an increase in power of 29.5%. However for the second group, the urban canyon configuration had more accelerating effect than the staggered urban configuration since the acceleration above the vaulted roof reached 1.13U and 1.15U which corresponds to an increase in power of 44% and 52% for the 12m case and the 24m case respectively. As for the staggered urban configuration cases, the acceleration reached 1.10U and 1.13U which

corresponds to 33% and 44% increase in power for the 12m and 24m cases respectively. In light of these results, identifying the effect of surrounding urban configuration on wind flow above the roof is achieved.

It can be concluded that the case of mounting a micro-wind turbine above an isolated building is not so common within the built environment except for high rise buildings where the surrounding buildings would have a negligible effect on local wind flow above the roof. Due to the complexity of the built environment, simplification is needed for these studies where all the variables are fixed except for one variable to investigate its effect on local wind flow. However, for low rise buildings, they will still have an accelerating effect on wind flow above the roof which requires a complete assessment of wind flow to determine the potential locations for mounting a wind turbine to take advantage of the accelerating effect.

6.4 Recommendations for future work

This work contributes to understanding urban wind flow and wind flow around isolated buildings, specifically around different roof shapes for the purpose of mounting wind turbines. To the best knowledge of the researcher, it can be argued that this is the first research to investigate and compare wind flow above the previously mentioned roof shapes in addition to investigating the building height and urban configuration effect on wind flow above a barrel vaulted roof building. However, it should be noted that this work is not definitive as the study was limited by the available computational power and the investigated cases were hypothetical and lacking the details of the real built environment. Thus, the recommendations for future work in the field can cover:

6.4.1 *CFD simulation:*

In light of the obtained results comparing the accelerating effect above the barrel vaulted roof with different heights placed within different urban configuration, a difference in flow patterns was observed between the cases when the building was lower or the same height as the surrounding urban configuration and when the building was higher than the surrounding urban configuration. It is hypothesised that this difference is attributed to the way in which the CFD code solves the flow near the ground which affects the flow above the investigated cases. Thus, more research is required to investigate

the reason behind these differences and whether they are related to the CFD code, the geometry of the investigated cases or it is just a result of the interaction between the wind, ground and the investigated urban settings. More sophisticated CFD simulations techniques which yield more consistent results can be implemented to investigate this case.

With the advancements in computer technology and the increased computational power, it can be possible to use more sophisticated turbulence models such as DNS, LES and URANS for investigating urban wind flow, these turbulence models are more accurate and yield more consistent results than the used RANS model in this thesis. Thus, it is recommended to implement those turbulence models in investigating similar flow problems and compare the results with the obtained results in this thesis to identify the accuracy of different turbulence models in predicting urban wind flow and whether or not it is worth using more sophisticated turbulence models which takes longer time to run and requires more computational power.

6.4.2 *Buildings:*

Integrating wind turbines within buildings is either through retrofitting existing buildings with wind turbines or designing new buildings with the integration of wind turbines in mind. In the first case, a complete assessment of the structural integrity of the existing building is mandatory and more research is needed in this area especially in light of the obtained results in this research for the proposed roof mounting locations of wind turbines which might conflict with the structural integrity of the building.

As for the newly designed buildings with wind turbines' integration in mind, the structural integrity of the building is counted for at the early stages of the design. However, these designs tend to have aerodynamic forms which might affect the architectural spaces inside the buildings. More research is needed in this area to identify how the spaces are affected by aerodynamically shaping buildings for the purpose of integrating wind turbines to take advantage of the accelerating effect that happens.

As mentioned earlier, the studied cases in this research are hypothetical cases where the geometries where simplified. However, in the real built environment,

more elements exist that would affect wind flow at roof level. Also, roofs exist in more complicated forms and it would be recommended to investigate wind flow above more complicated roof shapes for the purpose of identifying the optimum mounting locations of roof mounted wind turbines. Also, it is recommended to include more of the elements forming the built environment in the model to have a more realistic prediction of wind flow around the investigated buildings. However, it should be noted that this would be computationally expensive.

In light of the obtained results for the turbulence intensities above the barrel vaulted roof covering 6m, 12m and 24m buildings, it was noticed that the turbulence intensity increases with the increase in building height but locations of maximum recorded turbulence intensities for all three cases were the same, however one of the recommendations from the Encraft Warwick Wind Trials Project (2009) and the WINEUR report (2007) suggests a relationship between the vertical range of turbulence above the building and its height which was not recorded in this research. Thus, more research investigating the relationship between building height and the vertical range of turbulence above the building is required since the methodologies for collecting turbulence data in both the Encraft Warwick Wind Trials Project (2009) and the WINEUR report (2007) were not clear and the used instruments have limitations in recording turbulence intensities.

6.4.3 *Wind turbines:*

The technology of large scale wind turbines is quite developed. However, small and micro scale wind turbines are still under development and the field is promising especially for the purpose of integrating wind turbines within the built environment. More research on wind turbines capable of withstanding high levels of turbulence and generating electricity under low mean wind velocities is required.

Also, it is recommended to undergo research on the performance of existing wind turbines integrated within the built environment as data in that field is scarce. In addition, the field of assessing the performance of multiple wind turbines mounted on top of buildings' roofs is another potential area of investigation since it is expected that the rotating blades on top of a roof would change the wind flow regime around the wind turbine and would affect the

energy yield of adjacent installed wind turbines if more than one turbine is proposed for installation.

6.4.4 *Education:*

Since urban wind turbines or small scale wind turbines are another way of having buildings that are near to self-sufficiency in terms of energy, it is important to look at those systems as part of a holistic approach to tackling climate change. Architects and planners play a major role through their designs in mitigating climate change. However, they lack the required knowledge of these systems that might be an added value to the design. Accordingly, it is recommended to include in the curricula of planners and architects subjects that address building physics and the integration of different renewable systems in buildings.

6.5 Closing remarks

Urban wind turbines is a relatively new field which is developing and has high potentials with the advancements in small and micro scale wind turbines technologies and the continues investigation of taking advantage of the accelerating effect of different buildings' shapes. This thesis goes some way towards addressing the developing wind turbines technologies to be integrated within buildings in addition to investigating the accelerating effect of different roof shapes. However, from a practical and architectural point of view, how can the results of this research be implemented?

In order to answer this question, it should be noted that the idea of integrating wind turbines in urban areas is still questionable due to the low mean wind speed and high levels of turbulence in addition to the difficulty of assessing, to a high degree of accuracy, the wind resources at the proposed mounting location. However, when it comes to mounting wind turbines near buildings in rural areas or on top of isolated buildings' roofs in open fields, the integrated wind turbines would have more potential in terms of being mounted at the optimum mounting location to take advantage of the accelerating effect of the building.

These areas are usually located away from the grid and energy consumption is minimal which makes the idea of integrating renewables more attractive. For roof mounting wind turbines, the case will either be retrofitting an existing

building with a roof mounted wind turbine or a new building is being built and the decision has been made to rely on wind energy as part of energy supply of the building. In the first case, the wind resources can be assessed to a high degree of accuracy due to the simplicity of the surrounding context. Thus, the optimum mounting location can be determined. However, the structural integrity of the building and any other potential problems from retrofitting the existing building with the wind turbine should always be assessed before installing the wind turbine.

As for the second case and in light of the obtained results in this research, a recommendation can be made to the developer on which roof shape to be used and how to orient the building in a way in which the roof mounted wind turbine could benefit from the prevailing wind direction and its interaction with the proposed roof shape. Accordingly, the optimum mounting location can be determined and the anticipated energy yield can be calculated before the inception of the project which will help in deciding about the feasibility of roof mounting a wind turbine. However, it should always be noted that there will be a compromise between the orientation of the building, the roof shape and other architectural requirements whether being ecological, functional or even certain specific requirements by the developer. But it can be argued that such integration can result in a new type of buildings, especially when the whole building is shaped to harness wind power, where the form of the building will follow its function from a power related point of view.

Appendices

Appendices

Appendix 1: Table comparing the obtained results in this work for the specific lengths of the flow to the published results of in-situ measurements, wind tunnel tests and CFD simulations

Sp : Saddle point

St : Stagnation point

Rx2 : Roof reattachment length

Rx1 : Reattachment length in the leeward direction of the cube

CpW : Maximum recorded pressure coefficient on the windward façade

CpR : Maximum recorded pressure coefficient on the roof

CpL : Maximum recorded pressure coefficient on the leeward façade

	Sp	St	Rx2[1]	Rx1[2]	CpW	CpR	CpL
CFD simulation in this work	0.80h	0.80h	0.32h	1.60h	0.81 at 0.8h	-0.97 at 0.05h	-0.17 at 0.85h
Richards *et al.* (2001) and Richards and Hoxey (2006) (In-situ	NA	0.81h	0.6h	NA	0.86 at 0.81h	-0.9 at 0.15h	-0.1 along the line
Castro and Robins (1977) (Wind tunnel)	NA[3]	0.85h	0.3h	NA	0.78 at 0.85h	-0.9 at 0.1h	-0.1 along the line

[1] X2 is the distance measured from the windward edge of the roof towards the roof leeward edge

[2] X1 is the distance measured from the leeward façade ins the streamwise direction of the flow

[3] NA = Not Available

	Sp	St	Rx2[1]	Rx1[2]	CpW	CpR	CpL
Hölscher and Niemann (1998) (Average of 15 wind tunnels)	NA	0.75h	NA	NA	0.87 at 0.75h	-1.0 at 0.27h	-0.2 along the line
Vardoulakis *et al.* (2011) (CEDVAL wind tunnel)	NA	0.64h	NA	1.50h	NA	NA	NA
Vardoulakis *et al.* (2011) (ATREUS wind tunnel)	NA	0.70h	NA	1.34h	NA	NA	NA
Richards *et al.* (2007) (Wind tunnel)	NA	0.81h	NA	NA	0.75 at 0.81h	-1.1 at 0.2h	-0.2 along the line
Beyers *et al.* (2004) (CFD)	NA	0.63h	0.00[4]	2.74h	0.98 at 0.63h	-0.95 at 0.05h	-0.2 along the line
Paterson and Apelt (1989) (CFD)	NA	0.84h	0.65h	2.00h	0.89 at 0.84h	-1.5 at the edge	-0.3 along the line
Seeta Ratnam and Vengadesan (2008) (CFD)							

[4] 0.00 means no separation occurred

	Sp	St	Rx2[1]	Rx1[2]	CpW	CpR	CpL
DNS	1.20h	0.60h	0.50h	1.50h	NA	NA	NA
Standard k–ε,	0.80h	0.58h	0.40h	2.20h	NA	NA	NA
Low-Reynolds number k–ε,	1.58h	0.60h	0.60h	2.30h	NA	NA	NA
Non-linear k–ε model,	1.50h	0.60h	0.55h	2.00h	NA	NA	NA
Standard k–ω	1.40h	0.55h	0.30h	2.20h	NA	NA	NA
Improved k–ω	1.29h	0.60h	0.50h	2.20h	NA	NA	NA
Rodi (1997) (CFD)							
LES	0.81h to	NA	0.00 to	NA	NA	NA	NA
RANS	0.64h to	NA	0.00 to	NA	NA	NA	NA
Yang (2004a) (CFD)							
CFX5 k-ε	NA	0.82h	NA	NA	0.95 at 0.82h	-1.56 at 0.05h	-0.3 at 0.24h
CFX5 RNG	NA	0.80h	NA	NA	0.90 at 0.8h	-0.85 at 0.05h	-0.40 at 0.19h

Appendices from 2 to 31

For all TI plots, X axis: normalised TI, Y axis: H = 6m and is measured from directly above the roof.

For all Streamwise velocity plots, X axis: normalised streamwise velocity, Y axis: H = 6m and is measured from directly above the roof.

For all plots: C (flat roof), d (domed roof), g (gabled roof), p (pyramidal roof), v (barrel vaulted roof) and w (wedged roof).

Appendix 2: Turbulence intensity plots for all roof shapes at 0^0 wind direction

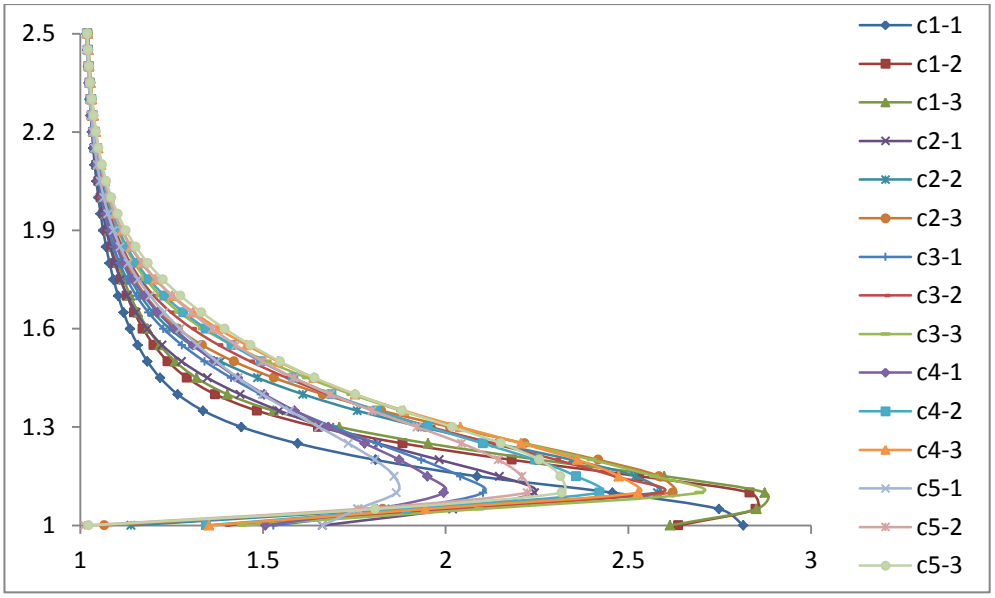

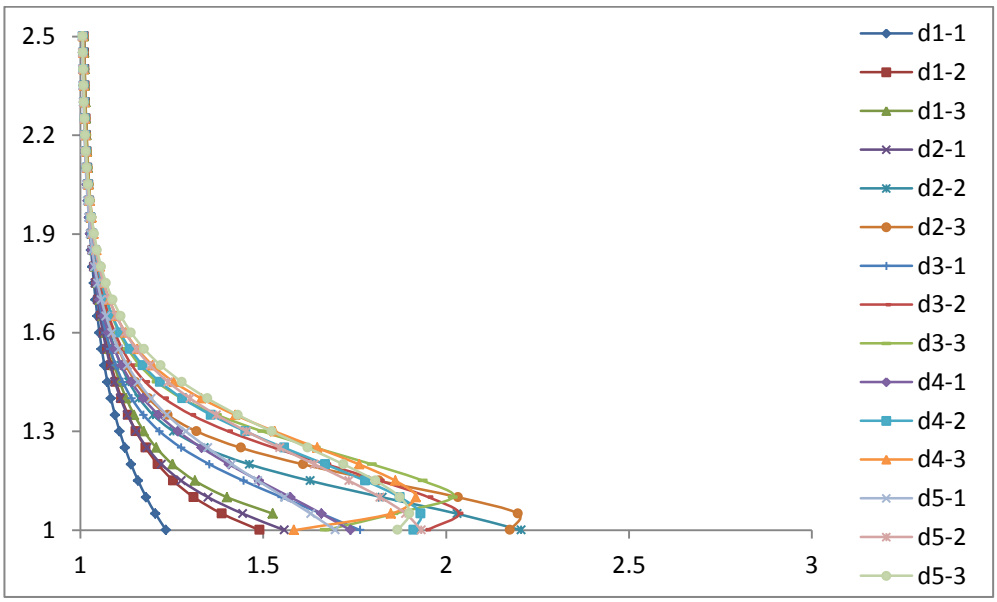

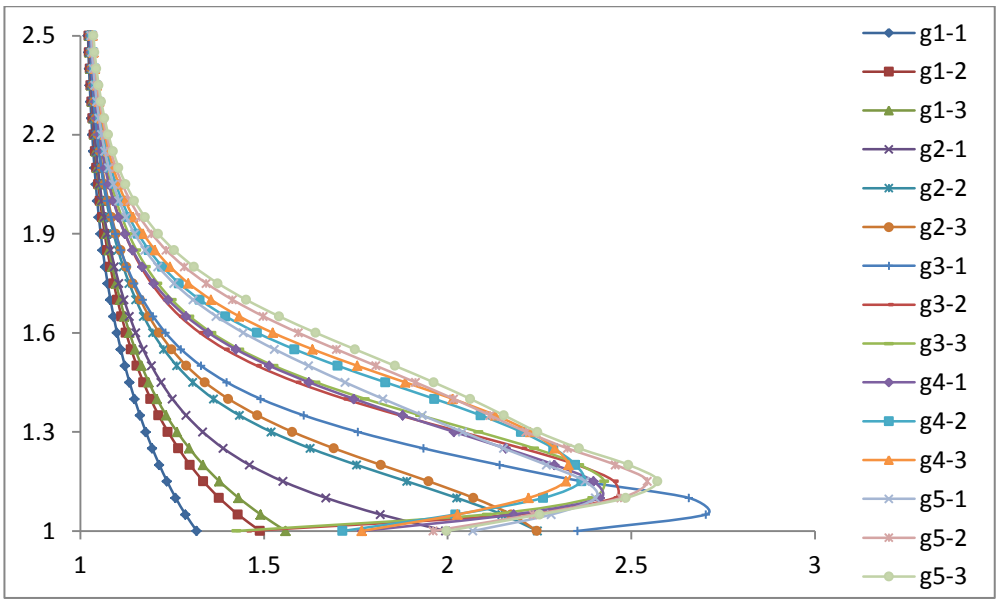
2.5
2.2
1.9
1.6
1.3
1
1
1.5
2
2.5
3
g1-1
g1-2
g1-3
g2-1
g2-2
g2-3
g3-1
g3-2
g3-3
g4-1
g4-2
g4-3
g5-1
g5-2
g5-3

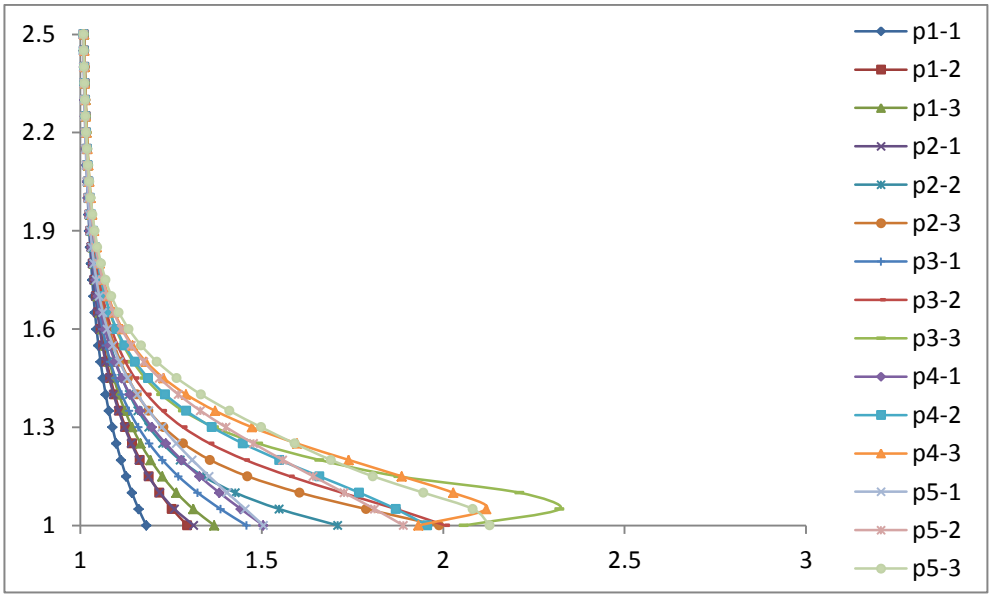
2.5
2.2
1.9
1.6
1.3
1
1
1.5
2
2.5
3
p1-1
p1-2
p1-3
p2-1
p2-2
p2-3
p3-1
p3-2
p3-3
p4-1
p4-2
p4-3
p5-1
p5-2
p5-3

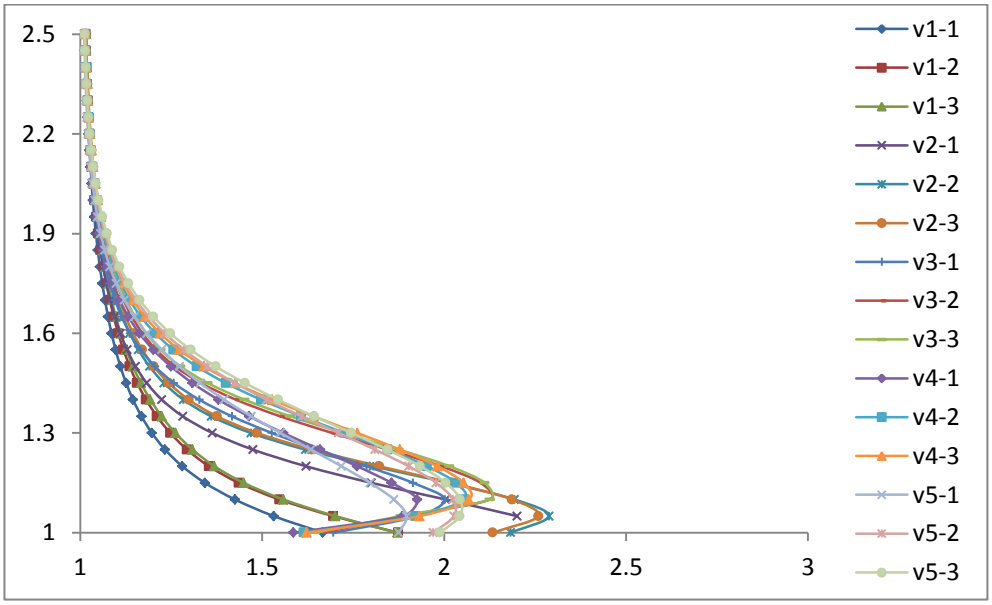
2.5
2.2
1.9
1.6
1.3
1
1
1.5
2
2.5
3
v1-1
v1-2
v1-3
v2-1
v2-2
v2-3
v3-1
v3-2
v3-3
v4-1
v4-2
v4-3
v5-1
v5-2
v5-3

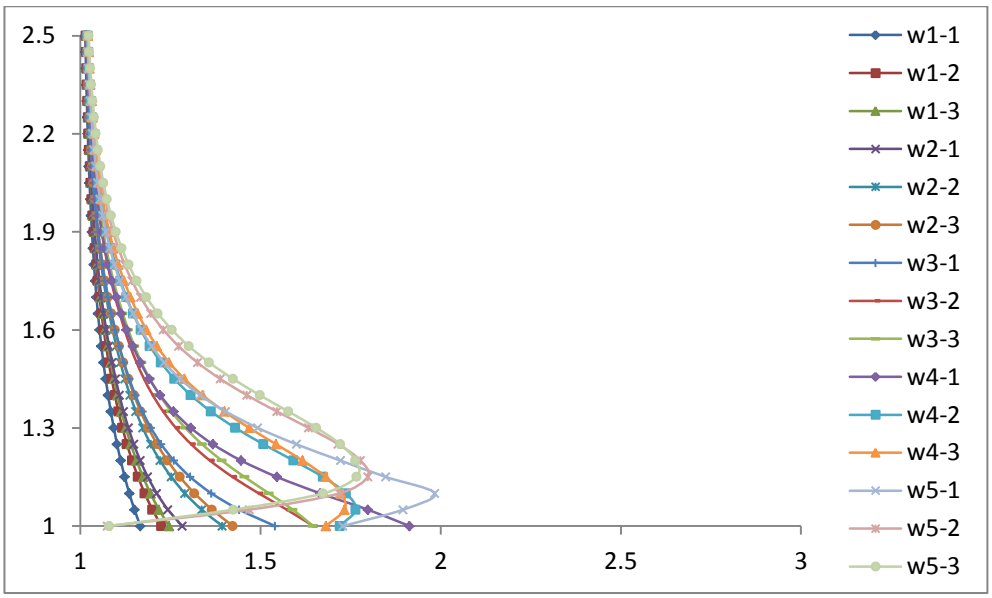

Appendix 3: Streamwise velocity plots for all roof shapes at 0^0 wind direction

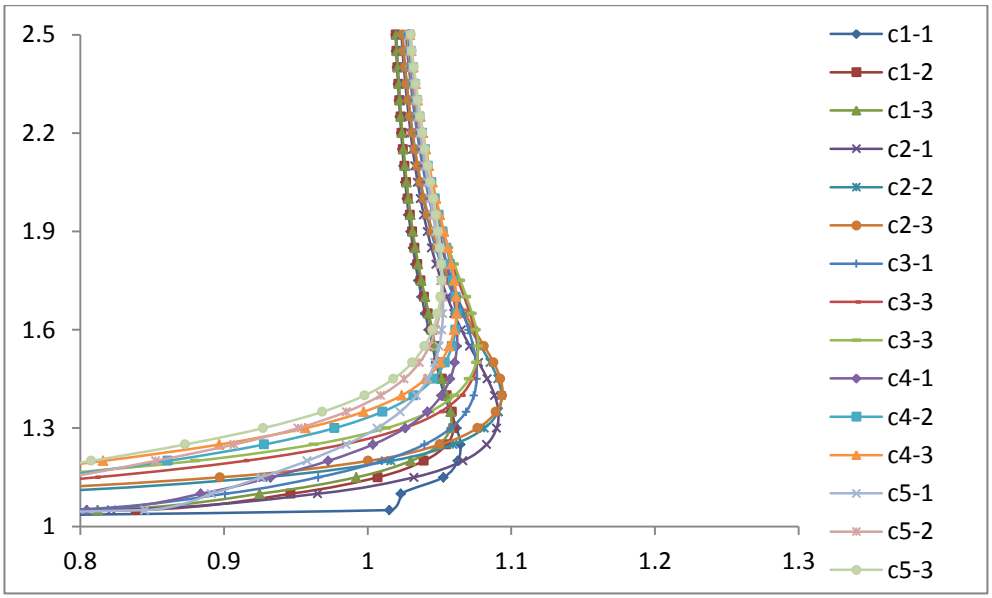

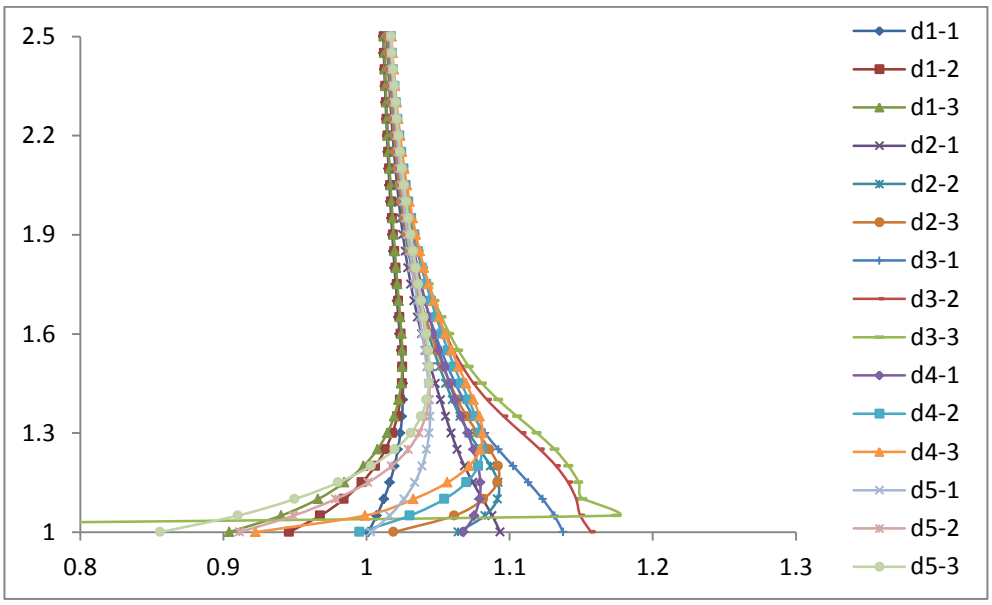

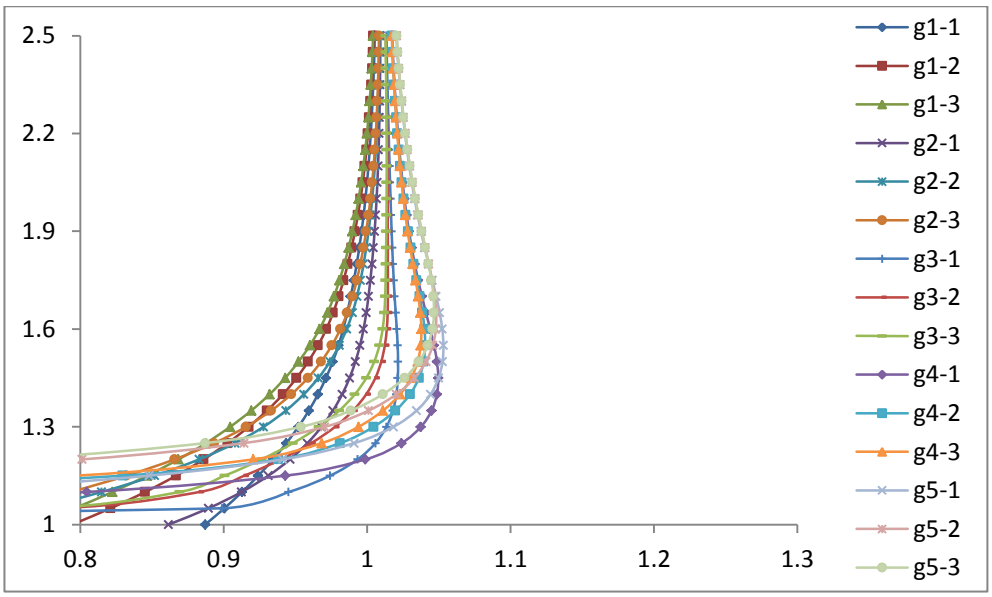
2.5
2.2
1.9
1.6
1.3
1
0.8
0.9
1
1.1
1.2
1.3
g1-1
g1-2
g1-3
g2-1
g2-2
g2-3
g3-1
g3-2
g3-3
g4-1
g4-2
g4-3
g5-1
g5-2
g5-3

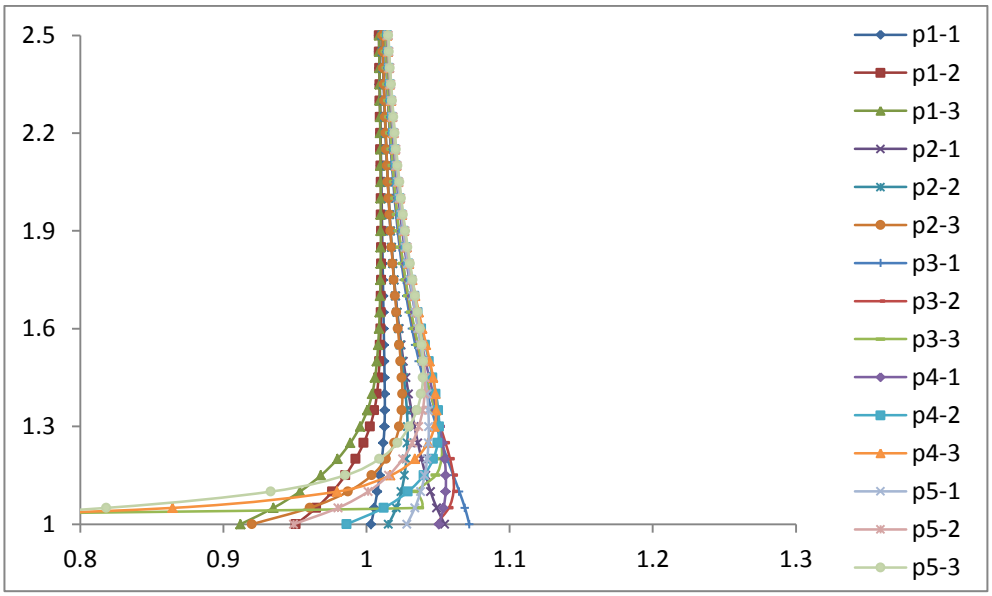
2.5
2.2
1.9
1.6
1.3
1
0.8
0.9
1
1.1
1.2
1.3
p1-1
p1-2
p1-3
p2-1
p2-2
p2-3
p3-1
p3-2
p3-3
p4-1
p4-2
p4-3
p5-1
p5-2
p5-3

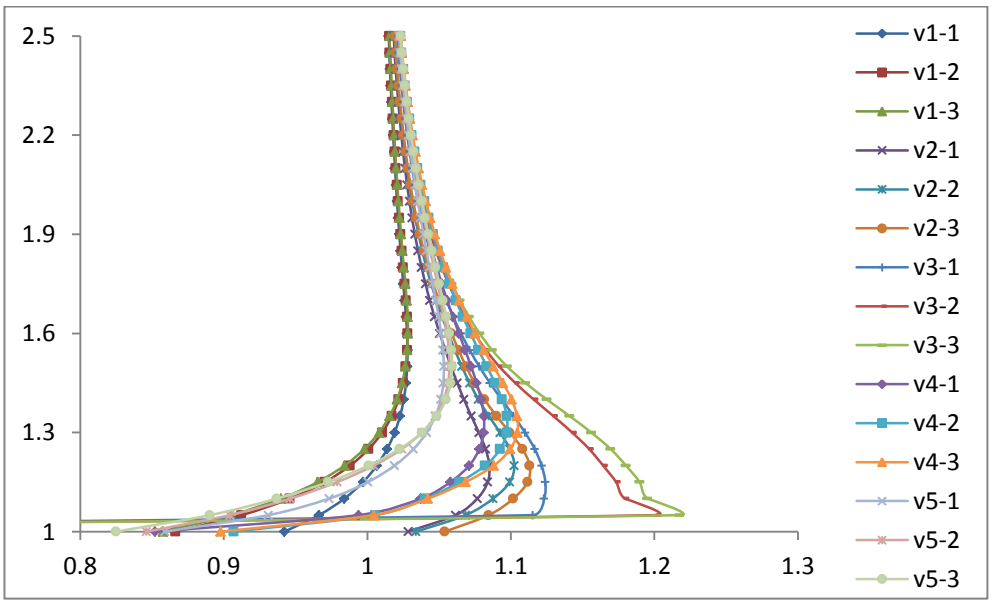
2.5
2.2
1.9
1.6
1.3
1
0.8
0.9
1
1.1
1.2
1.3
v1-1
v1-2
v1-3
v2-1
v2-2
v2-3
v3-1
v3-2
v3-3
v4-1
v4-2
v4-3
v5-1
v5-2
v5-3

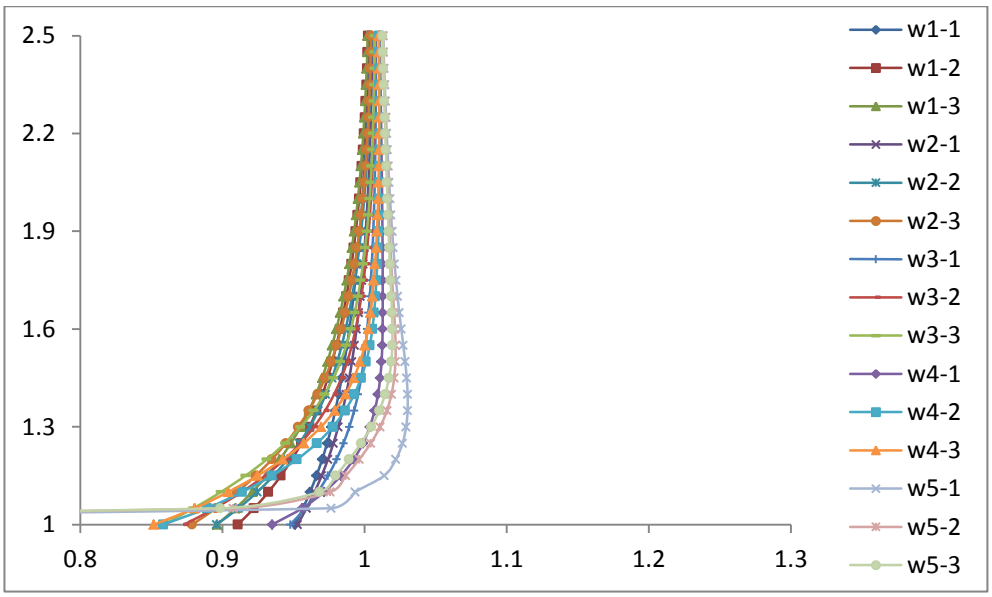

Appendix 4: Turbulence intensity plots for all roof shapes at 45^0 wind direction

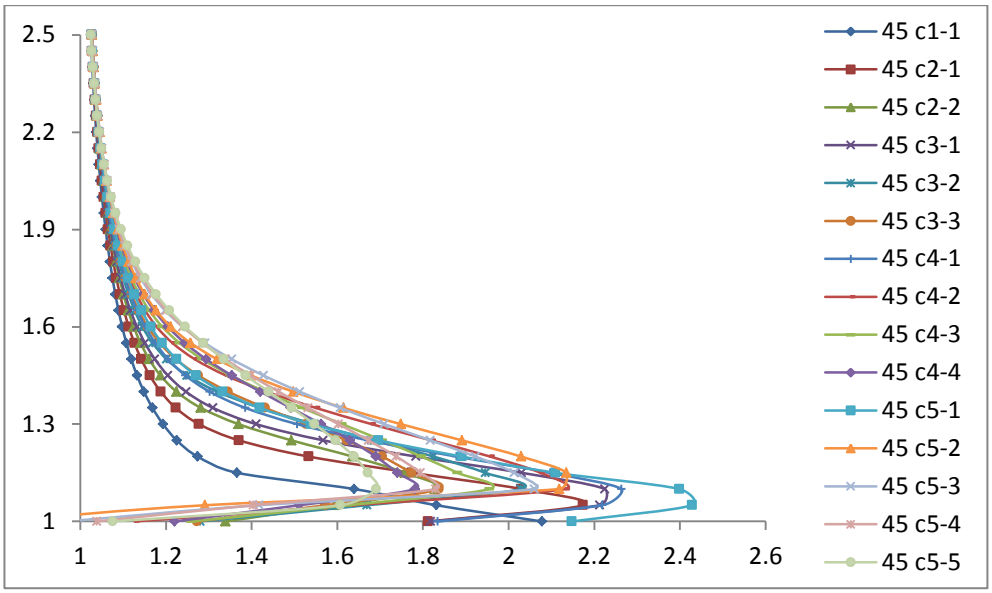

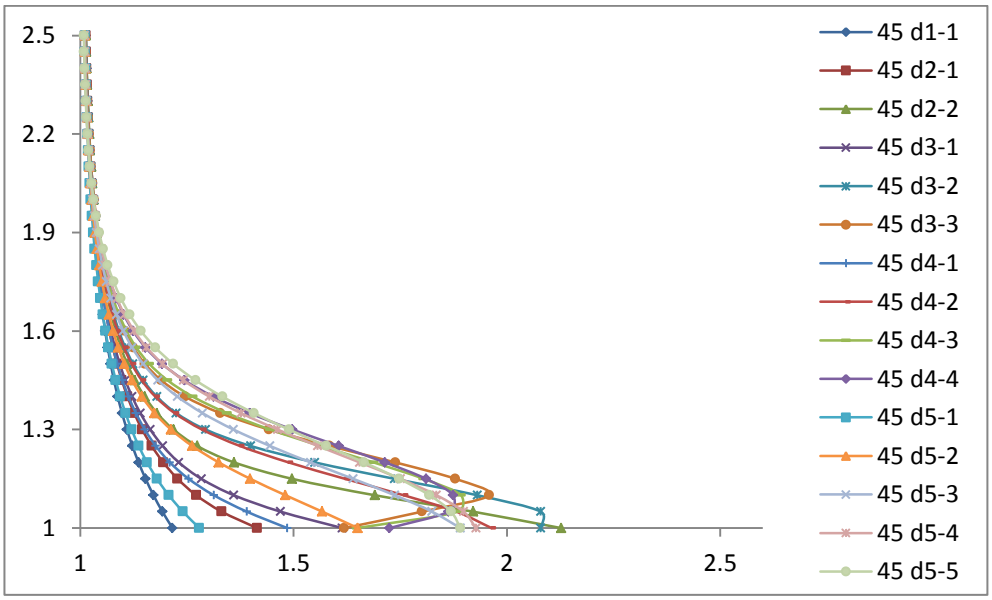

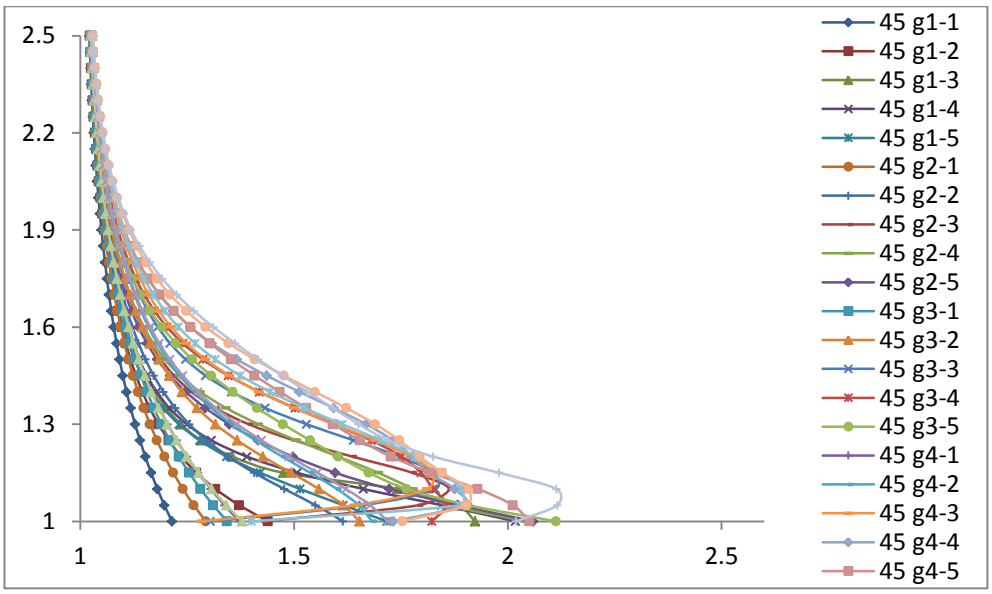
2.5
2.2
1.9
1.6
1.3
1
1
1.5
2
2.5
45 g1-1
45 g1-2
45 g1-3
45 g1-4
45 g1-5
45 g2-1
45 g2-2
45 g2-3
45 g2-4
45 g2-5
45 g3-1
45 g3-2
45 g3-3
45 g3-4
45 g3-5
45 g4-1
45 g4-2
45 g4-3
45 g4-4
45 g4-5

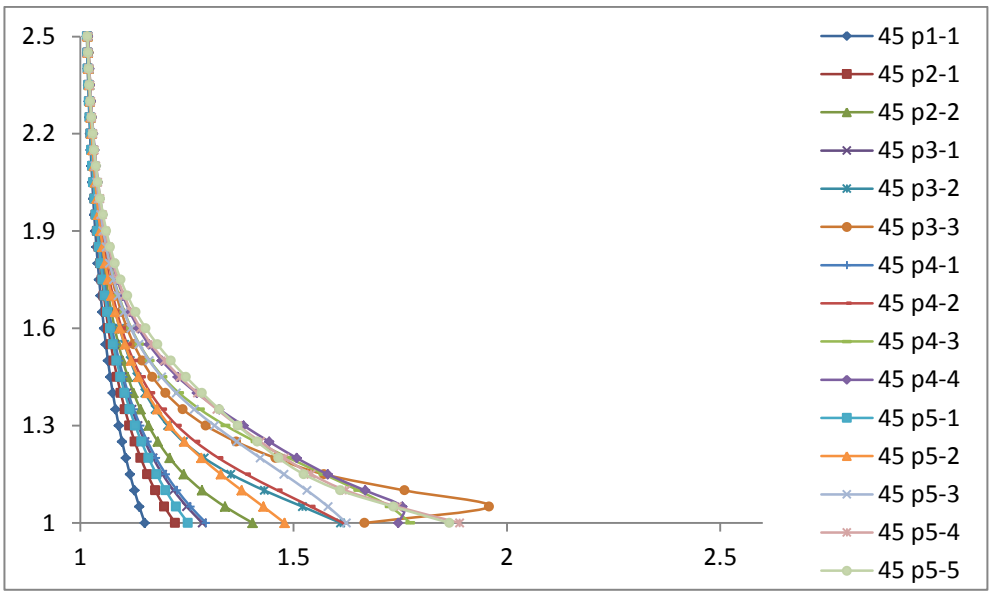
2.5
2.2
1.9
1.6
1.3
1
1
1.5
2
2.5
45 p1-1
45 p2-1
45 p2-2
45 p3-1
45 p3-2
45 p3-3
45 p4-1
45 p4-2
45 p4-3
45 p4-4
45 p5-1
45 p5-2
45 p5-3
45 p5-4
45 p5-5

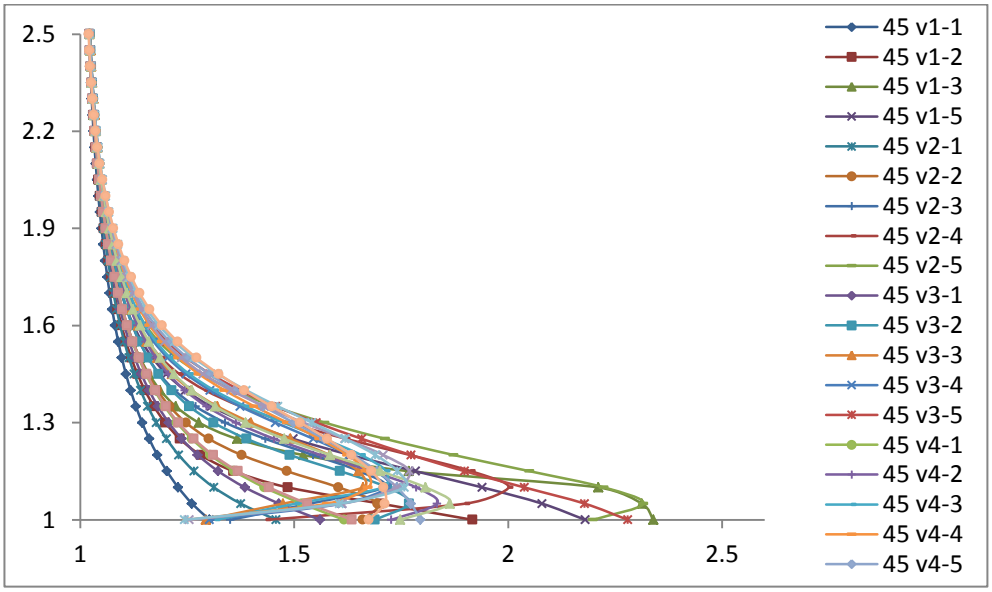
2.5
2.2
1.9
1.6
1.3
1
1
1.5
2
2.5
45 v1-1
45 v1-2
45 v1-3
45 v1-5
45 v2-1
45 v2-2
45 v2-3
45 v2-4
45 v2-5
45 v3-1
45 v3-2
45 v3-3
45 v3-4
45 v3-5
45 v4-1
45 v4-2
45 v4-3
45 v4-4
45 v4-5

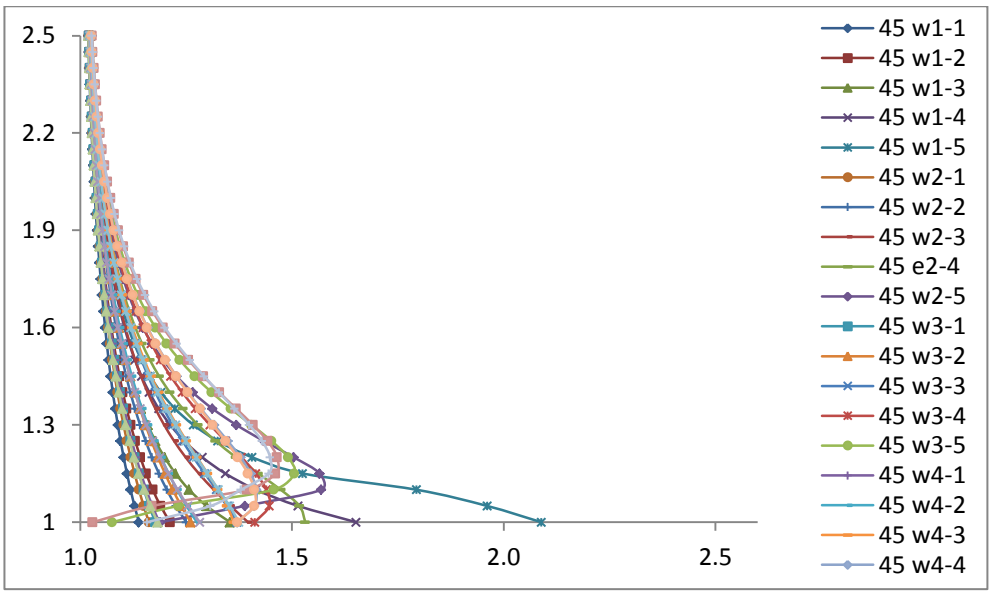

Appendix 5: Streamwise velocity plots for all roof shapes at 45^0 wind direction

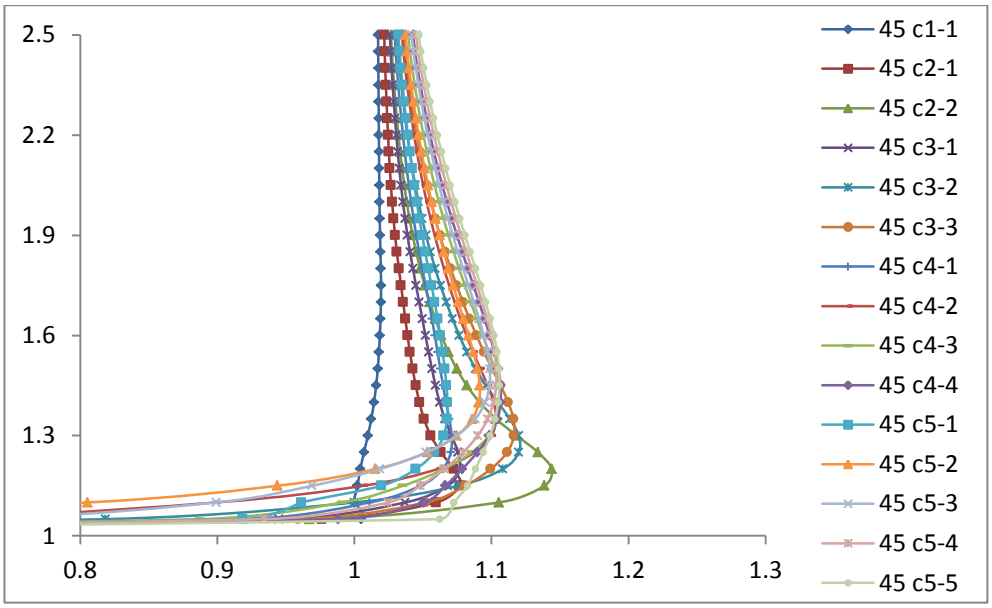

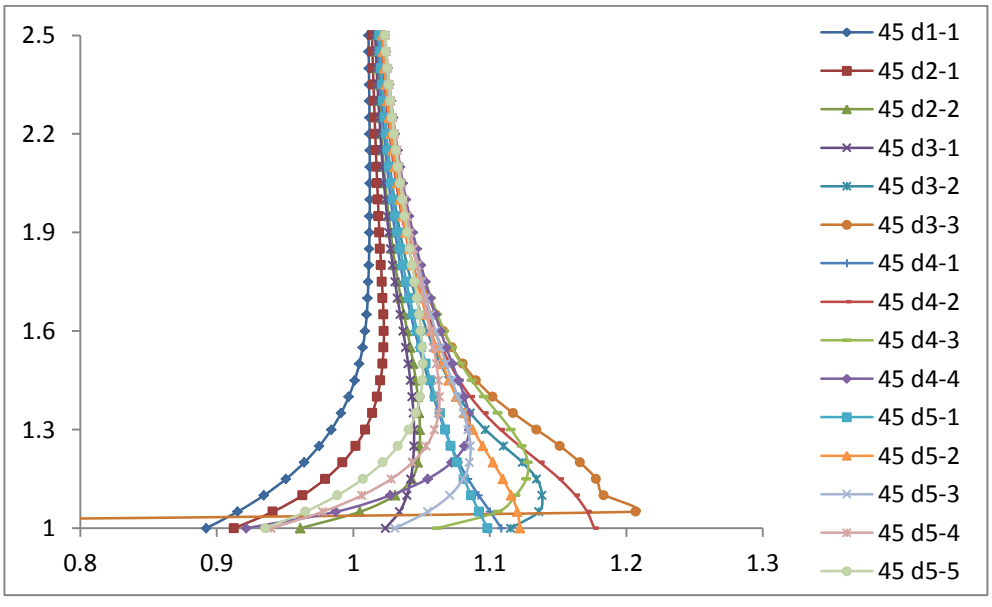

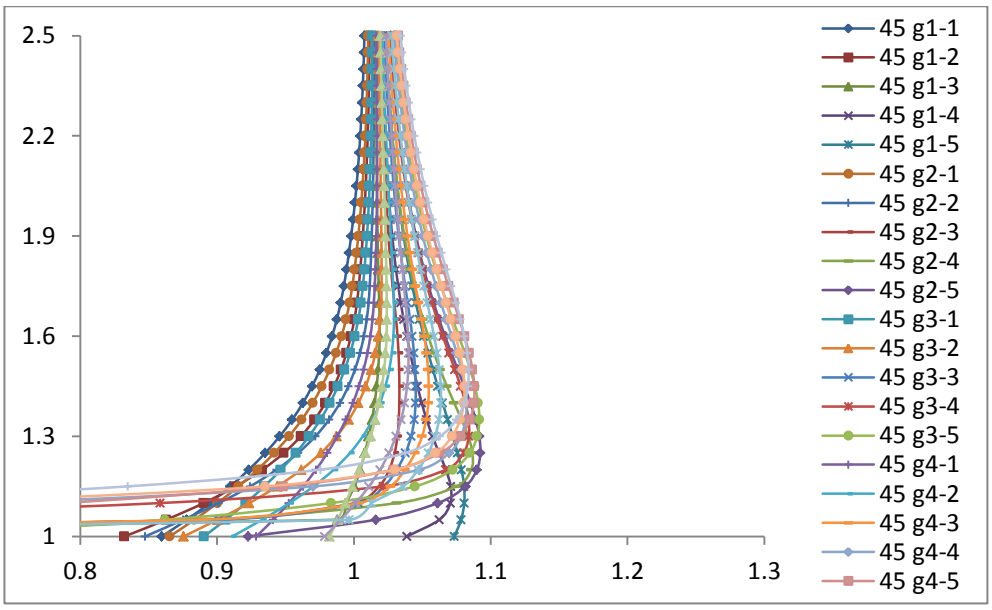
2.5
2.2
1.9
1.6
1.3
1
0.8
0.9
1
1.1
1.2
1.3
45 g1-1
45 g1-2
45 g1-3
45 g1-4
45 g1-5
45 g2-1
45 g2-2
45 g2-3
45 g2-4
45 g2-5
45 g3-1
45 g3-2
45 g3-3
45 g3-4
45 g3-5
45 g4-1
45 g4-2
45 g4-3
45 g4-4
45 g4-5

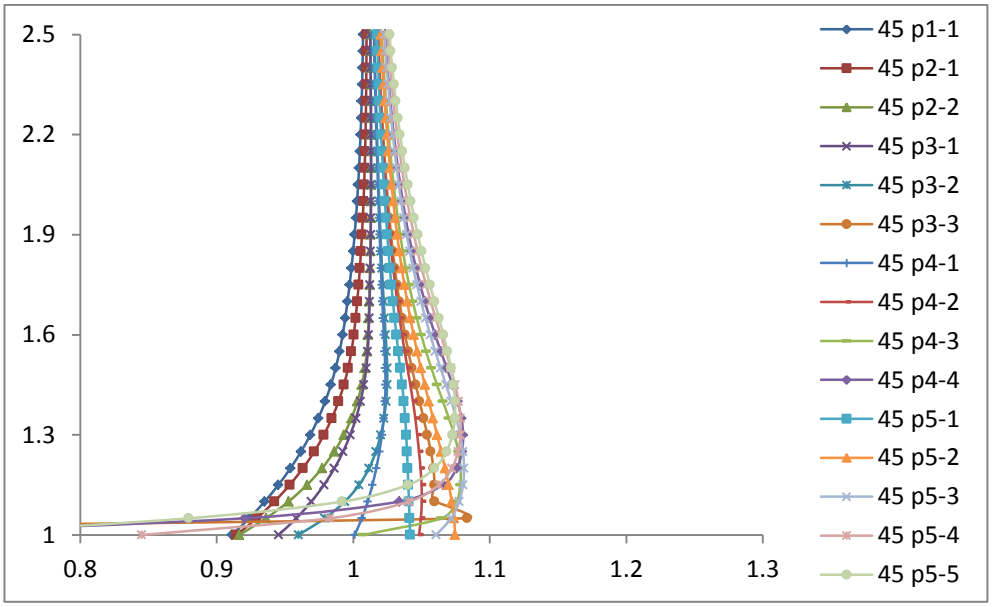
2.5
2.2
1.9
1.6
1.3
1
0.8
0.9
1
1.1
1.2
1.3
45 p1-1
45 p2-1
45 p2-2
45 p3-1
45 p3-2
45 p3-3
45 p4-1
45 p4-2
45 p4-3
45 p4-4
45 p5-1
45 p5-2
45 p5-3
45 p5-4
45 p5-5

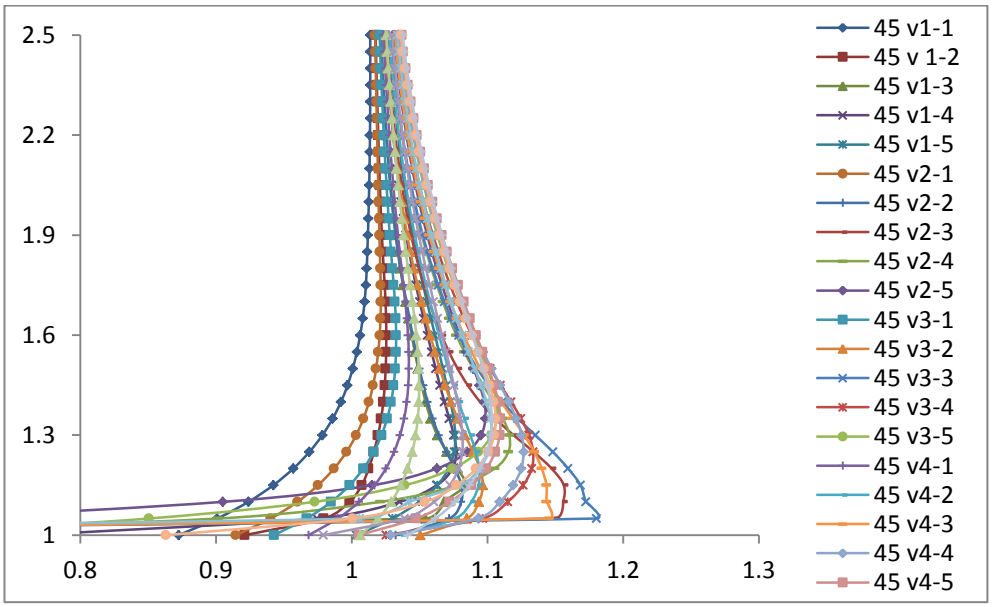
2.5
2.2
1.9
1.6
1.3
1
0.8
0.9
1
1.1
1.2
1.3
45 v1-1
45 v 1-2
45 v1-3
45 v1-4
45 v1-5
45 v2-1
45 v2-2
45 v2-3
45 v2-4
45 v2-5
45 v3-1
45 v3-2
45 v3-3
45 v3-4
45 v3-5
45 v4-1
45 v4-2
45 v4-3
45 v4-4
45 v4-5

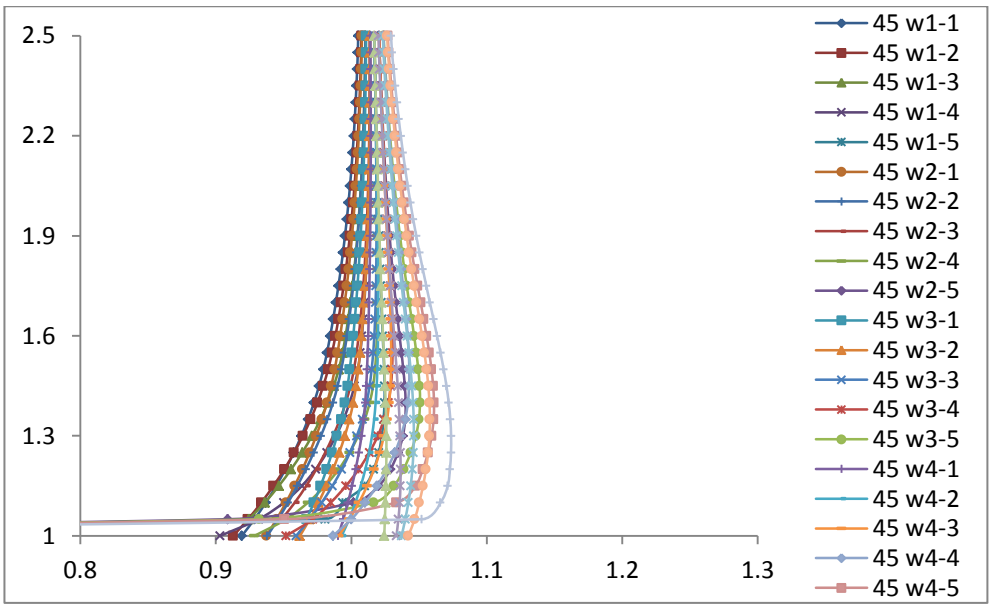

Appendix 6: Turbulence intensity plots for the gabled, vaulted and the wedged roofs at 90^0 wind direction

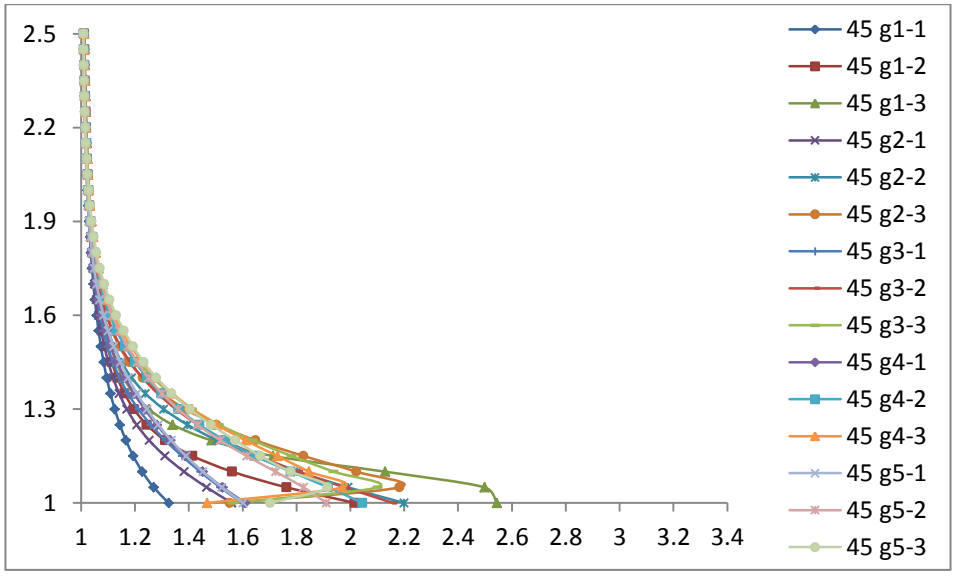

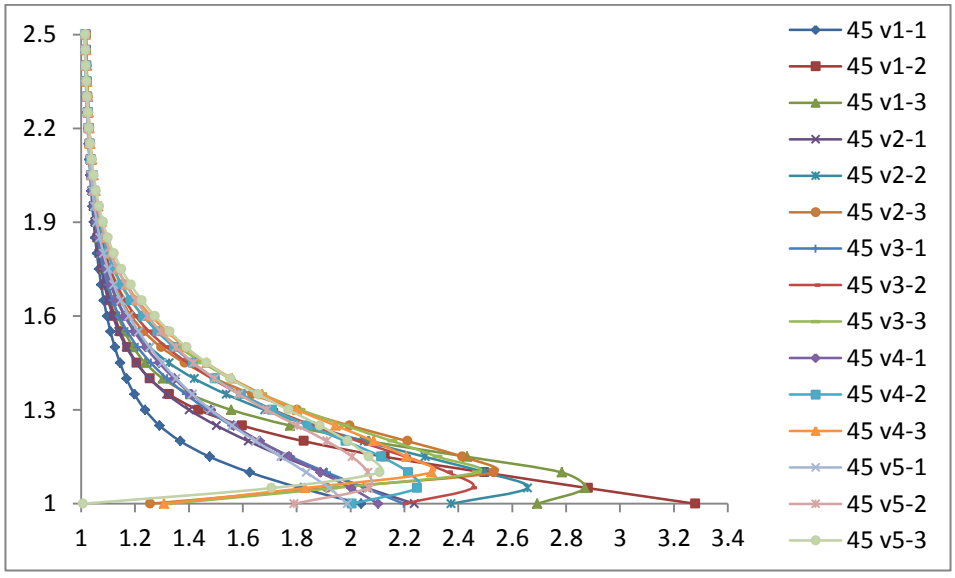

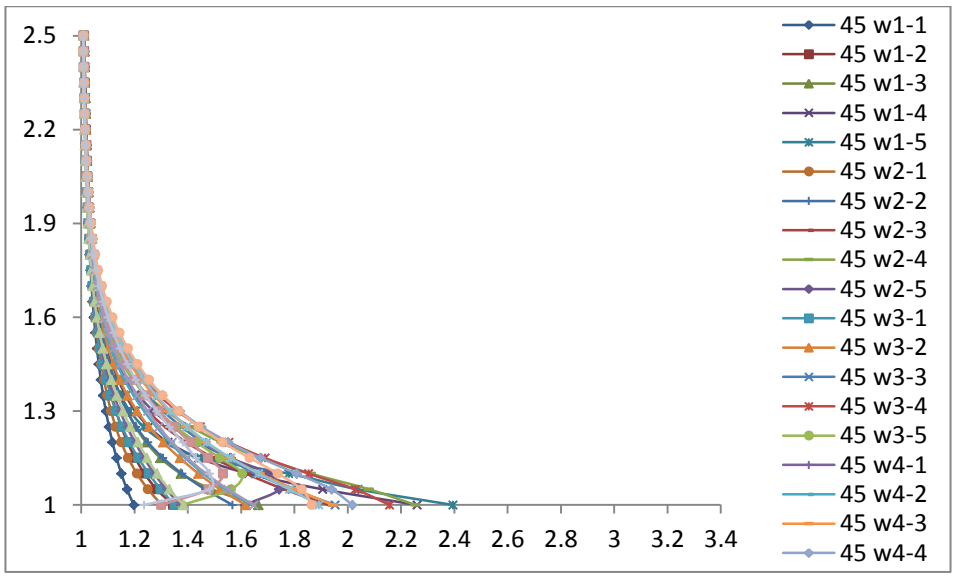

Appendix 7: Streamwise velocity plots for the gabled, vaulted and the wedged roofs at 90^0 wind direction

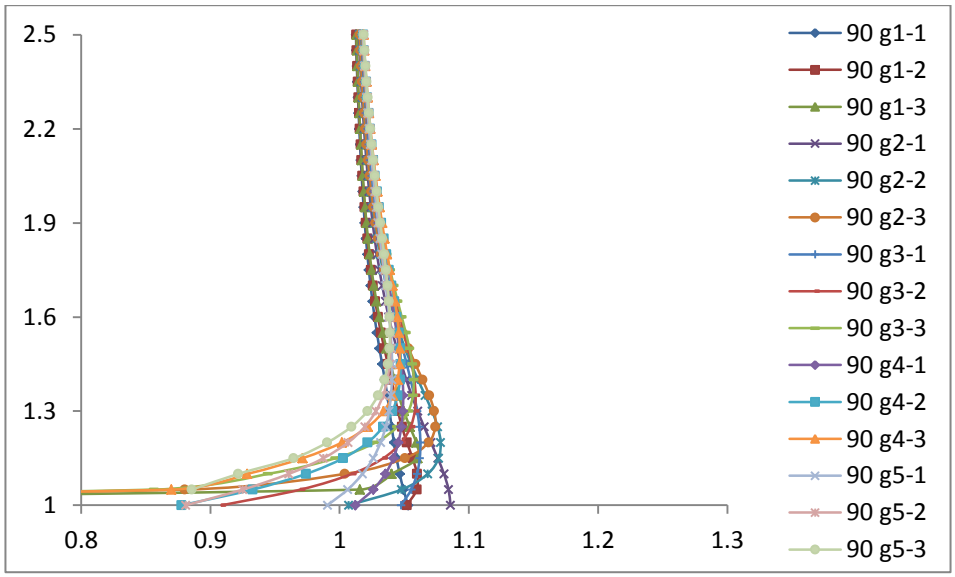

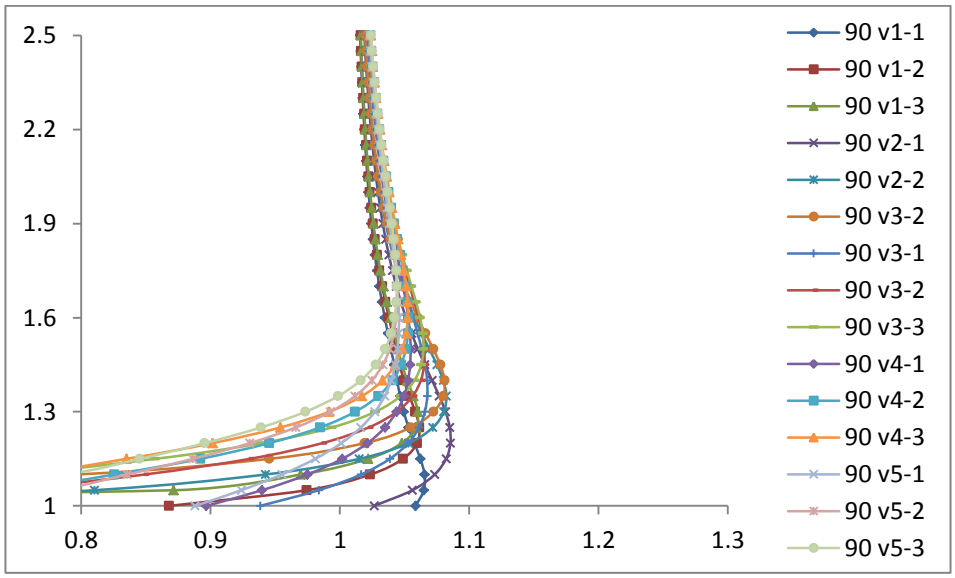

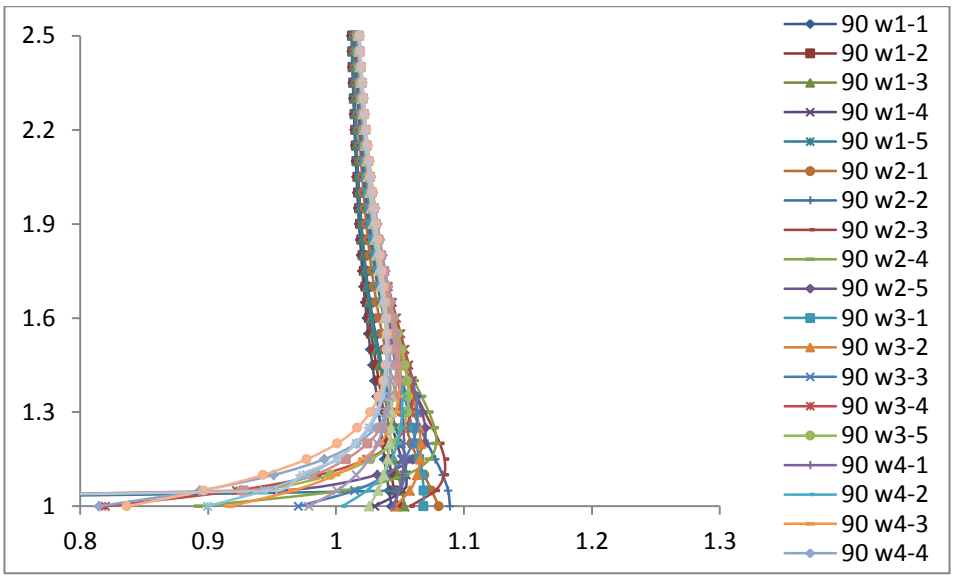

Appendix 8: Turbulence intensity plots for the wedged roofs at 135^0 wind direction

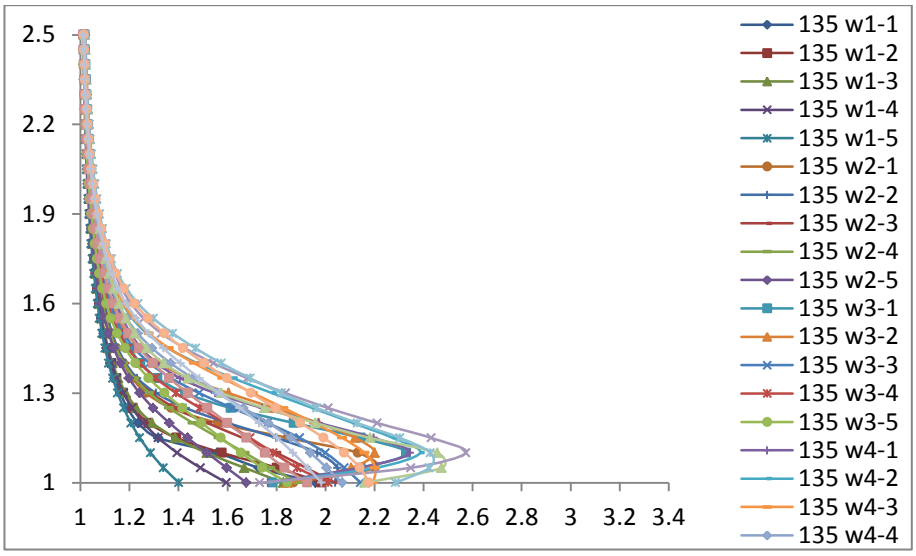

Appendix 9: Streamwise velocity plots for the wedged roofs at 135^0 wind direction

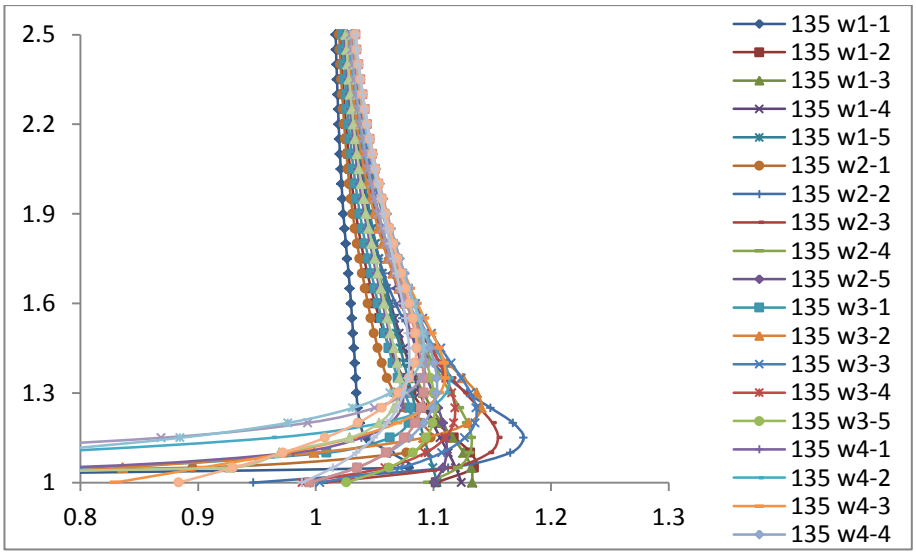

Appendix 10: Turbulence intensity plots for the wedged roofs at 180^0 wind direction

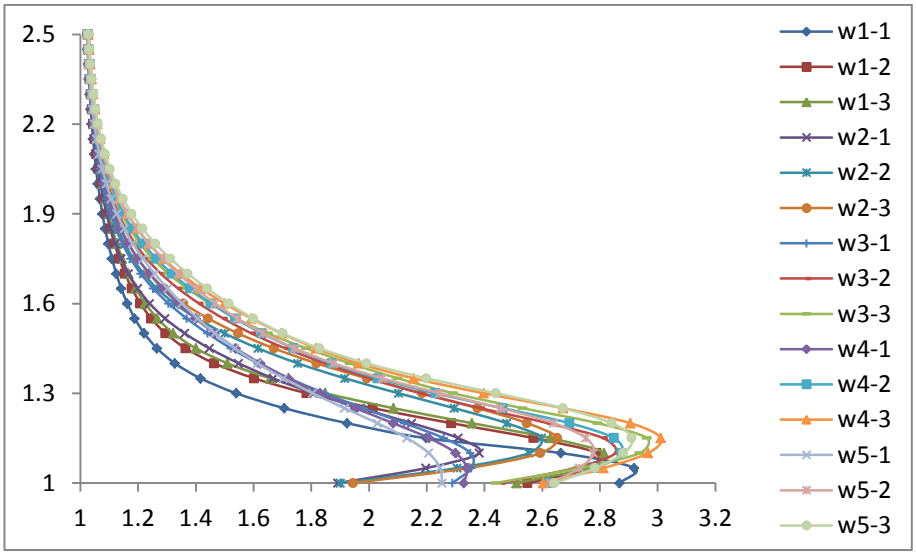

Appendix 11: Streamwise velocity plots for the wedged roofs at 180^0 wind direction

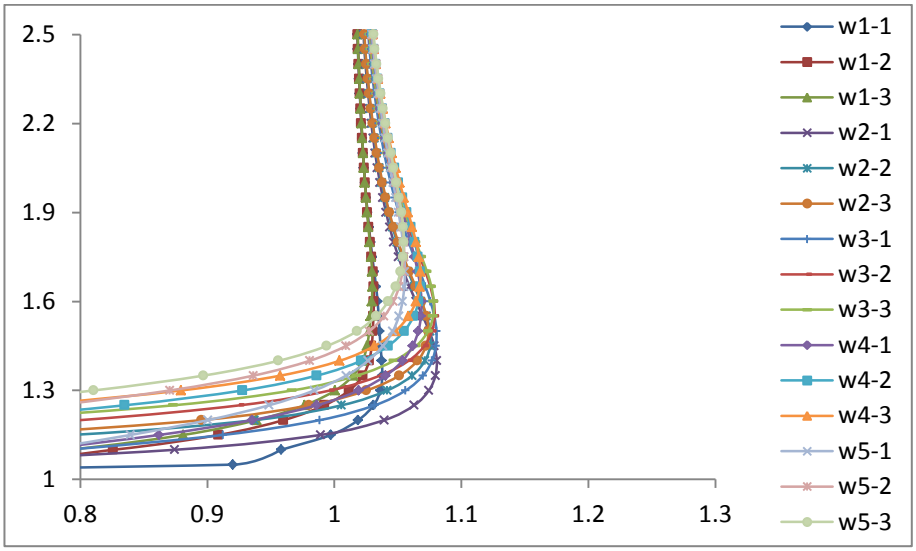

Appendix 12: Turbulence intensity plots for the 12m vaulted roof building

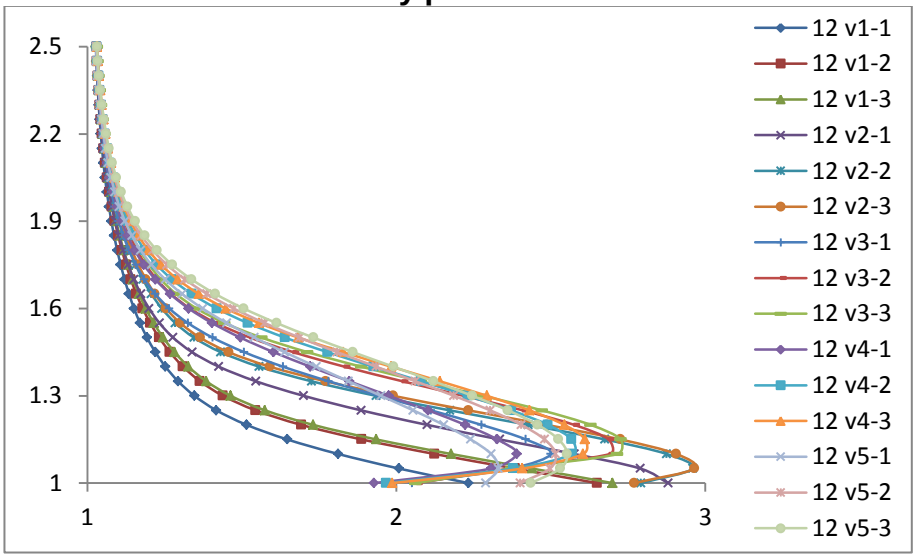

Appendix 13: Streamwise velocity plots for the 12m vaulted roof building

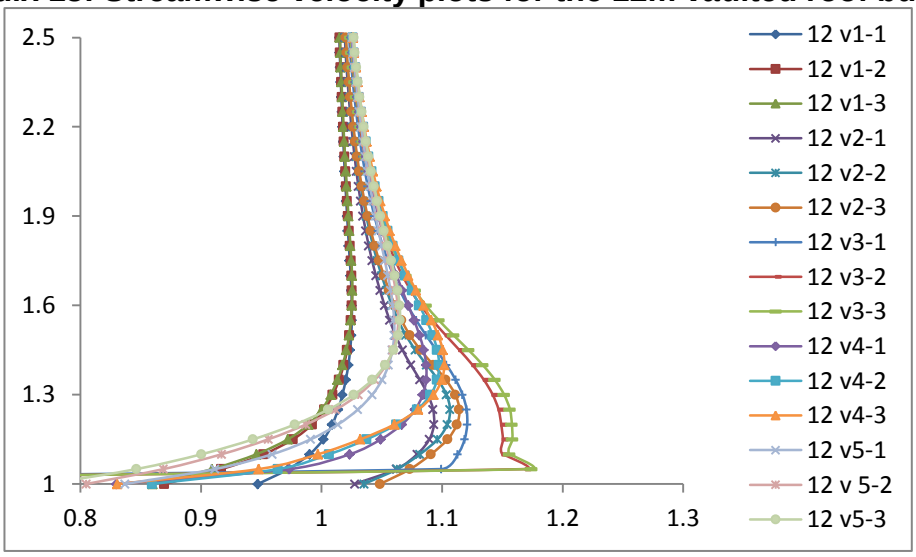

Appendix 14: Turbulence intensity plots for the 24m vaulted roof building

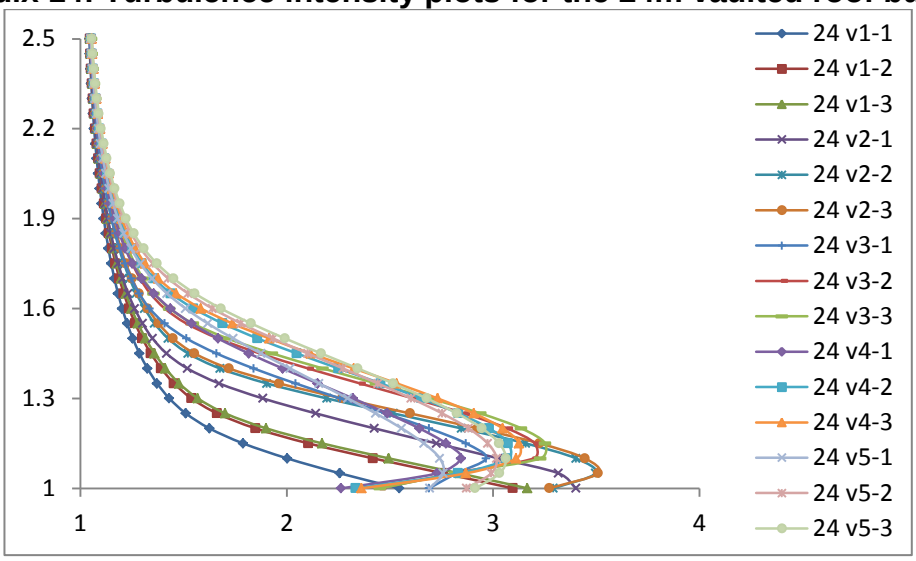

Appendix 15: Streamwise velocity plots for the 24m vaulted roof building

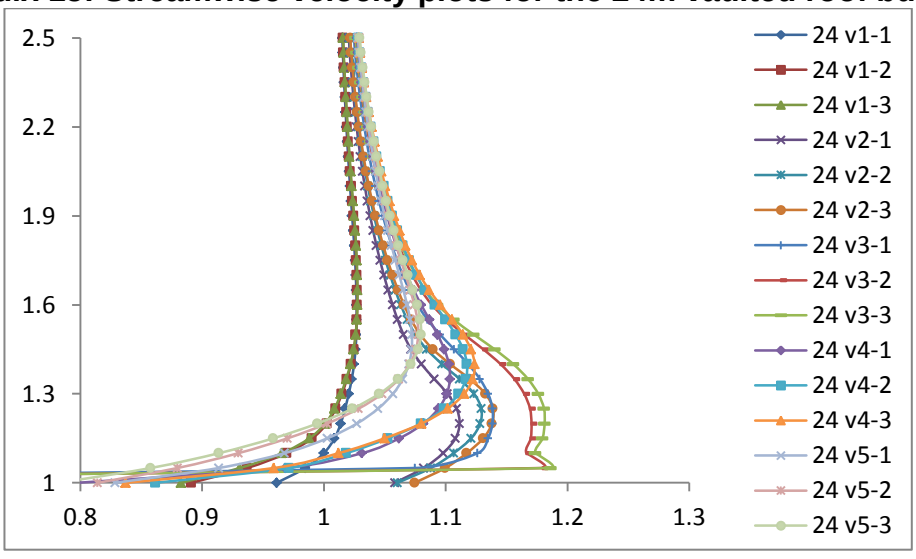

Appendix 16: Turbulence intensity plots for the 4.5m vaulted roof building within an urban canyon configuration

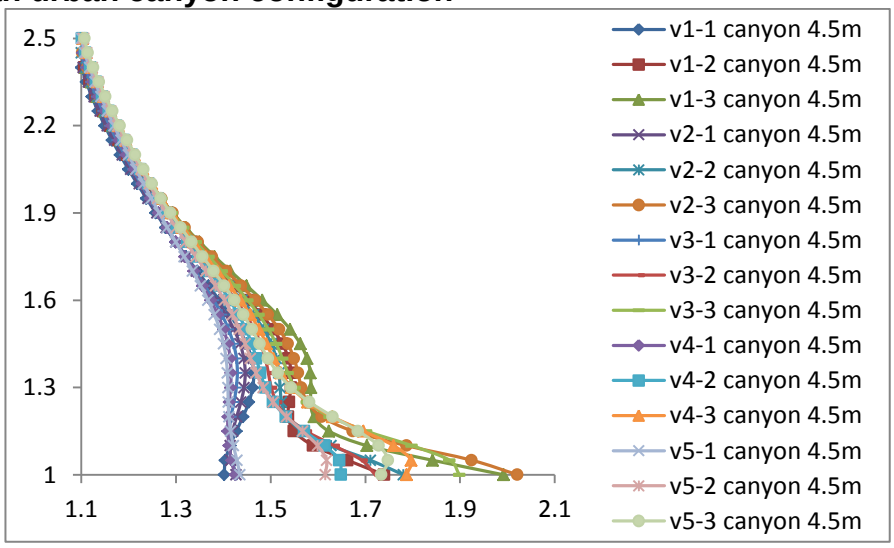

Appendix 17: Turbulence intensity plots for the 4.5m vaulted roof building within staggered urban configuration

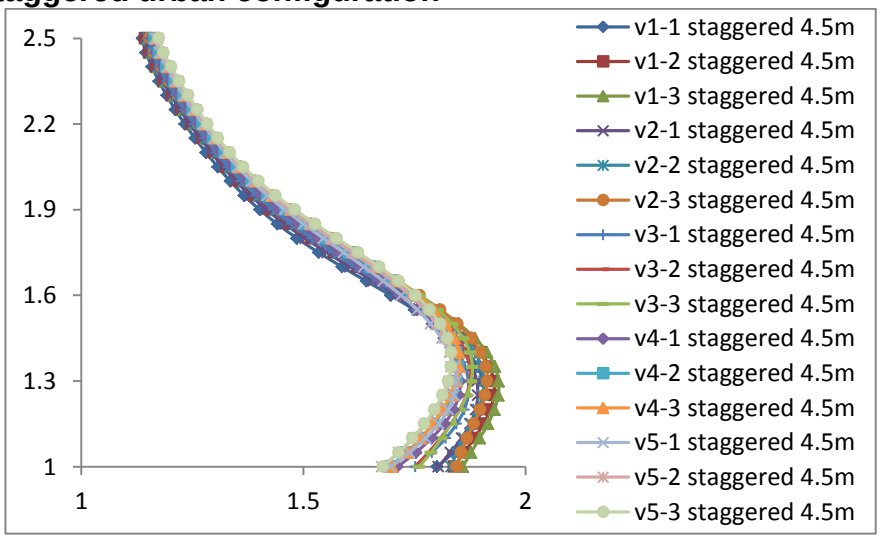

Appendix 18: Turbulence intensity plots for the 6m vaulted roof building within an urban canyon configuration

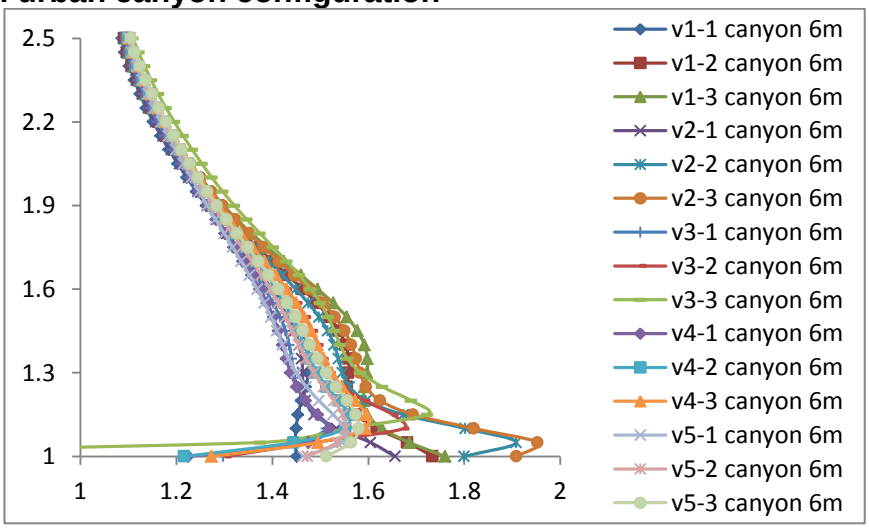

Appendix 19: Turbulence intensity plots for the 6m vaulted roof building within staggered urban configuration

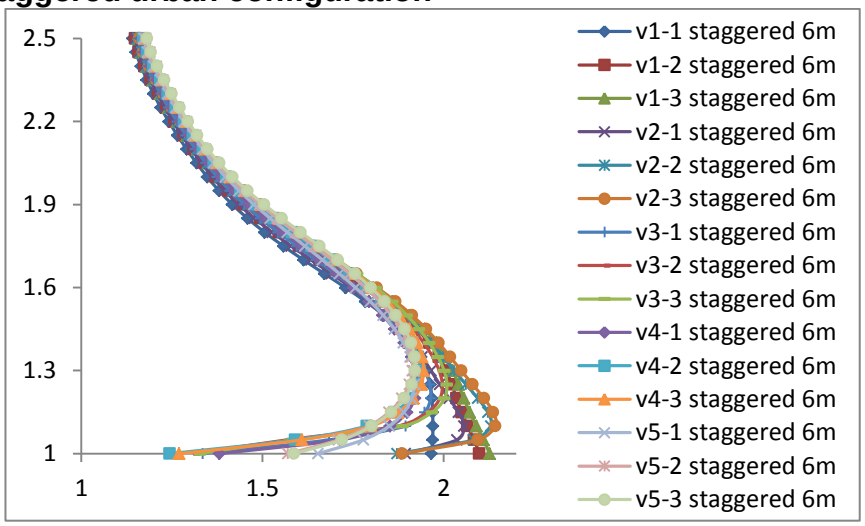

Appendix 20: Turbulence intensity plots for the 12m vaulted roof building within an urban canyon configuration

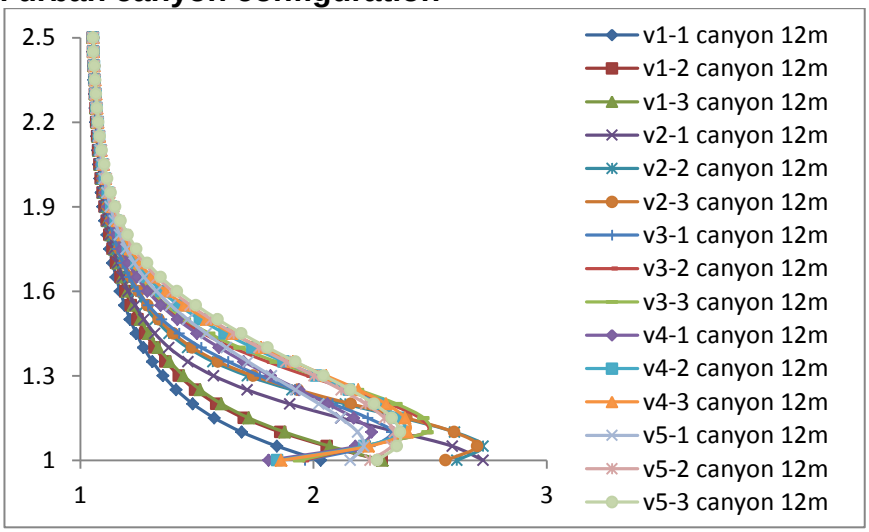

Appendix 21: Turbulence intensity plots for the 12m vaulted roof building within staggered urban configuration

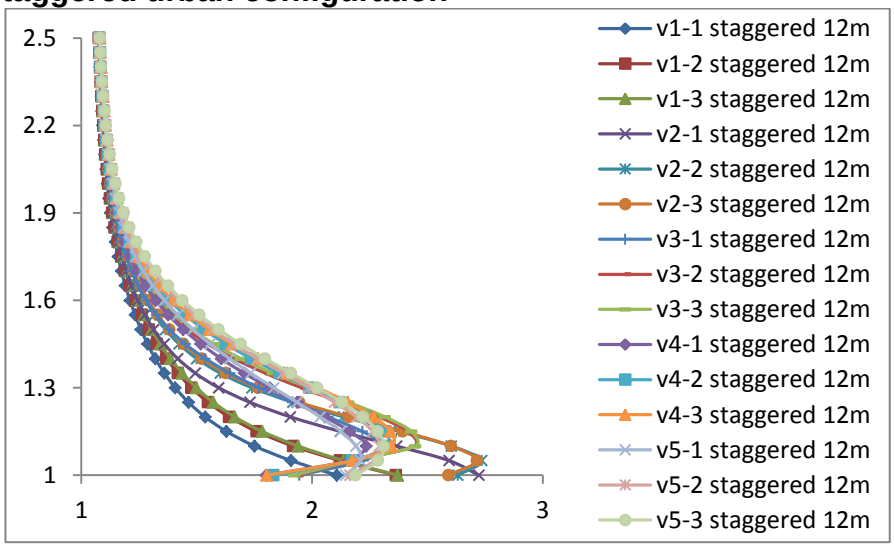

Appendix 22: Turbulence intensity plots for the 24m vaulted roof building within an urban canyon configuration

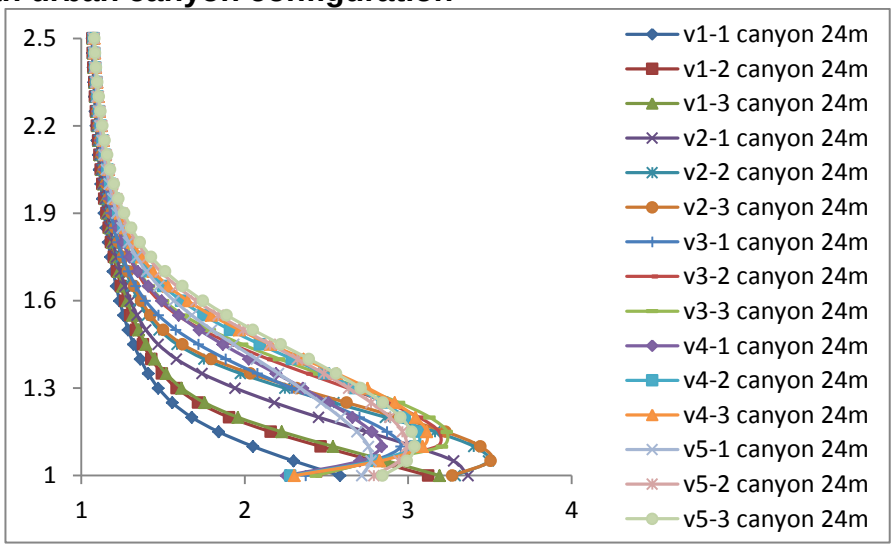

Appendix 23: Turbulence intensity plots for the 24m vaulted roof building within staggered urban configuration

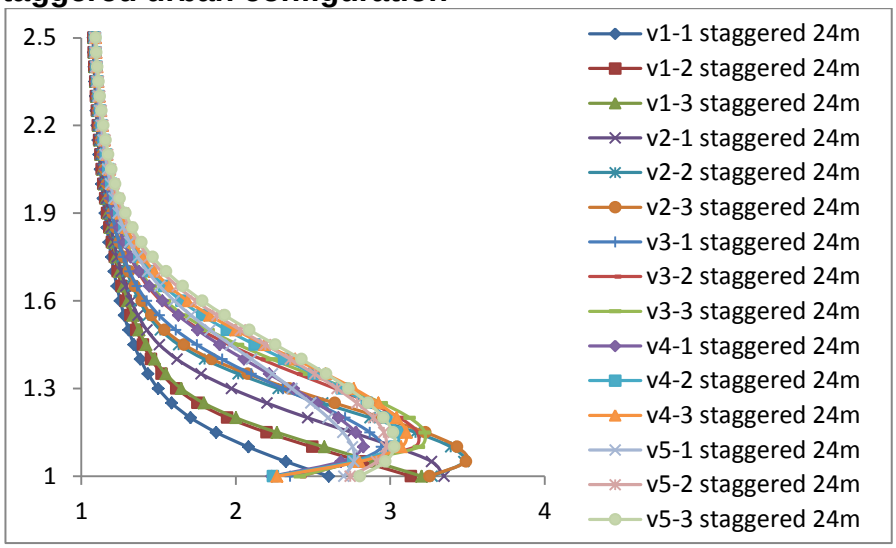

Appendix 24: Streamwise velocity plots for the 4.5m vaulted roof building within urban canyon configuration

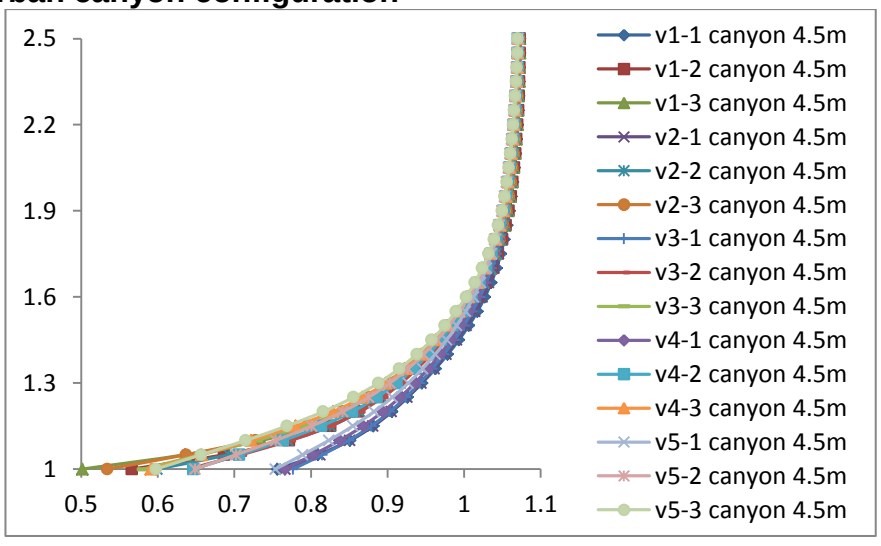

Appendix 25: Streamwise velocity plots for the 4.5m vaulted roof building within staggered urban configuration

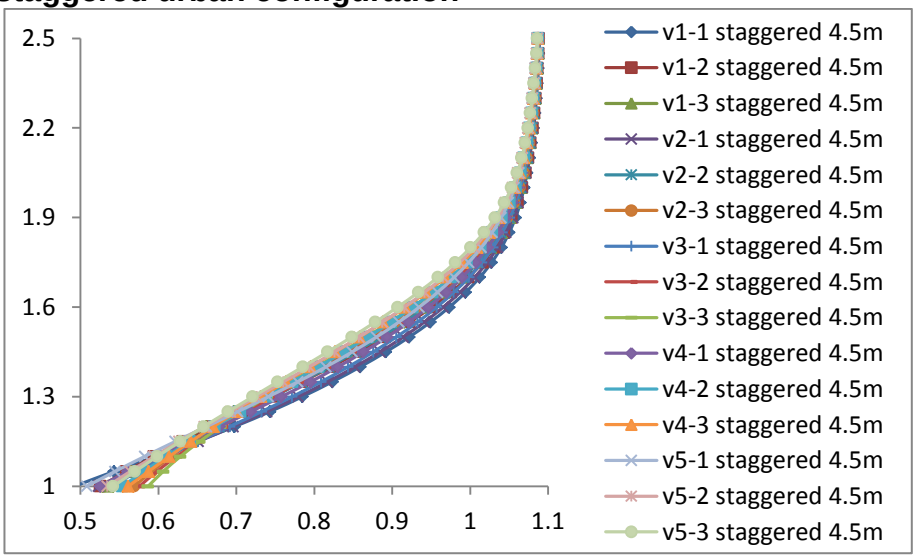

Appendix 26: Streamwise velocity plots for the 6m vaulted roof building within urban canyon configuration

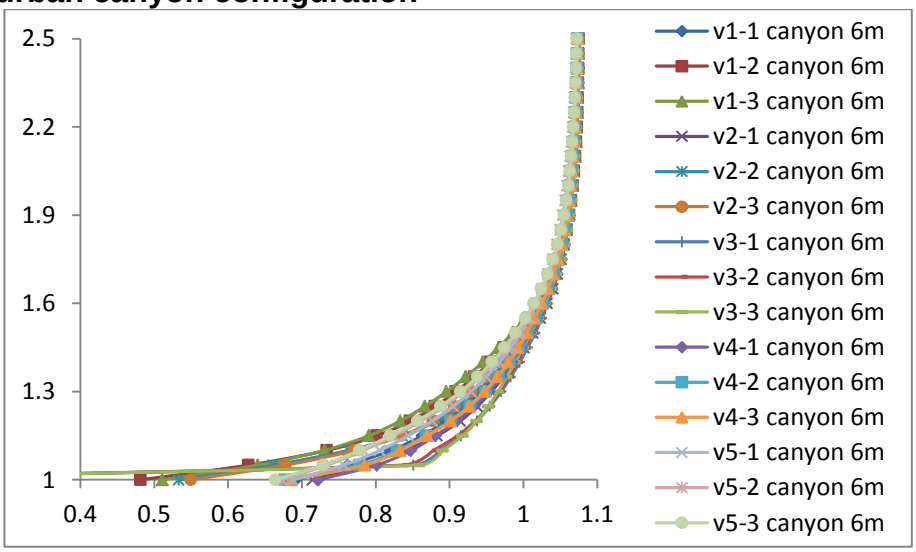

Appendix 27: Streamwise velocity plots for the 6m vaulted roof building within staggered urban configuration

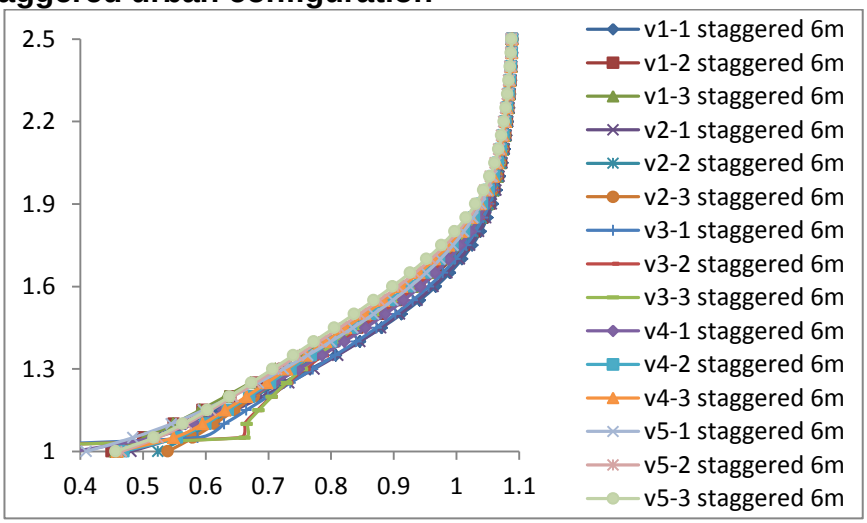

Appendix 28: Streamwise velocity plots for the 12m vaulted roof building within urban canyon configuration

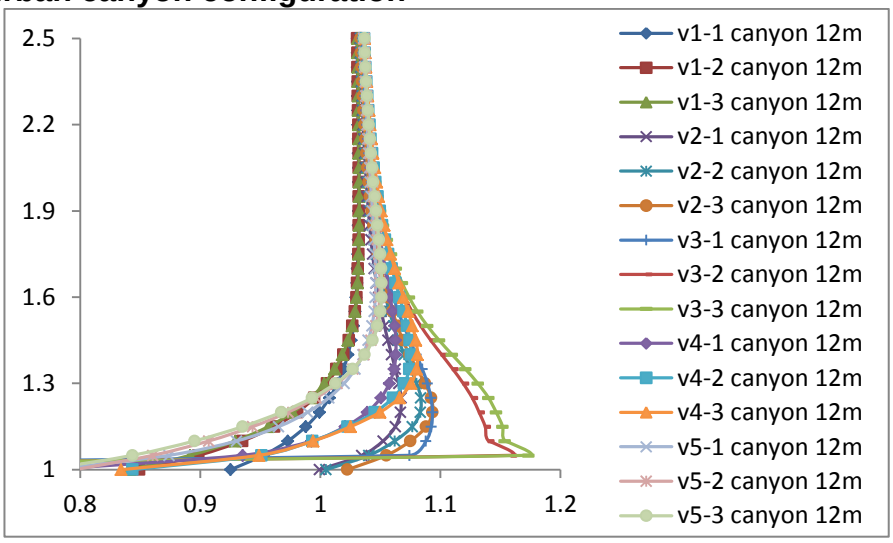

Appendix 29: Streamwise velocity plots for the 12m vaulted roof building within staggered urban configuration

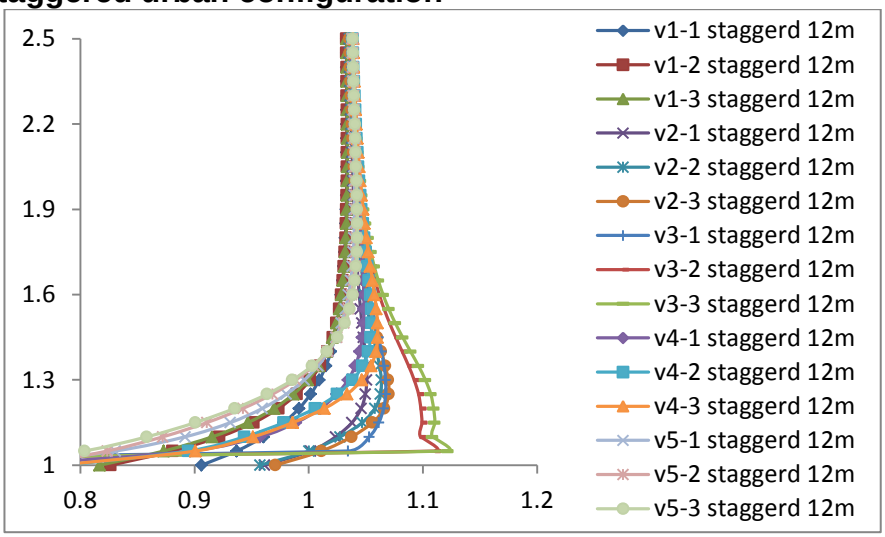

Appendix 30: Streamwise velocity plots for the 24m vaulted roof building within urban canyon configuration

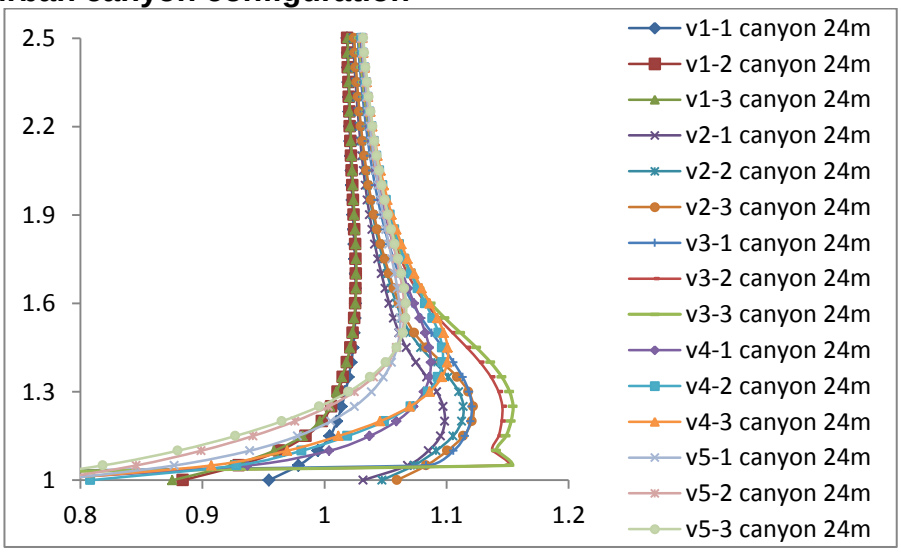

Appendix 31: Streamwise velocity plots for the 24m vaulted roof building within staggered urban configuration

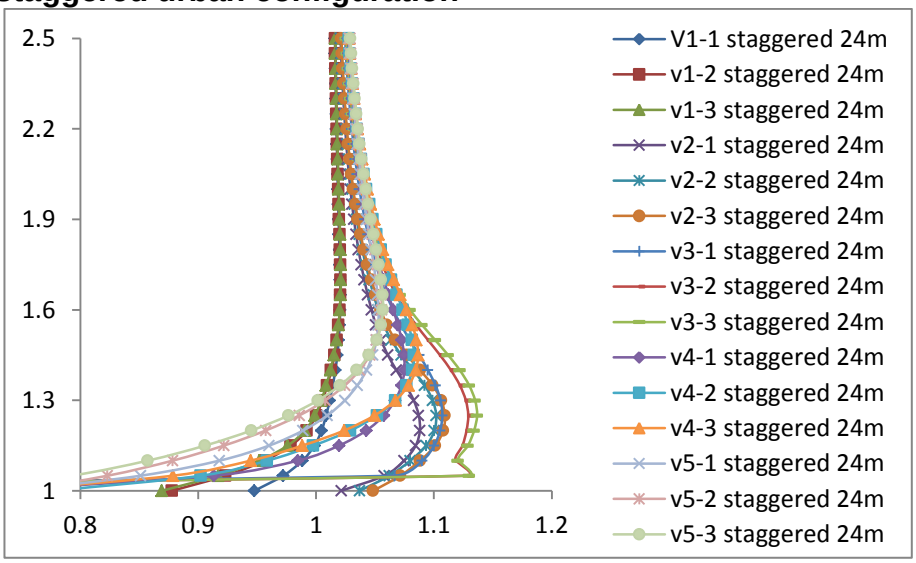

References

References

Ackermann, T. and Söder, L. (2002) 'An overview of wind energy-status 2002', *Renewable and Sustainable Energy Reviews*, 6(1-2), pp. 67-127.

Ages, E.M. (2010) 'History of wind power', *Wind Power Overview*, p. 23.

Aguiló, A., Taylor, D., Quinn, A. and Wiltshire, D.R. (2009) *Computational Fluid Dynamic Modelling of wind speed enhancement through a building augmented wind concentration system*. Available at: http://www.2004ewec.info/files/23_1400_derektaylor_01.pdf (Accessed: 20-01-2010).

Ahshan, R., Iqbal, M.T. and Mann, G.K.I. (2008) 'Controller for a small induction-generator based wind-turbine', *Applied Energy*, 85(4), pp. 218-227.

Allen, S.R., Hammond, G.P., Harajli, H.A., Jones, C.I., McManus, M.C. and Winnett, A.B. (2008a) 'Integrated appraisal of micro-generators: methods and applications', *Proceedings of the Institution of Civil Engineers, Energy*, 161(2), pp. 73-86.

Allen, S.R., Hammond, G.P. and McManus, M.C. (2008b) 'Energy analysis and environmental life cycle assessment of a micro-wind turbine', *Proceedings of the Institution of Mechanical Engineers, Part A: Journal of Power and Energy*, 222(7), pp. 669-684.

Andersen, P.D. (2007) *Review of historical and modern utilization of wind power*. Wind Energy & Atmospheric Physics Dept., Risø National Laboratory.

Anderson, D., Whale, J., Livingston, P.O. and Chan, D. (2008) *Rooftop Wind Resource Assessment using a Three-Dimensional Ultrasonic Anemometer*. Available at: http://www.ontario-sea.org/Storage/26/1798_A_Wind_Resource_Assessment_on_a_Rooftop_Using__3D_Ultrasonic_Anemometer.pdf (Accessed: 20-01-2010).

Anderson, J. (1995) *Computational Fluid Dynamics, The Basics with Applications*. New York: McGraw-Hill Science/Engineering/Math.

Ariff, M., SALIM, S.M. and CHEAH, S.C. (2009a) 'Wall Y+approach for dealing with turbulent flow over a surface mounted cube: Part 1 – High Reynolds number', *Seventh International Conference on CFD in the Minerals and Process Industries*. CSIRO, Melbourne, Australia, 9-11 December 2009. pp. 1-9. Available at: http://www.cfd.com.au/cfd_conf09/PDFs/142SAL.pdf.

Ariff, M., SALIM, S.M. and CHEAH, S.C. (2009b) 'Wall Y+approach for dealing with turbulent flow over a surface mounted cube: Part 2 – High

Reynolds number', *Seventh International Conference on CFD in the Minerals and Process Industries*. CSIRO, Melbourne, Australia, 9-11 December 2009. pp. 1-9. Available at: http://www.cfd.com.au/cfd_conf09/PDFs/142SAL.pdf.

ASCE (1996) 'Wind-tunnel studies if building and structures', *Journal of Aerospace Engineering, American Society of Civil Engineers* Vol. 9(1), pp. 19-36.

Asfour, O.S. and Gadi, M.B. (2007) 'A comparison between CFD and Network models for predicting wind-driven ventilation in buildings', *Building and Environment*, 42(12), pp. 4079-4085.

Asfour, O.S. and Gadi, M.B. (2008) 'Using CFD to investigate ventilation characteristics of vaults as wind-inducing devices in buildings', *Applied Energy*, 85(12), pp. 1126-1140.

Augenbroe, G. (2004) 'Trends in building simulation', in Malkawi, A.M. and Augenbroe, G. (eds.) *Advanced Building Simulation*. Oxfordshire: Spon Press, pp. 04-24.

Ayata, T. (2009) 'Investigation of building height and roof effect on the air velocity and pressure distribution around the detached houses in Turkey', *Applied Thermal Engineering*, 29(8-9), pp. 1752-1758.

Bahaj, A.S., Myers, L. and James, P.A.B. (2007) 'Urban energy generation: Influence of micro-wind turbine output on electricity consumption in buildings', *Energy and Buildings*, 39(2), pp. 154-165.

Balduzzi, F., Bianchini, A., Carnevale, E.A., Ferrari, L. and Magnani, S. (2012) 'Feasibility analysis of a Darrieus vertical-axis wind turbine installation in the rooftop of a building', *Applied Energy*, (0).

Barbason, M., van Moeseke, G. and Reiter, S. (2010) *7th Conference on Indoor Air Quality, Ventilation and Energy Conservation in buildings (IAQVEC 2010)*. Syracuse, USA.

Baskaran, A. and Kashef, A. (1996) 'Investigation of air flow around buildings using computational fluid dynamics techniques', *Engineering Structures*, 18(11), pp. 861-873.

Baskaran, A. and Stathopoulos, T. (1994) 'Prediction of wind effects on buildings using computational methods — review of the state of the art', *Canadian Journal of Civil Engineering*, 21(5), pp. 805-822.

Beyers, J.H.M., Sundsbø, P.A. and Harms, T.M. (2004) 'Numerical simulation of three-dimensional, transient snow drifting around a cube', *Journal of Wind Engineering and Industrial Aerodynamics*, 92(9), pp. 725-747.

Bhutta, A., Mahmood, M., Hayat, N.F., Ahmed, U., Ali, Z., Jamil, S.R. and Hussain, Z. (2012) 'Vertical axis wind turbine – A review of various

configurations and design techniques', *Renewable and Sustainable Energy Reviews*, 16(4), pp. 1926-1939.

Blackmore, P. (2008) *Siting micro-wind turbines on house roofs*. Watford: BRE.

Blackmore, P. (2010) *Building-mounted micro-wind turbines on high-rise and commercial buildings*. Watford: BRE.

Blazek, J. (2001) *Computational Fluid Dynamics: Principles and Applications*. First edition edn. Oxford: ELSEVIER.

Blocken, B. and Carmeliet, J. (2004) 'Pedestrian Wind Environment around Buildings: Literature Review and Practical Examples', *Journal of Thermal Envelope and Building Science*, 28(2), pp. 107-159.

Blocken, B. and Carmeliet, J. (2006) 'The influence of the wind-blocking effect by a building on its wind-driven rain exposure', *Journal of Wind Engineering and Industrial Aerodynamics*, 94(2), pp. 101-127.

Blocken, B., Carmeliet, J. and Stathopoulos, T. (2007a) 'CFD evaluation of wind speed conditions in passages between parallel buildings--effect of wall-function roughness modifications for the atmospheric boundary layer flow', *Journal of Wind Engineering and Industrial Aerodynamics*, 95(9-11), pp. 941-962.

Blocken, B., Moonen, P., Stathopoulos, T. and Carmeliet, J. (2008) 'Numerical Study on the Existence of the Venturi Effect in Passages between Perpendicular Buildings', *Journal of Engineering Mechanics*, 134(12), pp. 1021-1028.

Blocken, B. and Persoon, J. (2009) 'Pedestrian wind comfort around a large football stadium in an urban environment: CFD simulation, validation and application of the new Dutch wind nuisance standard', *Journal of Wind Engineering and Industrial Aerodynamics*, 97(5-6), pp. 255-270.

Blocken, B., Stathopoulos, T. and Carmeliet, J. (2007b) 'CFD simulation of the atmospheric boundary layer: wall function problems', *Atmospheric Environment*, 41(2), pp. 238-252.

Blocken, B., Stathopoulos, T., Carmeliet, J. and Hensen, J. (2010) *Application of CFD in building performance simulation for the outdoor environment: an overview*. Available at: http://sts.bwk.tue.nl/WindEngineering/pdf/2010_JBPS_Preprint_BB_TS_JC_JH.pdf (Accessed: 18 October 2010).

Blocken, B., Stathopoulos, T., Carmeliet, J. and Hensen, J.L.M. (2011) 'Application of computational fluid dynamics in building performance simulation for the outdoor environment: an overview', *Journal of Building Performance Simulation*, 4(2), pp. 157-184.

Booker, J.D., Mellor, P.H., Wrobel, R. and Drury, D. (2010) 'A compact, high efficiency contra-rotating generator suitable for wind turbines in the urban environment', *Renewable Energy*, 35(9), pp. 2027-2033.

Bradshaw, V. (2006) *The building environment : active and passive control systems*. Chichester: Wiley ; John Wiley.

Bright, J., Langston, R., Bullman, R., Evans, R., Gardner, S. and Pearce-Higgins, J. (2008) 'Map of bird sensitivities to wind farms in Scotland: A tool to aid planning and conservation', *Biological Conservation*, 141(9), pp. 2342-2356.

Burns, R.B. (2000) 'Introduction to research methods', *London: Thousand Oaks, Calif*.

Burton, T. (2001) *Wind energy : handbook*. Chichester ; New York: J. Wiley.

Campos-Arriaga, L. (2009) *Wind energy in the built environment: a design analysis using CFD and wind tunnel modelling approach*. PhD thesis. University of Nottingham [Online]. Available at: http://etheses.nottingham.ac.uk/806/.

Carpentieri, M., Hayden, P. and Robins, A.G. (2012) 'Wind tunnel measurements of pollutant turbulent fluxes in urban intersections', *Atmospheric Environment*, 46(0), pp. 669-674.

Carrete, M., Sánchez-Zapata, J.A., Benítez, J.R., Lobón, M., Montoya, F. and Donázar, J.A. (2012) 'Mortality at wind-farms is positively related to large-scale distribution and aggregation in griffon vultures', *Biological Conservation*, 145(1), pp. 102-108.

Castro, I.P. and Graham, J.M.R. (1999) 'Nymerical Wind Engineering: The way ahead?', *Proceedings of the ICE - Structures and Buildings*, 163(4), pp. 275-277.

Castro, I.P. and Robins, A.G. (1977) 'The flow around a surface-mounted cube in uniform and turbulent streams', *Journal of Fluid Mechanics*, vol. 79, pp. 307-335.

Cebeci, T. (2005) *Computational fluid dynamics for engineers from panel to Navier-Stokes methods with computer programs*. 1st edn. Long Beach, Calif. Berlin: Horizons Pub. Inc. ; Springer.

Cheatham, S.A.B.J.P.C.B.Z. (2003) '26 p.', *Simulation of Flow and Dispersion Around a Surface-Mounted Cube* [Internet Resource Date of Entry: 20080513]. Available at: http://handle.dtic.mil/100.2/ADA417469 (Accessed: 23 December 2010).

Chen, Q. (2004) 'Using computational tools to factor wind into architectural environment design', *Energy and Buildings*, 36(12), pp. 1197-1209.

Chen, Q. and Srebric, J. (2002) 'A procedure for verification, validation and reporting of indoor environment CFD analyses', *HVAC&R Research*, 8(2), pp. 201-216.

Chen, Q. and Zhai, Z. (2004) 'The use of Computational Fluid Dynamics tools for indoor environmental design', in Malkawi, A.M. and Augenbroe, G. (eds.) *Advanced Building Simulation*. Oxfordshire: Spon Press.

Chen, T.Y. and Liou, L.R. (2011) 'Blockage corrections in wind tunnel tests of small horizontal-axis wind turbines', *Experimental Thermal and Fluid Science*, 35(3), pp. 565-569.

Cheng, Y., Lien, F.S., Yee, E. and Sinclair, R. (2003) 'A comparison of large Eddy simulations with a standard k-[var epsilon] Reynolds-averaged Navier-Stokes model for the prediction of a fully developed turbulent flow over a matrix of cubes', *Journal of Wind Engineering and Industrial Aerodynamics*, 91(11), pp. 1301-1328.

Cheung, J.O.P. and Liu, C.-H. (2011) 'CFD simulations of natural ventilation behaviour in high-rise buildings in regular and staggered arrangements at various spacings', *Energy and Buildings*, 43(5), pp. 1149-1158.

Chiras, D. (2010) *Wind Power Basics*. Gabriola Island, Canada: New Society Publishers.

Clifford, M.J., Everitt, P.J., Clarke, R. and Riffat, S.B. (1997) 'Using computational fluid dynamics as a design tool for naturally ventilated buildings', *Building and Environment*, 32(4), pp. 305-312.

Cochran, B. and Damiani, R. (2008) *Integrating Wind Energy into the Design of Tall Buildings – A Case Study of the Houston Discovery Tower*. Available at: http://www.cppwind.com/support/papers/papers/windenergy/Building-Integrated_Turbines.pdf (Accessed: 27 January 2010).

Collins, J. (2004) 'A microgeneration manifesto', *Green Alliance, London*.

Committee on Climate Change (2008) *Building a low-carbon economy, the UK's contribution to tackling climate change*. London: TSO.

Cook, N.J. (1985) *The designer's guide to wind loading of building structures*. Watford, London ; Boston: Dept. of the Environment ; Butterworths.

Cóstola, D., Blocken, B. and Hensen, J.L.M. (2009) 'Overview of pressure coefficient data in building energy simulation and airflow network programs', *Building and Environment*, 44(10), pp. 2027-2036.

Cowan, I.R., Castro, I.P. and Robins, A.G. (1997) 'Numerical considerations for simulations of flow and dispersion around buildings', *Journal of Wind Engineering and Industrial Aerodynamics*, 67-68, pp. 535-545.

Danish Wind Industry Association (2003) *Guided Tour on Wind Energy* Available at: http://www.motiva.fi/myllarin_tuulivoima/windpower%20web/en/tour/wtrb/syncgen.htm (Accessed: 21 March 2012).

Dannecker, R.K.W. (2002) *Wind energy in the built environment: an experimental and numerical investigation of a building integrated ducted wind turbine module*. Ph.D. thesis. University of Strathclyde.

Date, A.W. (2005) *Introduction to computational fluid dynamics*. Cambridge Univ Pr.

Denoon, R., Cochran, B., Banks, D. and Wood, G. (2008) *Harvesting Wind Power from Tall Buildings*. Available at: http://www.ctbuh.org/Portals/0/Repository/T8_DenoonWood.357b6d8b-96e3-4988-b1d6-240cbafe12e3.pdf (Accessed: 20-01-2010).

Department of Energy and Climate Change (2011a) *Low Carbon Building Programme, Householder's Project Case Study – Wind Turbine*. Available at: http://www.decc.gov.uk/assets/decc/11/meeting-energy-demand/microgeneration/2118-project-case-study-wind-turbine.pdf (Accessed: 13 December 2011).

Department of Energy and Climate Change (2011b) *Low Carbon Buildings Programme, Communities Project Case Study – Wind Turbine*. Available at: http://www.decc.gov.uk/assets/decc/11/meeting-energy-demand/microgeneration/2122-communities-case-study-beckington.pdf (Accessed: 13 December 2011).

Department of Energy and Climate Change (2011c) *Microgeneration Strategy*. London: Crown. [Online]. Available at: http://www.decc.gov.uk/publications/basket.aspx?filetype=4&filepath=11%2fmeeting-energy-demand%2fmicrogeneration%2f2015-microgeneration-strategy.pdf&minwidth=true#basket (Accessed: 12 December 2011).

Department of Energy and Climate Change (2011d) *Planning our electric future: a White Paper for secure, affordable and low carbon electricity*. Norwich: TSO. [Online]. Available at: http://www.official-documents.gov.uk/document/cm80/8099/8099.pdf (Accessed: 12 December 2011).

Devinant, P., Laverne, T. and Hureau, J. (2002) 'Experimental study of wind-turbine airfoil aerodynamics in high turbulence', *Journal of Wind Engineering and Industrial Aerodynamics*, 90(6), pp. 689-707.

Dobbyn, J. and Thomas, G. (2005) 'Seeing the light: the impact of micro-generation on our use of energy', *Sustainable Consumption Roundtable*.

Dutton, A.G., Halliday, J.A. and Blanch, M.J. (2005) *The Feasibility of Building Mounted/Integrated Wind Turbines (BUWTs): Achieving their Potential for Carbon Emission Reductions.* [Online]. Available at: http://www.eru.rl.ac.uk/BUWT.htm.

Easom, G. (2000) *Improved Turbulence Models for Computational Wind Engineering*. PhD thesis. University of Nottingham.

El-Okda, Y.M., Ragab, S.A. and Hajj, M.R. (2008) 'Large-eddy simulation of flow over a surface-mounted prism using a high-order finite-difference scheme', *Journal of Wind Engineering and Industrial Aerodynamics*, 96(6-7), pp. 900-912.

El-Samanoudy, M., Ghorab, A.A.E. and Youssef, S.Z. (2010) 'Effect of some design parameters on the performance of a Giromill vertical axis wind turbine', *Ain Shams Engineering Journal*, 1(1), pp. 85-95.

Eliasson, I., Offerle, B., Grimmond, C.S.B. and Lindqvist, S. (2006) 'Wind fields and turbulence statistics in an urban street canyon', *Atmospheric Environment*, 40(1), pp. 1-16.

Eltham, D.C., Harrison, G.P. and Allen, S.J. (2008) 'Change in public attitudes towards a Cornish wind farm: Implications for planning', *Energy Policy*, 36(1), pp. 23-33.

Encraft (2009) *Encraft Warwick Wind Trials Project*. Available at: http://www.warwickwindtrials.org.uk/resources/Warwick+Wind+Trials+Final+Report+.pdf (Accessed: 29 January 2010).

Endalew, A.M., Hertog, M., Delele, M.A., Baetens, K., Persoons, T., Baelmans, M., Ramon, H., Nicolaï, B.M. and Verboven, P. (2009) 'CFD modelling and wind tunnel validation of airflow through plant canopies using 3D canopy architecture', *International Journal of Heat and Fluid Flow*, 30(2), pp. 356-368.

Eriksson, S., Bernhoff, H. and Leijon, M. (2008) 'Evaluation of different turbine concepts for wind power', *Renewable and Sustainable Energy Reviews*, 12(5), pp. 1419-1434.

Fellows, R. and Liu, A. (2008) *Research methods for construction*. Blackwell Pub.

Ferziger, J.H. and Peric, M. (2002) *Computational methods for fluid dynamics*. 3rd, rev. ed edn. Berlin, London: Springer.

FLUENT (2006) *FLUENT 6.3 User's Guide*. Available at: http://my.fit.edu/itresources/manuals/fluent6.3/help/pdf/ug/flug.pdf (Accessed: 25 June 2010).

Founda, D. and Giannakopoulos, C. (2009) 'The exceptionally hot summer of 2007 in Athens, Greece — A typical summer in the future climate?', *Global and Planetary Change*, 67(3-4), pp. 227-236.

Franke, J. (2007) 'Introduction to the Prediction of Wind Loads on Buildings by Computational Wind Engineering (CWE)', in Stathopoulos, T. and Baniotopoulos, C.C. (eds.) *Wind Effects on Buildings and Design of Wind-Sensitive Structures*. Springer Vienna, pp. 67-103.

Franke, J., Hellsten, A., Schlünzen, H. and Carissimo, B. (2007) *Best Practice Guideline for the CFD Simulation of Flows in the Urban Environment, Action 732* (732). Brussels: Hamburg, U.o. [Online]. Available at: http://www.mi.uni-hamburg.de/fileadmin/files/forschung/techmet/cost/cost_732/pdf/BestPractiseGuideline_1-5-2007-www.pdf.

Franke, J., Hirsch, C., Jensen, A.G., Kliis, H.W., Schatzmann, M., Westbury, P.S., Miles, S.D., Wlisse, J.A. and Wright, N.G. (2004) *Recommendations of the COST action C14 on the use of CFD in predicting pedestrian wind environment*. [Online]. Available at: http://www.kuleuven.be/bwf/projects/annex41/protected/data/Recommendations%20for%20CFD%20in%20wind%20engineering.pdf.

Freathy, P. and Salt, J. (2010) *Glossary of Wind Terms used in Construction*. Available at: http://www.ice.org.uk/Information-resources/Document-Library/Glossary-of-wind-terms-used-in-construction (Accessed: 22 March 2010).

Frechette, R. and Gilchrist, R. (2008) *Towards Zero Energy, A Case Study of the Pearl River Tower, Guangzhou, China*. Available at: http://www.ctbuh.org/Portals/0/Repository/T6_FrechetteGilchrist.cc3a16e5-f3b1-471f-b6f2-fc7545ad1beb.pdf (Accessed: 23 January 2010).

Freitas, C.I. (1993) *Journal of Fluids Engineering Editorial Policy, Statement on the Control of Numerical Accuracy*. Available at: http://journaltool.asme.org/Templates/JFENumAccuracy.pdf (Accessed: 05 November 2010).

Gao, Y. and Chow, W.K. (2005) 'Numerical studies on air flow around a cube', *Journal of Wind Engineering and Industrial Aerodynamics*, 93(2), pp. 115-135.

Glass, A. and Levermore, G. (2011) 'Micro wind turbine performance under real weather conditions in urban environment', *Building Services Engineering Research and Technology*.

Gomes, M.S.d.P., Isnard, A.A. and Pinto, J.M.d.C. (2007) 'Wind tunnel investigation on the retention of air pollutants in three-dimensional recirculation zones in urban areas', *Atmospheric Environment*, 41(23), pp. 4949-4961.

Gosman, A.D. (1999) 'Developments in CFD for industrial and environmental applications in wind engineering', *Journal of Wind Engineering and Industrial Aerodynamics*, 81(1-3), pp. 21-39.

Grant, A., Johnstone, C. and Kelly, N. (2008) 'Urban wind energy conversion: The potential of ducted turbines', *Renewable Energy*, 33(6), pp. 1157-1163.

Grant, A. and Kelly, N. (2004) 'A ducted wind turbine model for building simulation', *Building Service Engineering*, 25(4), pp. 339-349.

Greenblatt, D., Schulman, M. and Ben-Harav, A. (2012) 'Vertical axis wind turbine performance enhancement using plasma actuators', *Renewable Energy*, 37(1), pp. 345-354.

Haggett, C. (2011) 'Understanding public responses to offshore wind power', *Energy Policy*, 39(2), pp. 503-510.

Hang, J., Li, Y. and Sandberg, M. (2011) 'Experimental and numerical studies of flows through and within high-rise building arrays and their link to ventilation strategy', *Journal of Wind Engineering and Industrial Aerodynamics*, 99(10), pp. 1036-1055.

Hargreaves, D.M. and Wright, N.G. (2007) 'On the use of the k-[epsilon] model in commercial CFD software to model the neutral atmospheric boundary layer', *Journal of Wind Engineering and Industrial Aerodynamics*, 95(5), pp. 355-369.

Hau, E. (2006) *Wind turbines: fundamentals, technologies, application, economics*. Springer Verlag.

He, J. and Song, C.C.S. (1997) 'A numerical study of wind flow around the TTU building and the roof corner vortex', *Journal of Wind Engineering and Industrial Aerodynamics*, 67-68, pp. 547-558.

He, J. and Song, C.C.S. (1999) 'Evaluation of pedestrian winds in urban area by numerical approach', *Journal of Wind Engineering and Industrial Aerodynamics*, 81(1-3), pp. 295-309.

Heath, M.A., Walshe, J.D. and Watson, S.J. (2007) 'Estimating the potential yield of small building-mounted wind turbines', *Wind Energy*, 10(3), pp. 271-287.

Herzog, N., Schreiber, M., Egbers, C. and Krautz, H.J. (2012) 'A comparative study of different CFD-codes for numerical simulation of gas–solid fluidized bed hydrodynamics', *Computers & Chemical Engineering*, (0).

Hölscher, N. and Niemann, H.-J. (1998) 'Towards quality assurance for wind tunnel tests: A comparative testing program of the Windtechnologische Gesellschaft', *Journal of Wind Engineering and Industrial Aerodynamics*, 74–76(0), pp. 599-608.

Houkema, M., Siccama, N.B., Lycklama à Nijeholt, J.A. and Komen, E.M.J. (2008) 'Validation of the CFX4 CFD code for containment thermal-hydraulics', *Nuclear Engineering and Design*, 238(3), pp. 590-599.

Howell, R., Qin, N., Edwards, J. and Durrani, N. (2010) 'Wind tunnel and numerical study of a small vertical axis wind turbine', *Renewable Energy*, 35(2), pp. 412-422.

Hu, C.-H. (2003) *Proposed Guidelines of Using CFD and the Validity of the CFD Models in the Numerical Simulations of Wind Environments around Buildings*. PhD thesis. Heriot-Watt University.

Hu, D., Hua, O. and Du, Z. (2006) 'A study on stall-delay for horizontal axis wind turbine', *Renewable Energy*, 31(6), pp. 821-836.

Huang, S., Li, Q.S. and Xu, S. (2007) 'Numerical evaluation of wind effects on a tall steel building by CFD', *Journal of Constructional Steel Research*, 63(5), pp. 612-627.

Huang, Y., Hu, X. and Zeng, N. (2009) 'Impact of wedge-shaped roofs on airflow and pollutant dispersion inside urban street canyons', *Building and Environment*, 44(12), pp. 2335-2347.

Hussein, H.J. and Martinuzzi, R.J. (1996) 'Energy balance for turbulent flow around a surface mounted cube placed in a channel', *Physics of fluids*, vol. 8(3), pp. 764-780.

Hyams, E. (2005) *Delivering the Government's 2020 vision for local energy generation*. London.

Jha, A.R. (2010) *Wind Turbine Technology*. Hoboken: CRC Press.

Jiang, Y., Liu, H., Zhang, B., Zhu, F., Liang, B. and Sang, J. (2008) 'Wind flow and wind loads on the surface of a towershaped building: Numerical simulations and wind tunnel experiment', *Science in China Series D: Earth Sciences*, 51(1), pp. 103-113.

Jones, C.R. and Richard Eiser, J. (2010) 'Understanding 'local' opposition to wind development in the UK: How big is a backyard?', *Energy Policy*, 38(6), pp. 3106-3117.

Jones, P.J., Alexander, D. and Burnett, J. (2004) 'Pedestrian Wind Environment Around High-Rise Residential Buildings in Hong Kong', *Indoor and Built Environment*, 13(4), pp. 259-269.

Jones, P.J. and Whittle, G.E. (1992) 'Computational fluid dynamics for building air flow prediction--current status and capabilities', *Building and Environment*, 27(3), pp. 321-338.

Joselin Herbert, G.M., Iniyan, S., Sreevalsan, E. and Rajapandian, S. (2007) 'A review of wind energy technologies', *Renewable and Sustainable Energy Reviews*, 11(6), pp. 1117-1145.

Jung, S.N., No, T.-S. and Ryu, K.-W. (2005) 'Aerodynamic performance prediction of a 30 kW counter-rotating wind turbine system', *Renewable Energy*, 30(5), pp. 631-644.

Kaganov, E.I. and Yaglom, A.M. (1976) 'Errors in wind-speed measurements by rotation anemometers', *Boundary-Layer Meteorology*, 10(1), pp. 15-34.

Kaldellis, J.K. and Zafirakis, D. (2011) 'The wind energy (r)evolution: A short review of a long history', *Renewable Energy*, 36(7), pp. 1887-1901.

Kastner-Klein, P., Fedorovich, E. and Rotach, M.W. (2001) 'A wind tunnel study of organised and turbulent air motions in urban street canyons', *Journal of Wind Engineering and Industrial Aerodynamics*, 89(9), pp. 849-861.

Kastner-Klein, P. and Plate, E.J. (1999) 'Wind-tunnel study of concentration fields in street canyons', *Atmospheric Environment*, 33(24-25), pp. 3973-3979.

Killa, S. and Smith, R.F. (2008) *Harnessing Energy in Tall Buildings: Bahrain World Trade Center and Beyond*. Available at: http://www.ctbuh.org/Portals/0/Repository/T3_KillaSmith.cfce5b62-fc35-4de7-ba53-90eeca647d94.pdf (Accessed: 23 January 2010).

Kim, H., Lee, S., Son, E., Lee, S. and Lee, S. (2012) 'Aerodynamic noise analysis of large horizontal axis wind turbines considering fluid–structure interaction', *Renewable Energy*, 42(0), pp. 46-53.

Kim, J.-J. and Kim, D.-Y. (2009) 'Effects of a building's density on flow in urban areas', *Advances in Atmospheric Sciences*, 26(1), pp. 45-56.

Kim, T., Kim, K. and Kim, B.S. (2009) 'A wind tunnel experiment and CFD analysis on airflow performance of enclosed-arcade markets in Korea', *Building and Environment*, 45(5), pp. 1329-1338.

Kindangen, J., Krauss, G. and Depecker, P. (1997) 'Effects of roof shapes on wind-induced air motion inside buildings', *Building and Environment*, 32(1), pp. 1-11.

Kirklees Metropolitan Council (2006) *Detailed technical information: Civic Centre 3 – Energy from the Sun and the Wind*. Available at: http://www.kirklees.gov.uk/community/environment/renewable/CivicCentre3casestudy.pdf (Accessed: 18 February 2010).

Kitson, M. and Moran, H. (2006) *Taking the Built Environment to New Heights*. Available at: http://www.fluent.com/about/news/newsletters/06v15i2/a5.pdf (Accessed: 16 February 2010).

Kjellin, J., Bülow, F., Eriksson, S., Deglaire, P., Leijon, M. and Bernhoff, H. (2011) 'Power coefficient measurement on a 12 kW straight bladed vertical axis wind turbine', *Renewable Energy*, 36(11), pp. 3050-3053.

Lakehal, D. and Rodi, W. (1997) 'Calculation of the flow past a surface-mounted cube with two-layer turbulence models', *Journal of Wind Engineering and Industrial Aerodynamics*, 67-68, pp. 65-78.

Lawson, T.V. (2001) *Building Aerodynamics*. London: Imperial College Press

Ledo, L., Kosasih, P.B. and Cooper, P. (2011) 'Roof mounting site analysis for micro-wind turbines', *Renewable Energy*, 36(5), pp. 1379-1391.

Lee, B.E. and Evans, R.A. (1984) 'The measurement of wind flow patterns over building roofs', *Building and Environment*, 19(4), pp. 235-241.

Lee, S., Kim, H., Son, E. and Lee, S. (2012) 'Effects of design parameters on aerodynamic performance of a counter-rotating wind turbine', *Renewable Energy*, 42(0), pp. 140-144.

Lei, L., Fei, H., Xue-Ling, C., Jin-Hua, J. and Xiao-Guang, M. (2006) 'Numerical simulation of the flow within and over an intersection model with Reynolds-averaged Navier–Stokes method', *Chinese Physics*, 15(1), pp. 149-155.

Li, Y., Tagawa, K. and Liu, W. (2010) 'Performance effects of attachment on blade on a straight-bladed vertical axis wind turbine', *Current Applied Physics*, 10(2, Supplement), pp. S335-S338.

Liaw, K.F. (2005) *Simulation of Flow around Bluff Bodies and Bridge Deck Sections using CFD*. PhD thesis. University of Nottingham [Online]. Available at: www.etheses.nottingham.ac.uk/125/1/KFL_thesis.pdf.

Lim, H.C., Thomas, T.G. and Castro, I.P. (2009) 'Flow around a cube in a turbulent boundary layer: LES and experiment', *Journal of Wind Engineering and Industrial Aerodynamics*, 97(2), pp. 96-109.

Liu, C.-h., Leung, D., Man, A. and Chan, P. (2010) 'Computational fluid dynamics simulation of the wind flow over an airport terminal building', *Journal of Zhejiang University - Science A*, 11(6), pp. 389-401.

Lu, L. and Ip, K.Y. (2009) 'Investigation on the feasibility and enhancement methods of wind power utilization in high-rise buildings of Hong Kong', *Renewable and Sustainable Energy Reviews*, 13(2), pp. 450-461.

Mahmood, M. (2011) 'Experiments to study turbulence and flow past a low-rise building at oblique incidence', *Journal of Wind Engineering and Industrial Aerodynamics*, 99(5), pp. 560-572.

Makkawi, A., Celik, A.N. and Muneer, T. (2009) 'Evaluation of micro-wind turbine aerodynamics, wind speed sampling interval and its spatial variation', *Building Services Engineering Research and Technology*, 30(1), p. 7.

Malcolm, A.H., John, D.W. and Simon, J.W. (2007) 'Estimating the potential yield of small building-mounted wind turbines', *Wind Energy*, 10(3), pp. 271-287.

Manwell, J.F., McGowan, J.G. and Rogers, A.L. (2002) *Wind energy explained*. Wiley Online Library.

Manwell, J.F., McGowan, J.G. and Rogers, A.L. (2009) *Wind energy explained : theory, design, and application*. 2nd edn. Hoboken, NJ: John Wiley.

Martinot, E., Dienst, C., Weiliang, L. and Qimin, C. (2007) 'Renewable energy futures: Targets, scenarios, and pathways', *Annu. Rev. Environ. Resour.*, 32, pp. 205-239.

Martinuzzi, R. and Tropea, C. (1993) 'The Flow Around Surface-Mounted, Prismatic Obstacles Placed in a Fully Developed Channel Flow (Data Bank Contribution)', *Journal of Fluids Engineering*, 115(1), pp. 85-92.

Mejía, E.R., Filipek, J.W. and Tovar Salazar, J. (2003) 'A cheap, reliable and efficient regulator for small horizontal-axis wind-turbines', *Applied Energy*, 74(1–2), pp. 229-237.

Menter, F., Hemstrom, B., Henriksson, M., Karlsson, R., Latrobe, A., Martin, A., Muhlbauer, P., Scheuerer, M., Smith, B., Takacs, T. and Willemsen, S. (2002) *CFD Best Practice Guidelines for CFD Code Validation for Reactor-Safety Applications*. [Online]. Available at: http://domino.grs.de/ecora/ecora.nsf/16edc336e8a342f580256502004d0e8b/684c0ed5f389add8c1256fcd002e7cb8/$FILE/D01_WP1.pdf.

Mertens, S. (2006) *Wind energy in the built environment : concentrator effects of buildings*. Essex: Multi-Science.

Mithraratne, N. (2009) 'Roof-top wind turbines for microgeneration in urban houses in New Zealand', *Energy and Buildings*, 41(10), pp. 1013-1018.

Mochida, A., Murakami, S., Ojima, T., Kim, S., Ooka, R. and Sugiyama, H. (1997) 'CFD analysis of mesoscale climate in the Greater Tokyo area', *Journal of Wind Engineering and Industrial Aerodynamics*, 67-68, pp. 459-477.

Molnarova, K., Sklenicka, P., Stiborek, J., Svobodova, K., Salek, M. and Brabec, E. (2012) 'Visual preferences for wind turbines: Location, numbers and respondent characteristics', *Applied Energy*, 92(0), pp. 269-278.

Morris, V.R., Barnard, J.C., Wendell, L.L. and Tomich, S.D. (1992) *Comparison of anemometers for turbulence characterization*.

Müller, G., Jentsch, M.F. and Stoddart, E. (2009) 'Vertical axis resistance type wind turbines for use in buildings', *Renewable Energy*, 34(5), pp. 1407-1412.

Murakami, S. and Mochida, A. (1988) '3-D numerical simulation of airflow around a cubic model by means of the k-[epsilon] model', *Journal of Wind Engineering and Industrial Aerodynamics*, 31(2-3), pp. 283-303.

Murakami, S., Zeng, J. and Hayashi, T. (1999) 'CFD analysis of wind environment around a human body', *Journal of Wind Engineering and Industrial Aerodynamics*, 83(1-3), pp. 393-408.

Ozgener, O. (2006) 'A small wind turbine system (SWTS) application and its performance analysis', *Energy Conversion and Management*, 47(11–12), pp. 1326-1337.

Parent, O. and Ilinca, A. (2011) 'Anti-icing and de-icing techniques for wind turbines: Critical review', *Cold Regions Science and Technology*, 65(1), pp. 88-96.

Paterson, D.A. and Apelt, C.J. (1989) 'Simulation of wind flow around three-dimensional buildings', *Building and Environment*, 24(1), pp. 39-50.

Peacock, A.D., Jenkins, D., Ahadzi, M., Berry, A. and Turan, S. (2008) 'Micro wind turbines in the UK domestic sector', *Energy and Buildings*, 40(7), pp. 1324-1333.

Pedersen, E. and Larsman, P. (2008) 'The impact of visual factors on noise annoyance among people living in the vicinity of wind turbines', *Journal of Environmental Psychology*, 28(4), pp. 379-389.

Pedersen, E., van den Berg, F., Bakker, R. and Bouma, J. (2010) 'Can road traffic mask sound from wind turbines? Response to wind turbine sound at different levels of road traffic sound', *Energy Policy*, 38(5), pp. 2520-2527.

Peel, D. and Lloyd, M.G. (2007) 'Positive Planning for Wind-Turbines in an Urban Context', *Local Environment: The International Journal of Justice and Sustainability*, 12(4), pp. 343 - 354.

Peter, I., John, K., Jamieson, R. and Andrea, F. (2008) 'Wind and tall buildings: negatives and positives', *The Structural Design of Tall and Special Buildings*, 17(5), pp. 915-928.

Phillips, R. (2007) *Micro-wind turbines in urban environments : an assessment*. Bracknell: IHS BRE Press for BRE Trust.

Pindado, S., Meseguer, J. and Franchini, S. (2011) 'Influence of an upstream building on the wind-induced mean suction on the flat roof of a low-rise building', *Journal of Wind Engineering and Industrial Aerodynamics*, 99(8), pp. 889-893.

Plate, E.J. (1999) 'Methods of investigating urban wind fields--physical models', *Atmospheric Environment*, 33(24-25), pp. 3981-3989.

Pope, K., Rodrigues, V., Doyle, R., Tsopelas, A., Gravelsins, R., Naterer, G.F. and Tsang, E. (2010) 'Effects of stator vanes on power coefficients of a zephyr vertical axis wind turbine', *Renewable Energy*, 35(5), pp. 1043-1051.

Pospisil, J., Jicha, M., Niachou, K. and Santamouris, M. (2005) 'Computational modelling of airflow in urban street canyon and comparison with measurements', *International Journal of Environment and Pollution*, 25(1-4), pp. 191-200.

Quick, D. (2010) *World's biggest wind turbine to take a spin in Norway*. Available at: http://www.gizmag.com/worlds-biggest-wind-turbine/14215/ (Accessed: 29 March 2012).

Rafailidis, S. (1997) 'Influence of Building Areal Density and Roof Shape on the Wind Characteristics Above a Town', *Boundary-Layer Meteorology*, 85(2), pp. 255-271.

Reiter, S. (2008) *The European Built Environment CAE Conference*. London, 5-6 june.

Reiter, S. (2010) 'Assessing wind comfort in urban planning', *Environment and Planning B: Planning and Design*, 37(5), pp. 857-873.

RenewableUK (2011a) *Generate Your Own Power, Your Guide to Installing a Small Wind System*. Available at: http://www.bwea.com/pdf/publications/RenewableUK_SWS_Consumer_Guide.pdf (Accessed: 12 December 2011).

RenewableUK (2011b) *Small Wind Systems UK Market Report 2011*. Available at: http://www.bwea.com/pdf/small/Small_Wind_Systems_Market_Report_2011.pdf (Accessed: 12 December 2011).

Ricciardelli, F. and Polimeno, S. (2006) 'Some characteristics of the wind flow in the lower Urban Boundary Layer', *Journal of Wind Engineering and Industrial Aerodynamics*, 94(11), pp. 815-832.

Richards, P.J. and Hoxey, R.P. (1993) 'Appropriate boundary conditions for computational wind engineering models using the k-[epsilon] turbulence model', *Journal of Wind Engineering and Industrial Aerodynamics*, 46-47, pp. 145-153.

Richards, P.J. and Hoxey, R.P. (2002) 'Unsteady flow on the sides of a 6 m cube', *Journal of Wind Engineering and Industrial Aerodynamics*, 90(12-15), pp. 1855-1866.

Richards, P.J. and Hoxey, R.P. (2004) 'Quasi-steady theory and point pressures on a cubic building', *Journal of Wind Engineering and Industrial Aerodynamics*, 92(14-15), pp. 1173-1190.

Richards, P.J. and Hoxey, R.P. (2006) 'Flow reattachment on the roof of a 6 m cube', *Journal of Wind Engineering and Industrial Aerodynamics*, 94(2), pp. 77-99.

Richards, P.J. and Hoxey, R.P. (2008) 'Wind loads on the roof of a 6 m cube', *Journal of Wind Engineering and Industrial Aerodynamics*, 96(6-7), pp. 984-993.

Richards, P.J., Hoxey, R.P., Connell, B.D. and Lander, D.P. (2007) 'Wind-tunnel modelling of the Silsoe Cube', *Journal of Wind Engineering and Industrial Aerodynamics*, 95(9-11), pp. 1384-1399.

Richards, P.J., Hoxey, R.P. and Short, L.J. (2001) 'Wind pressures on a 6 m cube', *Journal of Wind Engineering and Industrial Aerodynamics*, 89(14-15), pp. 1553-1564.

Riegler, H. (2003) 'HAWT versus VAWT: Small VAWTs find a clear niche', *Refocus*, 4(4), pp. 44-46.

Ritchie, A. and Thomas, R. (2009) *Sustainable urban design : an environmental approach*. 2nd edn. London ; New York: Taylor & Francis.

Roaf, S., Crichton, D. and Nicol, F. (2009) *Adapting buildings and cities for climate change, A 21st Century Survival Guide*. Elsevier.

Rodi, W. (1997) 'Comparison of LES and RANS calculations of the flow around bluff bodies', *Journal of Wind Engineering and Industrial Aerodynamics*, 69–71(0), pp. 55-75.

Ross, I. and Altman, A. (2011) 'Wind tunnel blockage corrections: Review and application to Savonius vertical-axis wind turbines', *Journal of Wind Engineering and Industrial Aerodynamics*, 99(5), pp. 523-538.

Roth, M. and Oke, T.R. (1993) 'Turbulent transfer relationships over an urban surface. I. Spectral characteristics', *Quarterly Journal of the Royal Meteorological Society*, 119(513), pp. 1071-1104.

Royal instutute of British Architects (RIBA) (2006) *Low or Zero Carbon Energy Sources: Strategic Guide*. First edn. London: NBS.

Salim, S.M. and Cheah, S.C. (2009) *The International MultiConference of Engineers and Computer Scientists*. Hong Kong. Newswood Limited. Available at: http://www.iaeng.org/publication/IMECS2009/IMECS2009_pp2165-2170.pdf.

Sara Louise, W. (2011) 'Building mounted wind turbines and their suitability for the urban scale—A review of methods of estimating urban wind resource', *Energy and Buildings*, 43(8), pp. 1852-1862.

Schaffrath, A., Fischer, K.-C., Hahm, T. and Wussow, S. (2007) 'Validation of the CFD code fluent by post-test calculation of a density-driven ROCOM experiment', *Nuclear Engineering and Design*, 237(15–17), pp. 1899-1908.

Schmidt, S. and Thiele, F. (2002) 'Comparison of numerical methods applied to the flow over wall-mounted cubes', *International Journal of Heat and Fluid Flow*, 23(3), pp. 330-339.

Seeta Ratnam, G. and Vengadesan, S. (2008) 'Performance of two equation turbulence models for prediction of flow and heat transfer over a wall mounted cube', *International Journal of Heat and Mass Transfer*, 51(11–12), pp. 2834-2846.

Shah, K.B. and Ferziger, J.H. (1997) 'A fluid mechanicians view of wind engineering: Large eddy simulation of flow past a cubic obstacle', *Journal of Wind Engineering and Industrial Aerodynamics*, 67-68, pp. 211-224.

Sharma, R.N. and Madawala, U.K. (2012) 'The concept of a smart wind turbine system', *Renewable Energy*, 39(1), pp. 403-410.

Sharpe, T. and Proven, G. (2010) 'Crossflex: Concept and early development of a true building integrated wind turbine', *Energy and Buildings*, 42(12), pp. 2365-2375.

Sievert, T. (2009) *Product Pick of the Week - The Mag-Wind™ wind turbine*. Available at: http://windfair.net/press/5739.html (Accessed: 19 April 2011).

Slowe, J. (2006) *Roof-top Wind Turbines, Large Potential - But Can They Deliver?* Available at: http://www.delta-ee.com/downloads/09_Delta_Micro_Wind_Research_Brief.pdf (Accessed: 19 April 2011).

Smith, F.J. (2010) *Conducting your pharmacy practice research project: a step-by-step approach*. Pharmaceutical Pr.

Smith, P.F. (2003) *Sustainability at the cutting edge : emerging technologies for low energy buildings*. Oxford: Architectural Press.

Smith, P.F. (2005) *Architecture in a Climate of Change*. Architectural Press.

Sørensen, D.N. and Nielsen, P.V. (2003) 'Quality control of computational fluid dynamics in indoor environments', *Indoor Air*, 13(1), pp. 2-17.

Sovacool, B.K. (2012) 'The avian benefits of wind energy: A 2009 update', *Renewable Energy*, (0).

Spalart, P.R. (2000) 'Strategies for turbulence modelling and simulations', *International Journal of Heat and Fluid Flow*, 21(3), pp. 252-263.

Spalding, D.B. (1981) 'A general purpose computer program for multi-dimensional one- and two-phase flow', *Mathematics and Computers in Simulation*, 23(3), pp. 267-276.

Srebric, J. and Chen, Q. (2002) 'An example of verification, validation, and reporting of indoor environment CFD analyses (RP-1133)', *TRANSACTIONS-AMERICAN SOCIETY OF HEATING*

REFRIGERATING AND AIR CONDITIONING ENGINEERS, 108(2), pp. 185-194.

Stankovic, S., Campbell, N. and Harries, A. (2009) *Urban wind energy*. London: Earthscan.

Stathopoulos, T. (2006) 'Pedestrian level winds and outdoor human comfort', *Journal of Wind Engineering and Industrial Aerodynamics*, 94(11), pp. 769-780.

Stathopoulos, T. and Baskaran, B.A. (1996) 'Computer simulation of wind environmental conditions around buildings', *Engineering Structures*, 18(11), pp. 876-885.

Summers, D.M., Hanson, T. and Wilson, C.B. (1986) 'Validation of a computer simulation of wind flow over a building model', *Building and Environment*, 21(2), pp. 97-111.

Sun, H. and Huang, S. (2001) 'Simulation of Wind Flow Around a Building with a k –ε Model', *Theoretical and Computational Fluid Dynamics*, 14(4), pp. 283-292.

Swaddiwudhipong, S., Anh, T., Liu, Z. and Hua, J. (2007) 'Modelling of wind load on single and staggered dual buildings', *Engineering with Computers*, 23(3), pp. 215-227.

Syngellakis, K. and Traylor, H. (2007) *Urban Wind Resource Assessment in the UK, An introduction to wind resource assessment in the urban environment*. Chineham. [Online]. Available at: http://www.urbanwind.net/pdf/Reports_UrbanWindResourceAssessment_UK.pdf (Accessed: 28 January 2010).

Theodoridis, G. and Moussiopoulos, N. (2000) 'Influence of Building Density and Roof Shape on the Wind and Dispersion Characteristics in an Urban Area: A Numerical Study', *Environmental Monitoring and Assessment*, 65(1), pp. 407-415.

Thomas, T.G. and Williams, J.J.R. (1999) 'Generating a wind environment for large eddy simulation of bluff body flows', *Journal of Wind Engineering and Industrial Aerodynamics*, 82(1-3), pp. 189-208.

Tieleman, H.W. (2003) 'Wind tunnel simulation of wind loading on low-rise structures: a review', *Journal of Wind Engineering and Industrial Aerodynamics*, 91(12-15), pp. 1627-1649.

Tominaga, Y. and Mochida, A. (1999) 'CFD prediction of flowfield and snowdrift around a building complex in a snowy region', *Journal of Wind Engineering and Industrial Aerodynamics*, 81(1-3), pp. 273-282.

Tominaga, Y., Mochida, A., Shirasawa, T., Yoshie, R., Kataoka, H., Harimoto, K. and Nozu, T. (2004) 'Cross Comparisons of CFD Results of Wind Environment at Pedestrian Level around a High-rise Building and

within a Building Complex', *Journal of Asian Architecture and Building Engineering*, 3(1), pp. 63-70.

Tominaga, Y., Mochida, A., Yoshie, R., Kataoka, H., Nozu, T., Yoshikawa, M. and Shirasawa, T. (2008) 'AIJ guidelines for practical applications of CFD to pedestrian wind environment around buildings', *Journal of Wind Engineering and Industrial Aerodynamics*, 96(10-11), pp. 1749-1761.

Tominaga, Y. and Stathopoulos, T. (2009) 'Numerical simulation of dispersion around an isolated cubic building: Comparison of various types of k-[var epsilon] models', *Atmospheric Environment*, 43(20), pp. 3200-3210.

Tong, W. (2010) *Wind Power Generation and Wind Turbine Design*. Wit Pr/Computational Mechanics.

Tu, J., Yeoh, G.H. and Liu, C. (2008) *Computational Fluid Dynamics - A Practical Approach*. USA: Elsevier.

Tutar, M. and Oguz, G. (2002) 'Large eddy simulation of wind flow around parallel buildings with varying configurations', *Fluid Dynamics Research*, 31(5-6), pp. 289-315.

Tutar, M. and Oğuz, G. (2004) 'Computational Modeling of Wind Flow Around a Group of Buildings', *International Journal of Computational Fluid Dynamics*, 18(8), pp. 651 - 670.

Van Hooff, T., Blocken, B. and van Harten, M. (2011) '3D CFD simulations of wind flow and wind-driven rain shelter in sports stadia: Influence of stadium geometry', *Building and Environment*, 46(1), pp. 22-37.

Vardoulakis, S., Dimitrova, R., Richards, K., Hamlyn, D., Camilleri, G., Weeks, M., Sini, J.-F., Britter, R., Borrego, C., Schatzmann, M. and Moussiopoulos, N. (2011) 'Numerical Model Inter-comparison for Wind Flow and Turbulence Around Single-Block Buildings', *Environmental Modeling and Assessment*, 16(2), pp. 169-181.

Versteeg, H.K. and Malalasekera, W. (2007) *An introduction to computational fluid dynamics : the finite volume method*. 2nd edn. Harlow: Prentice Hall.

Wainwright, J. and Mulligan, M. (2004) *Environmental modelling : finding simplicity in complexity*. Chichester: Wiley.

Walker, N. (2007) *Generating Wind Power*. Crabtree Publishing Company.

Walker, S.L. (2012) 'Can the GB feed-in tariff deliver the expected 2% of electricity from renewable sources?', *Renewable Energy*, 43(0), pp. 383-388.

Watson, J., Sauter, R., Bahaj, B., James, P., Myers, L. and Wing, R. (2008) 'Domestic micro-generation: Economic, regulatory and policy issues for the UK', *Energy Policy*, 36(8), pp. 3095-3106.

Webb, A. (2007) *The Viability of Domestic Wind Turbines for Urban Melbourne*. Melbourne. [Online]. Available at: http://www.advocacypanel.com.au/documents/Applic246Windturbinevi ablity.pdf (Accessed: 28 January 2010).

Willemsen, E. and Wisse, J.A. (2002) 'Accuracy of assessment of wind speed in the built environment', *Journal of Wind Engineering and Industrial Aerodynamics*, 90(10), pp. 1183-1190.

Willemsen, E. and Wisse, J.A. (2007) 'Design for wind comfort in The Netherlands: Procedures, criteria and open research issues', *Journal of Wind Engineering and Industrial Aerodynamics*, 95(9-11), pp. 1541-1550.

WINEUR (2005) *Wind energy integration in the urban environment,Technology inventory report*. [Online]. Available at: http://www.bwea.com/pdf/small/wineur.pdf (Accessed: 29 January 2010).

WINEUR (2007) *Wind Energy Integration in the Urban Environment: Report on Resource Assessment* (5.1). [Online]. Available at: http://www.iee-library.eu/images/all_ieelibrary_docs/514%20wineur.pdf (Accessed: 29 January 2010).

Wit, S.D. (2004) 'Uncertainty in building simulaton', in Malkawi, A.M. and Augenbroe, G. (eds.) *Advanced Building Simulation*. Oxfordshire: Spon Press, pp. 25-59.

Wolsink, M. (2000) 'Wind power and the NIMBY-myth: institutional capacity and the limited significance of public support', *Renewable Energy*, 21(1), pp. 49-64.

Wu, Z. and Wang, H. (2012) 'Research on Active Yaw Mechanism of Small Wind Turbines', *Energy Procedia*, 16, Part A(0), pp. 53-57.

Xiaomin, X., Zhen, H. and Jiasong, W. (2006) 'The impact of urban street layout on local atmospheric environment', *Building and Environment*, 41(10), pp. 1352-1363.

Yakhot, A., Liu, H. and Nikitin, N. (2006) 'Turbulent flow around a wall-mounted cube: A direct numerical simulation', *International Journal of Heat and Fluid Flow*, 27(6), pp. 994-1009.

Yang, T. (2004a) *CFD and Field Testing of a Naturally Ventilated Full-scale Building*. PhD thesis. University of Nottingham [Online]. Available at: http://etheses.nottingham.ac.uk/91/.

Yang, T. (2004b) *CFD and Field Testing of a Naturally Ventilated Full-scale Building*. PhD thesis. UNIVERSITY OF NOTTINGHAM.

Yang, Y., Gu, M., Chen, S. and Jin, X. (2009) 'New inflow boundary conditions for modelling the neutral equilibrium atmospheric boundary layer in computational wind engineering', *Journal of Wind Engineering and Industrial Aerodynamics*, 97(2), pp. 88-95.

Yassin, M.F., Kato, S., Ooka, R., Takahashi, T. and Kouno, R. (2005) 'Field and wind-tunnel study of pollutant dispersion in a built-up area under various meteorological conditions', *Journal of Wind Engineering and Industrial Aerodynamics*, 93(5), pp. 361-382.

Yu, D. and Kareem, A. (1998) 'Parametric study of flow around rectangular prisms using LES', *Journal of Wind Engineering and Industrial Aerodynamics*, 77-78, pp. 653-662.

Yuen, C., Zanchetta, M. and Battle, G. (2004) 'Performance of a Building Integrated Wind Farm', *The 21st Conference on Passive and Low Energy Architecture (Plea)*. The Netherlands. Available at: http://alexandria.tue.nl/openaccess/635611/p0563final.pdf (Accessed: 28 January 2010).

Zhang, A., Gao, C. and Zhang, L. (2005) 'Numerical simulation of the wind field around different building arrangements', *Journal of Wind Engineering and Industrial Aerodynamics*, 93(12), pp. 891-904.

Zhang, R., Zhang, Y., Lam, K.P. and Archer, D.H. (2010) 'A prototype mesh generation tool for CFD simulations in architecture domain', *Building and Environment*, 45(10), pp. 2253-2262.

Zhang, Y.W., Gu, Z.L., Lee, S.C., Fu, T.M. and Ho, K.F. (2011) 'Numerical Simulation and In Situ Investigation of Fine Particle Dispersion in an Actual Deep Street Canyon in Hong Kong', *Indoor and Built Environment*, 20(2), p. 206.

Zhe, C., Guerrero, J.M. and Blaabjerg, F. (2009) 'A Review of the State of the Art of Power Electronics for Wind Turbines', *Power Electronics, IEEE Transactions on*, 24(8), pp. 1859-1875.